GENOTOXICITY OF COMPLEX CHEMICAL MIXTURES

A Dissertation

by

TRACIE DENISE PHILLIPS

Submitted to the Office of Graduate Studies of
Texas A&M University
in partial fulfillment of the requirements for the degree of

DOCTOR OF PHILOSOPHY

December 2006

Major Subject: Toxicology

GENOTOXICITY OF COMPLEX CHEMICAL MIXTURES

A Dissertation

by

TRACIE DENISE PHILLIPS

Submitted to the Office of Graduate Studies of
Texas A&M University
in partial fulfillment of the requirements for the degree of

DOCTOR OF PHILOSOPHY

Approved by:

Chair of Committee,	Kirby C. Donnelly
Committee Members,	Robin L. Autenrieth
	Thomas J. McDonald
	Stephen S. Safe
Chair of Faculty of Toxicology,	Robert C. Burghardt

December 2006

Major Subject: Toxicology

ABSTRACT

Genotoxicity of Complex Chemical Mixtures.
(December 2006)
Tracie Denise Phillips, B.S., Texas A&M University
Chair of Advisory Committee: Dr. K.C. Donnelly

Complex chemical mixtures are ubiquitous in the environment. Humans are frequently exposed to these mixtures; therefore, it is important to understand potential interactions of chemical mixtures. Mixture interactions may influence the absorption, distribution, metabolism or excretion of the components of a complex mixture. The research conducted for this dissertation has coupled chemical fractionation with *in vitro* and *in vivo* bioassays to assess the potential carcinogenic risk of complex mixtures. A non-aqueous phase liquid from a wood treatment plant was separated into acid (AF), base (BF) and neutral fractions (NF). The NF was further enriched using column chromatography to produce a polychlorinated dinbenzo-*p*-dioxin (PCDD) and a polycyclic aromatic hydrocarbon (PAH) fraction. The genotoxicity of these mixtures were assessed via analytical quantification, *in vitro* (*Salmonella* microsome and *E. coli* prophage induction) and *in vivo* (^{32}P-postlabeling) bioassays. The NF was further tested to measure bulky DNA adducts and induction of tumor formation. The AF contained the highest level of pentachlorophenol and the highest concentration of total PAHs. Although the carcinogenic PAHs were highest in the PCDD fraction, the highest concentrations of benzo(a)pyrene (BAP), indeno(1,2,3-cd)pyrene and dibenz(a,h)anthracene were detected in the PAH fraction. A positive genotoxic response in *Salmonella* was induced by the crude extract, the PAH and BF, whereas the AF and BF induced a positive response in the *E. coli* assay. *In vivo,* the PAH fraction induced the highest DNA adduct frequencies in the lung. The NF, reconstituted mixture (RM) (which includes equivalent concentrations of seven carcinogenic PAHs in the NF), BAP and the NF amended with BAP (NF+BAP) were all tested in an infant mouse

model. At the highest dose, after a 24 hr exposure, NF+BAP had the highest total DNA adducts measured in liver which was three to seven times higher than with other treatments. Adduct levels were comparable to the control after 280 days. The highest incidence of tumors was observed in the liver. At the high dose, NF+BAP elicited the highest incidence of tumors. The results of this research confirm previous studies and indicate that the carcinogenic potential of PAH mixtures may be greater than predicted by chemical analysis.

DEDICATION

To my Mother, Father, two Sisters and Cat, for all of the love and support they gave me during my graduate studies.

ACKNOWLEDGMENTS

I would like to thank my committee chair, Dr. Donnelly, and my committee members, Dr. Safe, Dr. McDonald, and Dr. Autenrieth for their guidance and support during my graduate studies. A special thanks goes to Lorna Safe, who provided guidance and aid during the course of this research.

I would also like to thank my friends, collegues and the department faculty and staff at Texas A&M University. Their friendship and experience helped to make my time here one to remember. Specifically, I would like to thank the people who aided me in this research: Dr. Henry Hubener, Dr. Mindy Wiles, Dr. Leslie Cizmas, Dr. Ling-Yu He, Dr. Annika Gillespie, Nancy White, Molly Richardson, Rebecca Lingenfelter, Christine Naspinski and Ziad Naufal. I would like to thank Dr. Guo-Dong Zhou, whithout whom I would not have been able to postlabel. His encouragement, guidance and expertise were indispensable. I would like to thank Dr. Yaorong Qian and the Texas A&M University Geochemical and Environmental Research Group for their help with dioxin elution and analysis. I would like to thank Dr. Moorthy and his lab for the use of their equipment and their help during dissections. I would like to thank Dr. Lisa Cheng for her expertise as a pathologist, and her help in interpreting the histology part of this research. I would like to thank Dr. James Calvin and Mandy Hering with the Texas A&M Statistics Department, who helped with the statistics for this research. I am also grateful to the National Institute of Environmental Health Sciences' Superfund Basic Research Program Grant which funded this work. I am also extremely grateful to the National Intitute of Environmntal Health Sciences' Training Grant, which also supported this research.

Finally, I would like to thank my family for all of their encouragement, love and support throughout my graduate studies.

TABLE OF CONTENTS

CHAPTER Page

CHAPTER Page

LIST OF FIGURES

FIGURE Page

FIGURE Page

FIGURE Page

FIGURE Page

FIGURE Page

LIST OF TABLES

TABLE Page

TABLE Page

TABLE Page

LIST OF ABREVIATIONS

ABBREVIATION	TERMINOLOGY
TCDD	2,3,7,8-tetrachlorodibezno-*p*-dioxin
2NF	2-nitrofluorene
2AA	2-aminoanthracene
^{32}P	Radioactive phosphorus isotope
ADP	Adenosine diphosphate
AF	Acid fraction
ATP	Adenosine tri-phosphate
ATSDR	Agency for Toxic Substances and Disease Registry
BAP	Benzo[a]pyrene
BF	Base fraction
CERCLA	Comprehensive Environmental Response, Compensation, and Liability Act
CHX	Cyclohexane
COC	Contaminant of concern
CPM	Counts per minute
DCM	Dichloromethane
DNAPL	Dense non-aqueous phase liquid
GC/MS	Gas chromatography/mass spectroscopy
GERG	Geochemical and Environmental Research Group
HRS	Hazardous Ranking System
IRIS	Integrated Risk Information System
MEOH	Methanol
NAPL	Non-aqueous phase liquid
NCP	National Contingency Plan
NF	Neutral fraction
NPL	National Priorities List
PAH	Polycyclic aromatic hydrocarbon

ABBREVIATION	TERMINOLOGY
PCA	Polychlorinated aromatic
PCDD	Polychlorinated dibenzo-*p*-dioxin
PCDF	Polychlorinated dibenzofuran
PCP	Pentachlorophenol
PEI	Polyethyleneimine
PNK	Polynucleotide kinase
RAL	Relative adduct labeling
RfD	Reference dose
RM	Reconstituted mixture
ROD	Record of Decision
S9	Rat liver supernatant 9000
SARA	Superfund Amendments and Reauthorization Act
SSC	Sodium citrate + sodium chloride
TEF	Toxic equivalency factor
TLC	Thin layer chromatography
TOL	Toluene
USEPA	United States Environmental Protection Agency
VBMM	Vogel-Bonner minimal medium
WPW	Wood preserving waste

CHAPTER I
INTRODUCTION

1.1 Background

Complex mixtures are ubiquitous in the environment. Mixtures of organic and inorganic chemicals have been detected in food, air, water and soil. Exposure to chemical mixtures is common, and could lead to potentially harmful outcomes including cancer, respiratory and cardiovascular disease. Polycyclic aromatic hydrocarbons (PAHs) and polychlorinated aromatic compounds (PCAs) are among the most common environmental contaminants. These compounds cause DNA adducts and cancer in animal models. The research described in this dissertation represents a series of experiments designed to obtain information to better define potential risks associated with exposure to chemical mixtures. Studies were conducted using microbial cells in culture and animal models to assess the genotoxic potential of complex PAH mixtures. These included tests using the crude extract of a complex mixture, as well as fractionated components of the mixture and model compounds. Information will be provided in this introductory chapter to describe the history of toxicology, as well as provide background information on the metabolism and toxicity of mixtures of PAHs and PCAs.

1.1.1 History of Toxicology

Toxicology is the study of poisons. In a broader sense, toxicology encompasses studying the adverse effects that a chemical may have on living organisms. The study of toxicology can be dated back to pre-recorded history when poisons from plants and animals were used for a variety of purposes. The first attempt at classifying poisons was made by Greek physician Dioscorides. The initial categories described by Dioscorides were used for more than sixteen centuries. Later, Maimonides and Hippocrates conducted studies to improve information about bioavailability. Most toxicology efforts during this time period were intended for disposal of ones enemies. In Italy, Toffana, an

---

This dissertation follows the style of Environmental and Molecular Mutagenesis.

infamous figure in the early Renaissance period, sold arsenic-containing cosmetics as a form of assassination (Klaassen 2001; Langman and Kapur 2006; Monosson 2005; Schonwalder and Olden 2003).

The individual who had the most profound influence on the development of toxicology was Paracelsus. This early scientist is credited with the phrase: "The right dose differentiates a poison from a remedy." (Klaassen 2001; Langman and Kapur 2006; Schonwalder and Olden 2003). Paracelcus had many revolutionary views for the time in which he lived (Klaassen 2001; Mann 1993). These views can still be seen today in the structure of toxicology, as well as in pharmacology and therapeutics. Paracelcus believed that the "toxicon" (toxic agent) is of primary importance. He had four main views, which are still largely followed today, 1) experimentation is necessary in determining responses to chemicals, 2) therapeutic properties are not the same as toxic properties of chemicals, 3) dose does not always separate these properties, and 4) specificity of chemicals, along with the therapeutic and toxic effects, can be determined (Klaassen 2001). Paracelcus introduced mercury as a treatment for syphilis, one of the first forms of the dose-response relationship having been put to work (Klaassen 2001; Mann 1993).

During the 15th century, several investigators recognized the hazards of occupational exposures. Ellenbog and Paracelcus published works on toxicity of mercury and lead in goldsmithing and mining, respectively. In 1775, Sir Percival Pott recognized a connection between scrotal cancer in chimney sweeps and soot. This was the first report of toxicity associated with mixtures of polycyclic aromatic hydrocarbons. Paracelcus and Ramazzini, an occupational toxicologist, both expressed concern for the toxicity of soot, as well as smoke (Klaassen 2001; Monosson 2005).

As the 19th century approached, the science of toxicology advanced at a rapid rate. The advent of the industrial revolution was associated with the synthesis of more than 10,000 organic chemicals by the year 1880. The introduction of these chemicals into the workplace and the environment produced a need for tests that could be used to measure their toxicity. Orfila established the use of autopsy material and chemical analysis to

prove poisoning, laying a path for forensic toxicology. Magendie established adsorption and distribution studies; while, Bernard established mechanisms of action studies, specifically on carbon monoxide. Schmiedeberg focused on liver and its detoxification mechanisms. Lewin's work included chronic toxicity of narcotics, along with toxicity of chemicals such as methanol, glycerol, acrolein and chloroform (Breathnach 1987; Klaassen 2001; Koch-Weser and Schechter 1978; Langman and Kapur 2006; Monosson 2005; Morabia 2006; Shampo and Kyle 1987).

The tools available to measure the mechanistic effects of toxic chemicals have changed appreciably over time. Some of these changes may be attributed to significant events in the history of the world. For example, chemical warfare agents were first used in World War I (Roffey et al. 2002). The novel by Upton Sinclair, "The Jungle", described adverse work conditions that affected not only worker health, but also the quality of food in the United States (Schonwalder and Olden 2003; Sinclair 2003). Significant advances in toxicology occurred following World War II. This included the study of organophosphate insecticides, antimalarials, and radionuclides, as well as the beginning of inhalation toxicology (Borm 2002; Bullman and Kang 1994). In the early 1960's, Rachel Carson's "Silent Spring" described potential adverse effects to wildlife caused by exposure to organochlorine pesticides (Carson 1962; Schonwalder and Olden 2003). Around the same time Love Canal was discovered. Love canal was a canal that had been used as a toxic waste landfill by Hooker Chemical Corporation. The discovery of Love Canal raised awareness of the potential toxic effects from chemicals that are released into the environment (Brown and Clapp 2002).

In the last 50 years, the changes to toxicology have been even more dramatic. Prior to the late 1900's, infectious disease was a major cause of death. Since the discovery of antibiotics and immunizations, cancer and heart disease have become the major causes of death in most industrialized countries (CDC 2003a; Mann 1993). In the United States, approximately 1.3 million new cases of cancer were diagnosed in 2003 with about 1,500 deaths per day (CDC 2003b). For any individual, the risk of cancer is affected by genetic, lifestyle and environmental factors. The significance of each of

these factors is greatly dependent on the individual, where they live and work, and whether they smoke or have other lifestyle factors that may increase risk.

In order to improve methods for prevention and treatment of cancer, it is important to better understand the molecular mechanisms that precede the formation of a malignant cancer cell. Laboratory studies have demonstrated that the initial step in the transformation of a normal cell to a malignant cell is a point mutation. Chemicals that are capable of binding with DNA forming a bulky adduct may increase mutations in protooncogenes or tumor suppressor genes. In order to obtain information regarding the potential of chemical mixtures to induce cancer, toxicologists have developed a variety of methods to detect chemicals that are capable of modifying genetic material. Point mutation bioassays were developed in the late 1960's and early 1970's (Ames et al. 1975; Malling 1971). In 1981, Randerath et al. developed a protocol for labeling bulky DNA adducts using radioactive ATP. This ^{32}P-postlabeling method is widely recognized as one of the most sensitive methods for detecting genotoxic compounds in environmental media (Reddy 2000; Williams et al. 1996). Today, technologies such as the Polymerase Chain Reaction (PCR) and microarray allow toxicologists to measure single nucleotide polymorphisms and measure the impact of chemicals and chemical mixtures on gene expression (Majtan et al. 2004; Nakayama et al. 2006). These new technologies have provided toxicologists tools to look inside the mammalian genome to investigate mechanisms of complex mixture interactions, as well as the impact of genetic polymorphisms on sensitivities to chemical exposures.

1.1.2 History of Superfund

The United States Congress has passed legislation to establish institutes for the promotion of research into causes of cancer, as well as to reduce the release of carcinogenic chemicals into the environment from industrial operations. In 1930, the National Institute of Health (NIH) was established under the presidency of Herbert Hoover. Approximately thirty years later, the United States government established the National Center for Toxicologic Research (NCTR) and the National Institute of

Environmental Health Sciences (NIEHS). The need to regulate the release of toxic chemicals to air, water and soil resulted in the establishment of the United States Environmental Protection Agency (USEPA) in 1970. Concern over hazardous wastes, chemical dumps, and accurate reporting of hazardous chemical inventories grew with the discovery of Love Canal in the 1970s. The recognition of the existence of a large number of uncontrolled hazardous waste sites by the USEPA led to the Toxic Substances Control Act (1976) and in 1980 to the Superfund bill (1980). The goal of this legislation was described as cradle to grave. In principle, this meant that all hazardous chemicals would be carefully tracked from synthesis to final disposal (USEPA 2005b, USEPA 2005c).

The Resource Conservation and Recovery Act (RCRA) was passed due to concern over the impact from releasing hazardous chemicals into environmental media (USC 1976). The RCRA set standards for all facilities that treat, store or generate hazardous waste. To deal with those sites which appeared to represent a more immediate threat to health and the environment, Congress passed the Comprehensive Environmental Response, Compensation and Liability Act (CERCLA) (USC 1980). This act included provisions for the Superfund program. The Superfund program included a tax on hazardous chemicals that would provide funds to assess and reclaim those sites which required remediation. The program also established a methodology for estimating the non-cancer and cancer risk associated with contaminated environmental media. The Risk Assessment Guidelines for Superfund (USEPA 1986) defined a four step process for ranking uncontrolled hazardous waste sites. These steps include hazard identification, toxicity assessment, exposure assessment and risk characterization. The process allowed regulators to produce an estimate of the non-cancer or lifetime cancer risk associated with exposure to contaminated media at a specific site. This information could then be utilized to rank sites and identify those which required more immediate action.

CERCLA also provided Federal authority to respond directly to threatened or actual releases of hazardous substances which may endanger public health or the

environment. The three major legislative initiatives that CERCLA provided for include; 1) establish prohibitions and requirements concerning closed and abandoned hazardous waste sites, 2) provide for liability of persons responsible for releases of hazardous waste, and 3) establish a trust fund to provide for cleanup when no responsible party could be identified. CERCLA also enabled the National Contingency Plan (NCP) to be revised. The NCP is the legislation that provides the guidelines and procedures needed to respond to threatened and actual releases of hazardous substances, pollutants, or contaminants. On October 17, 1986, CERCLA was amended by the Superfund Amendments and Reauthorization Act (SARA). Several important changes and additions were made to the program. SARA reflected the EPA's experience in administering CERCLA during its first six years. SARA's revisions included: 1) stressing the importance of permanent remedies and innovative treatment technologies, 2) requiring Superfund actions to consider the standards and requirements found in other State and Federal environmental laws and regulations, 3) providing new enforcement authorities and settlement tools, 4) increasing State involvement in every phase of CERCLA, 5) increasing the focus on human health problems, 6) encouraging greater citizen participation in making decisions regarding sites, and 7) increasing the size of the trust fund for site assessment and remediation to $8.5 billion. SARA also stipulated that the EPA update the Hazardous Ranking System (HRS) for accuracy (USEPA 2005a; USEPA 2005b; USEPA 2005c; USEPA 2005d; USEPA 2006e). The HRS is used to prioritize those sites where contaminants represent a threat to human or ecological health. There are currently 1,609 sites on the EPA's National Priorities List, although it is estimated that by the year 2033 more than 294,000 sites will be identified (USEPA 2006e).

A major concern at many of these sites is the potential for human exposure to complex chemical mixtures. Two of the most common classes of contaminants detected in environmental media are mixtures of PAHs and chlorinated aromatic hydrocarbons (Mueller et al. 1991; Ramesh et al. 2004; Samanta et al. 2002). PAHs have been detected at 47 % of the 1609 Superfund sites in the United States (USEPA 2006e).

PAH mixtures may be present at wood preserving sites, refineries and petroleum production facilities, coal gasification sites, and other sites where petroleum products were stored or disposed of. In addition, PAH mixtures are common combustion by-products. Thus, sources of human exposure to PAH mixtures includes not only the release of hazardous chemicals, but also ingestion of cooked foods and inhalation of cigarette smoke or other combustion by-products.

1.1.3 Environmental Mixtures

Complex chemical mixtures are ubiquitous in the environment. Sources of complex mixtures include cooked foods, combustion by-products, and releases associated with hazardous waste facilities. The release of hazardous chemicals from industrial facilities is a concern because these chemicals may add to the burden of chemicals to which a population is normally exposed. Sir Percivall Pott (1775) observed that young men employed as chimney sweeps had an excess frequency of scrotal cancer. It is likely that the accumulation of complex mixtures of polycyclic hydrocarbons from the soot in the chimneys was a significant factor affecting the incidence of cancer in these young men. PAH mixtures are common contaminants of petroleum and petrochemical facilities, wood preserving facilities, and any industry utilizing combustion sources. Hydrocarbon mixtures are also common at Department of Defense and Department of Energy facilities. The release of hydrocarbon mixtures to the environment may result in contamination of air, surface water, soil, sediment and/or groundwater. PAH mixtures are generally persistent in the environment. PAHs are relatively insoluble in water, and thus concentrate in soil and sediment near the hazardous waste facilities that released them into the environment. PAH mixtures may also represent a threat to human and/or ecological health when they are concentrated in the food chain.

1.2 Human Health

1.2.1 Exposure to Environmental Mixtures

Humans are constantly exposed to complex environmental mixtures in air, food and water. Populations living near hazardous waste facilities may be exposed to higher concentrations of chemicals. Brender et al. (2006) reported higher rates of cancer in populations living within one mile of a Superfund site. The EPA has established a procedure that can be used to estimate the risk associated with exposure to contaminated media at a Superfund site. The National Academy of Science recommends four steps in the risk assessment process (Figure 1.1). The initial step in this process is to identify the hazard at a specific site. Hazard Identification is designed to develop a qualitative assessment of risk. The existing data for a specific site is collected and reviewed. Concentrations of each contaminant at a site are compared to Risk Based Concentrations (USEPA 2006a) to determine which chemicals represent the greatest health threat. Hazard identification is typically used to develop a list of Contaminants of Concern, or the 10-15 chemicals which appear to represent the greatest threat to environmental health. (USEPA 2006a)

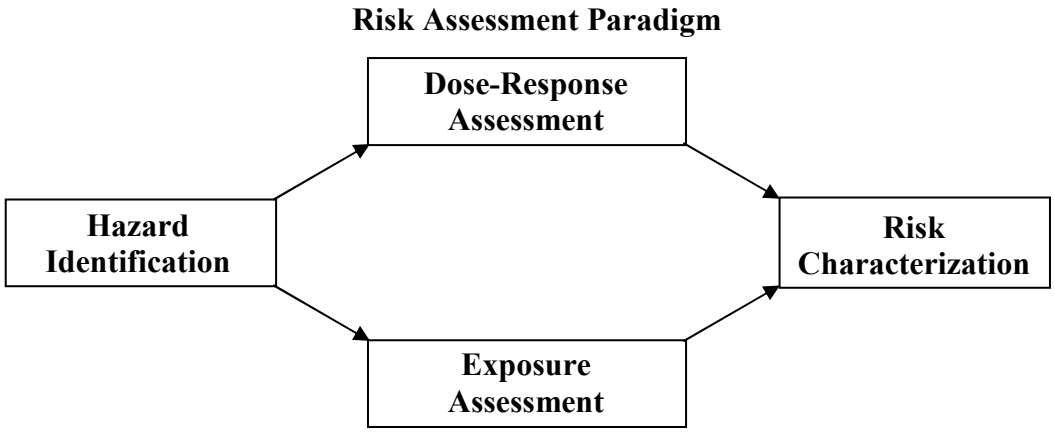

Figure 1.1. Diagram of the four elements of the NAS risk assessment as used by USEPA's IRIS database. A similar paradigm can be found in the USEPA's *Risk Assessment Guidelines for Superfund* (RAGS) *Part A* where hazard identification would be called data collection:data evaluation and dose-response assessment would be called toxicity assessment (USEPA 1986; USEPA 1989).

The second step in the risk assessment is the toxicity or dose-response assessment. In most cases, the EPA's Integrated Risk Information System (IRIS) is used to identify a Reference Dose (RfD) for non-cancer effects, and/or a Cancer Slope Factor (CSF) for cancer effects. Although toxicity values have been established for a large number of chemicals, there is a great deal of uncertainty in many of these values. Sources of uncertainty include species extrapolation, and extrapolation from large doses used in toxicity studies to the relatively small doses that generally occur in environmental exposures. More importantly, there is no widely accepted protocol for interpreting the interactions of chemical mixtures. Most risk assessments assume additive effects. Data are not available at the present time to accurately assess the potential interactions of complex mixture carcinogens and non-carcinogens. (USEPA 1986)

The USEPA has developed five categories to describe the carcinogenic potential of a specific chemical. These include: 1) Class A—evidence of carcinogenicity in humans, 2) Class B—probable human carcinogen (limited evidence in humans and adequate evidence in animals), 3) Class C—possible human carcinogen (adequate evidence in animals), 4) Class D—not classifiable for human carcinogenicity, and 5) Class E—evidence for non-carcinogenicity in humans. The cancer slope factor is used by the USEPA to rank the carcinogenic potency of various chemicals. For example, methylene chloride is considered a weak carcinogen (Class B2) and has an oral cancer slope factor of 7.5×10^{-3} (mg/kg)/day, while vinyl chloride is considered a potent human carcinogen (Class A) and has an oral cancer slope factor of 7.2×10^{-1} (USEPA 1995, USEPA 2000a). The model carcinogenic PAH benzo(a)pyrene (BAP), is considered a Class B carcinogen and has an oral cancer slope factor of 1.2×10^{-1} (mg/kg)/day (USEPA 1994b). Mixture interactions may affect risk by affecting the uptake, distribution, metabolism or elimination of other chemicals. Thus, low molecular weight PAHs that are capable of inducting Phase I liver enzymes may enhance the toxicity of high molecular weight PAHs. Alternatively, studies by Falahatpisheh et al. (2004) observed

that chrysene could inhibit the toxicity of BAP through competition for metabolizing enzymes.

The third step in the risk assessment process is the exposure assessment. All completed exposure pathways at a site for both on-site workers and off-site residents must be determined. This includes exposure to soil, air, groundwater, surface water, sediment, or food products that may have become contaminated due to chemicals released from the site. For each completed exposure pathway, the concentration of each contaminant of concern in a specific media is estimated. This estimate may use a mean value, an upper 90^{th} percentile value or a maximum value depending on the quantity and quality of existing data. These values are used to estimate a Cumulative Daily Intake for each exposure pathway and each contaminant of concern. Major sources of uncertainty in the exposure assessment include assumptions regarding intake variables for contaminated media, estimate of chemical concentrations in the media, and rates of absorption from various exposure pathways. (USEPA 2006b)

The final stage in the risk assessment is the characterization of both the non-cancer and cancer risk. The non-cancer risk is a sum of the Hazard Quotient, or a value obtained by dividing the Cumulative Daily Intake by the Reference Dose. Contaminate concentrations are considered acceptable as long as the estimated daily intake is not greater than an estimate of a No Observable Adverse Effect Level (or the Reference Dose). Hazard Quotients for each chemical and each exposure pathway are summed. The Lifetime Cancer Risk is calculated as a product of the Cancer Slope Factor and the cumulative Daily Intake. Residential sites are considered acceptable as long as the sum of Lifetime Cancer Risk for all chemicals and all exposure pathways does not exceed one in one million. These risk calculations provide a means of ranking sites and assessing acceptable levels for clean-up. However, as stated previously, significant sources of uncertainty exist in each step of the risk assessment process. One of the major sources of uncertainty is knowledge of the potential interactions of complex chemical mixtures (USEPA 1986; USEPA 2000b). The research conducted as part of

this dissertation has investigated the ability of model compounds and complex mixtures for form DNA adducts and tumors in mouse models.

1.2.2 Chemical Carcinogenesis

Cancer is a multi-stage process that may involve multiple chemical exposures over many years. Most animal or occupational studies that have been used to identify chemicals that are capable of causing cancer have involved high dose exposures over a relatively short time period. Thus, limited information exists to accurately characterize the risk associated with long-term, low dose exposure to chemical mixtures. Occupational studies have clearly shown that exposure to PAH mixtures in coke oven emissions is capable of causing lung, upper respiratory and alimentary tract cancers (Bertrand et al. 1987; Heinrich et al. 1986; Lloyd 1971; Mazumdar et al. 1975; Redmond et al. 1976; Rockette and Redmond 1976). In order to understand the risk of an environmental mixture, it is important to have information regarding the mechanism through which the mixture induces carcinogenesis. Farber and Sarma (1987) developed a model for tumor formation in the liver. These steps were largely determined through the use of the resistant hepatocyte model created in 1976 by Solt and Farber (Figure 1.2). This model was used to establish that three major steps follow exposure to a chemical carcinogen prior to the development of a malignant tumor. The chemical must first be adsorbed and distributed into systemic circulation. Once in circulation, the chemical may be transformed through metabolizing enzymes into its ultimate carcinogenic form. The first major step is initiation. Initiation occurs when a carcinogen binds with DNA resulting in a mutation. This mutation leads to the formation of abnormal, initiated cells. The growth of these initiated cells is promoted through further mutations, to tumor suppressor genes or oncogenes that alter normal cellular growth. Promoted cells for small foci have a variety of altered biochemical characteristics. Continued exposure may cause these foci to progress into neoplastic cells. The nodules formed by these cells may be visible, but may also be small enough to grow unnoticed with minimal effect on the host. If these neoplastic cells become malignant, they have the capability to outgrow

the normal architecture of the tissue in which they reside, and may break off from a primary tumor and migrate to another location in the host forming a secondary tumor (Solt and Farber 1976).

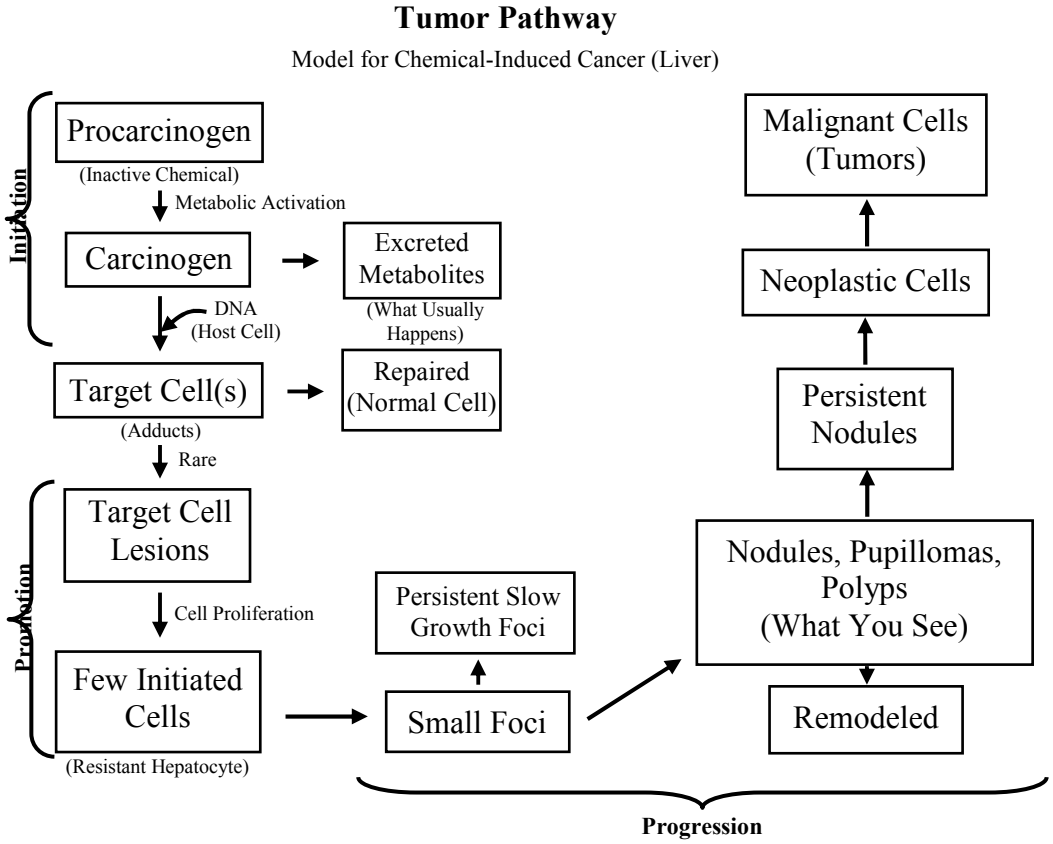

Figure 1.2. Diagram of the tumor pathway model for chemical-induced liver cancer. Adapted from Farber and Sarma (1987).

1.2.3 Models for Human Carcinogenesis

The International Agency for Research on Cancer (IARC), part of the World Health Organization (WHO), has identified approximately 400 chemicals as human carcinogens (potential and definite) (IARC 2004). A human carcinogen is any chemical that has the ability to transform a normal cell into a malignant cancer cell. Carcinogens may be classified as genotoxic or epigenetic. Epigenetic carcinogens induce cancer by

mechanisms that do not involve binding to DNA (e.g. tissue injury, hormonal imbalance, immunologic effects, or promotional activity on cells that have been altered by genotoxic carcinogens). Genotoxic carcinogens covalently bind to DNA. Most genotoxic carcinogens are procarcinogens. That is, they require conversion into an electophilic metabolite prior to binding with DNA. A complex environmental mixture is likely to contain both genotoxic and epigenetic carcinogens. In addition, given the multiple interactions that occur in a biological system, chemicals may exhibit both genotoxic and epigenetic effects (Weisburger and Williams 1988).

Occupational exposures to PAHs can occur among different manufacturing processes including: petroleum processing (all operations from drilling to refining), metalworking, coke production, anode manufacturing, aluminum production, and through the use of specific complex mixtures during the manufacturing processes such as coal tar, pitch, asphalt, creosote, soot and anthracene oil. The main occupational route of exposure depends on the specific manufacturing process. For workers in petroleum refinement and coal mining, the main route of exposure is generally inhalation, with a significant risk from dermal absorption as well (ATSDR 1995; Borm 2002; USEPA 2006c). For coke oven workers and metalworkers, the main route of exposure is dermal absorption. Lung and scrotal cancer has been observed in metal workers who use refined mineral oils in their machining operations (Jarvholm et al. 1981). PAHs are highly lipophilic compounds which may be difficult to detect in human tissues. One way of assessing exposure to PAHs is to use biomarkers. 1-Hydroxypyrene can be analytically monitored in urine. Although this biomarker of exposure can confirm that a person has been exposed to PAHs, it does not provide a quantitative measure of the potential for an adverse health effect. It is important to take into account individual PAH exposures outside of the occupational situation when calculating exposure. Other biomarkers of exposure for PAHs include 1-nitropyrene and BAP, determining PAH-DNA adducts in urine, blood and other tissues as well as cellular macromolecules (hemoglobin, globin, large serum proteins) (ATSDR 1995).

Although humans are constantly exposed to PAHs and PCAs, the variability of these exposures and the variability of the human population make it difficult to study cancer incidence (Barrett 1995; DHHS 2004). In addition, the latency from exposure to tumor development in humans may be more than 20 years. Animal models, because of their uniform genetics and uniform dosing, are a valuable tool for measuring the genotoxic interactions of chemical mixtures (Barrett 1993; DHHS 2004). When animal data can be combined with epidemiological data, a more accurate prediction can be made about the compound(s) in question (Wogen et al. 2004; Miller and Miller 1971; DHHS 2004).

Epidemiological studies are the most relevant studies to human carcinogenicity, especially occupational exposure studies (Krewski and Thomas 1992; DHHS 2004). However, these studies are often wrought with difficulties, and variances must be accounted for when looking at this data. Within epidemiological studies, there are interspecies differences (age, sex, rate of metabolic processes, etc.) that must be considered. In addition, exposure in human populations is often highly variable. Once a tumor has formed, the cells have lost their ability for normal cell function (Wogan et al. 2004). Biomarkers, such as metabolites (often PAHs for creosote exposure) and DNA adduct formation, may be monitored in exposed populations to determine exposure and response relationships as accurately as is possible (DHHS 2004; Grimmer et al. 1997; Malkin et al. 1996; Melber et al. 2004). Epidemiological studies have shown that exposure to creosote can cause skin cancer, along with other symptoms (depending on source and duration of exposure) (ATSDR 2002; Melber et al. 2004).

Human exposure to PAHs and PCBs is common. However, due to the genetic variability of the human population and the wide ranges in dose and durations of exposure to these compounds, it is difficult to characterize the carcinogenic potential of these compounds in humans (Barrett 1995; DHHS 2004). The latency of most solid tumors, often as long as 20 years, can make it difficult to link a previous chemical exposure to a specific cancer. Animal models, because of their uniform genetics and the ability to administer consistent dosages, are a valuable tool for studying the genotoxic

interactions of chemical mixture (Barrett 1995; DHHS 2004). The most accurate information from which to access the ability of a chemical or chemical mixture to induce cancer is a combination of *in vitro*, *in vivo* and epidemiologic studies (DHHS 2004; Miller and Miller 1971; Wogen et al. 2004).

Occupational studies, due to the potential for high and frequent exposure, are often some of the most relevant data from which to judge the ability of a chemical or chemical mixture to induce cancer (DHHS 2004; Krewski and Thomas 1992). However, it is rare for accurate information regarding cumulative exposures to be available for an occupational study. In addition, humans may display significant differences in susceptibility to chemical carcinogenesis due to the effect of age and size on metabolic processes, as well as genetic differences that may influence not only metabolism, but also tumor suppressor genes, oncogenes, and other factors. A neoplastic lesion has a variety of morphological and biochemical properties which differentiate the cell from a normal cell (Wogan et al. 2004). Biomarkers of abnormal cells can be identified as changes in enzyme levels and the cell cycle. Levels of oncogenes and proto-oncogenes present in a cell, as well as p53 can help determine if a cell has become abnormal or not. Oncogenes, which may control cell growth, once mutated can allow for abnormal division and replication of the cell. Proto-oncogenes are genes that encode proteins which stimulate cell growth. Some proteins from proto-oncogenes are growth factors, intracellular signal transducers (G proteins), protein kinases, cyclins, and nuclear transcription factors. Over expression of these proteins may also have an effect on the growth of abnormal cells. One of the most studied is the p53 tumor suppressor gene. This transcription factor helps to induce apoptosis in response to cell damage or stress (Klaassen 2001; Ress et al. 2002). Abnormal cell growth is one piece of a complicated process which may end in tumor formation.

This research was designed to add to current knowledge regarding the genotoxic potential of complex chemical mixtures. Microbial genotoxicity studies will be used to identify fractions from mixtures that are capable of causing mutations in DNA. Data will also be obtained from animal studies to improve information regarding the

relationship between the initiation of the carcinogenic process through the formation of DNA adducts, and the ultimate formation of neoplastic lesions including benign and malignant tumors.

1.3 Contaminants of Concern

1.3.1 Complex Chemical Mixtures

Feron et al. (1995) defined a complex mixture as a substance that contains from ten to more than one thousand chemical components. For the majority of environmental mixtures, the composition is not qualitatively or quantitatively known (Groten et al. 2001). The properties, both chemical and toxicological, of the components of a mixture may be altered by component interactions. Chemical mixtures are common in air, food and water. Specific examples of complex mixtures that may contain PAHs include cigarette smoke, diesel exhaust, cooked foods, and coal tar creosote (Fay and Feron 1996). Due to the widespread use of petroleum products in the United States, complex mixtures of PAHs are frequently detected in a broad range of environmental media (Johnson and DeRosa 1995). The toxicity and genotoxicity of complex mixtures is often difficult to assess because they may contain low concentrations of the most potent compounds (e.g. benzo(a)pyrene or tetrachlorodibenzo-*p*-dioxin), and relatively high concentrations of chemicals with a less significant toxic effect. However, it is important to develop methods that can be used to characterize the toxicity of various components of a mixture, as well as the potential interactions of these compounds (Fay and Feron 1996).

Complex mixtures are difficult to characterize due matrix interferences and the close structural similarity of many of the components. Each compound within a complex mixture may have different physical and chemical properties. For example, creosote as a whole is not considered to be water soluble; however, specific compounds within the mixture are highly water soluble while others are much less soluble. Specific physical and chemical properties of individual compounds can be found in ATSDRs ToxProfiles (ATSDR 1995; ATSDR 2001; ATSDR 2002). Exposure assessments

generally do not take into account interactions among the multiple chemicals in complex mixtures (Groten et al. 2001). An important component of complex mixture research is to study the mixtures as a whole, and to break them down into fractions for study (Fay and Feron 1996; Johnson and DeRosa 1995). The mixture as a whole presents a problem as each chemical's toxicity role may be quite different than depending on the dose. As difficult as testing the whole mixture is, testing individual compounds is practically unobtainable. The entire composition of the whole mixture is not known, and the possible interactions of individual compounds are almost endless. Thus, fractionation of the whole mixture is an appropriate method for determining genotoxic or mutagenic chemical compounds or groups of compounds (Fay and Feron 1996). The concept of fractionating chemical mixtures to better understand toxicity is characterized by Fay and Feron (1996) as being "better to have a shattered image of reality than a combined image of unreality". Other methods that have been recommended for testing complex mixtures include identification of the top ten chemicals, and the formation of composite standards (Fay and Feron 1996).

Human exposures are generally to environmental complex mixtures, and not to single compounds or even simple mixtures (Gennings 1995; Teuschler and Hertzberg 1995). These are usually low dose exposures, through various exposure pathways. Limited data exist to characterize the toxicity of complex mixtures. However, the USEPA has published *Guidelines for the Health Risk Assessment of Chemical Mixtures* (Teuschler and Hertzberg 1995; USEPA 1986). Guidelines for conducting a risk assessment for a chemical mixture are shown in Figure 1.3. Three approaches have been recommended for chemical mixtures, including a Surrogate Approach, a Comparative Potency Approach, and a Relative Potency Approach (Teuschler and Hertzberg 1995). The Surrogate Approach assumes that there is data from occupational or animal studies for a similar, or surrogate, mixture. This data can then be used to extrapolate a toxicity value for the mixture of concern. The Comparative Potency Approach assumes that the mixture may be compared to another mixture for which extensive toxicity data are available. Thus, the potency of the mixture of concern is adjusted based on a

comparison with a better characterized mixture. The Relative Potency Approach is the most widely used approach. This approach assumes primarily additive interactions and sums the toxicity of a mixture based on the chemical analysis of components. Ideally, risk assessment should be done based on chemical mixture specific information, or on classes of compounds found within a particular mixture (Teuschler and Hertzberg 1995; USEPA 1986).

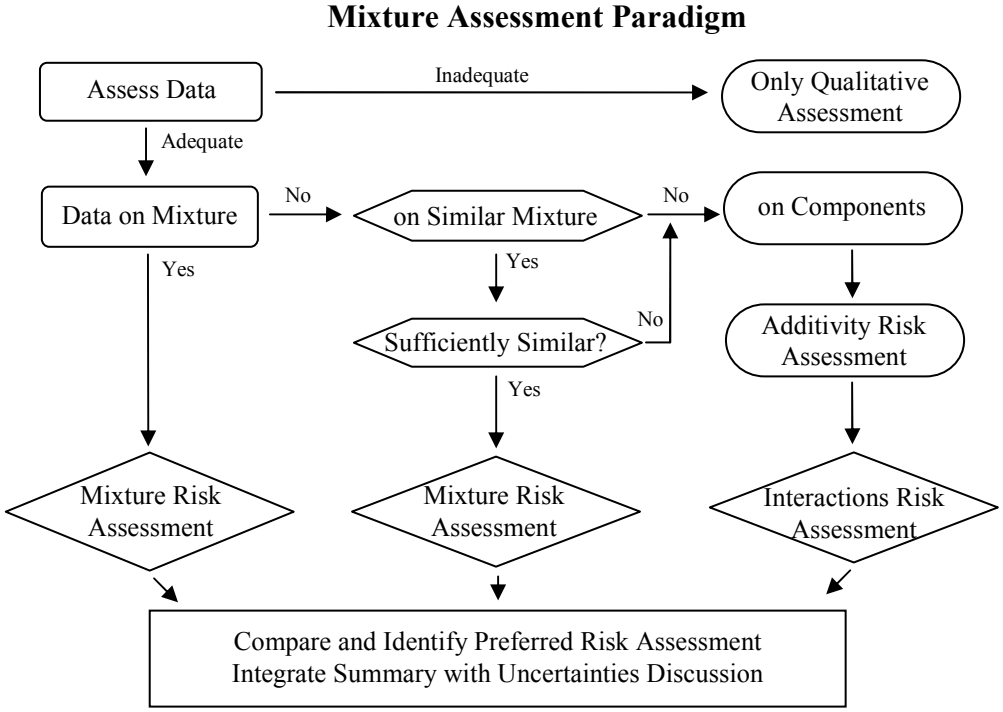

Figure 1.3. Diagram of mixture assessment paradigm found in USEPA's *Guidelines for the Health Risk Assessment of Chemical Mixtures.* Adapted from Teuschler et al.. 1995 and USEPA 1986.

The complex mixture that was characterized as a portion of this dissertation is creosote. Creosote is a coal tar distillate that rarely occurs naturally in the environment. There are six main classes of chemicals in creosote; 1) aromatic hydrocarbons, 2) tar acids/phenols, 3) tar bases/nitrogen-containing heterocycles, 4) aromatic amines, 5) sulfur-containing heterocycles, and 6) oxygen-containing heterocycles (ATSDR 2002; Melber et al. 2004). Approximately 400 compounds have been identified in creosote, with approximately 10,000 total compounds making up the mixture (ATSDR 2002; Culp et al. 1998). The components of creosote can be found in multiple matrices (air, water, sediment, soil, and biota), due to the vast differences in properties of the compounds within. Creosote is a particularly difficult complex mixture to characterize as its constituents are influenced by the origin of the coal used and the nature of the distilling process. Polycyclic aromatic hydrocarbons constitute approximately 85-90% of creosote, while other constituents are generally less than 1% (Melber et al. 2004; Mueller et al. 1989). Creosote has been used for many purposes, including, wood preservation, water-proofing agent for structures (land and water), railway crossing timbers, railroad ties, decking (bridge and pier), poles, log homes, fencing, equipment for children's play grounds, anti-fouling applications for marine pilings, insecticide, animal dip, fungicide, and components in roofing pitch, and fuel oil. Major environmental sinks for creosote compounds are sediment, soil and groundwater, making creosote an important complex mixture to characterize and understand (Melber et al. 2004).

1.3.2 Polycyclic Aromatic Hydrocarbon Compounds

PAHs are ubiquitous environmental contaminants. These chemicals may be found in cooked foods, absorbed to air particulate, as well as in soil, and sediment. PAHs may be released from both natural and anthropogenic sources. High concentrations of PAHs are present in crude oil, coal and oil shale. These petroleum and petrochemical products are used to produce extensively used fuels and synthetics (fibers and plastics) (Harvey 1997). The widespread use of petroleum products has resulted in increased levels of

these compounds in the environment. PAHs may also be released into the environment from volcanic eruptions, forest fires, burning of coal, burning of wood, expulsion fumes from manufacturing industries, and smoking. Due to the ubiquitous sources of PAHs in the environment, exposure to these compounds is common (ATSDR 1995; Ramesh et al. 2004; Samanta et al. 2002).

The majority of atmospheric contamination with PAHs can be attributed to industrial activities (50% of BAP emissions in the United States) and vehicle emissions (35% of PAH air contamination in the United States). Natural sources account for much of the remaining atmospheric contamination with PAHs (Harvey 1997). The composition and concentration of PAHs resulting from combustion of fuels depends on the conditions in which they were generated. High temperatures in the absence of oxygen produce simple unsubstituted PAHs, while at lower temperatures, larger and more alkyl substituted PAHs will be produced. Conditions in the atmosphere also determine the extent of PAH deposition. For example, a rise in PAH emissions is generally seen in colder months, presumably because more fossil fuels are consumed in these months. Atmospheric conditions, such as temperature inversions, may also increase PAH concentrations near ground level. Density, temperature and emission sources are also factors in PAH distribution. PAHs transition from the gas phase into the solid phase (fly ash) when temperatures are below 150°C. Accordingly, most PAH atmospheric contamination is seen as particulate matter, and can be respirable if less than 5 μm (Harvey 1997).

Soil contamination with PAHs is fairly significant, with the most significant contamination generally occurring near industrialized areas, or areas with high traffic volumes (Harvey 1997; Ciganek et al. 2004; Marr et al. 2004; Johnsen et al. 2006). The National Institutes of Health published a paper on traffic PAH exposure in Mexico City in 2004 (Marr et al. 2004). This study clearly shows high levels of PAHs concentrated in areas where vehicles operate. Ciganek et al. (2004) collected samples at high and low traffic areas in the Czech Republic. They found BAP concentrations of 0.64 $ng \cdot m^{-3}$ in the high traffic area and 0.38 $ng \cdot m^{-3}$ in the low traffic area, with total PAH

concentrations of 46.2 $ng \cdot m^{-3}$ and 20.7 $ng \cdot m^{-3}$, respectively. Another study done by Johnsen et al. in 2006 not only clearly showed high levels of PAHs at a motorway site, they also showed steady contamination of the soil near the asphalt. They suggest that this steady influx of PAH exposure will most likely accumulate and add to human exposure. PAH contamination of surface water is also common. There are many diverse sources for water contamination, with the major source being deposition of particulates from the atmosphere. Other sources of PAHs in surface water include direct pollution from household use, discharge of used crankcase oil, and effluents from industrial uses. PAH contamination of surface water may result in distribution of these compounds into the food chain. Because PAHs are lipophilic, PAHs in the food chain are likely to bioaccumulate (Harvey 1997).

Direct contamination of food with PAHs has also been observed. PAHs have been detected in leafy plants, at low levels in seafood, and in cooked meats. Studies done by Kulhanek et al. (2005) and Jakszyn et al. (2004) report levels of PAHs found in leafy vegeTables. The Kulhanek study reportes bioconcentration factors in leafy vegeTables from the Czech Republic. The factor for BAP was 4.92×10^{-6} without attached soil and 0.01 with soil. The Jakszyn study put together a database on foods and concentrations of chemicals found in them. They report the following values for leafy greens: collar greens (raw) 0.48 μg/kg BAP; mixed greens 0.14 μg/kg BAP; lettuce 0.007 μg/kg BAP and 2.61 μg/kg total PAHs (tPAHs); and spinach 0.10 μg/kg BAP. Meats that have been fried or charcoal broiled are especially high in PAH content (Harvey 1997). The Jakszyn database reports these values for meat and fish: bacon (pork) 0.35 μg/kg BAP and 6.80 μg/kg tPAHs; beef (cooked) 0.40 μg/kg BAP and 9.70 μg/kg tPAHs; chicken (barbecued) 4.60 μg/kg BAP and 60.20 μg/kg tPAHs; ham (cooked) nd BAP and 2.60 μg/kg tPAHs; codfish (cooked) 0.026 μg/kg BAP and 0.58 μg/kg tPAHs; herring 400/dry weight (dw) μg/kg BAP and 1300 μg/kg tPAHs; salmon (raw) 3.90 μg/kg BAP and 86.6 μg/kg tPAHs; shrimp (raw) nd BAP and 9.30 μg/kg tPAHs; and tuna (raw) 0.015 μg/kg BAP. Visciano et al. (2006) also reported PAH levels in salmon, fresh and smoked. They found that the mean concentration of BAP in raw salmon was 3.67 ± 3.99

ng/g dw and 3.20 ± 2.05 ng/g dw in smoked salmon. Overall, eleven PAHs were quantified, with a total of 231.77 ± 46.56 ng/g dw in raw salmon and 226.27 ± 38.12 ng/g dw in smoked salmon. PAHs have also been detected in meteorites, and interstellar clouds (Harvey 1997).

PAHs were first linked to human cancer by Sir Percival Pott in 1775, who observed an elevated incidence of scrotal cancer in chimney sweeps exposed to soot. Later, Cook et al. (1933) isolated a single PAH, 1:2-benzpyrene which is now called benzo(a)pyrene, from a coal tar pitch and observed its capabilities for tumor production in rodents. This study involved isolation of BAP from the complex mixture using a distillation extraction process. Briefly, alcohol extract of pitch distillate (coal tar) was distilled and dissolved in benzene. The liquid phase of benzene was shaken with 5% sulfuric acid. The benzene was distilled off, and the residue dissolved in acetic acid. Picric acid was added, and then crystallized 4 to 5 times from benzene. The liquid phase was shaken with sodium carbonate and distilled at 3 mm. The distillate was then re-crystallized three times with benzene and alcohol. 1:2-benzpyrene then crystallized and was collected. This fraction was found to be strongly carcinogenic in mice, causing skin cancer (methods not described). After these early studies, BAP became one of the most studied PAHs, and still is extensively studied (Miller 1978). Exposure to PAH mixtures can occur through ingestion, inhalation and dermal absorption. A review by Ramesh et al. (2004) indicates that PAHs have been found to induce cancer, hematotoxicity, cardiotoxicity, renal toxicity, neurotoxicity, immunotoxicity, reproductive toxicity, and developmental toxicity in animals and humans.

PAHs have been categorized into two groups, peri-condensed PAHs and cata-condensed PAHs. Peri-condensed PAHs form a cycle as their lines connect the ring centers. Within peri-condensed there are two subgroups, alternate and non-alternate. Alternate peri-condensed PAHs are formed of six-membered rings. Non-alternate peri-condensed PAHs are formed of five- and six-membered rings. Cata-condensed PAHs do not form cycles, these can be classified as branched or non-branched. PAH structure plays a very important role in the biological activity of the compound.

Depending on structure, PAHs may have varying regions; the K region, the L region, the bay region, the distal bay region, and the peri position. These regions are important structural characteristics in determining biological activity. The most biologically active of the regions in the model carcinogen BAP is the bay region. The bay region is an open inner corner of a phenanthrene moiety. When a PAH is metabolized by mammalian enzymes, it can be excreted from the body, or it can be activated and bound to nucleic acids in DNA. The reaction of the 7,8,9,10 benzo(a)pyrene-diolepoxide with the N-2 of guanine results in the formation of a DNA adduct.

In general, PAHs are lipophilic compounds which readily penetrate cellular membranes. In the absence of metabolic transformations, the majority of an absorbed dose of PAHs would remain in the body. The process of Phase I oxidative metabolism of PAHs modifies the structure of the parent compound resulting in a metabolite that is usually more water-soluble, and thus more readily excreted from the body. There are multiple pathways for metabolic conversion of PAHs (Figure 1.4). The Phase I and Phase II enzymes for metabolism of PAHs are common in mammalian systems. Generally, the highest level of metabolizing enzymes is in the liver, followed by the kidney and lungs. The rate and extent of PAH metabolism also depends on structure of the specific compound. For instance, alternate PAHs are processed differently than non-alternate PAHs. Because PAHs consist of multiple fused benzene rings, there structures are similar. This similarity explains why they, as a group, undergo similar biotransformations. BAP, the most extensively studied compound among PAHs, is used as a model compound for the metabolism of PAHs (Figure 1.5). BAP undergoes metabolism by the cytochrome P-450 enzymes. Uno et al. (2001; 2004) have shown that CYP1A1 is essential for not only PAH-mediated toxicity, but it is also essential for detoxification of oral BAP. In 2001 Uno et al. showed that when CYP1A1 is not present (*Cyp1a1*(-/-) knockout mice), mice were protected against liver toxicity and death. They

concluded that this was due to the decrease in production of the normally large amounts of toxic metabolites. However, in 2004 Uno et al. showed that CYP1A1 was necessary for the detoxification of orally dosed BAP. Higher levels of DNA adducts were detected in the *Cyp1a1*(-/-) mice as compared to the levels seen in *Cyp1a1*(+/+) mice.

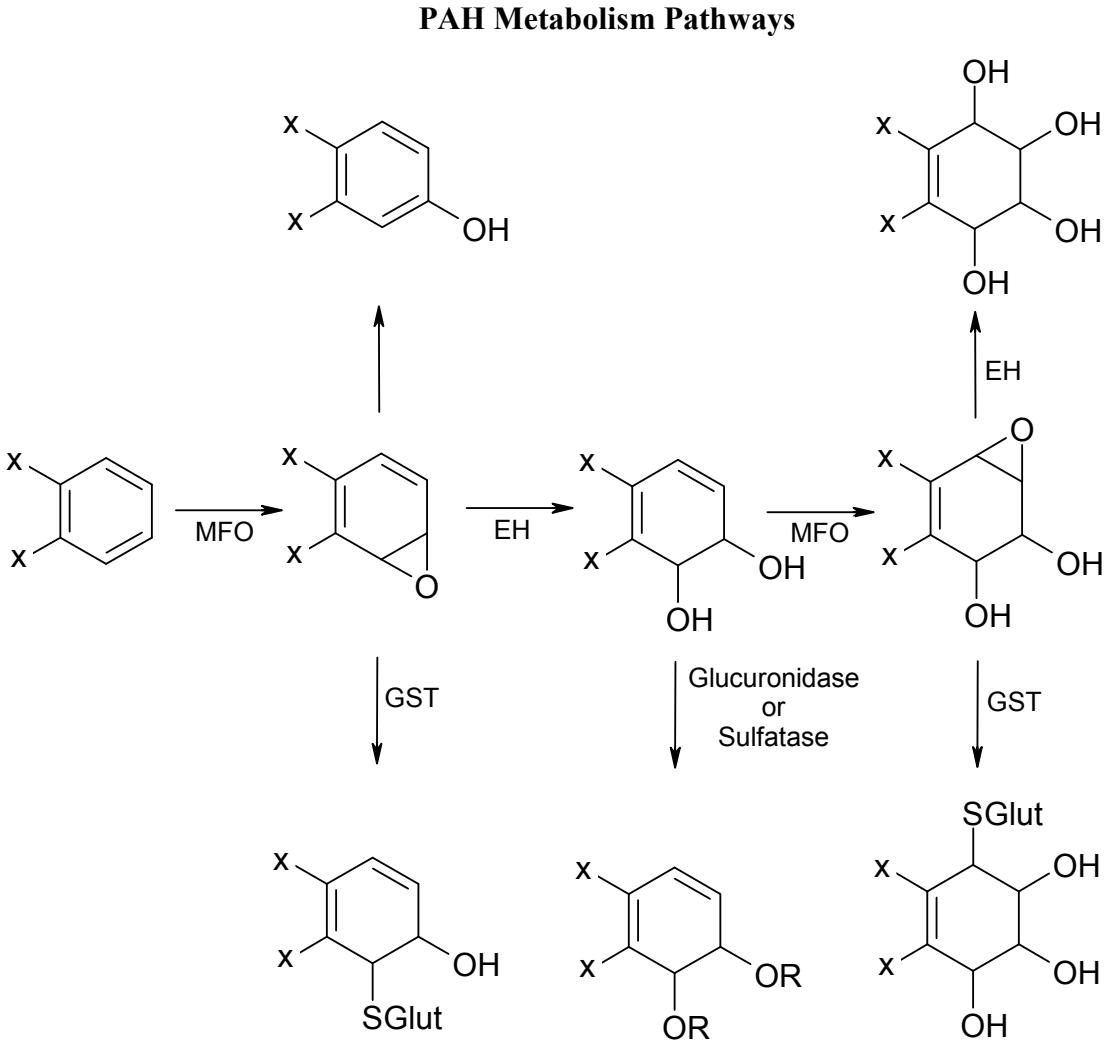

Figure 1.4. Metabolic pathways of PAH metabolism (Harvey 1991). MFO is mixed function oxidase, EH is epoxide hyrolase, GST is glutathione-S-transferase, R = glucuronate or sulfate.

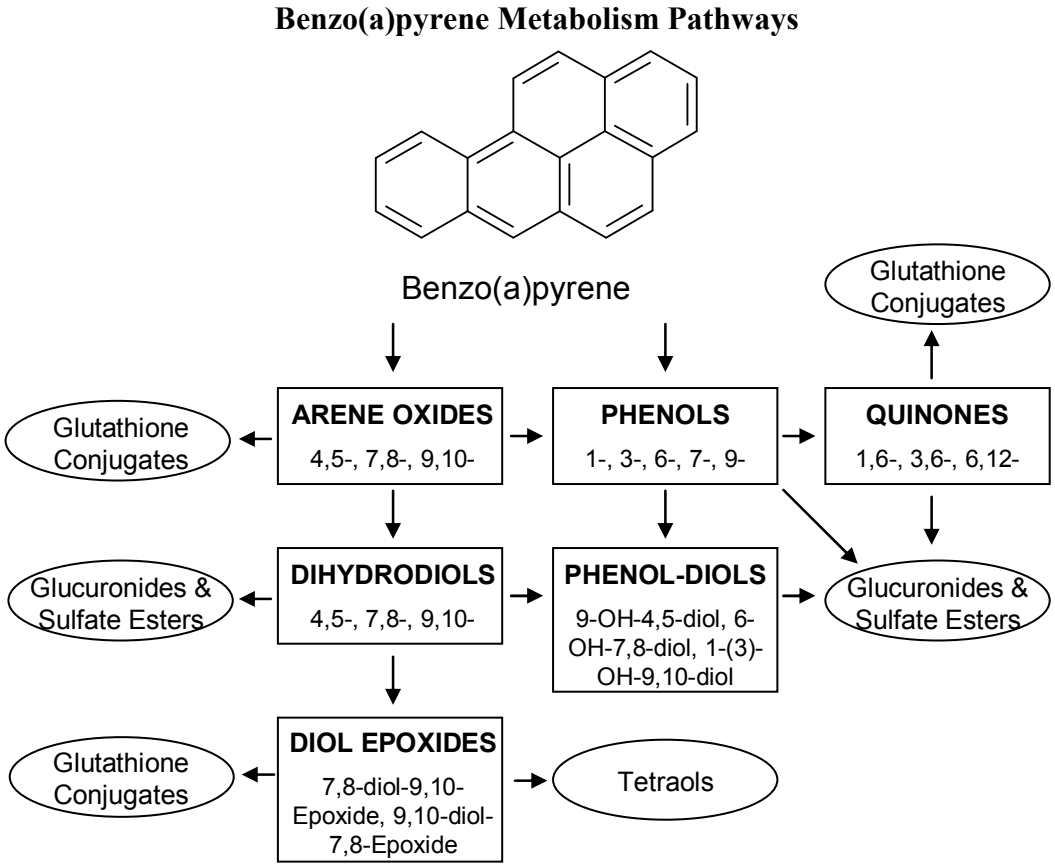

Figure 1.5. Scheme depicting the several different pathways for metabolic activation of benzo(a)pyrene. These pathways are assumed to apply generally to all PAHs, due to the structural similarities of these compounds. Scheme was modified from a Figure in ATSDR 1995.

These Phase I oxidation reactions generally produces arene oxides. Arene oxides may then be transformed into several different structures including phenols by spontaneous reaction, trans-dihydrodiols by hydration which is catalyzed by microsomal epoxide hydrolase, or the arene oxide may bind to glutathione covalently by spontaneous reaction in glutathione-S-transferase catayzation. At this point, 6-hydroxybenzo(a)pyrene has been formed, and is then oxidized to 1,6-, 3,6-, or 6,12-quinones via spontaneous or metabolic reaction. Two further phenols may be oxidized; 3-hydroxybenzo(a)pyrene to 3,6-quinone and 9-hydroxybenzo(a)pyrene to the K-region 4,5-oxide. The 4,5-oxide can then be hydrated to 4,5-dihydrodiol (4,5,9-triol). Glucuronides and sulfate esters may then be conjugated from the phenols, quinones, and dihydrodiols, while glutathione conjugates can be formed from the quinones as well. Conjugation is not the only reaction that the dihydrodiols may undergo. More oxidative metabolism may also modify the structure of the dihydrodiols via cytochrome P-450 enzymes. This reaction generally results in the formation of the 7,8-dihydrodiol-9,10-epoxide. There are two types of reactions that can conjugate diol epoxides, spontaneous reaction or glutathione-S-transferase reaction. Alternatively, the diol epoxides may form tetrols via spontaneous hydrolization. The 7,8-dihydrodiol-9,10-epoxide is generally thought of as being the major compound responsible for carcinogenic activity of BAP (ATSDR 1995).

The USEPA considers seven PAHs to be potentially carcinogenic to humans. BAP (Figure 1.6) is listed as a class B2 probable human carcinogen. Pure BAP appears as pale yellow needles or plates in the solid form (Harvey 1997; USEPA 1994b). The carcinogenic potential of BAP has been demonstrated in numerous animal assays via several different routes of administration and numerous genotoxic assays(Culp et al. 1998; Gaylor et al. 2000; Ramesh and Knuckles 2006; Rodriguez et al. 1997; USEPA 1994b).

Animals showing positive carcinogenic responses include rats, mice, hamsters, and guinea pigs. Routes of exposure reported as carcinogenic in animals include dietary, gavage, inhalation, intratracheal instillation, dermal studies, intraperitoneal injection, subcutaneous injection, intravenous, transplacentally, implantation in the stomach wall, lung, renal parenchyma and brain, injection into the renal pelvis, and vaginal painting. In oral exposure, the type of tumors seen include forestomach, squamous cell papillomas and carcinomas. BAP, often considered a model carcinogen, has multiple areas for metabolic activation, including a bay-region. The pathway for binding to DNA is shown in Figure 1.7. The benzo(a)pyrene diol epoxide attached to the N^2 of deoxyguanosine is shown in Figure 1.8. In a review done by the USEPA (1991), the report shows that intraperitoneal injections have higher numbers of injection site tumors in mice and rats. Neal and Rigdon (1967) administered BAP at 0, 1, 10, 20, 30, 40, 45, 50, 100 and 250 ppm in the diet of male and female CFW-Swill mice. Forestomach tumors were detected in the 20+ ppm dose ranges. Tumor of incidence was also observed to increase with dose. Brune et al. (1981) fed 0.15 mg/kg BAP to Sprague-Dawley rats. Dose times ranged from every nine days to 5 times a week until death, making the average dose 6 or 39 mg/kg respectively. Tumors were observed in the forestomach, esophagus and larynx. A statistical trend for tumor incidence was also observed based on dose.

USEPA Class B2 Carcinogenic PAHs

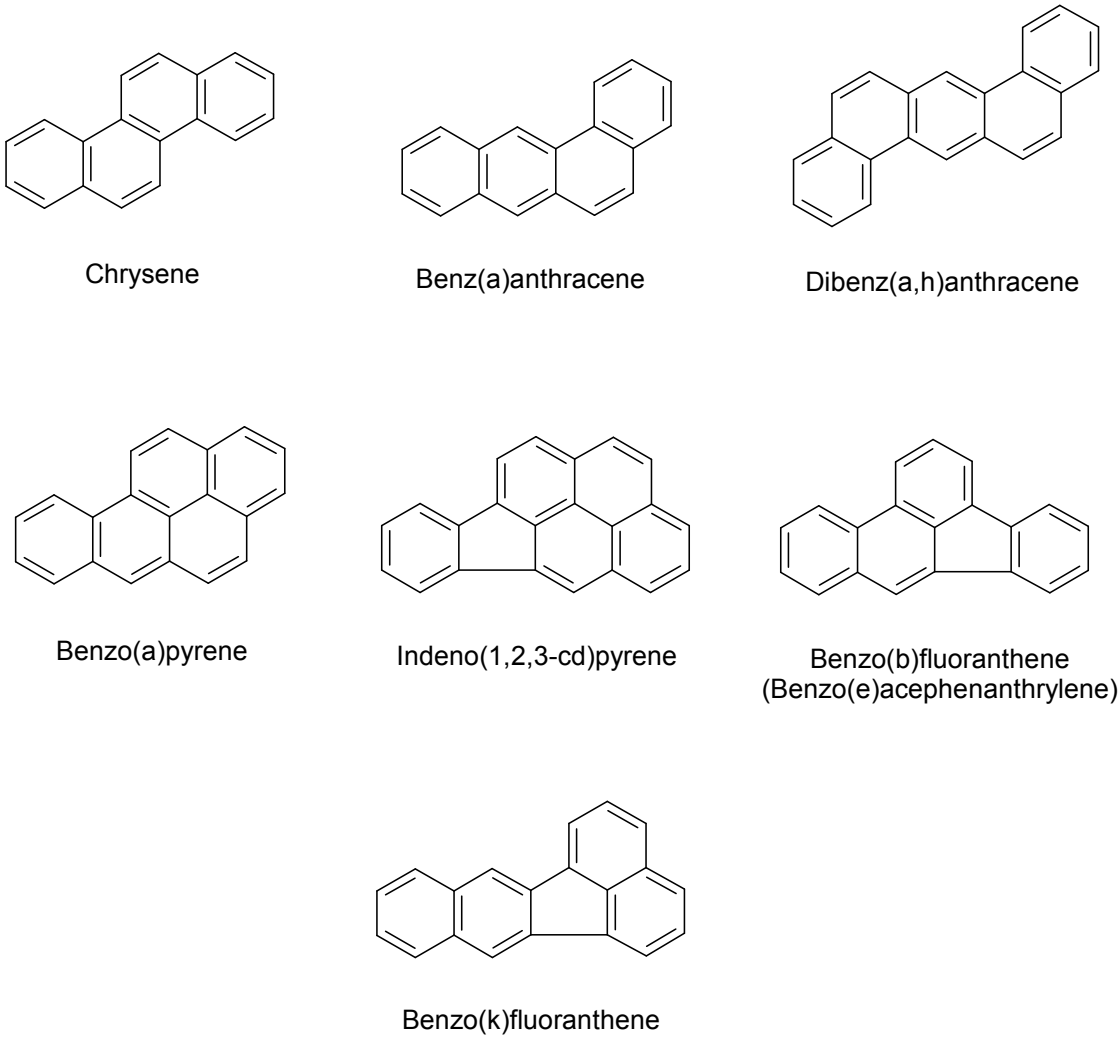

Figure 1.6. PAHs classified as class B2 carcinogens by the USEPA (Harvey 1991; USEPA 2006b).

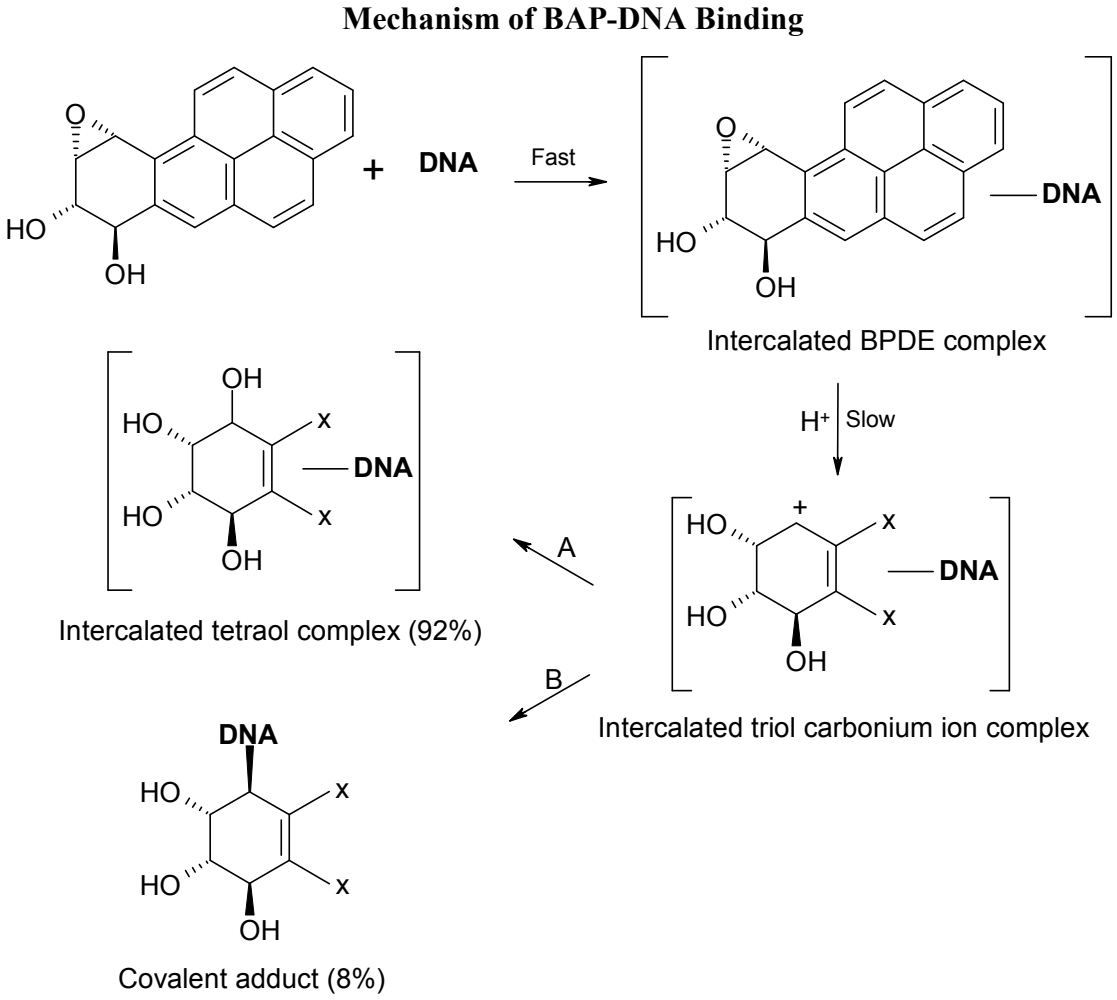

Figure 1.7. Mechanism by which the *anti* configuration of benzo(a)pyrene diol epoxide binds to DNA covalently (Harvey 1991).

BPDE N^2-dG Adduct

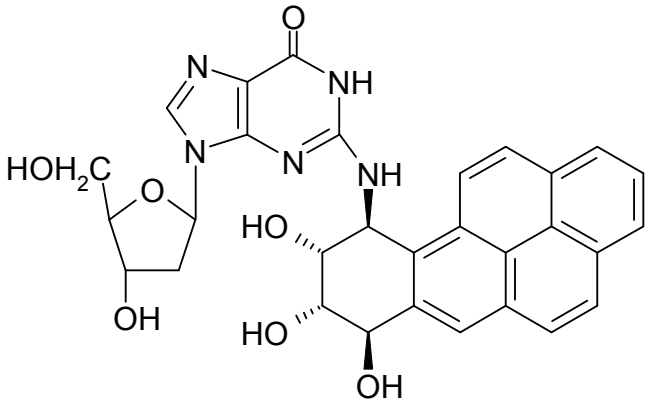

anti-BPDE N^2-dG

Figure 1.8. Benzo(a)pyrene diol epoxide, *anti* configuration, adduct attached at the N^2 position of deoxyguanosine (Harvey 1991).

Benz(a)anthracene (BAA) (Figure 1.6) is also classified as a class B2 probable human carcinogen by the USEPA IRIS database. According to the USEPA's IRIS database, BAA has been shown to produce tumors *in vivo* in mice via gavage, intraperitoneal injection, subcutaneous injection, intramuscular injection, and topical application. It has also been shown to produce mutations *in vitro* via bacterial cells and mammalian cells. There is no human carcinogen data for BAA, although an excess rate of cancer has been observed in humans exposed to complex mixtures that include BAA including cigarette smoke, coal tar, and soot. The mechanisms of action and metabolic activation for PAHs in general fit BAA for carcinogenic potential, as this compound does posess a bay region (ATSDR 1995; USEPA 1994a). Wislocki et al. (1986) injected 90-100 male and female CD-1 mice intraperitoneally with BAA in DMSO at 1, 8, and 15 days of age for a total dose of 638 μg/mouse. A statistical incidence of tumor adenomas or carcinomas was observed in the male mice, while pulmonary adenomas were observed in the female mice as statistically significant level. Steiner and Falk (1951)

injected C57Bl mice subcutaneously with BAA in tricaprylin. Sacromas were observed at the site of injection nine months later, with a survival rate of ~70%.

The third Class B2 carcinogenic PAH is benzo(b)fluoranthene (BBF) (Figure 1.6), also called benz(e)acephenanthrylene. The USEPA's IRIS database indicates that BBF has been found to produce tumor in mice via lung implantation, intraperitoneal injection, subcutaneous injection, and skin painting. In 1987, LaVoie et al. injected male and female CD-1 mice intraperitoneally with BBF in DMSO at 1, 8, and 15 days old. The total dose given was approximately 126 μg/mouse. After 52 weeks of age, the mice were sacrificed and tumor incidence observed. Liver adenomas and hepatomas were significant in males, while lung adenomas were reported in both males and females. Wynder and Hoffmann (1959) conducted skin painting assays with BFF and female Swiss mice. Mice were treated with doses of 0.01, 0.1 or 0.5% BFF solutions in acetone were three times a week. By eight months 100% of the high dose mice had papillomas, while 90% had carcinomas. The middle dose produced 65% papillomas and 85% carcinomas by 12 months, while the low dose produced one papilloma in 10 animals that survived to 14 months. As with the other PAHs, there is no human carcinogenicity data for this compound, although it is linked to human cancer via complex mixtures such as cigarette smoke, coal tar, and soot. The structure of BBF includes a bay-region, thus allowing it to fall into the current theories on mechanisms of action and metabolic activation of PAHs (ATSDR 1995; USEPA 1994c).

Benzo(k)fluoranthene (BKF) (Figure 1.8) is also listed by the USEPA as a class B2 probable human carcinogen. BKF has been demonstrated *in vitro* to be mutagenic via bacterial assays. BKF has also been shown to produce tumors *in vivo* in mice via lung implantation and skin painting (with a promoting agent for the latter). In 1987, LaVoie et al. injected male and female CD-1 newborn mice intraperitoneally with BKF in DMSO. A total dose of 126 μg/mouse was given at 1, 8, and 15 days of age. After 52 weeks of age, the mice were sacrificed. Hepatic adenomas and hepatomas were increased in the male mice, and lung adenomas were observed in both sexes. Skin painting assays were also preformed by Van Duuren et al. in 1966. A dose of 11 mg of

BDF was treated one time on Swiss mice. After 63 weeks, no tumors were observed. However, tumors were observed when promoting treatments of croton resin were added. Papillomas were observed in 18/20 animals, while carcinomas developed in 5/20 animals. BKF is another PAH which is present in complex mixtures such as cigarette smoke and soot that have been found to increase the risk of cancer in humans (USEPA 1994d).

Chrysene, a four ring PAH, is also defined by the USEPA as a class B2 probable human carcinogen (Figure 1.6). The review for chrysene indicates that this chemical has been shown to produce carcinomas, malignant lymphomas and chromosomal abnormalities *in vivo* in mice via intraperitoneal injection and dermal exposure and in hamster and mouse germ cells via gavage (respectively). Male and female CD-1 mice were injected intraperitoneally with chrysene dissolved in DMSO at 1, 8, and 15 days of age (Wislocki et al. 1986). Total doses were 0, 160 or 640 μg/mouse. A significant incidence of liver adenomas and carcinomas were observed in male mice, 29% and 11% in the low dose, and 41% and 75 in the high dose, respectively. Malignant lymphoma was significant in the male low dose (9%), but not in the high dose (0%). Lung adenomas were significantly elevated in males at the high dose, while female mice did not see a significant increase in any tumors. Buening et al. (1979) dosed male and female Swiss Webster BLU/Ha(ICR) mice with 320 μg/mouse of chrysene in DMSO at 1, 8, and 15 days of age via i.p. injection. After 38-42 weeks of age, mice were evaluated for tumor incidence. Lung tumors were elevated, 21% in males and 9% in females. Hepatic tumors in males were significantly higher (25%), while females had a 0% incidence. This compound has also shown positive genotoxicity in bacterial mutation assays and in transformed mammalian cells. Chrysene contains a bay-region, and is assumed to be metabolically activated through this structure (USEPA 1994e).

The USEPA IRIS database has also classified dibenz(a,h)anthracene (DA) (Figure 1.6) as a class B2 probable human carcinogen. DA has been shown *in vivo* to produce carcinomas and injection site tumors in mice and other species via oral or dermal exposures and subcutaneous or intramuscular injections (respectively). *In vitro*, DA has

demonstrated the ability to induce DNA damage, along with gene mutations in bacterial assays as well as mammalian cells. DA contains a bay-region structure, through which it is proposed to be metabolically activated for its carcinogenic potential (USEPA 1994f). Biancifiori and Caschera (1962) showed mammary carcinomas in female Balb/c (1/20) and pseudo-regnant (13/24) female mice. Mice were gavaged twice a week for 15 weeks with 0.5% DA for a total dose of 15 mg/mouse. Lubet et al. (1983) found fibrosarcoma development with subcutaneous injections of DA. Four strains of mice, C3H/HeJ, C57B1/6J, AKR/J and DBA/2J, were injected a single time with 150 mg DA in 0.05 mL trictanoin. After 9 months, animals were sacrificed. Tumor incidence was between 0 and 80%, strain dependent. The C3H and C57B1 mice had higher tumor incidence than the AKR or DBA mice. Fibrosarcoma development was inversely correlated with tumor incidence.

Indeno(1,2,3-cd)pyrene (IP) (Figure 1.6) is also a class B2 probable human carcinogen, according to the USEPA's IRIS database. IP has demonstrated the ability to produce tumors *in vivo* in mice via lung implants, subcutaneous injection and dermal exposure. Hoffmann and Wynder (1966) painted the skin of female Swiss albino Ha/ICR/Mil mice with IP in dioxane (0.05 and 0.1%) or acetone (0.01, 0.05 and 0.1%). Dioxane treatments did not induce tumor formation, however, acetone treatment did. The acetone treatments produced skin tumors in a dose-responsvie manner for the two highest doses. Six papillomas and three carcinomas were observed at 9 months in the 0.1% treatment, while seven papillomas and five carcinomas were observed in the 0.5% treatment with the first appearing at three months. Rice et al. (1986) applied IP dissolved in acetone to the shaved backs of Crl:CD-1(ICR)BR female mice. Treatments were applied every other day for 10 days, total IP dose was 1 mg. After 10 days, tetradecanoylphorbol was applied as a promoter (0.0025% in 100 mL acetone) three times a week for 20 weeks. Tumor incidence was observed to be 100%. *In vitro*, IP has also produced positive results in bacterial mutation assays. There is no human carcinogenicity data for IP. Generally, IP is found environmentally as part of complex mixtures. These complex mixtures may include coal tar, coke oven emissions, and

cigarette smoke. Because of the association of IP with these complex mixtures, it may also be associated with human cancer (USEPA 1994g).

The formation of bulky DNA adducts is generally believed to represent the initiation step in the three step process (initiation, promotion and progression) to transform a normal cell into a malignant cancer cell (Ramesh et al. 2004). Using a battery of *in vitro* and *in vivo* studies, this research will develop information regarding the ability of PAH mixtures to induce mutations and ultimately to cause tumor formation.

1.3.3 Polychlorinated Aromatic Compounds

The combustion of plastics produces mixtures of both PAHs and PCAs including the polychlorinated dibenzo-*p*-dioxins (PCDDs) and dibenzofurans (PCDFs). Another common complex environmental mixture containing both PCAs and PAHs is the waste stream from the treatment of wood with a mixture of diesel oil and pentachlorophenol. Many wood preserving facilties used creosote for treating utility poles and railroad ties, and pentachlorophenol for treating smaller wood products. Contamination of soil and groundwater with mixtures of PAHs and PCAs at wood preserving sites is common. Thus, much like the PAHs, PCAs are ubiquitous environmental contaminants. PCAs are recalcitrant in the environment due to the resistance of chlorinated molecules to oxidative degradation. The electrophilic nature of the chlorine substitution renders PCAs highly lipophilic. Thus, PCAs, especially PCDDs and pentachlorophenol (PCP), will partition into lipids or organic matter and are likely to bioaccumulate in the environment as well as in the food chain.

Environmental media contaminated with PCAs may contain several hundred different chemicals. These complex mixtures contain various isomers and congeners of the halogenated compounds. The chemical, physical and toxicological properties of the PCA congeners are dependent on the amount of halogens present in the aromatic ring (Safe et al. 1990). PCDDs include 75 different congeners, including 2,3,7,8-

tetrachlorodibenzo-*p*-dioxin (TCDD). TCDD is considered to be the most toxic congener of the PCDDs, and thus is the most widely studied (ATSDR 1998).

The most noted toxic response in humans from acute exposure to PCDDs is chloracne. Safe et al. (1990) indicate that PCDDs have also been shown to cause body weight loss, thymic atrophy, impairment of immune responses, hepatotoxicity and porphyria, dermal lesions, tissue-specific hypo and hyperplastic responses, carcinogenesis, teratogenicity and reproductive toxicity, and are highly species, sex and age specific. PCDDs are a class of chemicals that contain eight different congeners. Potency of these congeners depends upon their affinity for the AhR receptor. In general, the more chlorinated the congener, the less potent. TCDD is the most toxic congener, and the model compound for PCDDs (Anderson and Conolly 1998; DHHS 2004; Loertscher et al. 2002). However, it is important to note the species in which the PCDDs are being tested, as toxic effects vary greatly between species (Safe et al. 1990). There is large sensitivity among species, and even among strains, for example Long-Evan rats are sensitive to dioxins while Han/Wistar rats are resistant. However, mice, rats and hamsters have all shown affinity for dioxin toxicity (DHHS 2004; Viluksela et al. 2000).

1.3.3.1 Polychlorinated Dibenzodioxins and Furans

Because of the diverse structures of the many congeners (Figures 1.9 and 1.10) of the PCDDs and PCDFs these compounds may produce a broad range of toxic, genotoxic and epigenetic responses. As by-products of industrial processes and incomplete combustion, these compounds have been detected in environmental media in all parts of the world. In Hamburg, 3.5/0.23 pg/m^3 levels of TCDF/TCDD were detected in the atmosphere in a motorway tunnel (Rappe et al. 1988). Levels of TCDD/TCDFs have been detected in Lake Superior fish are 5.7-22 ppt/0.3-2.8 ppt (Zacharewski et al. 1989). The same study also reported levels Lake Ontario fish as 36-45 ppt/13-30 ppt. Adipose Tissue levels were reported by Nygren et al. (1988) as 3.9 ppt for TCDF, 54 ppt for PCDF, 3 ppt for TCDD and 15 ppt for PCDD. The major route of exposure for PCDDs and PCDFs is believed to be through food intake (Figure 1.11) (IOM 2003). In the

United States, there are 126 sites on the National Priority List where PCDDs are listed as a contaminant of concern. PCDDs may be classified into eight groups, based on the number of chlorine atoms, ranging from mono-chlorinated dioxins to octa-chlorinated dioxins. The chlorine atoms may be bound to any of eight carbon atom positions available on the aromatic rings. The toxicity of PCDDS is highly dependent on the number of chlorine atoms, and their position. The most toxic PCDD congener is TCDD. Thus, TCDD is the most studied of these compounds (ATSDR 1994). Since the production of most chlorinated chemicals has been reduced in recent years, there has been a corresponding reduction in the release of PCDDs into the environment. However, because these compounds are persistent and capable of bioaccumulation, there is still concern for their potential adverse human and ecological health effects.

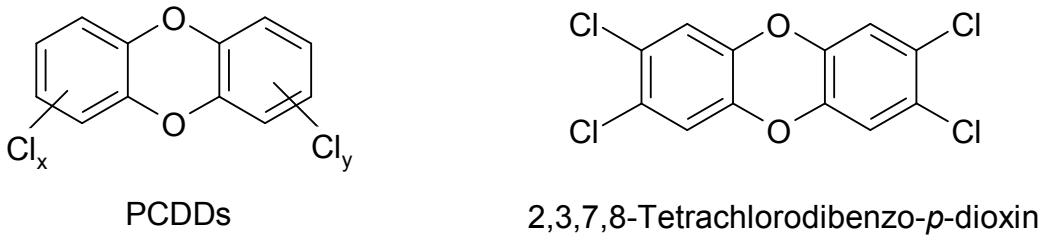

Figure 1.9. Polychlorinated dibenzo-*p*-dioxins and 2,3,7,8-tetrachlorodibenzo-*p*-dioxin (Poland 1984).

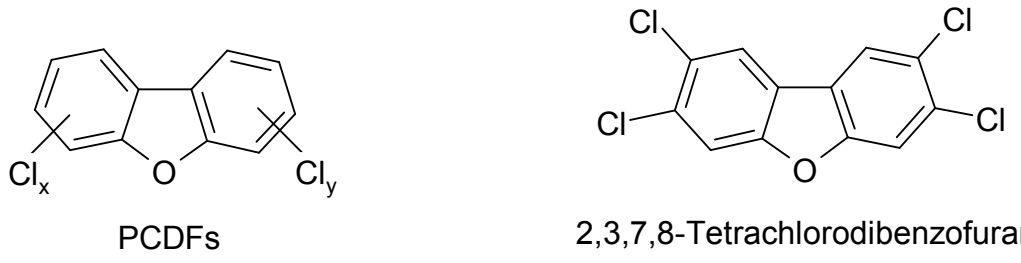

Figure 1.10. Polychlorinated dibenzofurans and 2,3,7,8-tetrachlorodibenzofuran (Poland 1984).

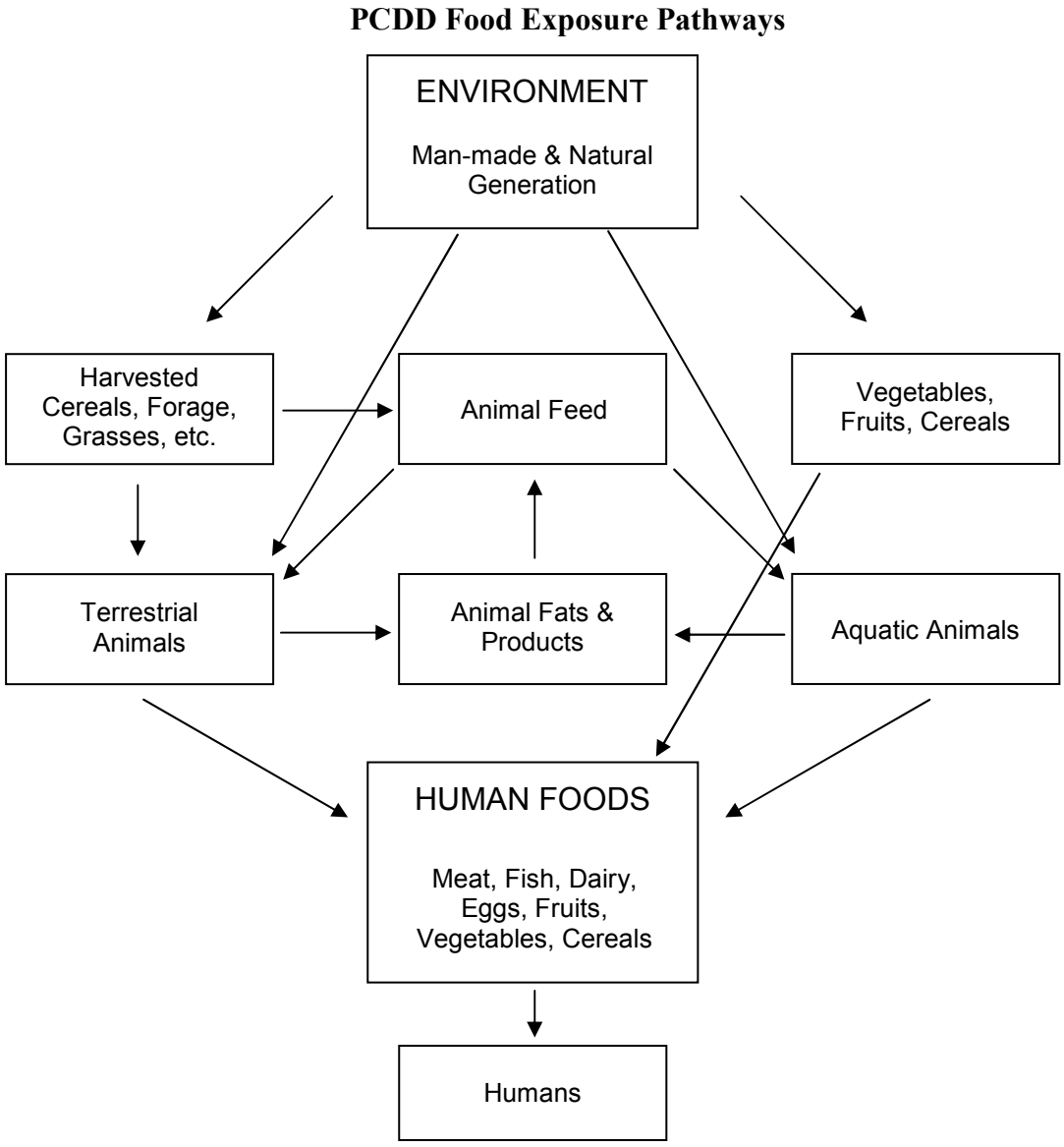

Figure 1.11. Pathways for the major source of exposure to PCDDs, food exposure. Light arrows depict smaller contribution sources than the dark arrows. Adapted from Figure 4-1 in the book *Dioxins and Dioxin-like Compounds in the Food Supply*, Institute of Medicine of the National Academies, 2003.

PCDDs may be released into the environment via unintentional byproducts of combustion, metals smelting and refining, chemical manufacturing, biological and photochemical processes, and reservoirs of PCDDs. During these processes PCDDs are created and released into the environment. Reservoirs of PCDDs are stores which can

release and recirculate PCDDs via short, long and intermediate releases. Atmospheric transportation is the major cause for release to the environment. Due to the low water solubility and high lipophilicity of these compounds, they tend to be transported through air, and then soil. When in the water column, PCDDs bind to particles in the water, and are eventually removed through sedimentation (IOM 2003). The largest impact on PCDD contamination can be attributed to anthropomorphic practices such as incineration and combustion processes. PCDDs are almost always accompanied by PCDFs, due to the processes in which they are formed, and their similar structure. These same reasons account for their association with chlorinated phenols as well. This tendency makes it difficult to discern PCDD and PCDF effects from exposure in human populations. TCDD is the most toxic and most studied compound, it is considered to be the model compound for PCDD toxicity. Toxic Equivalent Factors (TEFs) were developed as a way of expressing toxicity of dioxin-like compounds as a fraction of the toxicity of TCDD. Potency of the PCDD and PCDF congeners is thought to depend highly on their AhR affinity. Therefore, dioxin like compounds are compared to TCDD, which has the highest affinity for AhR. The TEF value for TCDD is 1.0, with all others based on their fractional potency relative to TCDD (ATSDR 1998; Finley et al. 2003; Safe et al. 1990). The AhR protein has a binding specificity for aromatic hydrocarbons. AhR can be set free from its chaperone proteins by ligand binding. This allows it to enter the nucleus and bind to ARNT. This ligand-AhR-ARNT comlpex enhances transcription of multiple genes (CYP1A1, 1A2, 1B1, and glutathione-S-transferase) (Franc et al. 2001a). TCDD has a high affinity for the AhR (Franc et al. 2001a; Franc et al. 2001b).

PCDDs have a half life of elimination of 8.5 years in adults (ATSDR 1998). TCDD promotes tumor formation and altered hepatice foci (Pitot et al. 1980; Walker et al. 2000; Wyde et al. 2002). TCDD also depletes hepatic vitamin A (Fattore et al. 2000); (Fletcher et al. 2001). This reduction of hepatic viatamin A along with decreasd weight gain can be a biomarker for TCDD exposure in laboratory animals. Poland et al. (1982) demonstrated TCDDs ability to promote tumor formation. In HRS/J hairless mouce,

exposure to a carcinogen followed by repeated exposures to TCDD produced papillomas in *hr/hr* mice, but not *hr/+* mice. In mice treated with *N*-methyl-*N'*-nitro*N*-nitrosoguanidine (MNNG), 55-100% tumor incidence was observed (doses from 3.75 ng to 15 ng). Randerath et al. (1988) studied on the DNA adduct levels after TCDD and PCDD exposure. Rats treated with these compounds did not form appreciable levels of DNA adducts, thus confirming ealier findings that TCDD was not genotoxic.

Occupational and environmental exposures to PCDDs and PCDFs occur frequently, since these compounds are ubiquitous and highly persistent in the environment due in part to their lipophilic nature. Humans are exposed to these compounds in the diet and their lipophilicity results in bioaccumulation in human adipose tissues and the environment. Several epidemiological studies have been done regarding PCDDs and PCDFs. The most well known effect is the dermal effect, chloracne. Eventhough multiple epidemiological studies have been done on PCDDs and PCDFs, there is inconclusive evidence for carcinogenicity of PCDDs and PCDFs (Asp et al. 1994; Becher et al. 1996; Bertazzi et al. 1997; Green 1991; Hooiveld et al. 1998; Kogevinas et al. 1997). The most obvious exposure sign was chloracne. However, Steenland et al. (1999) did a follow up study on an industrial cohort and showed that approximately 334 out of an expected 113 people died from cancer after exposure. They conclude that TCDD exposure does cause cancer. Unfortunately, statistically this study does not provide good evidence for a link to cancer (Cole et al. 2003).

TCDD is classified as a human carcinogen by the 11th Report on Carcinogens (DHHS 2004). This classification is based on data observed in epidemiological studies. Not much is known about the mechanisms of action in humans for PCDDs and PCDFs. The mechanism includes binding to the AhR the first and most important step. Most dioxin-like compounds, including PCDFs, are thought to act through similar mechanisms of action due to their structural similarities. It is possible to monitor exposure through biomarkers of exposure. Adipose tissue and liver generally exhibit the highest concentrations of PCDDs and PCDFs. Due to the lipophilicity, these tissues are the primary storage sites for PCDDs and PCDFs. PCDDs and PCDFs are measured in

these tissues as biomarkers of exposure. Other biomarkers of exposure include breast milk, and reverse transcriptase polymerase chain reaction (RT-PCR). The RT-PCR can measure CYP1A1 mRNA levels in blood lymphocytes. When TCDD is present, CYP1A1 has been demonstrated to increased by 21 times. Biomarkers of effect, chloracne and biochemical changes are also observed (ATSDR 1998).

1.3.3.2 Pentachlorophenol

The National Priorities List (NPL) includes 313 sites where PCP has been identified as a contaminant of concern. This chemical is listed by the USEPA as a a class B2 probable human carcinogen. Pentachlorophenol has a chemical formula of C_6HCl_5O (Figure 1.12) and a molecular weight of 266.35. Pure PCP appears as colorless crystals (ATSDR 2001; USEPA 1993). PCP is produced using a catalyst stepwise process that chlorinates phenols (ATSDR 2001). The USEPA oral cancer slope factor for PCP is 1.2×10^{-1} (USEPA 1993). The cancer slope factor is based on the finding that animals administered PCP developed hepatocellular adenomas, carcinomas, adrenal medulla pheochromocytomas, malignant pheochromoxytomas, hemangiosarcomas and hemangiomas. Although occupational and environmental exposures to this compound are common, the USEPA believes that there is inadequate data for the human carcinogenicity of PCP (USEPA 1993).

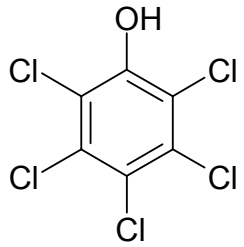

Pentachlorophenol

Figure 1.12. Pentachlorophenol.

PCP was widely used as a pesticide/biocide in the United States before its restriction in 1987. This all purpose biocide (herbicide, defoliant, mossicide, and disinfectant) was used in multiple applications including, but not limited to leather tanning, wood preservation, and in paints (ATSDR 2001; Klaassen 2001; USEPA 1993). The use of PCP as a wood preservative began in the 1930s. Shortly after, in 1947, some 3,200 metric tons were used in wood preservation. In 2002, approximately 11 million pounds of PCP were consumed in the United States due to restrictions on use (USEPA 1993). Exposure to PCP is generally to the technical grade, which contains a number of impurities including lower chlorinated phenols, polychlorinated dibenzo-*p*-dioxons and dibenzofurans (Ahlborg and Thunberg 1980). Occupational exposures generally occur through inhalation and dermal contact. Environmental exposures may occur when a person comes in contact with contaminated media. Exposure routes of concern are inhalation of contaminated air and volatilized PCP, as well as ingestion of contaminated food and dermal contact with contaminated soils or surfaces.

Several case studies have suggested that there is a relationship between occupational exposure to PCP and cancer (Dahlgren et al. 2003; Demers et al. 2006; Eriksson et al. 1990; Hardell et al. 1994; Jappinen et al. 1989). Oral administration of PCP to animals has shown several target organs. These target organs include the liver, kidney, central nervous system, endocrine system, immune system and the reproductive system (IARC 1998a; Seiler 1991). A proposed mechanism of action for PCP is the uncoupling of oxidative phosphorylation. This results in an acceleration of aerobic metabolism and the production of heat. Although no single organ or tissue is specifically targeted, multiple organs may exhibit signs of PCP toxicity following exposure (ATSDR 2001).

PCP contains a benzene ring with a single hydroxyl substituent and five chlorine substituents. This structure results in a nonpolarity for this compound which decreases water solubility and increases lipid solubility. These attributes facilitate the transfer of PCP across cell membranes. PCP also has an affinity for binding to plasma proteins,

which allow for distribution via the blood streem. PCP is not easily metabolized, and therefore generally persists in mammalian systems as the parent compound (Ahlborg et al. 1974; Braun et al. 1979; Larsen et al. 1972). PCP can be monitored through biomarkers of exposure (Chou and Bailey 1986; Drummond et al. 1982; Edgerton et al. 1979; Holler et al. 1989; Jorens and Schepens 1993). Because PCP remains unchanged for a large part, it can be quantified in urine, a major route of excretion (Benvenue et al. 1968; Needham et al. 1981). PCP can also be quantified in blood serum and adipose tissue. PCP has also been detected in adipose tissue as an ester of palmitic acid (Kuehl and Dougherty 1980; Needham et al. 1981; Ohe 1979). However, this is not a specific biomarker for PCP, as other chemicals may be metabolized into PCP after exposure (lindane, etc.). Two other biomarkers of exposure are TCHQ in urine (still not specific to PCP) and 8-hydroxydeoxyguanosine in the liver (increased levels due to oxidative DNA damage) (Ahlborg et al. 1974; Jorens and Schepens 1993; Juhl et al. 1985; Sai-Kato et al. 1995; Umemura et al. 1996). Approximately 90% of PCP was eliminated in the urine and feces of volunteers withing 7 days (Ahlborg and Thunberg 1980). The liver and kidney are the two major target organs in humans and animals. Elevated serum ALT and AST levels in the liver and increased enzyme levels, blood urea nitrogen, and loss of proximal tubular alkaline phosphatesase activity for kidney are biomarkers of effects for PCP exposure (ATSDR 2001).

1.4 Toxicity Test Methods

Chemical analysis provides important information regarding the composition and concentration of compounds in a complex mixture. Bioassays provide a tool to investigate mechanisms and interactions of the components of a complex mixture. *In vitro* and *in vivo* bioassays play and important role in toxicity evaluation of chemicals and mixtures (Ciganek et al. 2004). Microbial genotoxicity assays provide a useful tool for screening complex mixtures and isolated fractions. A major limitation of microbial bioassays is their inability to replicate the pharmacokinetic (e.g., absorption, distribution, metabolism and excretion) factors that may influence mixture carcinogenicity. Thus, it

is important to use multiple assays when evaluating the toxicity or genotoxicity of a substance. The optimal protocol as defined by Maron and Ames (1983) would include multiple bioassays where "the strengths of one test can compensate for the inadequacies of another".

1.4.1 *In Vitro* Bioassays

In vitro bioassays provide a valuable tool for screening a large number of complex environmental mixtures. Microbial bioassays are inexpensive, provide a response within a short time frame, and are relatively easy to conduct. Short-term *in vitro* bioassays have been used in previous studies to screen potential carcinogens (McCann et al. 1975), to detect genotoxic compounds in complex environmental mixtures (Donnelly et al. 1998), and to identify genotoxic compounds in isolated fractions (DeMarini et al. 1990). Data collected from these assays can be used to prioritize mixtures or compounds for further study using *in vivo* assays.

1.4.1.1 *Salmonella/*microsome Assay

The most widely studied *in vitro* bioassay is the *Salmonella* mutagenicity test, also known as Ames assay. There have been multiple revisions to the original protocol, first validated by McCann et al. (1975). The protocol in current use was described in Maron and Ames (1983). The *Salmonella/*microsome assay has been used to detect mutagens in samples of cigarette smoke (Roemer et al. 2004), diesel exhaust (Seagrave et al. 2005), hazardous waste (Donnelly et al. 1987; Houk and Claxton 1986), surface waters (Ohe et al. 2004), sewage sludge (Perez et al. 2003), and soils (Watanabe et al. 2005). This bioassay has also been used to identify and characterize mutagens such as heterocyclic amines in cooked foods (Knize et al. 2003; Shishu and Kaur 2003; Sugimura et al. 2004).

McCann et al. (1975) report of the more than 300 chemicals that have been tested using this assay, 90% of the known carcinogens tested showed a positive mutagenic response. They also report that the correlation between carcinogenicity and

mutagenicity is 83%. In 1987, Tennant et al. (1987a) conducted a detailed comparison of short-term tests and rodent carcinogenicity. They observed that although the sensitivity was only 45% (percent of carcinogens yielding a positive result in microbial bioassay), 83% of the compounds that induced a positive response in the *Salmonella* microbial bioassay were also rodent carcinogens. Tennant et al. (1987b) also found that the majority of chemicals that are trans-sex/trans-species carcinogens are also genotoxic in microbial tests.

In analytical chemistry, a variety of systems may be used to detect different classes of chemicals. This is a result of the different chemical structures and properties and reflects knowledge gained from many years of environmental measurements. Similarly, microbial bioassays exhibit differing sensitivities to different classes of chemicals. Purchase et al. (1976) found that 95% of the PAHs that induced a mutagenic response in *Salmonella* were also rodent carcinogens. Although the *Salmonella* bioassay in a sensitive method for detecting carcinogenic PAHs, it is relatively insensitive towards carcinogenic PCAs. In addition, the *Salmonella* bioassay is relatively insensitive to compounds that may be cytotoxic at low doses (Maron and Ames 1983). These limitations need to be considered when designing a protocol using multiple bioassays. The research described in this dissertation used two microbial mutagenicity bioassays to screen model carcinogenic chemicals and complex mixtures. Compounds and isolated complex mixtures that tested positive in the microbial bioassay were further tested using an infant mouse model to measure the ability of these to induce tumors. The results from this battery of bioassays were then compared with the composition of the mixtures as determined by quantitative chemical analysis. Standard *Salmonella* tester strains include TA89, TA90, TA92, TA94, TA97, TA98, TA100, TA102, TA110, TA1530, TA1534, TA1535, TA1538, TA1950, TA1964, TA1975, TA1978, TA2410, TA2631, and TA2641. The standard tester strains that are recommended for general mutagenesis testing include TA97, TA98, TA100 and TA102. These microbial strains have been engineered to be sensitive to different classes of genotoxic compounds.

A variety of mutations and deletions have been incorporated into the *Salmonella typhimurium* tester strains in order to increase their sensitivity towards certain classes of carcinogens. All of the tester strains were originally derived from *S. typhimurium LT2.* The different tester strains of bacteria contain a primary deletion in the histidine operon. These include a *his*G46, *his*D3052, *his*D6610, and *his*G428 deletion. Strains TA98 and TA1538 were derived from the *hisG46* deletion, whereas the *hisD3052* deletion was used to derive strains TA100 and TA1535. This *hisG* gene codes for first enzyme in the process of histidine biosynthesis. Bacteria with a deletion in this gene are unable to grow in media that has not been supplemented with histidine. Thus, approximately 100,000 cells are added to an agar plate containing a minimal media. The media is supplemented with sufficient histidine to allow cells to undergo two replications. Chemicals that react with DNA inducing a reverse mutation produce a cell that is able to grow in minimal media and may be detected as a visible colony.

The deletion in the *hisG* operon results in the substitution of one G and one C (proline, -GGG- -CCC-) for an A and T (leucine, -GAG- -CTC-), respectively. The *his*D3052 mutation eliminated the function of the histidinol dehydrogenase enzyme. The mutation sequence for this is 8 repetitive -GC- near a -1 frameshift mutation (-CGCGCGCG- -GCGCGCGCG-). Thus, strains TA1538 and TA98 are generally more sensitive to compounds that induce frameshift mutations. During replication, pairing can become shifted in repetitive sequences. Frameshift mutagens can stabilize this by a frameshift mutation, restoring the correct reading frame. The *his*D6610 mutation, another frameshift mutation, also is located in the *his*D gene. However, this strain has an added cytosine. As a result, there are 6 repetitive cytosines in this sequence (-CCCCCC-), along with another run of alternating -GC- near the cytosines. The *his*G428 mutation is also located in the *his*G gene. This is called the ochre mutation (-TAA- -ATT-).

In addition to the primary mutation at the histidine operon, other mutations have been incorporated into the tester strains to increase sensitivity to certain types of chemical carcinogens. The deep rough, or *rfa,* mutation results in an increase in

permeability of the microbial cell membrane. As many carcinogens are high molecular weight compounds, this is an important mutation. Cells containing the deep rough mutation were isolated using a large phage that could only enter cells that were absent of their lipopolysaccarhide membrane. This membrane is located on the outer surface of the microbial cell wall. In the absence of this membrane, permeability to chemicals is greatly increased. Thus, large compounds, such as BAP are able to gain access to the cytoplasm of the microbe. Many cells also contain an *uvrB* mutation. This mutation affects the DNA excision repair system by a deletion in the gene code. Without a properly functioning excision repair system, the cell looses the ability to repair chemical induced mutations. The *uvrB* deletion eliminated both the excision repair and biotin synthesis enzymes. Thus, strains with this deletion will also require trace amounts of biotin for growth.

The addition of a plasmid that increased error prone repair was found to greatly increase the sensitivity of the *Salmonella* bioassay. The plasmid, pKM101 was added to strains TA1535 and TA1538 to produce TA98 and TA100. In fact TA97, TA98, TA100 and TA102 are all standard tester strains, and they all contain this plasmid. The strains containing this plasmid are reverted by a number of mutagens that test as weak positive, or negative in the other strains. This R-factor enhances chemical and spontaneous mutagenesis.

1.4.1.2 *E.coli* Prophage Induction Assay

This research was conducted to investigate the genotoxicity of complex mixtures containing chlorinated compounds and PAHs. Since it is known that the *Salmonella* bioassay is relatively insensitive to chlorinated compounds, a test battery was designed to include a system that could be used to detect genotoxic chlorinated compounds. The *E. coli* prophage induction assay, also known as the Microscreen prophage induction assay has been found to be sensitive to chlorinated compounds (DeMarini et al. 1990). The procedure for this bioassay was first described by Rossman et al. (1984) and revised slightly by DeMarini et al. (1990). Most chlorinated compounds are unable to induce

point mutations. As a result, reverse mutation assays, such as the *Salmonella* bioassay, are relatively insensitive to these compounds. Most chlorinated compounds induce genotoxic damage by causing DNA strand breaks or chromosomal aberrations. DeMarini et al. (1990) found that the microscreen prophage induction assay detected chlorinated compound toxicity.

The *E. coli* assay uses two bacterium, $WP2_s(\lambda)$, and TH008. $WP2_s(\lambda)$ is a lambda lysogen from *E. coli* B/r, while TH008 is an indicator strain from *E. coli* C. The $WP2_s(\lambda)$ lysogen has an ochre nonsense mutation. This particular mutation has the ability to block a part of the tryptophan synthesis process. For phage induction, the $WP2_s(\lambda)$ strain is grown overnight to mid-log phase and then inoculated into wells that contain the test sample and a minimal medium. The wells are incubated overnight, and then scored for turbidity. Turbid cells indicate that there is cell growth, where clear wells indicate there is no cell growth. No cell growth can be due either to cytotoxicity or to growth inhibition. The quantity of phage that is released to the media is a measure of the extent of DNA damage that has occurred. Introduction of a chemical turns the SOS response on inside the cell. Once the SOS response is activated, the prophage activates and turns into the phage. The phage reproduces, multiplies and the *E. coli* cell then lyses. An aliquot of the turbid cells is then diluted and plated with the indicator strain TH008. The indicator strain is sensitive to the phage, and is supplemented with streptomycin. The use of streptomycin is to select against the lysogen $WP2_s(\lambda)$. The phage lyses the indicator strain resulting in the formation of a plaque. If a chemical or mixture of chemicals is capable of producing a three-fold increase in plaque formation (compared to an acetone solvent control), the sample is considered to have induced a positive genotoxic response. Thus, the two *in vitro* bioassays described in this section are capable of detecting chemicals that induce point mutations or DNA strand breaks.

1.4.2 *In Vivo* Bioassays

Microbial bioassays are useful tools to measure the ability of a chemical or chemical mixture to react with DNA and induce genotoxic damage. However, as stated

previously, microbial bioassays are unable to replicate the pharmacokinetic factors that influence the potential of environmental mixtures to cause cancer in humans. Animal studies, in conjunction with *in vitro* and epidemiological studies, are important tools to identify environmental mixtures that increase the incidence of cancer in exposed populations.

1.4.2.1 DNA ^{32}P-postlabeling Assay

DNA adducts are formed when an exogenous compounds enters into a cell and binds with the DNA. DNA adducts can also be formed from indigenous compounds already present in the biological system. These DNA adducts are called I-compounds. I-compounds increase linearly with age of an animal, the older the animal, the more difficult it is to determine differences between I-compounds and bulky DNA adducts with exogenous compounds (Randerath et al. 1986; Randerath and Randerath 1994; Randerath et al. 1999; Reddy 2000). Analysis of exogenous DNA adducts can be used as a biomarker of exposure to toxic compounds, as well as an indication of potential carcinogenic effects a compound might pose. The process of identifying quantitatively DNA adducts, especially at low levels, requires very sensitive and specific methodologies. There are methods that contain the level of sensitivity necessary: ^{32}P-postlabeling (can detect 1 adduct in 10^7-10^{10} nucleotides), fluorescence detection methods (can detect 1 adduct in 10^6-10^7 nucleotides), immunoassays (can detect 1 adduct in 10^6-10^7 nucleotides)and gas chromatography/mass spectrometry (GC/MS) (Hemminki et al. 2000; Reddy and Randerath 1986). Of these methods, the ^{32}P-postlabeling assay is considered to be the most sensitive for DNA adduct. Although DNA adducts are detected readily with this method, it does have weaknesses. Probably the most obvious weakness is the inability to identify chemical structures with this assay. However, as with most weaknesses, there are ways to overcome. Internal standards can be included within the method, to aid in the structure identification. Co-and re-chromatography can also be preformed. This method involves scraping the spots off the

cellulose and running them on a highly sensitive technique, such as GC/MS or liquid chromatography/mass spectrometry (LC/MS) (Hemminki et al. 2000).

DNA adducts are formed when exogendous, or endogenous, compounds are converted into electrophiles by metabolic activation. Once an electrophile is formed, the nucleophilic centers found in nucleic acids and proteins attract them. This attraction causes a covalent bond to occur which binds the metabolite to DNA (Reddy and Randerath 1986). Once a DNA adduct is formed, a mutation can occur when the adducted DNA undergoes replication. An adducted base has the ability to cause multiple problems. Some of these problems include: misincorporation, slippage by DNA polymerase, and misrepair. All of these problems may lead to a mutation. Not all DNA mutation is caused by bulky DNA adducts, however, as endogenous DNA damage is possible, and mutations may spontaneously appear as well. The benzo(a)pyrene diol epoxide (BPDE), which has been shown to bind to the N^2 of guanine (N^2-G), has also been shown to cause a GC $\longrightarrow$ TA mutation by Jelinsky et al. in1995. Compounds that will bind to the DNA generally will bind at multiple places, creating multiple adducted sites (Hemminki et al. 2000).

DNA adducts have been identified in various known human carcinogens. For compounds such as aflatoxins, 4-aminobiphenyl, benzidine, ethylene oxide and tamoxifen DNA adducts have been identified *in vitro* and *in vivo* (animals, as well as in humans) (Hemminki 1993; Randerath et al. 1996). BAP has been studied extensively with ^{32}P-postlabeling assays. These assay have shown large levels of DNA adducts with after BAP treatment (Booth et al. 1999; Boysen and Hecht 2003; Godschalk et al. 1998; Gupta et al. 1982; Lu et al. 1986; Reddy and Randerath 1986; Reddy et al. 1984). There have also been studies on the association between levels of DNA adducts and tumor formation. Nesnow et al. (1995) did a study on linking DNA adducts and tumor formation of PAHs. They tested BAP, BBF, DA, 5-methlychrysene(5MC) and cyclopenta(cd)pyrene (CPP) in A/J male mice that were administered PAHs in tricaprylin with a single i.p. injectyion (0 - 200 mg/kg). With increasing levels of PAHs, the lung cancer incidence increased as well. However, there was not a strong difference

observed with regard to adduct formation, they did find that DBA, 5MC and CPP all had a much higher potency for tumor formation than BAP.

Otteneder and Lutz 1999 did a study on the correlation of DNA adduct levels with tumor incidence. They tested several compounds, including several PAHs, and found that fluoranthene (FA) exhibited the highest DNA adduct levels, follwed by CPP with BF and BAP at relatively the same potency. They also found it difficult to correlate DNA adduct levels with tumor incidence. One explanation that they offer for this is due to the reduction in DNA adduct levels after each replication. They suggest that DNA adducts are reduced by a factor of two when replication occurs. This in return would suggest that cell division is a confounder for interpretation of DNA adduct levels. Reddy and Randerath (1986) studied the DNA adduct levels of BAP, 7-12-dimethylebenz(a)anthracene (DMBA), debenzo(c,g)crabazole (DBC), and 4-aminobiphenyl (ABP). They showed that DBC had the highest DNA adduct levels, followed by DMBA, ABP and finally BAP. Booth et al. (1999) did a study on the effects of solvent on BAP DNA adduct formation. They found that the type of solvent used affected BAP adduct formation (*n*-dodecane showed less DNA adduct formation then tetrahydrofuran). However, they also observed no DNA adduct formation from the solvent controls, suggesting that carcinogens need to be present for DNA damage to occur. DNA adduct damage has also been observed in application of mixtures. Randerath et al. (1994) induced DNA damage in rat lung DNA from wood preserving wate (WPW) extracts *in vitro*. They demonstrated that it was possible to induce DNA adducts from WPW through *in vitro* application. Randerath et al. (1997) demonstated levels of DNA adducts in mice exposed to WPW extracts. Very diverse patterns of adducts were observed in this assay, and these included exogenous adducts and endogenous (I-compounds) adducts. They showed that a complex mixture induces type I I-Compounds (adducts), which areassociated with carcinogenesis (Moorthy et al. 1994; Randerath et al. 1988; Randerath et al. 1995). Randerath et al. (1999) found that sediment extracts also showed varying patterns of DNA adducts. They analyzed total adducts as well as the levels of spot 4 adducts, which is associated with the BAP diol

epoxide (Lu et al. 1986). Interestingly, the spot 4 adducts make up approximately half of the total adducts detected. Boysen and Hecht (2003) analyzed BAP DNA and protein adduct levels found in humans. They found that for the number of samples analyzed, 39% detected BPDE-DNA adducts while 59% detected BPDE-protein adducts, however no single exposure type (smoking, occupational, environmental, non-smoking) was associated with overwhelming levels of adducts. This study demonstrates the importance of studying PAHs and their ability to produce DNA adducts and tumors.

DNA adducts are a good quantitative measure of DNA damage, and potential carcinogenic outcome. However, they cannot be interpreted as a measure of the absolute carcinogenic potential of a compound. It is important to carry out a tumorigenesis model in order to identify if DNA adduct frequency correspons to carcinogenic potential of certain compounds (Hemminki et al. 2000).

1.4.2.2 Infant Male Mouse Tumor Model

DNA adducts can lead to a tumorigenic outcome, however, the presence of DNA adducts alone does not mean tumors will develop (Hemminki et al. 2000). It is important to determine if tumorigenesis is the endpoint of an exposure to certain compounds. This is the ultimate measurement of carcinogenic potential of a compound or chemical mixtures. The research reported in this dissertation was modeled after a study carried out by Rodriguez et al. in 1997. Male and female infant B6C3F1 mice were exposed one time via intraperitoneal injection to BAP or a complex mixture of manufactured gas plant residue (MGP). Maximum tolerable doses for BAP were determined previously (Rodriquez et al. 1997). In the current study, only the male mice were used, along with the same doses of BAP used by Rodriquez et al. (1997). Infant mice, 15 days old, were treated with six chemicals in the Rodriguez study. However, due to constraints from the breeder and the animal facility, mice in this study were received at 15 days, and treated at 21 days of age. Mice were weighed and then injected intraperitoneally with a single dose, and then sacrificed at 26, 39, and 52 weeks after exposure. Based on the data gathered, this study sacrificed animals at 280 days, 40

weeks, after exposure. Liver, lung, forestomach tissues were harvested from the mice for histopathology and tumor classification.

1.5 Objectives and Specific Aims

This research investigated the genotoxic interactions of various fractions isolated from a WPW oil. This material is a common contaminant of soil and groundwater in the United States. The WPW used in this study was a complex mixture of petroleum hydrocarbons, PAHs, chlorinated compounds and PCAs. Due to the prevalence of these compounds in the environment, and the potential for exposure to human and ecological receptors, detailed information regarding the genotoxic potential of WPW mixtures would be very useful for regulatory agencies. The overall hypothesis of the study is that isolation of high molecular weight PAHs from a complex mixture will allow increased expression of genotoxicity *in vitro* and *in vivo*. Research activities have included chemical separation and fractionation of a complex WPW mixture, analysis of chemical components and genotoxicity using microbial cell cultures and animal models, and for a limited number of samples, evaluation of carcinogenic potential in an infant mouse model.

The specific aims of this research include:

1. Separate a complex PAH mixture into acid, base and neutral fractions, enrich a PAH and PCDD fraction and analyze genotoxicity using *in vitro* and *in vivo* bioassays.
2. Investigate the frequency and persistence of bulky DNA adducts produced by the model carcinogen BAP, a reconstituted mixture and isolated fractions from WPW *in vivo*.
3. Investigate the relationship between the formation of DNA adducts and tumors in infant mice exposed to the model carcinogen (BAP), a reconstituted mixture, and the neutral fraction from WPW.

In order to accomplish the goals of this research, a series of experiments have been completed. Initially, a complex WPW was collected from a Superfund site in the Northwestern United States. This material was separated, using a liquid-liquid extraction method, into acid, base and neutral fractions. These fractions were initially screened for genotoxicity using *in vitro* microbial bioassays. Genotoxicity fractions were further analyzed *in vivo* using the ^{32}P-postlabeling assay. Next, a pure compound, reconstituted mixture and neutral fraction were evaluated for their ability to bind with DNA and form bulky adducts. Finally, a model compound, reconstituted mixture and the neutral fraction were evaluated using an infant male mouse tumor model. These studies have been conducted to determine if the formation of DNA adducts is a valid predictor of tumor incidence.

CHAPTER II
GENOTOXICITY OF A COMPLEX CHEMICAL MIXTURE AND ISOLATED FRACTIONS

2.1 Introduction

The ability of a complex chemical mixture to induce cancer in humans has been clearly demonstrated (IARC 1998a, IARC 1998b). Studies of populations exposed to PAH mixtures have demonstrated a link between these exposures and cancer of the lung, respiratory system and stomach (Bertrand et al. 1987; Krewski and Thomas 1992; Puisieux et al. 1991; and Vyskocil et al. 2004). Complex PAH mixtures have also been clearly shown to cause cancer in animals (Culp et al. 2000; Rodriguez et al. 1997; Vesselinovitch et al. 1975a; Vesselinovitch et al. 1975b; Von Tungeln et al. 1999). Although PAH mixtures are known to cause cancer in animals and humans, the potential interactions of carcinogenic and non-carcinogenic PAHs are poorly understood. Short-term *in vitro* and *in vivo* bioassays provide a useful tool for investigating potential interactions of chemical mixtures.

The use of creosote, a PAH mixture, to extend the life of wood is associated with extensive environmental contamination at treatment plants. A range of materials including creosote, PCP and heavy metals have been used as wood preservatives. Creosote is composed of PAHs, phenolic compounds, and heterocyclic compounds (N-, S-, and O-) at approximately 85%, 10%, and 5% respectively (Creosote-contaminated sites paper). PCP, a biocide, was widely used as a wood preservative in the United States until 1987, when its use was restricted (USEPA 2006d). Technical grade PCP contains trace levels of chlorinated dioxins that are by-products of the production process. In the United States, there are 26 wood preserving sites on the National Priorities List (NPL) with 18 on the Final NPL. In addition, there are 749 sites on the NPL where PAH mixtures are listed as contaminants of concern. Data are needed to more accurately characterize the genotoxic potential of the complex mixtures that are common in the environment.

There is currently no widely accepted protocol for risk assessment of complex mixtures. Complex mixtures typically contain hundreds of different chemical components. This may include components that are toxic or non-toxic, soluble or insoluble. These components may produce a broad range of chemical interactions that may result in additive, synergistic or antagonistic interactions. In some cases, it may be necessary to isolate similar components of a complex mixture in order to identify the most genotoxic constituents. The USEPA has published "Guidelines for the Health Risk Assessment of Chemical Mixtures" in an effort to produce consistent risk assessments concerning chemical mixtures. These guidelines define a mixture as any combination of more than one chemical. The guidelines suggest three different approaches to mixture assessment. The approaches are based on the amount of information that is available on the mixture of concern. When data is available on the mixture of concern, chronic and subchronic toxicities can be used in the risk assessment. When there is no data available for the mixture of concern, but there is a sufficiently similar mixture with data available, that data may be used. However, dissimilarity of the mixtures should be taken into consideration. Finally, when data is not available on the mixture of concern as well as any reasonably similar mixtures, toxic or carcinogenic properties of the individual components may be used. Most important, risk assessment should be tailored to the mixture of concern, taking into account the many levels of complexity a mixture poses.

An understanding of how chemicals will interact is extremely important when evaluating the risk associated with an exposure. Adsorption, distribution, metabolism, excretion and activity at the receptor site are all processes where chemical interactions may occur. Therefore, when a risk assessment is done on a chemical mixture, all assumptions and processes should be considered in order to have the most complete picture possible. The criteria specified include different approaches, tailored to the specific chemicals in question (USEPA 1986). The approaches, however, concentrate on what is known about specific chemicals in the mixture. The problem with complex mixtures is that most of the interactions that take place are unknown. It is important to

evaluate chemical mixtures as a whole, and in parts, in order to better understand the interactions that may take place.

The following text reports on experiments to isolate and characterized the most genotoxic components of a complex mixture. A complex WPW was seporated via a liquid-liquid extraction in order to obtain an acid, base and neutral fraction from which PAH and PCDD enriched fractions were isolated. A series of *in vitro* and *in vivo* bioassays were used to identify the most genotoxic fractions.

2.2 Materials and Methods

2.2.1 Site History

The material used for this study was collected from a former wood treatment facility. This facility was active for approximately 23 years, from 1946 to 1969. During operations, the site used waste pits to dispose of waste water and tank bottom sludge collected from wood-treating fluid tanks. Area homeowners detected contamination in their private wells around 1979, and the USEPA listed the site on the NPL in September of 1983. Two Record of Decisions (RODs) were filed, and direct the three stages of work that were agreed to by the responsible party. In 1988 the USEPA decided on the following remedy for cleaning and containing the source of contamination: 1) Excavation and consolidation of 45,000 cubic yards of contaminated soil and debris, treatment by biodegradation using microorganism, and disposal by capping in lined treatment cells, 2) Collection of contaminated ground water from the upper aquifer and above ground treatment by bioremediation using microorganisms, 3) Treating remaining contamination in situ by adding oxygen and nutrients through injection wells to the ground water, 4) Initiating pilot studies for evaluation of technologies for the lower aquifer, and 5) Monitoring the site for five years to ensure effectiveness. As of 2006, all excavation has been completed, while the bioremediation treatments of soil and groundwater are ongoing.

2.2.2 Sample Collection

The underground aquifer at this site became heavily contaminated with a dense non-aqueous phase liquid (DNAPL) from a WPW. The WPW collected for use in this study is a complex mixture of creosote compounds including PAHs, and elevated concentrations of PCP. Water from the contaminated aquifer is pumped from various wells into an oil/water separator prior to bioremediation. Oil and non-aqueous phase liquids from the aquifer accumulate in the bottom of the oil-water separator. The complex mixture used in this research was collected as an aliquot of the material accumulated at the bottom of an oil/water separator. The sample was collected in four 250 mL amber glass I-Chem bottles, from a spigot connected to the oil-water separator. In the laboratory the WPW was autoclaved in 100 mL aliquots three times each, for 45 min, at 121°C, 115 psi using an American sterilizer Company autoclave (Erie, PA). The WPW was then mixed thoroughly, and separated into four sterile 250 mL wide-mouth amber I-Chem bottles.

2.2.3 Chemicals and Materials

Sodium hydroxide (ASC reagent grade, 98.2% pure), and silica gel (ACS grade, 3-8 mesh size) were purchased from Fischer Scientific (Fairlawn, NJ). Sulfuric Acid (95-98% pure), methylene chloride (ACS reagent grade, 99.5% pure), and acetone (ACS reagent grade, 99.5% pure) were purchased from EM Science (Gibbstown, NJ). Pentachlorophenol (98% pure), benz(a)anthracene (99% pure), chrysene (98% pure), benzo(b)fluoranthene 98% pure), benzo(k)fluoranthene (98% pure), benzo(a)pyrene (97% pure), dibenz(a,h)anthracene (200µg/mL in CH_2Cl_2), tetradecane (olefine free, >99% pure), carbon (>99%), alumina (~150 mesh, 58/ standard grade), sodium sulfate (ACS grade), and sand (white quartz, -50 + 70 mesh) were purchased from the Sigma-Aldrich Group (St. Louis, MO). The following chemicals were purchased from Honeywell Burdick & Jackson (Muskegon, MI): hexane (capillary GC/MS solvent, 87.3% pure), methanol (high purity solvent, 99.9%+ pure), acetone (high purity solvent, 99.9%+ pure), toluene (high purity solvent, 99.9%+ pure), methylene chloride (high

purity solvent, 99.9%+ pure), and cyclohexane (high purity solvent, 99.9%+ pure). Indeno(1,2,3-c,d)pyrene (1000 μg/mL in CH_2Cl_2) was purchased from Absolute Standards (Hamden, CT). Glass fiber filter (type A/E 8"x10" sheet) was purchased from Pall Gelman Sciences (Ann Arbor, MI).

2.2.4 Animals

All animals were obtained from Harlan (Houston, TX). Strains used were Hsd:ICR (CD-1®) female mice, 15 weeks old, 21 to 24 g. These mice are outbread albino descents from Charles River Laboratories (Wilmington, MA) animals. Mice were shipped via Harlan truck in filtered shipping containers. Mice were housed in a barrier facility, 3 mice per filtered cage. Mice were fed ad libitum using sterilized food provided by the facility. Water was also ad libitum, using filtered and sterilized water provided by the facility.

2.2.5 Statistics

Statistics were preformed using Systat Software, Inc. SigmaStat 3.11 software and SPSS Inc. SigmaPlot 8.02 software. Simple statistics were preformed using this software, once all data was transformed to the log value of the raw data. Normality test used was Kolmogorow-Smirnov. One Way ANOVA test was preformed using the Holm-Sidak method for all pairwise multiple comparison procedures using $\alpha = 0.05$. P-values were equal to <0.001 for all ANOVAs preformed, except for the lung tissue total DNA adduct analysis. The p-value for that analysis was equal to 0.004. Descriptive statistics were also preformed, to obtain data for SigmaPlot graphs.

2.2.6 Extraction and Fractionation of Complex Mixture

Since the WPW was collected as pure oil, no extraction was necessary. The WPW oil was partitioned into acid, base and neutral fractions following the USEPA 3650B method (USEPA 1997a). A schematic of this separation is provided in Figure 2.1. All fractions were then analyzed for chemical content using GC/MS. A 120 mL volume

(119g) of WPW was fractionated into an acid/base/neutral fraction following the EPA's Standard Method 3650B. A 30 mL volume of WPW, 60 mL of CH_2Cl_2, and 60 mL of NaOH pH12 was added to a 2000 mL separatory funnel and shaken for 2 min. Once the phases separated, the upper aqueous layer was removed, and the lower organic layer (base/neutral fraction) extracted two more times. The three aqueous layers were combined and the pH adjusted to <2 with 1:1 H_2SO_4:dH_2O. In a clean separatory funnel, the aqueous layers and 60 mL of CH_2Cl_2 were shaken for 2 min, followed by the removal of the organic layer. The aqueous layer was then extracted two more times. The three organic layers were combined to form the acid fraction.

The base/neutral fraction plus three volumes (~633 mL) of 1N H_2SO_4 and 300 mL CH_2Cl_2 were then shaken in a new separatory funnel for 2 min. Once the phases separated, the organic phase was removed and the aqueous phase extracted one more time with 300 mL CH_2Cl_2. The two organic layers were combined to form the neutral fraction. The neutral fraction was further enriched for PCDDs and then for PAHs using column chromatography. The aqueous layers were combined and adjusted to a pH of 12 with 10N NaOH. This layer was then extracted with a volume of 600 mL, 300 mL, and 30 mL CH_2Cl_2, in succession. Each extraction was shaken for 2 min and the organic layer collected. The three organic layers were combined to make the base fraction. Fractions were concentrated on a Kuderna-Danish (K-D) apparatus after passing through anhydrous sodium sulfate (Na_2SO_4).

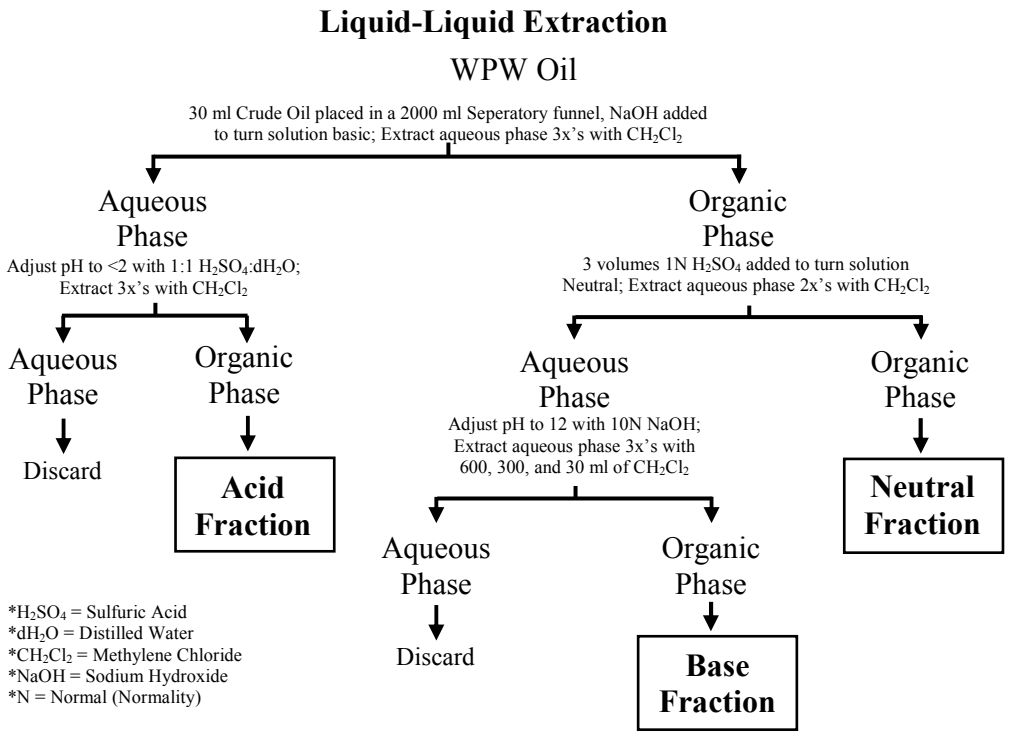

Figure 2.1. Schematic of the protocol used to partition WPW oil into acid, base and neutral fractions.

2.2.7 PCDD Enrichment

A total of 32 g of the neutral fraction, isolated from the WPW, was enriched for PCDDs following the protocol developed by the Texas A&M University Geochemical and Environmental Research Group (GERG) (Wang and Chambers 1997). A schematic of this enrichment is provided in Figure 2.2. For PCDD enrichment, 4.4g of neutral fraction, 200 mL of hexane, and 40g of 40% H_2SO_4/silica gel slurry were stirred for 2 hr (for quantification, 25 µl of tetradecane was added). The sample was then filtered through sodium sulfate, rinsed with hexane three times, and reduced to a volume of ~50 µl, using a rotary evaporator at 250 mbars. A mixed bed silica column was prepared by packing a 300 mm x 13 mm (i.d.) column with (bottom to top): a combusted glass wool plug, approximately 1 cm of combusted sand, 1 g activated room temperature silica gel, 4 g 33% 1N NaOH/silica gel, 1 g activated room temperature silica gel, 8 g H_2SO_4/silica gel acid slurry, 2 g activated room temperature silica gel, and approximately 1 cm combusted room temperature sodium sulfate. The column was pre-rinsed with 100 mL hexane. A 250 mL collecting flask was placed under the column, and the sample added, rinsing the flask three times with 2 mL of hexane. A 120 mL volume of hexane was added to the column, and allowed to drain.

The column eluate was collected and reduced to a volume of ~100 µl, using a rotary evaporator at 250 mbars. The eluate from the silica column was enriched further using a carbon column. The carbon column (1.2 cm i.d. x 13 cm) was prepared as follows: a glass wool plug was placed approximately 1 ½ in from the bottom, a 1 cm layer of activated silica gel was added, followed by 1 g of 5% AX-21 carbon/silica gel, and a second glass wool plug. The column was then inverted and primed by rinsing with a 5 mL volume of 1:1 dichloromethane:cyclohexane (DCM:CHX), inverted again, and rinsed a second time with a 5 mL volume of 1:1 DCM:CHX. Excess solvent was allowed to drain from the carbon column. Silica gel eluate was transferred to the carbon column by rinsing the flask three times with 2 mL volume of 1:1 DCM:CHX. An additional 6 mL of 1:1 DCM:CHX was added to the carbon column, bringing the total volume to 22 mL. A 20 mL volume of 75:20:5 dichloromethane:methanol:toluene

(DCM:MEOH:TOL) mixture was then added to the carbon column, and allowed to drain by gravity flow. The column was then inverted, and the PCDD fraction eluted. A 125 mL collecting flask was placed under the column, and two 25 mL volumes of toluene were added. The sample was then reduced on a rotary evaporator at 250 mbars, transferred by rinsing the flask three times with toluene to a pre-weighed glass vial, and dried under a stream of nitrogen. This process was preformed a total of seven times each.

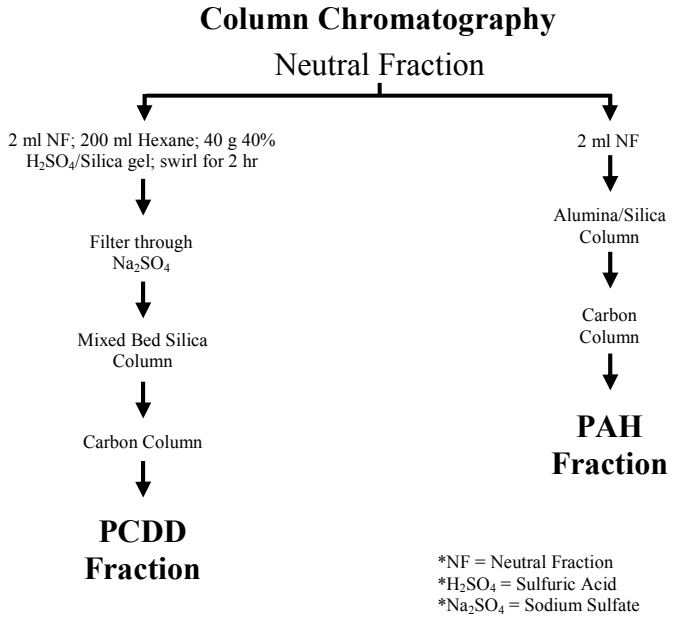

Figure 2.2. Schematic of the protocol used to produce enriched PCDD and PAH fractions.

2.2.8 PAH Enrichment

A 10 g aliquot from the neutral fraction was enriched for PAHs following the protocol developed by the Texas A&M University GERG (Wang and Chambers 1997). A schematic of this enrichment is provided in Figure 2.2. For PAH enrichment, a 1.6g mass of neutral fraction WPW was directly added to an alumina/silica column (13 mm x 300 mm i.d.). The alumina/silica column was prepared as follows: a glass wool plug, 10

g alumina (mixed with dichloromethane to reduce formation of air pockets), 20 g silica gel, and approximately 1 cm of anhydrous Na_2SO_4. The dichloromethane was allowed to drain from the column, after which a 100 mL volume of hexane was added. Once the hexane front was 1 cm from the Na_2SO_4 layer, a 1.6 g mass of the neutral fraction was added to the column. The enriched PAH fraction was then eluted from the column. First, an 80 mL volume of hexane was added to the column. Once the hexane reached the Na_2SO_4 layer, a 125 mL collecting flask was placed under the column and a 100 mL volume of toluene was added. The sample was then reduced to a volume of approximately 20 μL on a rotary evaporator at 80 mbars, and further enriched using a carbon column (as described above for the PCDD fraction). The sample eluate was collected in a flask and transferred by rinsing the flask three times with toluene to a pre-weighed glass vial, and dried under a stream of nitrogen. This process was conducted a total of six times each.

2.2.9 Preparation of a Reconstituted Mixture

A reconstituted mixture was prepared for comparison with the neutral fraction in the ^{32}P-postlabeling study. This mixture contains seven USEPA carcinogenic PAHs, as well as PCP. All of these compounds are defined as class B2 carcinogens by the USEPA. These chemicals were chosen because they represent the carcinogenic chemicals quantified in the neutral fraction, and include chrysene, BAA, DA, BAP, IP, BBF, BKF, and PCP (Figure 2.3).

Chemical Composition of Reconstituted Mixture

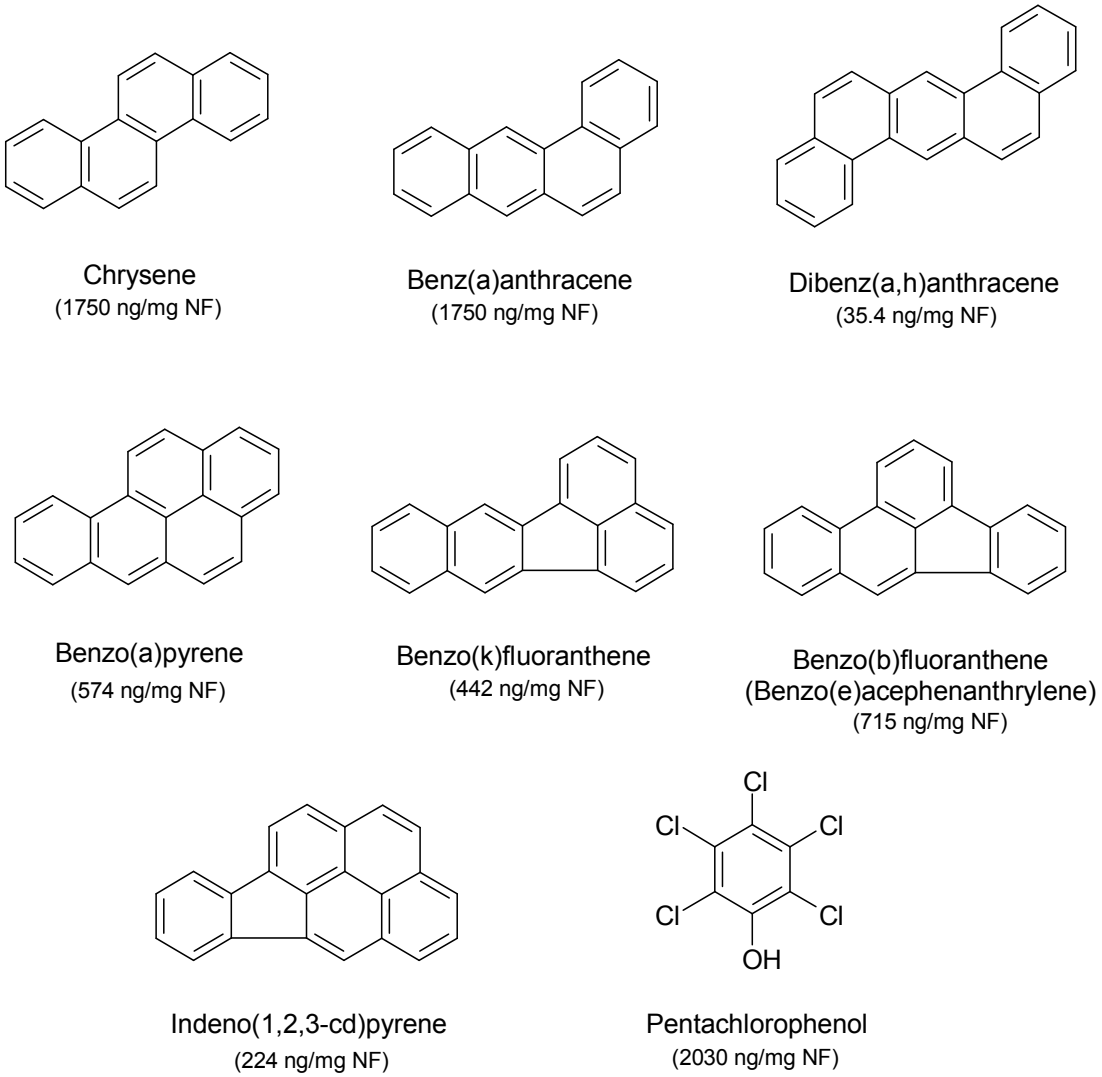

Figure 2.3. Structures and quantities of the eight class B2 USEPA carcinogens present in the reconstituted mixture.

Chemical analysis of the neutral fraction was used to calculate the mass of each of the eight chemicals that would be equivalent to the quantity detected in the neutral fraction for a 3 mg/mouse dose in the *in vivo* assay. Neutral fraction chemical analysis values were used to calculate mg fraction/mL dose volume. Calculations were prepared as follows:

Calculation for mg chemical/mL methylene chloride per mouse (highest dose shown):

$$\frac{\text{ng chemical}}{\text{mg fraction}} \times \frac{\text{3.0 mg fraction}}{\text{Mouse}} = \frac{\text{ng chemical}}{\text{Mouse}} \times \frac{\text{1 µg}}{\text{mg fraction}} \times \frac{\text{1 mg}}{\text{mg fraction}} = \frac{\text{mg chemical}}{\text{mouse}}$$

$$\frac{\text{mg chemical}}{\text{0.150 mL/ mouse}} = \frac{\text{mg chemical}}{\text{mL/mouse}} \quad \text{in highest dose}$$

Calculation for mg chemical needed for a 4 mL total volume:

$$\frac{\text{mg chemical}}{\text{mL/ mouse}} \times \text{4 mL vol. of highest dose} = \text{mg chemical/4 mL}$$

Calculation for µL of 5mg/mL stock solution needed to obtain mass of chemical calculated:

$$\frac{\text{5 mg chemical}}{\text{mL}} = \frac{\text{mg chemcial}}{\text{X mL}} \qquad \text{X} = \text{mL Stock} = \text{µL Stock}$$

All calculations were checked, and entered into excel spreadsheets. A 5 mg/mL stock solution was prepared for all chemicals, except chrysene, indeno(1,2,3-cd)pyrene and dibenz(a,h)anthracene. Due to the low solubility of chrysene, a 1 mg/mL stock solution was made. A 1 mg/mL and 0.2 mg/mL stock solution was made for indeno(1,2,3-cd)pyrene and dibenz(a,h)anthracene respectively as only neat solutions could be obtained and not crystals. The 5 mg/mL stock solutions were made by weighing 15 mL of chemical into a 5 mL glass vial using a Sartorius CP64 analytical balance, Aldinger Company, Dallas, TX. Next, 3 mL of methylene chloride were added to each vial. Once each chemical was dissolved, the calculated amount of stock solution, in µL, was added

to the 3 mg/mouse dose equivalent reconstituted mixture vial. After all chemicals were pipetted into the vial, a volume of methylene chloride was added to make the total volume in the vial 4 μL. The final solution in this vial was 20 mg/mL, a 3 mg/mouse dose equivalent. To make an 8 mg/mL solution, a 1.2 mg/mouse dose equivalent, 0.8 mL of the 20 mg/mL solution was added to a new vial with 1.2 mL of methylene chloride. An aliquot of 1 mL from the 20 mg/mL solution was put into another vial for chemical analysis. Each vial was sealed with a teflon lined cap, and put in the freezer for short-term storage. Vials were wrapped in teflon tape, and placed on ice for transport. Solutions were made one day prior to use.

2.2.10 Chemical Analysis

2.2.10.1 PAH Analysis

PAH analysis was conducted using a modified 8270B USEPA standard method (USEPA 1997b). Analysis was conducted on a Hewlett-Packard 5890 Series II gas chromatograph with a 5972 mass selective detector in selected ion monitoring mode. A 60m x 0.25mm ID x 0.25mm film thickness column (Agilent Technologies, Palo Alto, CA) was used. The injection port is maintained at 300°C and the transfer line at 280°C. The temperature program is as follows: 60°C for 6 min, increased at 12°C/min to 180°C and then increased at 6°C/min to 310°C and held for 11 min for a total run time of 47 min.

2.2.10.2 PCDD Analysis

PCDD analysis was done using an analytical method which is similar to USEPA Test method 1613 (USEPA 1997c). Dioxins/furans were analyzed by a high resolution gas chromatography (Hewlett Packard 6890 /high resolution mass spectrometer (VG Autospec) equipped with a DB-5ms column (60 m x 0.25 mm, i.d., J&W Science). The GC oven temperature was programmed to from 190ºC to 260ºC at a rate of 4ºC/min after holding at 190ºC for 2 min. The oven temperature was held at 260ºC for 3 min and then raised to 320ºC at a rate of 8ºC/min and was held for 10 min at 320ºC. Isotopically

labeled PCDDs and PCDFs were added to each sample prior to sample processing to facilitate the identification and quantitation of PCDDs and PCDFs.

2.2.11 *In Vitro* Bioassays

2.2.11.1 *Salmonella*/microsome Assay

The standard *Salmonella*/microsome assay, first described by Ames et al. (1975) and then revised by Maron and Ames (1983), was used to measure the mutagenicity of the WPW oil and acid, base, and neutral fractions. Briefly, a 50 µl volume of sample, 0.1 mL of TA98 *Salmonella* overnight culture, and 0.5 mL of 20% S-9 Rat Liver Enzyme (for +S-9 plates), or 0.5 mL PO_4 buffer (for –S-9 plates) were added to 2.5 mL minimal top agar. The agar was then poured onto the plate, swirled, and allowed to set. The plates were then inverted and incubated for 72 hr at 37ºC. After incubation, revertant colonies were enumerated using an Artek 880 automatic plate counter, Dynatech Laboratories Inc., Chantilly, VA. Positive controls included 2-nitrofluorene (2NF) (25 µg/plate) and BAP (10 µg/plate), while the negative control was dimethylsulfoxide (DMSO). The mixtures were tested at a dose of 50, 20, 10, 5, 2, and 1 mg/mL. A positive response is equal to a two fold increase over the solvent control (negative control). All samples were tested on duplicate plates in two independent experiments.

2.2.11.2 *E. coli* Prophage Induction Assay

The standard *E. coli* prophage induction assay, described by Rossman et al. (1984) and DeMarini et al. (1990), was used to screen the samples for DNA damage or inhibition of DNA replication. Briefly, a 250 µL volume of VBMM supplement was added to the first row of wells in the microtiter plate, and 150 µL of VBMM supplement were added to the remaining rows of the microtiter plate. A 50 µL volume of sample or control (acetone, VBMM supplement, 2NF for –S9 or 2AA for +S9) was added to the appropriate wells in the first row. A 2-fold dilution was then preformed by transferring 150 µL from row A sequentially through row H. 75 µL of *E. coli*

lambda lysogen WP2s(λ)18 and 25 μL of 2.5% S9 (for the +S9 microtiter plate) or VBMM (for the –S9 microtiter plates) were added to each of the eight wells. The microtiter plates were then covered with mylar film, wrapped in plastic wrap, and incubated for 24 hr. Two tubes of TH008 indicator strain were prepared as overnights via the following method. Frozen permanents, and oxoid broth were allowed to come to room temperature. A 100 μL volume of the frozen permanents was aseptically transferred to two oxoid broth tubes. The two inoculated oxoid broth tubes, plus one non-inoculated oxoid broth tube (control) were shaken/incubated overnight for 10 hr at 200 rpms and 37°C. After overnight growth, a volume of 250 μL of TH008 overnights were transferred aseptically to four tubes of room temperature oxoid broth tubes per microtiter plate for mid-log phase growth (approximately 1.5 hr). The microtiter plates were scored for cytotoxicity (clearing of media) and the five highest turbid wells were then sampled. The quantity of the phage released during this incubation is a measure of the extent of DNA damage. A 50 μL volume of diluted phage was then transferred to 5 mL of VBMM supplement and vortexed. A 200 μL volume of log-phase indicator cells was added to 2.5 mL volume of Luria broth top agar. Next, a 100 μL volume of diluted phage was added to two top agar + TH008 tubes (for A and B plate replicates), and vortexed. Top agar contents were then poured onto tryptone media plates, inverted, and incubated for 24 hr at 37°C. After incubation, plates were scored for plaque formation using a manual colony counter. The phage was quantified at the five highest, non-cytotoxic dose levels per treatment. The dose ranges tested were 2.5, 1.25, 0.625, 0.3125, and 0.15625 mg/mL in acetone. Positive controls used were 2-aminoanthracene (2AA) and 2NF, while negative controls used included VBMM and acetone. All samples were tested + and – S9 in two independent experiments.

2.2.12 *In Vivo* Bioassays

2.2.12.1 DNA Adducts in Mice, Topical Application

Dosing procedures were followed as previously described in Reddy and Randerath (1986). CD-1 female mice, 15-weeks old, were weighed and placed into groups to

ensure that the average weight for each group was approximately the same. Mice were then shaved and left for 24 hr. After 24 hr, the mice were shaved once more, allowing the chemicals to be applied directly to the skin, reweighed, and groups adjusted so any mice with nicked skin were not used. A 150 µl volume of sample in CH_2Cl_2 at doses of 3, 1.2, or 0.48 mg/mouse was topically applied. A total of eleven groups of mice, four mice per group, were treated with samples. Treatments included one each for crude oil, acid fraction, base fraction, PAH fraction and PCDD fraction at a dose of 3 mg/mouse. Three groups were treated with different concentrations of neutral fraction, for dose-response, at doses of 3 mg/mouse, 1.2 mg/mouse and 0.48 mg/mouse. Two groups were treated with different concentrations of reconstituted mixture, for dose-response, at doses of 3 mg/mouse and 1.2 mg/mouse. After 24 hr, mice were sacrificed, and exposed skin, lung and liver tissues were harvested. Tissues were immediatley stored in a -80°C freezer.

2.2.12.2 ^{32}P-postlabeling

DNA was extracted from mouse tissues, digested and labeled with γ^{32}P[ATP] following methods described previously by Reddy and Randerath (1986). A 0.2 to 0.5 g weight of minced mouse tissue was weighed into a 15 mL glass tube. A 3 mL volume of 1% SDS/1mM EDTA was added, and the tissue was homogenized for 30 to 60 sec at 15,000 to 20,000 rpm. Next, 100 to 150 µL proteinase K (15 mg/mL) was added to the homogenate, and the sample was then vortexed and incubated for 40 min at 38°C. The next step involves deproteinization using three solvent extractions. A 170 µL volume of 1M Tris-HCL, pH 8.0, and 35 µL 100 mM EDTA were added, and then vortexed. For the first extraction, a 3 mL volume of phenol saturated with 50 mM Tris-HCL, pH 8.0, 1 mM EDTA was added, and shaken for a minimum of 3 min. The sample was then spun for 10 min at 10000 rpm. The aqueous phase was transferred to a fresh tube. For the second extraction, a 3 mL volume of 1:1 mixture of saturated phenol and SEVAG (24 volumes Chloroform + 1 volume isoamyl alcohol) was added, and shaken for at least 3 min. The sample was then spun as described above. The aqueous phase was then

transferred to a fresh tube. For the third extraction, a 3 mL volume of SEVAG was added, and shaken as described above. The sample was then processed as previously described, and the aqueous phase was transferred to a fresh tube.

For precipitation of DNA (+RNA), 0.3 mL (=0.1 volume) 5 M NaCl + 3.3 mL ice-cold absolute ethanol are added, and vortexed. The sample was placed in -20°C freezer for 30 min. The sample was then spun for 10 min at 10000 rpm, and supernatant discarded. Precipitant was washed 2 times with 3 mL 70% ice-cold ethanol, and supernatant decanted. The sample was semi-dried for 4-5 min. The DNA (+RNA) was dissolved in 1 mL 0.01 SSC (150 mM NaCl, 15 mM Na citrate) + 10 µL 100 mM EDTA. Next, 50 µL 1 M Tris-HCL, pH 8.0, + 15 µL Rnase A (10 mg/mL) + 16.5 µL Rnase T1 (5,000 units/mL) are added to sample. The sample was then vortexed, and incubated for 40 min at 38°C. After incubation, 500 µL 0.01 x SSC was added to increase volume. Deprotieniztion was again carried out by solvent extraction. A 1.5 mL volume of SEVAG was added, and shaken for at least 3 mintues. The sample was processed as stated above, and the aqueous phase transferred to a fresh tube. DNA was precipitated by adding 150 µL 5 M NaCl + 1.5 mL ice-cold absolute ethanol. The sample was put in -20°C freezer for 30 min. The DNA was spun, washed, and semi-dried as stated above. DNA was redissolved in 0.3 to 0.6 mL 0.01 x SSC to reach the desired concentration of 2 µg/µL. The concentration of DNA was checked via UV-Vis Spectrophotometer, the A_{260} (DNA)/A_{280} (RNA) ratio should range from 1.6 to 1.8.

DNA digestion and labeling were preformed as follows: 10 µg of DNA in 5 µL of SSC and/or water were digested using 3 µL of 0.2 U micrococcal nuclease and 2.4 µg spleen phosphodiesterase per µL (MN/SPD) and 2.4 µL of IS-buffer mix (10 µg DNA, 100 mM $CaCl_2$ and 300 mM Na succinate) for 3.5 hr at 37°C. MN/SPD digestion cleaves the 5'-nucleotide-phosphate bonds, leaving the 3'-monophosphates of the normal and adducted deoxyribonucleosides. The DNA was then digested with 4.75 µL of nuclease P1 digestion mix (4 µg/µL nuclease P1, 1 M NaOAc and 1 mM $ZnCl_2$) for 40 min at 37°C. Nuclease P1 digestion cleaves the 3'-nucleotide-phosphate bonds on normal nucleotides only. It was reported that adducted nucleotides were mostly or

partially resistant to nuclease P1 3'-dephosphorylation (Reddy and Randerath 1986). The sample was then labeled using 3.86 µL of polynucleotide kinase (PNK) labeling mix (kinase buffer, 100 µC*i*/µL ATP and 30 U/µL PNK) and incubated for 40 min at 37°C. PNK labeling attaches the radioactive phosphate ([γ-^{32}P]ATP) at the 5'-hydroxyl group end of the adducted nucleotides through [^{32}P]phosphate transfer from ([γ-^{32}P]ATP). The normal nucleotides lost their 3'-phosphate during nuclease P1 digestion, so PNK will not phosphorylate them with the ([γ-^{32}P]ATP). Once samples were labeled, two specific activity (SA) tubes (2 pmol/µL dAP and 50 mM CHES, pH 9.5) were then labeled with 2.5 µL PNK labeling mix, and incubated same as the samples.

The samples, with the exception of the SA tubes, were then digested with 1.5 µL of 40 mU/µL potato apyrase for 30 min at 37°C. Apyrase digestion destroys the excess ATP by removing [^{32}P] from the ATP ([^{32}P]-ATP $\longrightarrow$ ADP + [^{32}P]). Once apyrase incubation was completed, normals and SA tubes were diluted. Normals are a qualitative check to make sure that each sample was digested and labeled well. Tubes contain 250 µL of 20 mM CHES, pH 9.5. 1 µL of sample was added to the corresponding tube, and then 5 µL per sample were spotted on PEI-cellulose sheets. SA dilution tubes contain 996 µL of 20 mM CHES, pH9.5. 4 µL of labeled SA tubes (d*pAp mix) were added to each corresponding SA tube, and then 5 µL were spotted on PEI-cellulose sheets. Normals and SA PEI-cellulose sheets were run in 0.28 M $NH_4(SO_4)_2$ + 50 mM NaH_2PO_4, pH 6.7 to 13 cm past the origin line, approximately 1 to 2 hr (Figure 2.4). While normals and SA sheets were running, labeled samples are spotted onto a PEI cellulose sheet (D1 development). D1 sheets were run in 80 mL of

2.3 M NaH_2PO_4, pH 5.75, for 16 hr (Figure 2.5). D1 development removes traces of normal nucleotides after the nuclease P1 treatment, as well as residual orthophosphate by pushing them to the wick at the top of the sheet, leaving the [^{32}P] adducted nucleotides behind. D1 sheets were developed on autoradiographic film, and locations of the spots were then drawn on the back of the PEI-cellulose sheets. Spots were then cutout from the D1 PEI-cellulose sheet and transferred to single PEI-cellulose sheets (2D maps) using a strong magnet (Figure 2.6). 2D maps were run vertically in 65 mL of 95% LFU, pH 3.35 + 5% dH_2O (D3 development) to top marked line after being pre-developed in 25 mL of dH_2O to the origin. 2D maps were then checked for transfer, cut at the second line from the top, washed twice in 250 mL of dH_2O for 7 min, dried, and a wick attached to the right side in preparation for the final development (D4 development) (Figure 2.7). For the D4 development, the 2D maps were run horizontally in 65 mL of 90% PTU, pH 8.20 + 10% dH_2O to the top of the wick after being pre-developed in 25 mL of 50% 0.8 M NaH_2PO_4, pH 8.2 + 50% dH_2O to the second line marked from the left side. 2D maps were then checked for separation, cut just below the wick, washed twice in 250 mL of dH_2O for 5 min, dried, and cut for autoradiographic development and imager reading (Figure 2.7). An instant imager was used to calculate counts per minute (CPM) per spot.

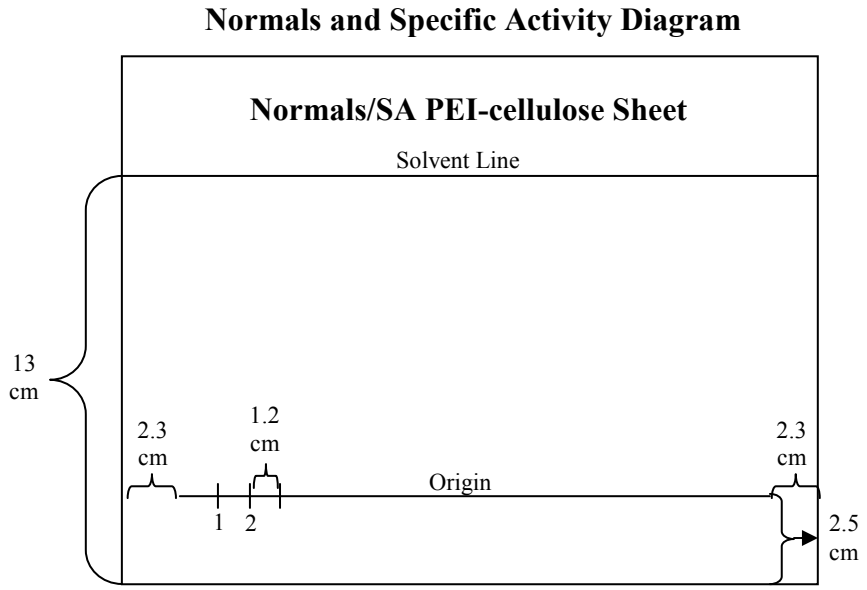

Figure 2.4. Diagram of how the normals and SA PEI-cellulose sheets are set up. An origin line is drawn 2.5 cm from the bottom of the sheet. Tick marks are drawn to represent where spotting of samples will occur. Tick marks begin 2.3 cm from the edge of the sheet and are placed 1.2 cm apart. Each tick mark represents a sample and are numbered accordingly (e.g. 1, 2, …n). The solvent line at the top of the sheet is 13 cm from the origin, and represents the point at which the sheet is removed from the developing solvent.

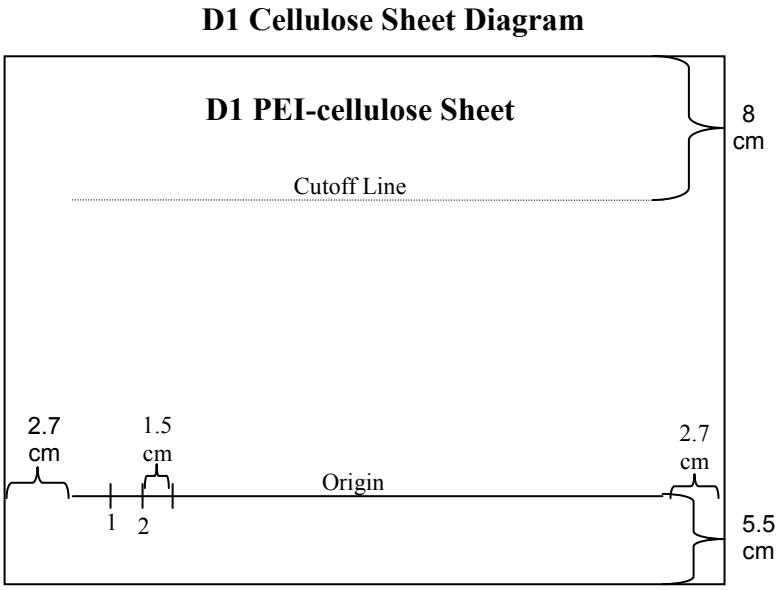

Figure 2.5. Diagram of how the D1 PEI-cellulose sheets are set up. An origin line is drawn 5.5 cm from the bottom of the sheet. Tick marks are drawn to represent where spotting of samples will occur. Tick marks begin 2.7 cm from the edge of the sheet and are placed 1.5 cm apart. Each tick mark represents a sample and are numbered accordingly (e.g. 1, 2, …n). The cutoff line at the top is 8cm from the top of the sheet, and represents the point at which the sheet will be cut, removing the wick which contains approximately 95% of the radioactivity.

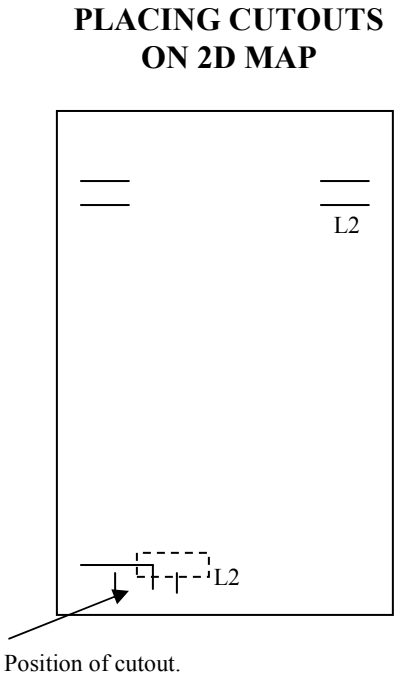

Figure 2.6. Diagram of how to place cutout spots on 2D map. Cutout spot should be placed cellulose-side down on the corresponding 2D map, with the origin on the 90° angle (shown by the hashed rectangle). Cutout should be secured to 2D map using a strong magnet.

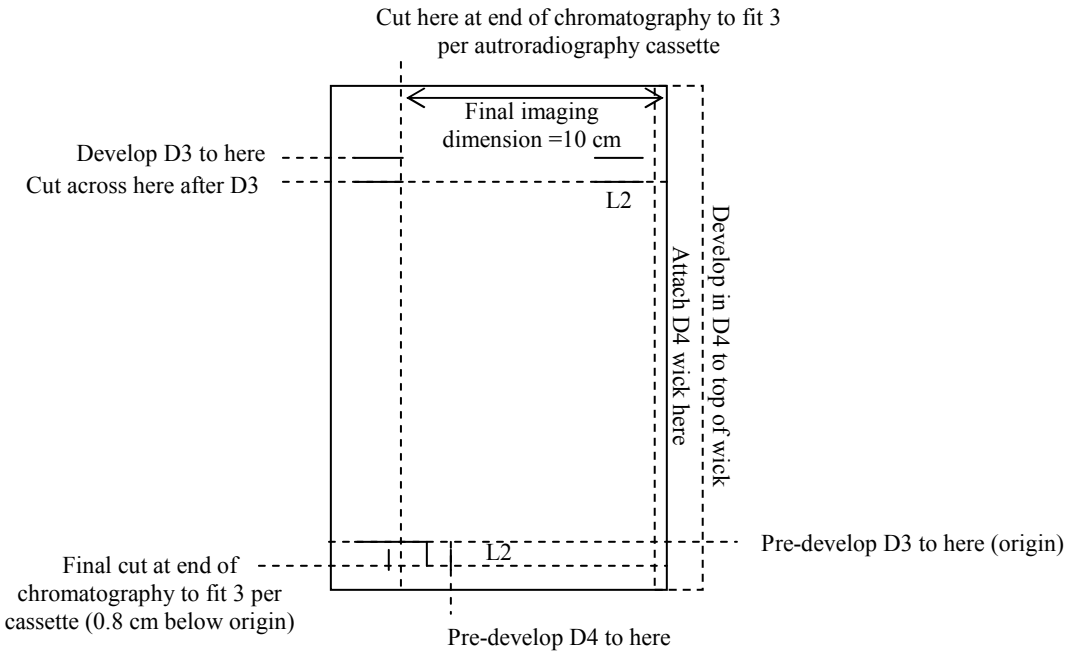

Figure 2.7. Diagram showing developing and trimming guidelines for the 2D map. For D3 development, predevelopment should be done to the first line from the bottom, and final development should be done to the top line. After development, the 2D map should be cut at the second line from the top. For D4 development, predevelopment should be done to the third line from the left, and final development should be done to the top of the wick (attached after D3 development). After development, the 2D map is cut just under the wick. Final cuts are 0.8 cm below the origin, and just to the left of the transfer point. Final cuts are done to fit 3 sheets per autoradiogram.

2.3 Results

2.3.1 Chemical Analysis

A total of sixty PAHs were quantified in each isolated fraction (Table 2.1). The chemical analysis of the fractions from the WPW oil confirmed that high levels of PCP were isolated in the acid fraction (6.93×10^5 ng/mg fraction, Table 2.2). The neutral fraction retained high levels of PAHs, while the base fraction retained a small amount of PAHs (1.75×10^3 ng/mg fraction BaA, 1.75×10^3 ng/mg fraction chrysene, 7.15×10^2 ng/mg fraction BbF, 4.42×10^2 ng/mg fraction BkF, 5.74×10^2 ng/mg fraction BAP, 2.24×10^2 ng/mg fraction IP, and 3.5×10^1 ng/mg fraction DA Table 2.2). PAH concentrations in the reconstituted mixture were shown to accurately reflect the concentrations of the neutral fraction carcinogenic PAHs (cPAHs) (Table 2.3). The cPAH values in the reconstituted mixture were as follows: 1.31×10^3 ng/mg fraction BaA, 1.61×10^3 ng/mg fraction chrysene, 7.16×10^2 ng/mg fraction BbF, 4.23×10^2 ng/mg fraction BkF, 5.33×10^2 ng/mg fraction BAP, 2.09×10^2 ng/mg fraction IP, 3.3×10^1 ng/mg fraction DA, and 2.28×10^3 ng/mg fraction PCP. Although the PCP concentration was highest in the acid fraction (6.93×10^5 ng/mg), the WPW oil and base fraction were also found to contain high concentrations of PCP (Figure 2.8). Total PAH concentrations ranged from 2.95×10^4 ng/mg in the base fraction to 7.78×10^5 ng/mg in the acid fraction. Although the carcinogenic PAH concentration was highest in the PCDD fraction (1.25×10^5 ng/mg), the PAH fraction was also found to have high concentrations of cPAHs (7.11×10^4 ng/mg). In addition, the high molecular weight PAHs, including BAP (1.50×10^4 ng/mg), IP (6.89×10^3 ng/mg) and DA (2.03×10^3 ng/mg) were enriched in the PAH fraction (Table 2.2 and Figure 2.9).

Table 2.1. List of the 60 PAHs quantified in WPW oil and fractions isolated from the WPW oil. Chemicals listed in **bold** are class B2 carcinogens according to USEPA 2006a.

PAHs Quantified in WPW Oil and Isolated Fractions

< 2-Ring PAHs:	Benzothiophene	Carbazole	Pyrene	C4-Chrysenes
Pentachlorophenol	C1-Benzothiophene	Anthracene	C1-Fluoranthenes/Pyrenes	> 4-Ring PAHs:
2-Ring PAHs:	C2-Benzothiophene	Phenanthrene	C2-Fluoranthenes/Pyrenes	**Benzo(b)fluoranthene**
Decalin	C3-Benzothiophene	C1-Phenanthrene/ Anthracene	C3-Fluoranthenes/Pyrenes	**Benzo(k)fluoranthene**
C1-Decalin	Biphenyl	C2-Phenanthrene/ Anthracene	Naphthobenzothiophene	Benzo(e)pyrene
C2-Decalin	3-Ring PAHs:	C3-Phenanthrene/ Anthracene	C1-Naphthobenzothiophene	**Benzo(a)pyrene**
C3-Decalin	Acenaphthylene	C4-Phenanthrene/ Anthracene	C2-Naphthobenzothiophene	Perylene
C4-Decalin	Acenaphthene	Dibenzothiophene	C3-Naphthobenzothiophene	**Indeno(1,2,3-c,d)pyrene**
Naphthalene	Dibenzofuran	C1-Dibenzothiophene	**Benz(a)anthracene**	**Dibenz(a,h)anthracene**
C1-Naphthalenes	Fluorene	C2-Dibenzothiophene	**Chrysene**	C1-Dibenz(a,h)anthracene
C2-Naphthalenes	C1-Fluorenes	C3-Dibenzothiophene	C1-Chrysenes	C2-Dibenz(a,h)anthracene
C3-Naphthalenes	C2-Fluorenes	4-Ring PAHs:	C2-Chrysenes	C3-Dibenz(a,h)anthracene
C4-Naphthalenes	C3-Fluorenes	Fluoranthene	C3-Chrysenes	Benzo(g,h,i)perylene

Table 2.2. Chemical analysis of PAH class B2 carcinogen content in WPW oil, acid fraction, base fraction, neutral fraction and reconstituted mixture using GC/MS. Data are presented as concentration in ng of compound per mg of sample.

	Chemical Concentration (ng/mg fraction)									
	PCP	**BaA**	**Chrysene**	**BbF**	**BkF**	**BAP**	**IP**	**DA**	**cPAHs**	**tPAHs**
WPW Oil	1.12E+04	2.15E+03	1.47E+03	8.06E+02	3.30E+02	5.84E+02	1.58E+02	4.30E+01	5.54E+03	1.47E+05
Acid Fraction	9.63E+05	7.51E+02	7.38E+02	2.84E+02	1.94E+02	2.34E+02	6.60E+01	7.00E+00	2.27E+03	7.78E+05
Base Fraction	4.58E+03	BDL*	BDL	BDL	BDL	BDL	BDL	BDL	BDL	2.95E+04
Neutral Fraction	2.03E+03	1.75E+03	1.75E+03	7.15E+02	4.42E+02	5.74E+02	2.24E+02	3.50E+01	5.49E+03	2.31E+05
Reconstituted Mixture	2.28E+03	1.31E+03	1.61E+03	7.16E+02	4.23E+02	5.33E+02	2.09E+02	3.30E+01	4.83E+03	4.83E+03
PCDD Fraction	2.32E+02	4.44E+04	5.93E+04	1.61E+04	4.62E+03	6.20E+01	1.50E+01	1.10E+01	1.25E+05	3.67E+05
PAH Fraction	1.93E+02	1.27E+04	1.18E+04	1.88E+04	3.87E+03	1.50E+04	6.89E+03	2.03E+03	7.11E+04	1.35E+05

*BDL = Below instrument detection limits

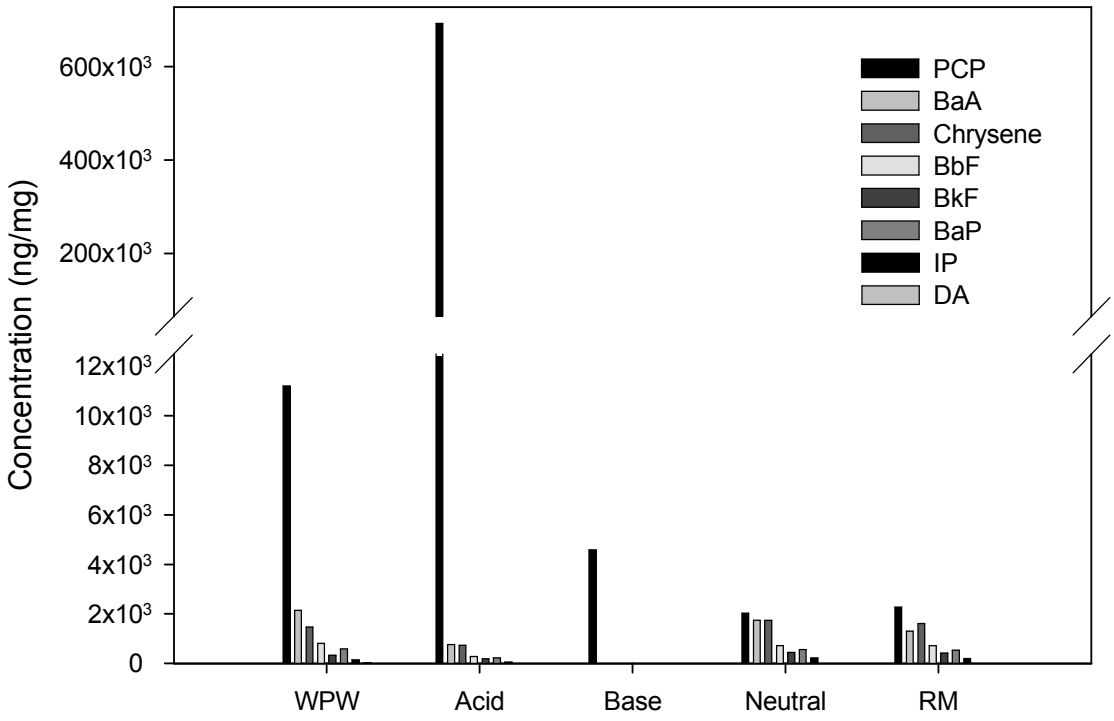

Figure 2.8. Chemical analysis concentrations of PCP and individual carcinogenic PAHs detected in WPW oil, isolated fractions, and reconstituted mixture. Data are presented as concentration in nanograms (ng) of compound per milligrams (mg) of sample.

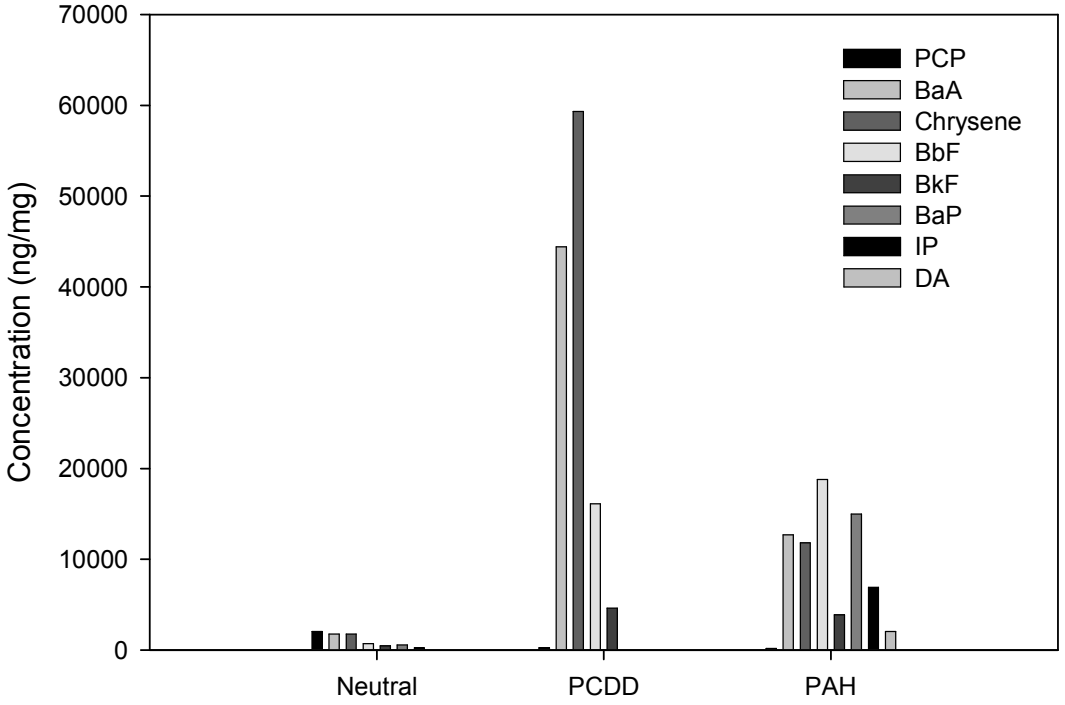

Figure 2.9. Chemical analysis concentrations of PCP and carcinogenic PAHs detected in neutral fraction from WPW oil, and PCDD and PAH enriched isolates. Data are presented as concentration in nanograms (ng) of compound per milligrams (mg) of sample.

Table 2.3. Results from preparation of a reconstituted mixture. Data are presented as ng of analyte per mL of sample calculated from weighing the samples out versus actual concentration from GC/MS.

Chemical Analysis of Reconstituted Mixture							
Predicted Concentration Based on Analytical Preparation (ng/mL)				Measured Concentration Based on GC/MS (ng/mL)			
tPAHs	**cPAHs**	**BAP**	**PCP**	**tPAHs**	**cPAHs**	**BAP**	**PCP**
1.50E+04	1.50E+04	1.15E+03	4.05E+03	1.42E+04	1.42E+04	1.06E+03	4.56E+03

Table 2.4. Results from the *in vitro* bioassays and chemical analysis for WPW oil, acid, base, and neutral fractions, and enriched PAH and PCDD fractions. Data are presented from one dose, 0.25 mg/plate ± SEM for *Salmonella,* one dose 62.5 g/mL for two experiments in *E. coli,* and ng of analyte per mg of sample.

	Biological Analysis				Chemical Analysis			
	Salmonella/microsome Assay (+S9)		*E.coli* Prophage Induction Assay (+S9)					
Sample	**Mean Revertants/Plate 0.25 mg/plate ± SEM**	**Summary Response**	**PFUs/Plate 62.5 µg/mL (2 Experiments)**	**Summary Response**	**tPAHs (ng/mg)**	**cPAHs (ng/mg)**	**BAP (ng/mg)**	**PCP (ng/mg)**
WPW Oil	57 ± 6	+	46/84	–	1.47E+05	1.67E+04	5.84E+02	1.12E+04
Acid Fraction	32 ± 4	–	303/426	++	7.78E+05	6.95E+05	2.34E+02	6.92E+05
Base Fraction	129 ± 8	++	16/76	±	2.90E+04	4.58E+03	BDL*	4.58E+03
Neutral Fraction	55 ± 1	±	33/62	–	2.31E+05	7.52E+03	5.74E+02	2.03E+03
PAH Fraction	90 ± 7	++	n/a	n/a	1.35E+05	7.13E+04	1.50E+04	1.93E+02
PCDD Fraction	33 ± 6	–	n/a	n/a	3.67E+05	1.25E+05	6.20E+01	2.32E+02

*BDL = Below instrument detection limits

Table 2.5. List of results from the *Salmonella*/microsome assay, *E. coli* prophage induction assay and dioxin/furan chemical analysis for neutral fraction and PCDD fraction. Data are presented from one dose, 0.25 mg/plate ± SEM for *Salmonella,* one dose 62.5 g/mL for two experiments in *E. coli,* and ng of analyte per mL of sample. (Note: Due to the limited volume of material available, samples were tested at the dose established as optimal for the neutral fraction.)

Chemical and Biological Analysis of Isolated and Enriched Fractions				
	Biological Analysis		Chemical Analysis	
	Salmonella/microsome Assay (+S9)			
Sample	Mean Revertants/Plate 0.25 mg/plate	Total Response	tPCDDs (ng/mL)	tPCDFs (ng/mL)
Neutral Fraction	29	–	4.15E+02	2.00E+01
PCDD Fraction	33	–	1.18E+03	8.89E+02

2.3.2 *Salmonella*/microsome Assay

All six fractions were tested with and without metabolic activation in the *Salmonella*/microsome assay. A positive genotoxic response was observed from the crude extract of the WPW, the base fraction, and the PAH isolate (Figure 2.10 and Table 2.1). The neutral fraction induced a weak positive response (doubling at only one dose), and all other fractions failed to induce a positive genotoxic response in *Salmonella*. The base fraction induced the maximum response of 129 ± 8 net revertants at a dose of 0.25 mg/plate. Although the PAH fraction had the highest concentration of BAP, this fraction induced a response of 90 ± 7 net revertants at a dose of 0.25 mg/plate (Table 2.4 and 2.5). The acid fraction, which had the highest concentration of total PAHs, failed to induce a positive response and induced only 32 ± 4 net revertants at the optimal dose. It is likely that the elevated concentration of PCP in the acid fraction was cytotoxic to the bacteria and inhibited mutagenicity.

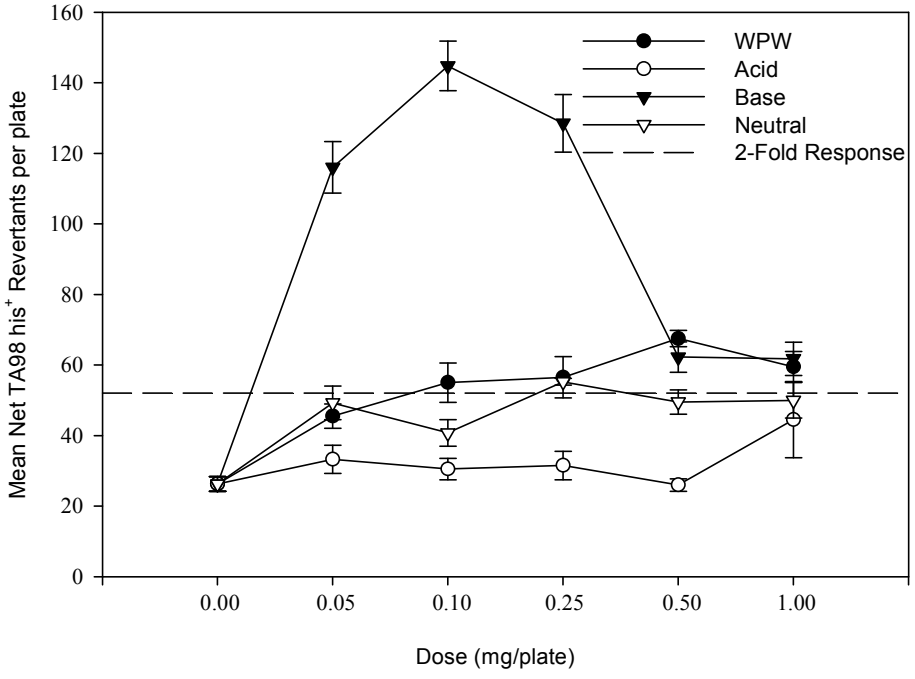

Figure 2.10. Microbial genotoxicity, as measured by *S. typhimurium* TA98 strain with metabolic activation of WPW oil and isolated fractions. 2-Fold response is equal to a two-fold increase over the solvent control. Data are presented as mean total net revertants per plate ± SEM.

2.3.3 *E. coli* Prophage Induction Assay

Due to limitation in volume of sample, only the crude, acid, base, and neutral fractions were tested in the *E. coli* prophage induction assay. The neutral fraction and crude oil did not induce a positive response in this assay at any of the doses tested. However, the acid fraction did show a strong positive response, while the base fraction showed a weak positive response (Figure 2.11 and Table 2.4). The acid fraction response was well above the three fold increase at doses of 16 μg/mL, 31 μg/mL and 63 μg/mL. This response was anticipated due to the large amount of PCP in this fraction. The base fraction exhibited a three fold increase at the 16 μg/mL concentration. The most likely source of the genotoxicity in the base fraction is the PCP that did not partition into the acid fraction during the liquid-liquid separation; it is also possible that nitroaromatics in the base fraction induced an increased level of plaque formation in *E. coli*.

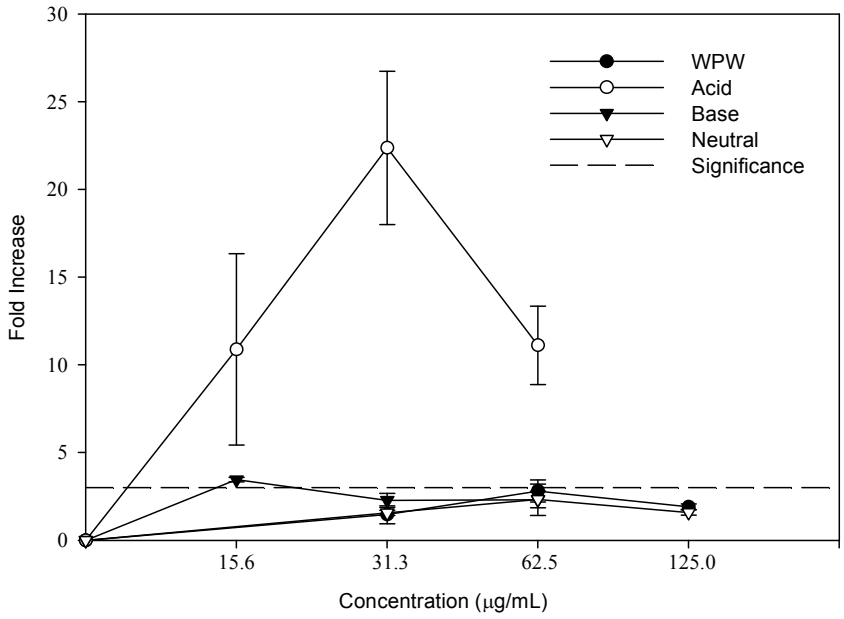

Figure 2.11. *E. coli* prophage induction assay, as measured by the indicator strain TH008 with metabolic activation of WPW oil, acid fraction, base fraction and neutral fraction. Fold Increase = # plaque forming unites (PFUs) per sample/# PFUs for solvent control. Significance was determined by a fold increase of 3, represented by the dashed line, for two or more doses, which is considered a positive mutagenic response. Data are graphed as the mean fold increase between two independent experiments with ± SEM.

2.3.4 ^{32}P-Postlabeling Assay

Autoradiograms displaying a typical DNA adduct pattern in the skin of animals treated with various complex mixtures is presented in Figure 2.12. Spots produced by the RM are much sharper compared to other chemicals. These sharper spots are due to the RM being a mixture of eight chemicals, whereas the other treatments are complex mixtures containing innumerous chemicals. Overall, the locations of the spots are similar for all treatments in the skin, with the base fraction as an exception. The base fraction appears to have an extra polar region in the upper right corner of the autoradiogram (Figure 2.12). The results from all tissues for total DNA adducts are presented in Table 2.6a, while the statistical significance of these data is presented in Table 2.6b. The PAH fraction, which induced a total DNA adduct relative adduct labeling value (RAL) of 109 ± 6.27 per 10^9 nucleotides in skin at a dose of 3 mg/mouse, induced the maximum level of adducts for all fractions. The PAH fraction treatment in skin (Figure 2.13) was the only treatment to produce a significantly larger response than all other treatments. Dose-response data for the NF and RM, in comparison to the PAH isolate, are presented in Table 2.7a, with the statistical significance presented in Table 2.7b. Both the NF and RM exhibited significant increased total adduct formation from the low to the high doses (Figure 2.14). Only the intermediate dose, 1.2 mg/mouse, was significantly higher in the NF as compared to the RM. The RM, a mixture of eight chemicals, is equivalent to the NF composition of those eight chemicals. Therefore, unknown components or compound interactions within the NF produced a larger response in the NF when compared to the RM.

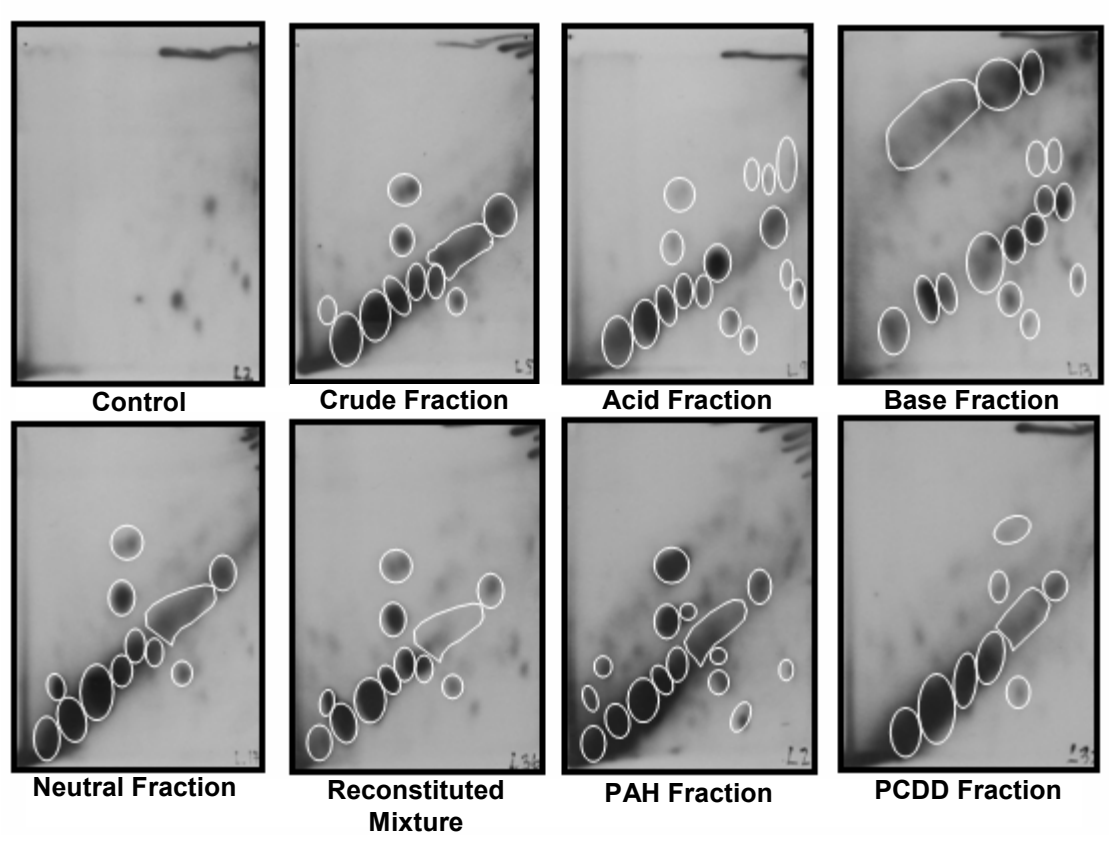

Figure 2.12. Autoradiograms of DNA adducts detected in the skin of CD-1 female mice.

Table 2.6a. Table of DNA adduct levels found in skin, lung and liver of CD-1 female mice treated with complex PAH fractions (dose is 3 mg/mouse). Data are presented as RAL per 10^9 nucleotides ± SEM.

Total DNA Adduct Frequency in Treated CD-1 Female Mice

	Mean Total DNA Adducts (RAL / 10^9 Nucleotides) for 3mg/mouse Dose						
Tissue	**Crude**	**Acid**	**Base**	**Neutral**	**RM**	**PAH**	**PCDD**
Skin	32.80 ± 1.80	30.70 ± 2.68	28.90 ± 3.00	37.40 ± 4.25	27.90 ± 1.74	109.00 ± 6.27	25.60 ± 2.03
Lung	79.00 ± 23.60	48.40 ± 8.65	178.00 ± 12.20	113.00 ± 27.60	47.50 ± 16.90	306.00 ± 81.90	125.00 ± 33.10
Liver	7.63 ± 0.74	7.12 ± 0.66	11.80 ± 0.21	11.10 ± 1.14	8.68 ± 0.92	383.00 ± 37.50	12.20 ± 0.43

Table 2.6b. Table of DNA adduct levels found in skin, lung and liver of CD-1 female mice treated with complex PAH fractions (3 mg/mouse dose). Data are presented as log transformed RAL per 10^9 nucleotides with statistical significance indicated ($\alpha = 0.05$; p-value = < 0.001 for skin and liver, p-value = 0.002 for lung).

Log Total DNA Adduct Frequency in Treated CD-1 Female Mice

	Log of RAL / 10^9 Nucleotides 3mg/mouse dose						
Tissue	**Crude**	**Acid**	**Base**	**Neutral**	**RM**	**PAH**	**PCDD**
Skin	1.51	1.48	1.45	1.56	1.44	2.03[a]	1.40
Lung	1.84	1.66	2.25[b]	1.99	1.57	2.44[c]	2.05
Liver	0.88	0.85	1.07[d]	1.04[d]	0.93	2.58[a]	1.09[d]

a = PAH is significantly greater than all other fractions

b = Base is significantly greater than RM Fraction

c = PAH is significantly greater than Acid and RM Fractions

d = Significantly greater than Crude and Acid Fractions

Table 2.7a. Table of DNA adduct levels found in skin, lung and liver of CD-1 female mice treated with isolated and complex PAH fractions. Data are presented as RAL per 10^9 nucleotides ± SEM.

Total and Spot 4 DNA Adduct Frequency in Treated CD-1 Female Mice

	Mean Total DNA Adducts (RAL / 10^9 Nucleotides)						
Tissue	**Control**	**NF 0.48 mg/mouse**	**NF 1.2 mg/mouse**	**NF 3 mg/mouse**	**RM 1.2 mg/mouse**	**RM 3 mg/mouse**	**PAH 3 mg/mouse**
Skin	3.45 ± 0.68	17.60 ± 1.14	23.30 ± 1.90	37.40 ± 4.25	13.60 ± 0.65	27.90 ± 1.74	109.00 ± 6.27
Lung	27.40 ± 6.29	52.10 ± 14.40	51.60 ± 12.00	113.00 ± 27.60	57.20 ± 18.80	47.50 ± 16.90	306.00 ± 81.90
Liver	59.40 ± 13.10	11.70 ± 1.83	9.79 ± 1.22	11.10 ± 1.14	9.53 ± 0.88	8.68 ± 0.92	383.00 ± 37.50
	Mean Spot 4 DNA Adducts (RAL / 10^9 Nucleotides)						
Tissue	**Control**	**NF 0.48 mg/mouse**	**NF 1.2 mg/mouse**	**NF 3 mg/mouse**	**RM 1.2 mg/mouse**	**RM 3 mg/mouse**	**PAH 3 mg/mouse**
Skin	0.30 ± 0.05	6.46 ± 0.44	8.58 ± 0.88	15.10 ± 2.11	5.46 ± 0.34	12.40 ±1.21	48.10 ± 3.76
Lung	4.10 ± 1.46	10.00 ± 3.10	15.00 ± 3.25	44.00 ± 13.20	7.53 ± 2.78	7.24 ± 2.90	160.40 ± 52.30
Liver	6.51 ± 0.16	1.46 ± 0.16	1.10 ± 0.07	1.33 ± 0.07	1.51 ± 0.12	1.35 ± 0.09	174.00 ± 33.40

Table 2.7b. Table of DNA adduct levels found in skin, lung and liver of CD-1 female mice. Data are presented as log transformed RAL per 10^9 nucleotides with statistical significance indicated (α = 0.05, p-value = $<$ 0.001).

Log Total and Spot 4 DNA Adduct Frequency in Treated CD-1 Female Mice

	Log Mean Total DNA Adducts (Log of RAL / 10^9 Nucleotides)						
Tissue	**Control**	**NF 0.48 mg/mouse**	**NF 1.2 mg/mouse**	**NF 3 mg/mouse**	**RM 1.2 mg/mouse**	**RM 3 mg/mouse**	**PAH 3 mg/mouse**
Skin	0.50	1.24[a]	1.36[a,b]	1.56[a,c]	1.13[a]	1.44[a,e]	2.03[a,f,g]
Lung	1.41	1.66	1.67	1.99	1.66	1.57	2.44[a,g]
Liver	1.75	1.05	0.98	1.04	0.97	0.93	2.58[a,f,g]
	Log Mean Spot 4 DNA Adducts (Log of RAL / 10^9 Nucleotides)						
Tissue	**Control**	**NF 0.48 mg/mouse**	**NF 1.2 mg/mouse**	**NF 3 mg/mouse**	**RM 1.2 mg/mouse**	**RM 3 mg/mouse**	**PAH 3 mg/mouse**
Skin	0.00	0.81[a]	0.93[a]	1.16[a,c,d]	0.74[a]	1.09[a,e]	1.68[a,f,g]
Lung	0.54	0.93	1.14	1.53[a]	0.75	0.72	2.14[a,g]
Liver	0.81	0.16	0.04	0.12	0.18	0.13	2.23[a,f,g]

a = Significantly greater than Control

b = NF 1.2 mg/mouse is significantly greater than RM 1.2 mg/mouse

c = NF 3 mg/mouse is significantly greater than NF 0.48 mg/mouse

d = NF 3 mg/mouse is significantly greater than NF 1.2 mg/mouse

e = RM 3 mg/mouse is significantly greater than RM 1.2 mg/mouse

f = PAH 3 mg/mouse is significantly greater than NF 3 mg/mouse

g = PAH 3 mg/mouse is significantly greater than RM 3 mg/mouse

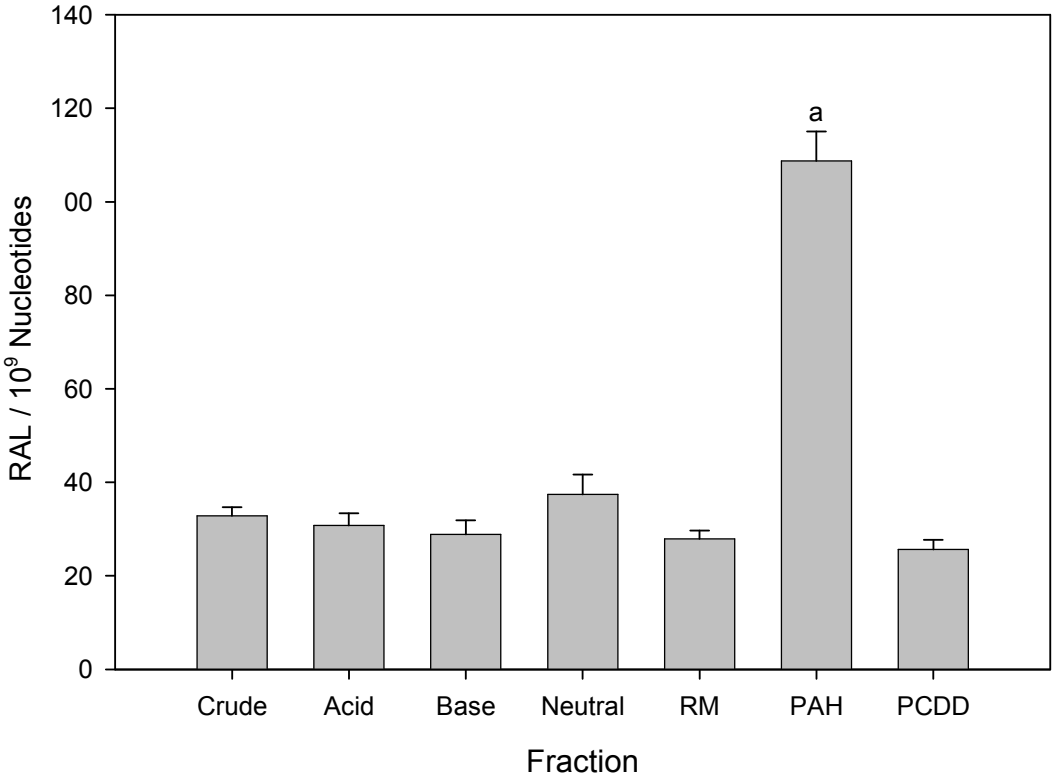

Figure 2.13. Total DNA adducts detected in DNA isolated from the skin of CD-1 mice treated with a 3 mg/mouse dose of complex PAH isolates or a reconstituted mixture. Data are presented as raw data of mean RAL per 10^9 nucleotides $\pm$ SEM. When data was transformed to log and analyzed, the following significant differences were observed: a = PAH is significantly larger than all other fractions (p-value = $<$0.001) (N=4, N=3 for PAH fraction).

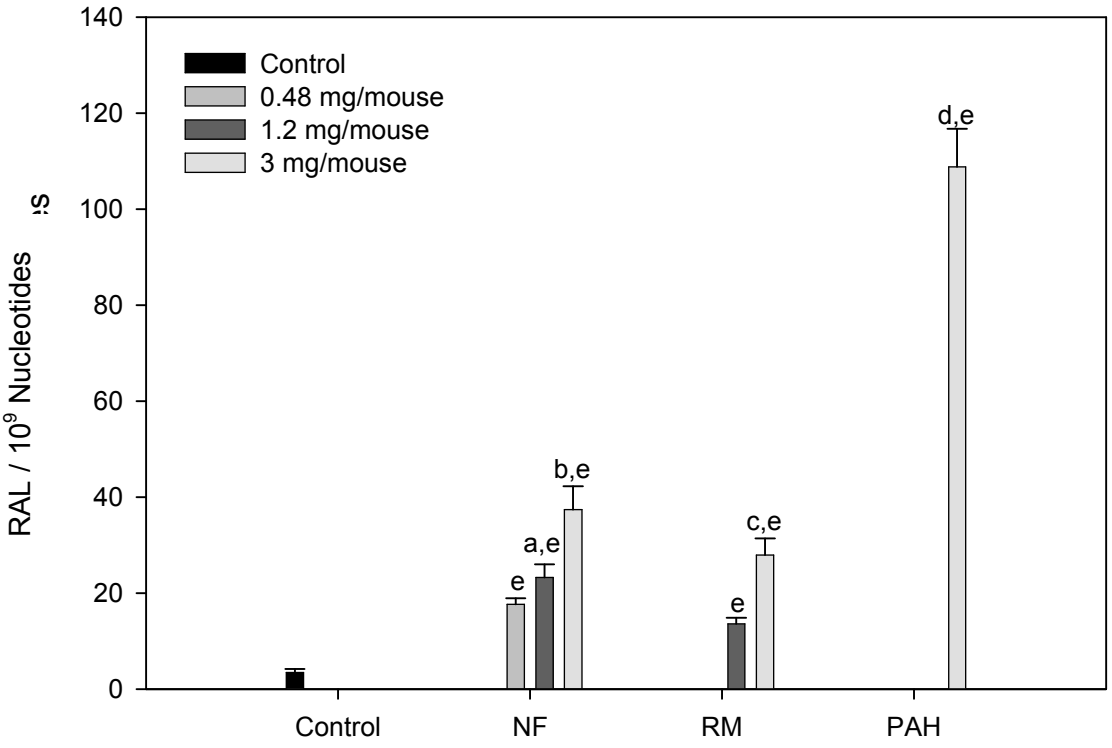

Figure 2.14. Total DNA adducts detected in DNA isolated from the skin of CD-1 mice treated with neutral fraction, reconstituted mixture and PAH fraction. Data are presented as raw data of mean RAL per 10^9 nucleotides ± SEM. When data was transformed to log and analyzed, the following significant differences were observed: a = NF 1.2 mg/mouse > RM 1.2 mg/mouse; b = NF 3 mg/mouse > 0.48 mg/mouse; c = RM 3 mg/mouse > RM 1.2 mg/mouse; d = PAH 3 mg/mouse > NF and RM 3 mg/mouse; e = > control (p-value = <0.001) (N=4, N=3 for PAH fraction).

Spot 4 is a bulky DNA adduct which has been previously shown to be associated with the BAP-diolepoxide (BPDE) adduct (Gupta et al. 1982; Lu et al. 1986). Similar results were observed for spot 4 (Tables 2.6a, 2.6b, 2.7a, 2.7b and Figure 2.15). The PAH fraction produced the maximum number of spot 4 adducts observed. At the highest dose tested, the PAH fraction induced approximately three times the number of adducts induced by the NF, and almost four times that induced by the RM (Table 2.7a). Again, a dose-response relationship was observed for spot 4 adducts with the NF and RM fractions (Table 2.7a). These data indicate that the level of adducts induced by the primary metabolite of BAP appear to be similar between the RM and NF.

Again, autoradiograms in the lung show a typical pattern for DNA adduct formation (Figure 2.16). As seen in the autoradiograms of skin adducts, the base fraction has a second polar region near the top right corner of the autoradiogram, and the RM spot are much sharper than those of the other treatments. All data are presented in Table 2.6a for total and spot 4 DNA adduct formation, while the statistical significance is presented in Table 2.6b. The PAH isolate, again, produced the maximum DNA adduct frequency, with a RAL of 306 ± 81.90 per 10^9 nucleotides (Table 2.6a). The PAH fraction elicited a significantly higher response than the RM and Acid fractions in this tissue, while the base elicited a significantly higher response than the RM as well (Figure 2.17). Dose-response relationship data, RAL and statistical, for NF and RM as compared to the PAH isolate are presented in Tables 2.6a and 2.7b. As observed in the analysis for all treatments, the PAH fraction elicited the highest response, and was significantly larger than the RM (Figure 2.18). No significant difference was observed between the RM and NF treatments.

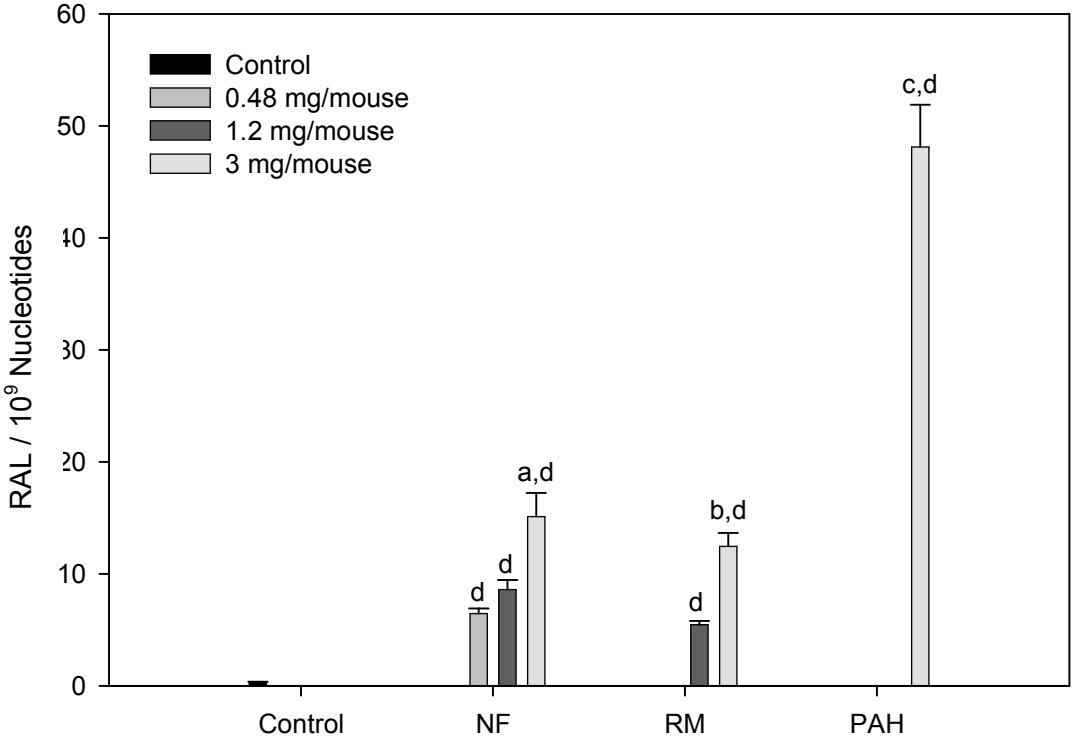

Figure 2.15. Spot 4 DNA adducts detected in DNA isolated from the skin of CD-1 mice treated with neutral fraction, reconstituted mixture and PAH fraction. Data are presented as raw data of mean RAL per 10^9 nucleotides ± SEM. When data was transformed to log and analyzed, the following significant differences were observed: a = NF 3mg/mouse > NF 1.2 and 0.48 mg/mouse; b = RM 3mg/mouse > RM 1.2 mg/mouse; c = PAH 3 mg/mouse > NF and RM 3 mg/mouse; d = > control (p-value = <0.001) (N=4, N=3 for PAH fraction).

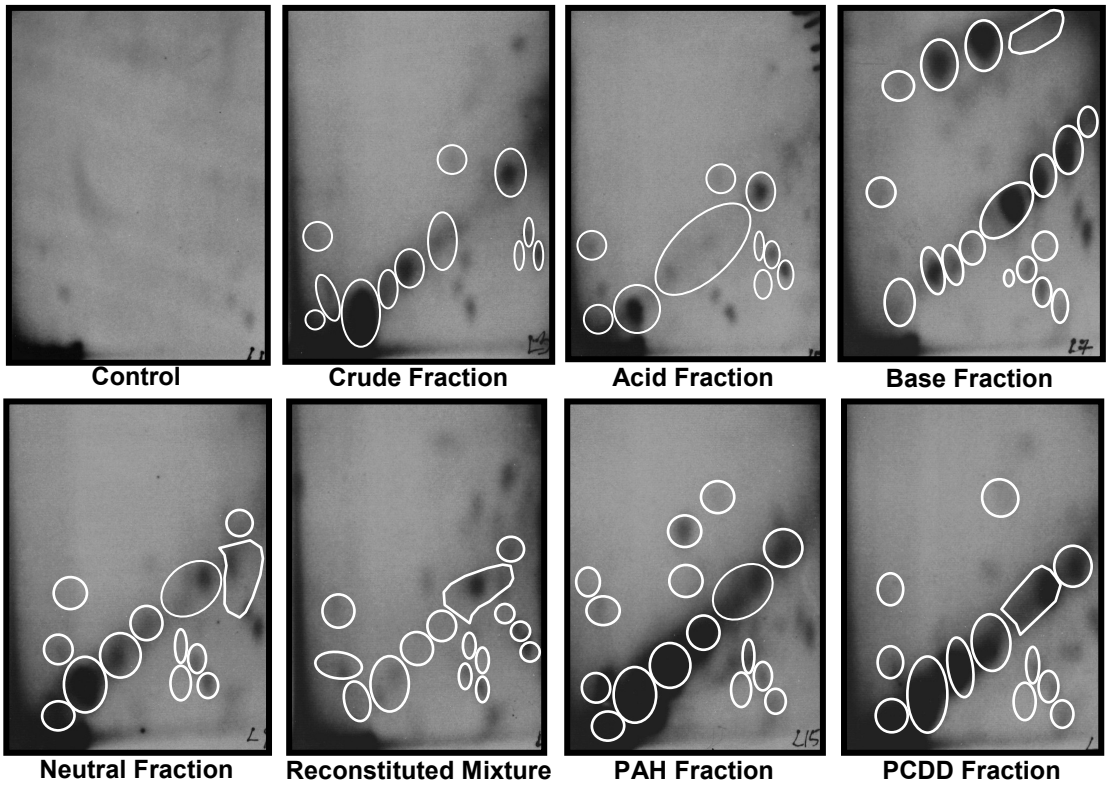

Figure 2.16. Autoradiograms of DNA adducts detected in the lung of CD-1 female mice.

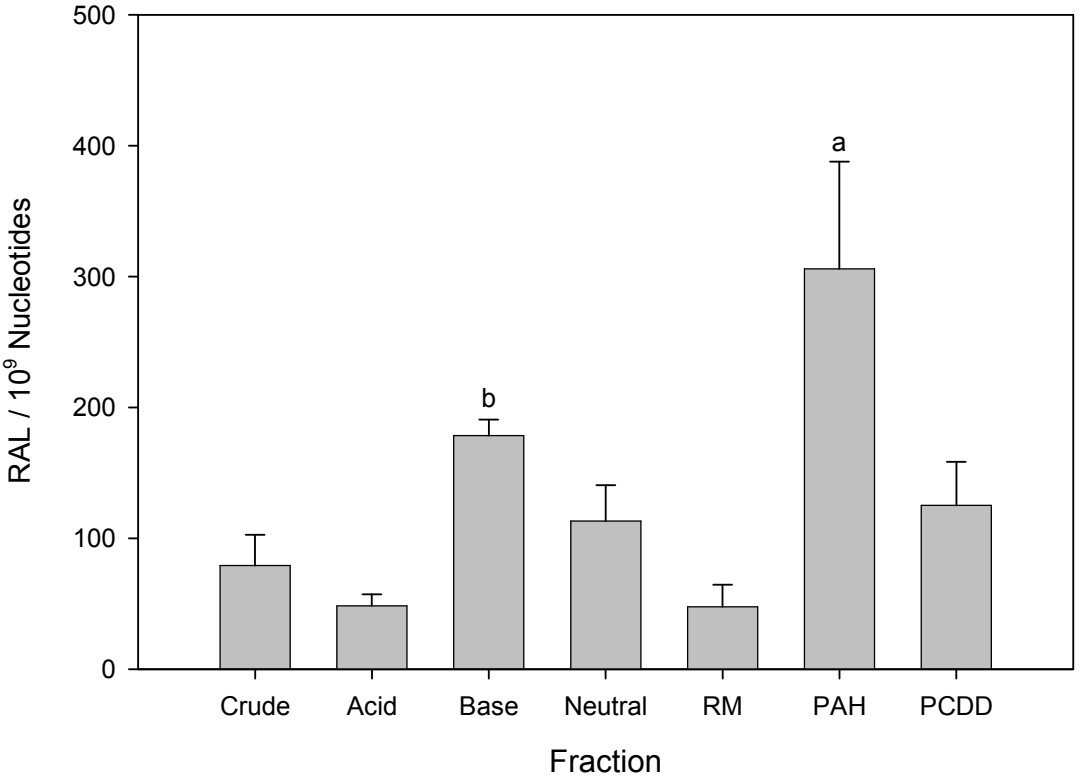

Figure 2.17. Total DNA adducts detected in DNA isolated from the lung of CD-1 mice treated with 3 mg/mouse of complex PAH isolates or a reconstituted mixture. Data are presented as raw data of mean RAL per 10^9 nucleotides $\pm$ SEM. When data was transformed to log and analyzed, the following significant differences were observed: a = PAH is significantly larger than RM and acid fractions; b = base is significantly larger than RM fraction (p-value = 0.002) (N=4, N=3 for PAH fraction).

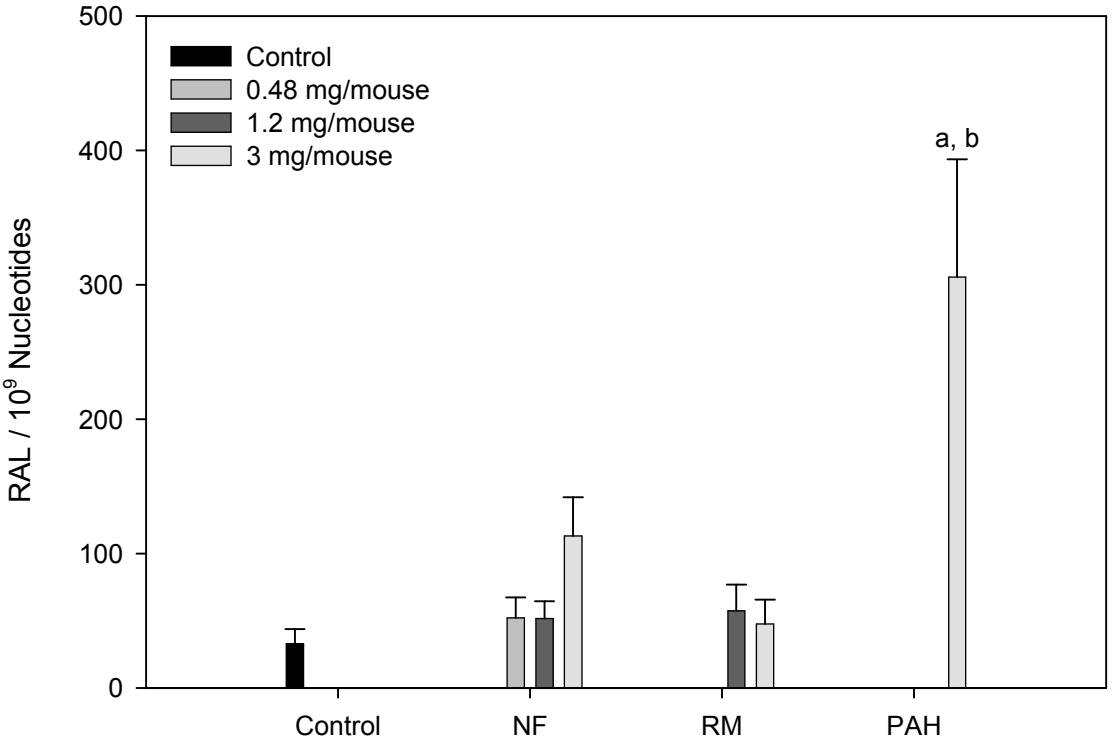

Figure 2.18. Total DNA adducts detected in DNA isolated from the lung of CD-1 mice treated with neutral fraction, reconstituted mixture and PAH fraction. Data are presented as raw data of mean RAL per 10^9 nucleotides ± SEM. When data was transformed to log and analyzed, the following significant differences were observed: a = PAH 3 mg/mouse > NF and RM 3 mg/mouse; b = > control (p-value = <0.001) (N=4, N=3 for PAH fraction).

Data for the spot 4 analysis are presented in Tables 2.6a and 2.6b, with statistical data in Tables 2.7a and 2.7b. Similar results were observed for spot 4 in this tissue that were observed for total DNA adduct formation. The PAH fraction elicited the highest DNA adduct formation for spot 4, and was significantly higher than that of the RM (Figure 2.19). The PAH fraction showed an increase of three times that of the NF, and about six times that of the RM (Table 2.7a). Responses are similar to those seen in the skin tissue.

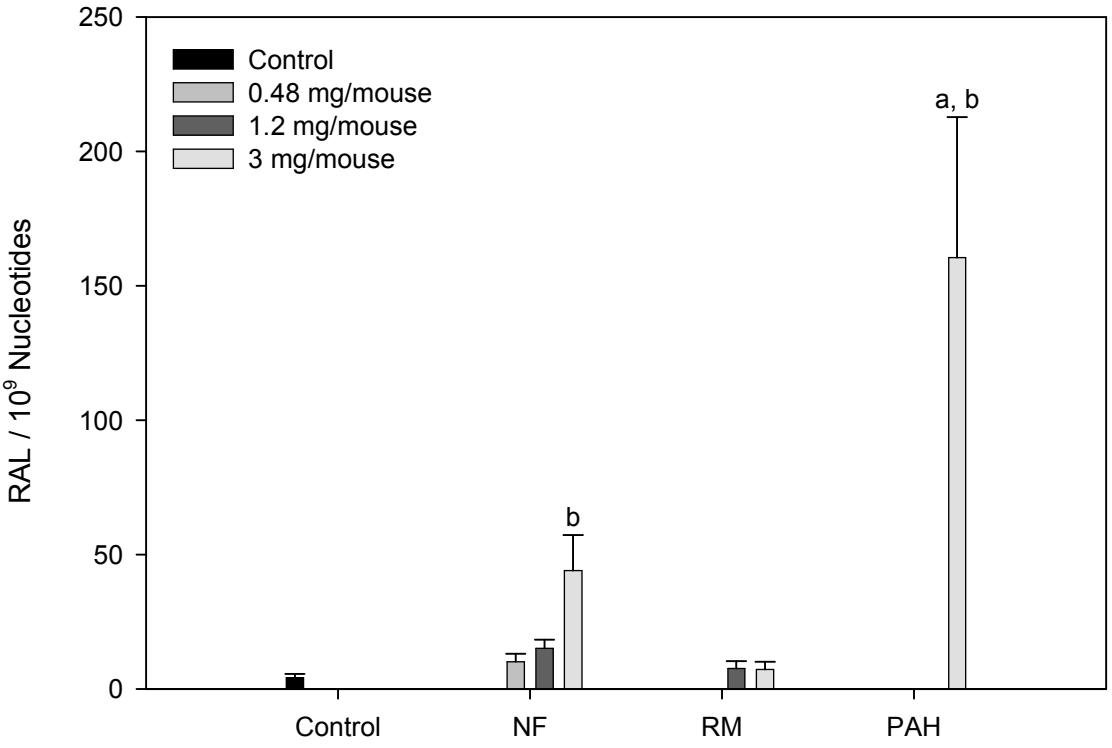

Figure 2.19. Total DNA adducts detected in DNA isolated from the lung of CD-1 mice treated with neutral fraction, reconstituted mixture and PAH fraction. Data are presented as raw data of mean RAL per 10^9 nucleotides ± SEM. When data was transformed to log and analyzed, the following significant differences were observed: a = PAH 3 mg/mouse > RM 3 mg/mouse; b = > control (p-value = <0.001) (N=4, N=3 for PAH fraction).

Finally, the autoradiograms for the liver tissue show a slightly different pattern than those of the skin and lung tissues (Figure 2.20). The autoradiograms are much darker, which is typical of liver tissue. However, even though the patterns have changed in this tissue, they still exhibit typical DNA adduct patterns. Even the base fraction is typical in this tissue, losing the extra polar region seen in the two previous tissues. Again, the RM is much sharper than the other treatments. All data for total and spot 4 DNA adducts are reported in Tables 2.6a and 2.6b, as well as the statistical data in

Tables 2.7a and 2.7b. Over all treatments, the PAH has once again produced the maximum level of DNA adducts, with a RAL of 383 ± 37.50 per 10^9 nucleotides. This value is approximately 31 times that of any other treatment (Table 2.6a). Even though the PAH fraction has produced the largest significant difference, the Base, NF and PCDD fractions all have produced significantly higher responses compared to the Acid and Crude fractions (Figure 2.21). When looking at the dose-response data, the PAH once again has produced the maximum response over the NF and RM. There are no other significant responses detected in this tissue for total DNA adducts (Figure 2.22).

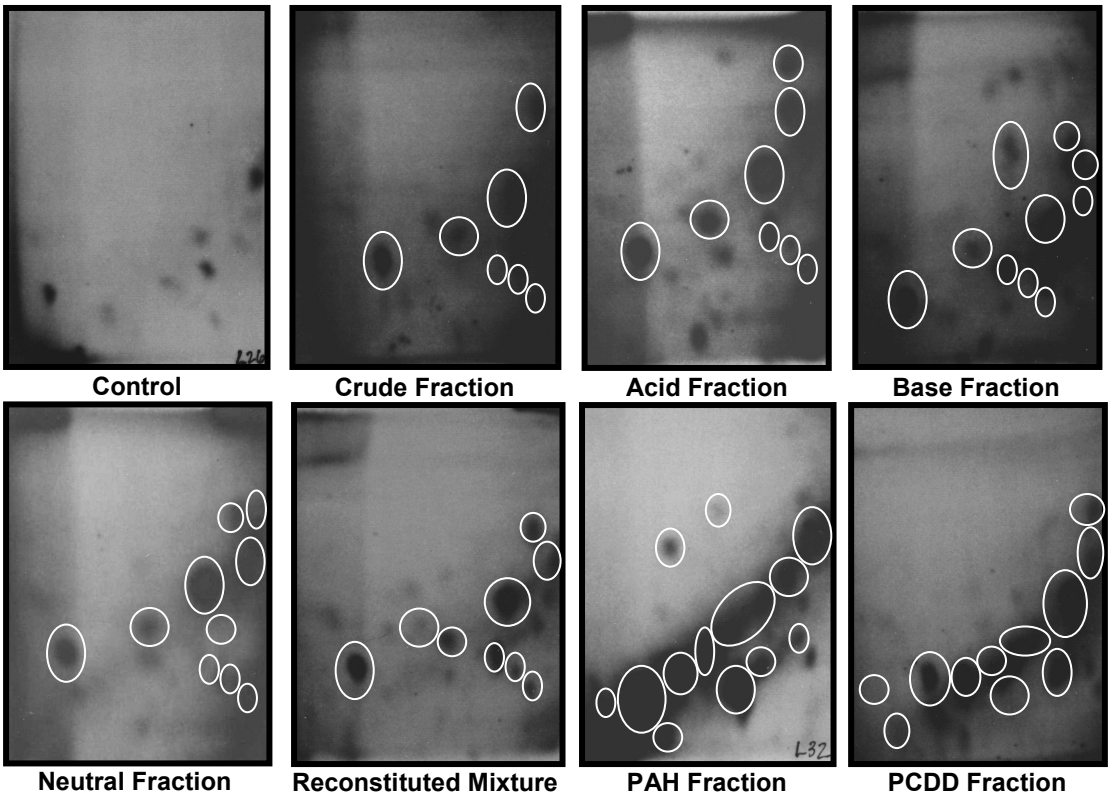

Figure 2.20. Autoradiograms of DNA adducts detected in the liver of CD-1 female mice. Liver tissue tends to yield "dirty" autoradiograms, due to the large amount of background noise.

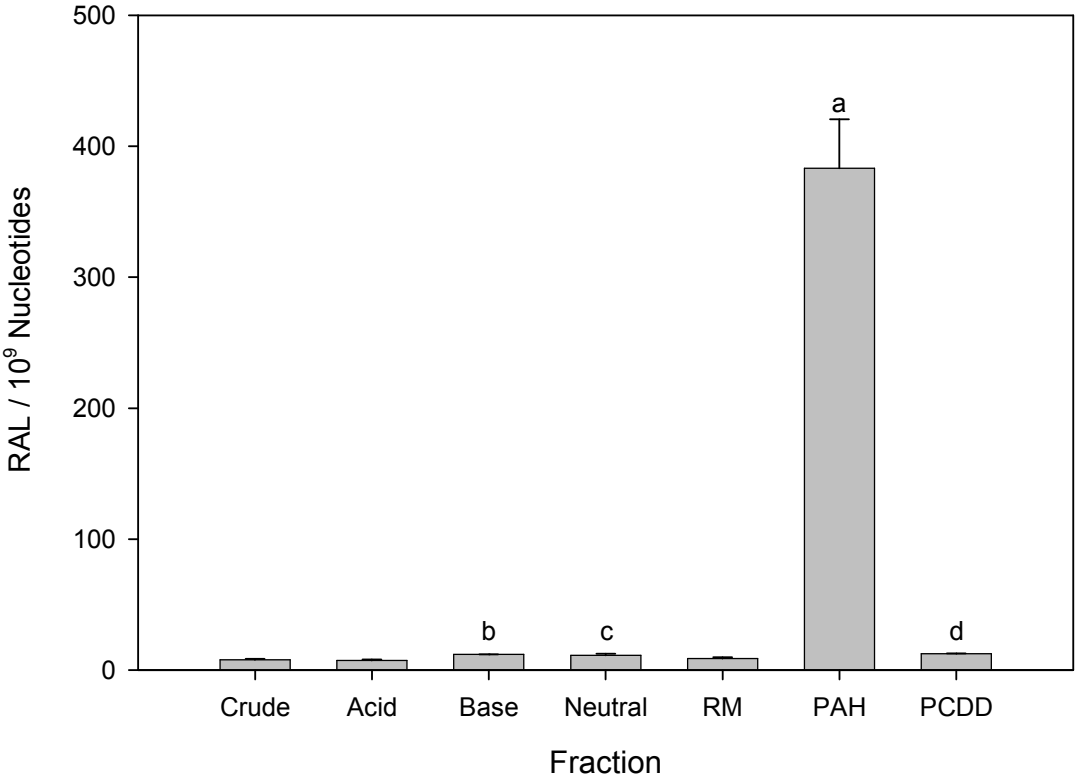

Figure 2.21. Total DNA adducts detected in DNA isolated from the liver of CD-1 mice treated with complex PAH isolates or a reconstituted mixture. Data are presented as raw data of mean RAL per 10^9 nucleotides $\pm$ SEM. When data was transformed to log and analyzed, the following significant differences were observed: a = PAH is significantly larger than all other fractions; b = base is significantly larger than acid and crude fractions; c = neutral is significantly larger than acid and crude fractions; d = PCDD is significantly larger than acid and crude fractions (p-value = $<$0.001) (N=4, N=3 for PAH fraction).

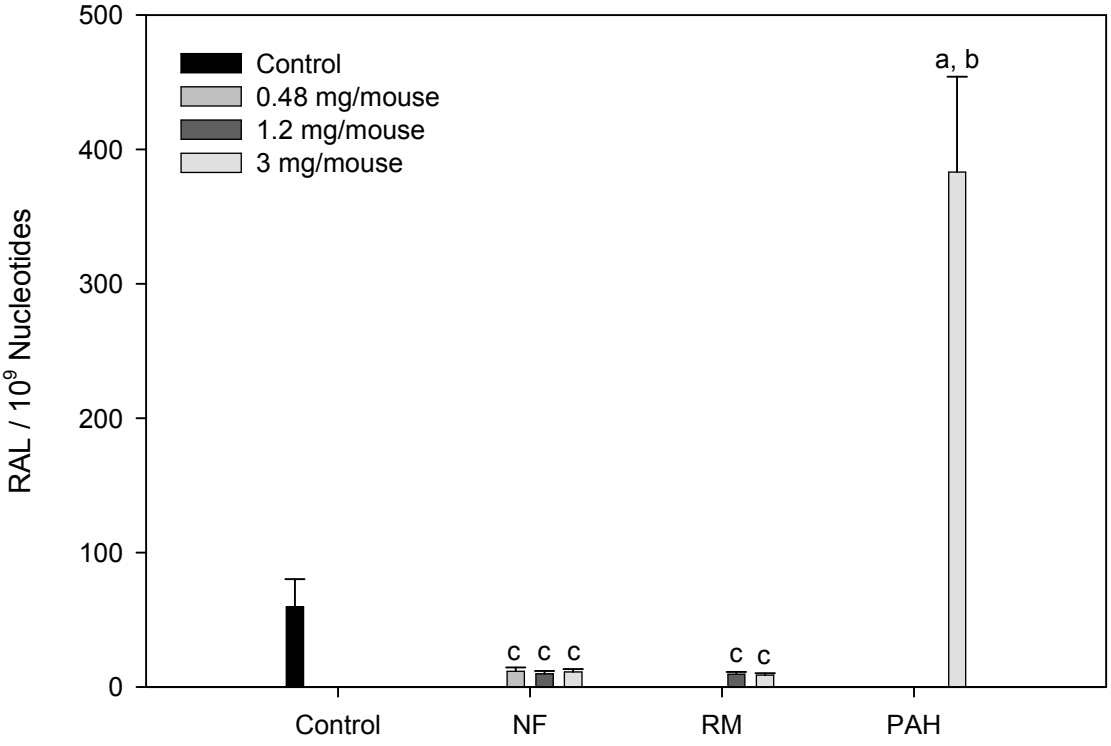

Figure 2.22. Total DNA adducts detected in DNA isolated from the liver of CD-1 mice treated with neutral fraction, reconstituted mixture and PAH fraction. Data are presented as raw data of mean RAL per 10^9 nucleotides ± SEM. When data was transformed to log and analyzed, the following significant differences were observed: a = PAH 3 mg/mouse > NF and RM 3 mg/mouse; b = > control; c = control > (p-value = <0.001) (N=4, N=3 for PAH fraction).

Spot 4 levels are, once again, similar to those observed in the total DNA adduct response analysis. The PAH fraction has produced the highest spot 4 response, approximately 119 times higher than the NF and RM. The NF and RM are not significantly different from the control and each other. In this tissue, the PAH fraction is the only treatment to have elicited a response.

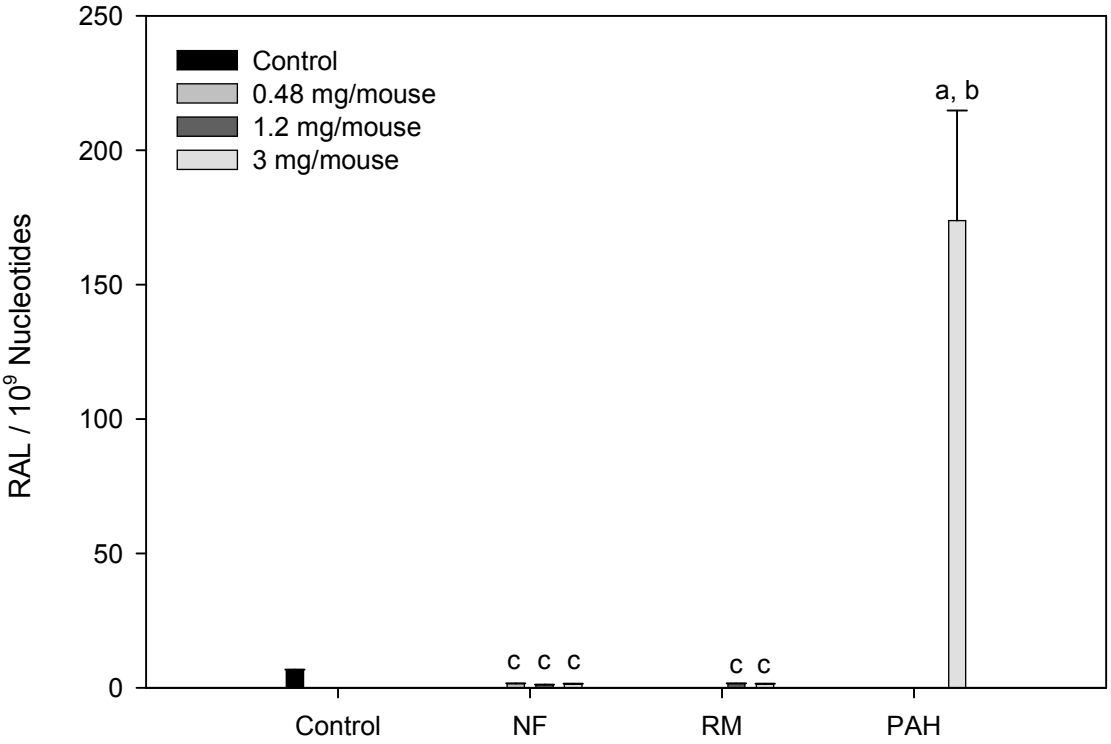

Figure 2.23. Spot 4 DNA adducts detected in DNA isolated from the liver of CD-1 mice treated with neutral fraction, reconstituted mixture and PAH fraction. Data are presented as raw data of mean RAL per 10^9 nucleotides ± SEM. When data was transformed to log and analyzed, the following significant differences were observed: a = PAH 3 mg/mouse > NF and RM 3 mg/mouse; b = > control; c = control > (p-value = <0.001) (N=4, N=3 for PAH fraction).

2.4 Discussion

Previous studies have shown that the *Salmonella*/microsome bioassay is a sensitive system for detecting carcinogenic PAHs as baterial mutagens (Chu et al. 1981; Donnelly et al. 1998; Purchase et al. 1976; Tennant et al. 1987a). In the current study the base and the crude fractions both had a positive response in the *Salmonella* microsome assay. The negative response observed for the acid fraction may be due either to the cytotoxicity of PCP, or the lack of sensitivity of this bioassay towards chlorinated compounds. The crude extract and neutral fraction both have a larger amount of carcinogenic PAHs present than the acid, base and reconstituted mixtures. Therefore, the mutagenicity of both the crude extract and the week response observed for the neutral fraction appear to be due to the presence of these carcinogenic PAHs. The neutral fraction, which had a lower response than the crude extract, had a larger number of total PAHs present (including low molecular weight PAHs) than the crude extract. Therefore, it appears that inhibition my have occurred via these other PAHs present (presumably by low molecular weight PAHs) which affected the neutral fraction. The base fraction induced the maximum genotoxic response for all mixtures tested. However, this compound has the lowest concentration of carcinogenic PAHs. Nitro aromatics are inherently present in this mixture, but were not analyzed in this research. Due to the lack of large amounts of carcinogenic PAHs, as well as a lower concentration of total PAHs, we speculate that the postitive response induced by the base fraction may be a result of nitro aromatics or other nitrogen containing aromatic compounds present in that fraction.

The *E. coli* prophage induction assay was used to complement the *Salmonella* assay in the battery because it detects DNA strand brakes, and is sensitive to chlorinated compounds (DeMarini et al. 1990). In the current study, the acid fraction induced a strong positive genotoxic response, while the base fraction induced a week positive response and the other fractions were negative. The positive response observed for the acid fraction is due to the presence of PCP, these results confirm the utility of this bioassay for detecting genotoxic chlorinated compounds. The base fraction had levels of PCP and this may be the reason for the positive response in this assay.

Bulky DNA adducts were measured in skin, lung and liver tissues collected from animals treated with complex PAH mixtures. Each of the complex mixtures induced a genotoxic response *in vivo*. The highest level of DNA adducts were consistently observed in lung tissue, whereas the lowest level of adducts were generally observed in the liver tissue. The exception to this was animals treated with the PAH fraction. The PAH fraction consistently induced the maximum level of total DNA adducts in each of the three tissues studied. In the liver, the PAH fraction induced a total adduct level that was more than 30 times greater than the level observed for any of the other fractions. In the lung tissue, the PAH fraction induced the maximum genotoxic response, although the PCDD fraction, the neutral fraction and the base fraction each induced more than 100 per 10^9 relative adducts. Spot 4 adducts are believed to represent the BAP diolepoxice (BPDE) metabolite of BAP (Lu et al. 1986). The pattern for spot 4 adducts follow the same general trend as the total adduct levels. Diffrerences observed between tissues can be attributed to adsorption and distribution of the chemical. The samples were applied to the skin. The chemicals had to be absorbed through the skin, and then be distributes through the body. Larger molecular weight chemicals will be slowed down in this process, which will effect the overall response.

Overall the *in vitro* bioassays were sensitive to selective classes of compounds. However, measuring DNA adducts in the animal model provides a useful system for incorporating interactions that may be influenced by pharmacokinetics. Using only the microbial bioassays, the two most genotoxic fractions appear to be the acid and base fractions, while a weak genotoxic response was observed for the crude, neutral and PAH fractions. However, in the animal model the PAH fraction was the most genotoxic, and this positive geonotxic response was observed for all of the fractions. These results indicate that while microbial bioassays provide a viable screen for identifying genotoxic mixtures, *in vivo* models are both more sensitive and appear to be more accurate. The sensitivity and accuracy of *in vivo* models can be attributed to these reasons as well: *in vivo* models allow for whole system testing of a chemical and its effects while these *in vitro* models do not; and *in vivo* model data is quantitiative, while the *in vitro* model data

is qualitative. Chemical analysis is important for quantification of the mixtures. However, it is apparent from the *in vitro* and *in vivo* assays that the biological measurements provide the most accurate assessment of genotoxic potential of complex mixtures based on the quantitative data collected.

CHAPTER III
FREQUENCY AND PERSISTENCE OF DNA ADDUCTS IN INFANT MALE MICE EXPOSED TO COMPLEX CHEMICAL MIXTURES

3.1 Introduction

Complex mixtures are ubiquitous in the environment. Chemical mixtures are present in air, water, soil and cooked foods. Due to the breadth of contamination in the environment, humans are exposed to chemical mixtures (Binkova and Sram 2004; Mueller et al. 1989; Mueller et al. 1991; Vyskocil et al. 2004). To reduce the occurrence of human disease from complex mixture exposure, it is important to obtain more accurate information regarding both the environmental and physiological fate of chemical mixtures. Mixture interactions may increase or decrease the relative toxicity of components due to alterations in absorption, metabolism, distribution or excretion.

WPW is a common environmental contaminant. WPW is a complex mixture of PAHs, PCDDs, and other numerous compounds. Many of these compounds are formed during combustion processes. The chemical properties of PAHs and the other components of WPW make them useful as biocides and wood preservatives. It is this use that has contaminated numerous sites throughout the United States. Certain PAHs are classified as carcinogenic compounds by the United States Environmental Protection Agency (USEPA 1992). Once a PAH carcinogen has entered into a biological organism they are considered to be a procarcinogen (inactive). Metabolic activation converts the procarcinogen into a carcinogen. The progression from a DNA adduct to an actual tumor is a rare process. It is more likely that the progression will be interrupted in some manor. However, this process does occur, making the carcinogenic potential of a chemical or group of chemicals very important. DNA adducts are thought to have a very important role in carcinogenesis. Therefore, it is important to identify DNA adducts formed by chemicals. ^{32}P-postlabeling is a very sensitive method used to determine DNA adducts in exposed tissues. Other methods used include fluorescence detection, gas chromatography/mass spectrometry and immunoassay.

The persistence of DNA adducts has been studied, and it has been shown that after about 48 hr, up to 80% of the DNA damage is no longer detected (Phillips 1997). It has also been shown in previous studies that the presence of DNA adducts does not mean the chemical is tumorigenic (Hemminki et al. 2000). However, by linking DNA adduct studies with tumor studies; it will help determine if ^{32}P-postlabeling is in fact a good assay for determining the carcinogenic potential of a chemical.

WPW produces DNA adduct formation in lung tissues by Randerath et al. in 1994. This study showed the potential of WPW to produce bulky DNA adducts *in vitro* using rat lung DNA. Again, this same group showed WPWs potential to produce bulky DNA adducts *in vivo* in mouse skin (Randerath et al. 1995; Randerath et al. 1997). In the study conducted in 1995, several tissues were tested for DNA adduct formation. The skin showed the highest levels, as it was the site of application, with the lung following behind. The liver exhibited the next highest levels of DNA adducts produced by the WPW. Persistence of the DNA adducts is the next concern, as this can determine how much damage, ultimately, the exogenous compounds may produce. In general, DNA adducts have shown to decrease rapidly within the first two weeks of exposure. Adducts that remain after this time are persistent, and are likely going to be the cause of larger problems (Randerath and Randerath 1994). Adducts that persist in the DNA can be detected up to 42 weeks after topical application (Reddy and Randerath 1986). However, the older the animal is, the more easily I-compounds will be detected. I-compounds are indigenous compounds already present in the biological system which may form bulky DNA adducts. These compounds increase linearly with age of an animal. The older the animal, the more difficult it is to determine differences between I-compounds and bulky DNA adducts with exogenous compounds (Randerath and Randerath 1994; Randerath et al. 1999; Reddy 2000).

The goal of this study is to investigate the frequency and persistence of bulky DNA adduct formation over time and dose in infant mice administered the model carcinogen BAP as well as complex mixtures containing BAP.

3.2 Materials and Methods

3.2.1 Sample Collection

The methods used for collection and extraction of the WPW were described in Chapter II.

3.2.2 Chemicals and Materials

The following chemicals were purchased from EM Science (Gibbstown, NJ): methylene chloride (ACS reagent grade, 99.5% pure), isopropyl alcohol (HPLC grade) and acetone (ACS reagent grade, 99.5% pure). Pentachlorophenol (98% pure), benz(a)anthracene (99% pure), chrysene (98% pure), benzo(b)fluoranthene 98% pure), benzo(k)fluoranthene (98% pure), benzo(a)pyrene (97% pure), dibenz(a,h)anthracene (200 μg/mL in CH_2Cl_2), guanidine HCl (99+% pure), and trizma base (>99.9%) were purchased from the Sigma-Aldrich Group (St. Louis, MO). Indeno(1,2,3-c,d)pyrene (1000 μg/mL in CH_2Cl_2) was purchased from Absolute Standards (Hamden, CT). The following were purchased from QIAGEN Sciences, Inc (Germantaown, MD): QIAGEN Genomic-tip 100/G and RNase A (17500 U). Proteinase K (recombinant, PCR grade, lyphilizate) was purchased from Roche Diagnostics (Indianapolis, IN). Tween-20 (enzyme grade) was purchased from Fisher Scientific (Pittsburgh, PA). Acide MOPS 3-(N-morpholino) propane sulfonique (Molecular Biology Grade) was purchased from VWR International (Batavia, IL). The following chemicals were purchased from EMD Biosciences, Inc. (San Diego, CA): $Na_2EDTA \bullet 2H_2O$, Triton X-100 and NaCl (ACS grade).

3.2.3 Animals

All animals were obtained from Harlan (Houston, TX). Strains used were B6C3F1/Hsd male mice, 21 days old, 7-11 g. These mice are inbred hybrid agouti offspring of a cross between a C57BL/6Nhsd inbred female mouse and a C3H/HeNHsd inbred male mouse. Mice were shipped via Harlan truck in filtered shipping containers. Mice are housed in a barrier facility, 3 mice per filtered cage. Mice were fed ad libitum

using sterilized food provided by the facility. Water was also ad libitum, using filtered and sterilized water provided by the facility.

3.2.4 Statistics

Statistics were carried out by the Department of Statistics at Texas A&M University using R software. All data underwent log transformation. Contrasts to be tested were entered into the program. Contrasts were determined based on scientific hypothesis determined for this study. For lung and forestomach tissues, a series of ANOVAs were preformed, building from 3x3x3 ANOVA (three chemicals, three doses and three times). Data was not collected at one time for one chemical, so it was ignored in order to make sure the full analysis would follow the same pattern as the smaller analysis. A 4x3x2 ANOVA (four chemicals, three doses and two times) was preformed. The one chemical with missing data was added, but the missing time ignored. Finally, the full analysis of four chemicals, three doses and three times (4x3x3) was preformed. All three analyses followed the same pattern. Only the 4x3x3 ANOVA analysis is reported in this paper. The same strategy was used for the liver tissue data. In the liver tissue, there are four times as one last time point of 280 days was added. Again, data was not collected for one chemical, but this time it was for two different times. A 3x3x4 ANOVA (three chemicals, three doses and four times) was preformed ignoring the one chemical. A three-way interaction was detected in the spot 4 liver response from the 3x3x4 analysis. A 4x3x2 (four chemicals, three doses and tow times) ANOVA was preformed ignoring two time points (7 days and 280 days). There was an inconsistency observed in this analysis. A three-way interaction showed significance (chemical-dose-time) where there were only two-way significant interactions previously. Therefore, contrasts in this final analysis must be done on a three-way interaction. Finally, the full 4x3x4 (four chemicals, three doses and four times) ANOVA was preformed. The data reported in this paper include: two-way 4x3x4 ANOVA interactions for the total adduct data, and three-way 4x3x4 ANOVA interactions for the spot 4 adduct data.

3.2.5 Preparation of a Reconstituted Mixture

The methods used for preparation of the RM was described in Chapter II. Table 3.1 lists the values of PAHs present for each treatment at the high dose. The NF was spiked with BAP to be equivalent to the level of pure BAP dosed. The RM was also spiked with BAP to be equivalent. NF was also tested without being spiked with extra BAP, to observe differences that may occur.

3.2.6 *In Vivo* Bioassays

3.2.6.1 DNA Adducts in Mice, Topical Application

DNA adducts were quantified in B6C3F1 21 day-old male mice exposed topically to 150 µl of sample (in CH_2Cl_2) at does of 3, 1.2, and 0.48 mg/mouse for 24 hr. Dosing procedures were followed as described by Reddy and Randerath (1986). Briefly, mice were weighed and placed into groups such that the average weight of each group is approximately equal. The backs of the mice were then shaved. After 24 hr, the mice were shaved a second time. This allowed the chemicals to be applied directly to the skin. Mice were then reweighed, groups readjusted, and any nicked mice were not treated. A total of 10 groups, 5 mice per group, were treated topically, including one control group.

Topical treatment was applied via capillary tubes and mice were left for 24 hr. Three groups at different concentrations (3 mg/mouse, 1.2 mg/mouse and 0.48 mg/mouse) for BAP, RM and NF+BAP mixtures were tested. Mice were sacrificed after 24 hr, and exposed skin, lung, and liver were collected and stored at -80°C.

Table 3.1. Comparison of PAHs present across treatments for the high dose (0.429 mg/g bw).

	Amount of PAH per High Dose (ug/mouse)							
Treatment	**PCP**	**BaA**	**Chrysene**	**BbF**	**BkF**	**BAP**	**IP**	**DA**
BAP	--	--	--	--	--	**3.75E+02**	--	--
RM	6.80E+00	3.90E+00	4.80E+00	2.10E+00	1.30E+00	**3.75E+02**	6.00E-01	1.00E-01
NF+BAP	6.10E+00	5.30E+00	5.30E+00	2.10E+00	1.30E+00	**3.75E+02**	7.00E-01	1.00E-01
NF	6.10E+00	5.30E+00	5.30E+00	2.10E+00	1.30E+00	**1.70E+00**	7.00E-01	1.00E-01

3.2.6.2 Infant Male Mouse Model

DNA adducts were quantified in male B6C3F1 mice using a protocol described by Rodriguez et al. (1997). Briefly, 21 day old male B6C3F1 mice were injected intraperitoneally (i.p.) one time with sample or control. The sample was dissolved in 50:50 DMSO:Corn oil. A total of 24 groups of mice were treated. For ice with a 280 day endpoint (tumor mice), there were 10 treated groups with 20 mice per group (Control, BAP, reconstituted mixture, and neutral fraction + BAP) and one treated group having 10 mice per group (neural fraction). BAP, reconstituted mixture and neutral fraction + BAP had three groups each, one for each dose concentration. Neutral fraction was dosed at the highest concentration only. Mice with a 1 day, 7 day and 21 day endpoint (DNA adduct mice), there were 13 treated groups with 15 mice per group (5 mice per sample endpoint). Groups included control, BAP, reconstituted mixture, neutral fraction + BAP, and neutral fraction. All treatments had three groups dosed with the dose-response concentrations. Dose concentrations administered to the mice included 0.429, 0.171, and 0.069 mg/g body weight in a volume of 7.14 µL vehicle/g body weight. Control was administered as a volume of 7.14 µL vehicle/g body weight. Calculations follow:

Before treatment administration, mice were taken from their mothers and weighed. After weight was determined, mice were injected according to weight (Figure 3.1). After intraperitoneal injection, tumor mice were watched daily for 3 months, and then bi-weekly until the 280 day endpoint. DNA adduct mice were watched daily until the endpoints of 1 day, 7 days and 21 days were reached. For DNA adduct mice, lung, liver and forestomach were collected and stored in a -80°C freezer. For tumor mice, lung, liver and forestomach were collected and immediately put into 10% formalin. A small piece of liver was collected from the first three mice of each group and stored at -80°C for DNA adduct testing.

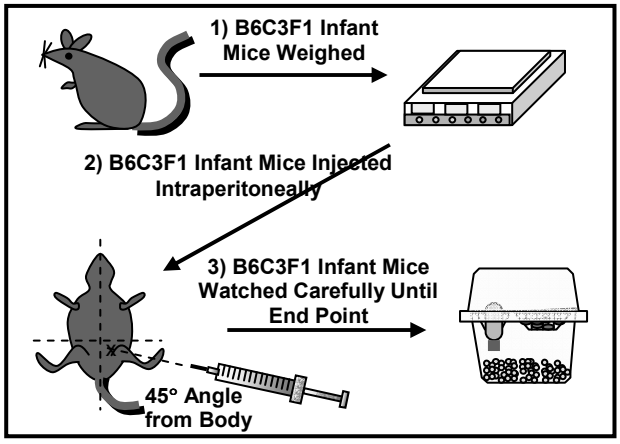

Figure 3.1. Diagram of the procedure for the infant male mouse model. Mice are weighed and then injected into the intraperitoneal cavity.

3.2.6.3 ^{32}P-Postlabeling

DNA was extracted from mouse tissues using Qiagen Genomic-tip 100/G tips. Digestion and labeled with γ^{32}P[ATP] following methods described previously by Reddy and Randerath (1986). The Qiagen extraction is briefly described, 0.08 to 0.1 g of minced mouse tissue were weighed into a 15 mL polypropylene centrifuge tube. 19 µL of RNase A stock solution (100mg/mL) and 9.5 mL buffer G2 were added to the tube. Tissues were then homogenized for 45 to 60 sec at 15,000 to 20,000 rpm. 0.5 mL of Proteinase k stock solution (20 mg/mL) was then added, and the sample was incubated at 50°C for 2 hr. Qiagen Genomic-tip 100/G tips were equilibrated with 4 mL of buffer QBT, and emptied via gravity flow. Samples were vortexed for 10 sec and poured onto the corresponding tip. Flow was regulated by gravity. Tips were then washed with 7.5 mL buffer QC twice via gravity flow. DNA was then eluted from the tips with 5 mL of buffer QF into a 50 mL polypropylene centrifuge tube. 3.5 mL of room temperature isopropanol was added to the tube. The samples were then vortexed and centrifuged at 10,000 rpm, 4°C, for 15 min. Supernatant was carefully poured off the DNA pellet. DNA was then washed with 2 mL of ice cold 70% ethanol, vortexed and spun in the centrifuge at 10,000 rpm for 10 min. Supernatant was carefully poured off, and DNA was washed a second time as described above. DNA was then dried for 10 min and

redissolved in 0.08 to 0.15 mL 0.01 x SSC. The desired concentration is 2μg/μL. Concentration was checked via UV-Vis Spectrophotometer, the A_{260} (DNA)/A_{280} (RNA) ratio should range from 1.6 to 1.8.

DNA digestion and labeling are described briefly: 10 μg of DNA in 5 μL of SSC and/or water were digested using 3 μL of 0.2U micrococcal nuclease and 2.4 μg spleen phosphodiesterase per μL (MN/SPD) and 2.4 μL of IS-buffer mix (10 μg DNA, 100 mM $CaCl_2$ and 300 mM Na succinate) for 3.5 hr at 37°C. MN/SPD digestion cleaves the 5'-nucleotide-phosphate bonds, leaving the 3'-monophosphates of the normal and adducted deoxyribonucleosides. The DNA was then digested with 4.75 μL of nuclease P1 digestion mix (4 μg/μL nuclease P1, 1 M NaOAc and 1 mM $ZnCl_2$) for 40 min at 37°C. Nuclease P1 digestion cleaves the 3'-nucleotide-phosphate bonds on normal nucleotides only. It was reported that adducted nucleotides were mostly or partially resistant to nuclease P1 3'-dephosphorylation (Reddy and Randerath 1986). The sample was then labeled using 3.86 μL of polynucleotide kinase (PNK) labeling mix (kinase buffer, 100 μC*i*/μL ATP and 30 U/μL PNK) and incubated for 40 min at 37°C. PNK labeling attaches the radioactive phosphate ([γ-^{32}P]ATP) at the 5'-hydroxyl group end of the adducted nucleotides through [^{32}P]phosphate transfer from ([γ-^{32}P]ATP). The normal nucleotides lost their 3'-phosphate during nuclease P1 digestion, so PNK will not phosphorylate them with the ([γ-^{32}P]ATP). Once samples are labeled, two specific activity (SA) tubes (2 pmol/μL dAP and 50 mM CHES, pH 9.5) were then labeled with 2.5 μL PNK labeling mix, and incubated same as the samples. All samples, with the exception of the SA tubes, were then digested with 1.5 μL of 40 mU/μL potato apyrase for 30 min at 37°C. Apyrase digestion destroys the excess ATP by removing [^{32}P] from the ATP ([^{32}P]-ATP$\longrightarrow$ADP + [^{32}P]). After apyrase incubation, normals and SA tubes were then diluted. Normals were a qualitative check to make sure that each sample was digested and labeled well. Tubes contain 250 μL of 20 mM CHES, pH 9.5. 1 μL of sample was added to the corresponding tube, and then μL per sample were spotted on PEI-cellulose sheets. SA dilution tubes contained 996 μL of 20 mM CHES, pH 9.5. 4 μL of labeled SA tubes (d*pAp mix) were added to each corresponding SA tube, and

then 5 µL are spotted on PEI-cellulose sheets. Normals and SA PEI-cellulose sheets were run in 0.28 M $NH_4(SO_4)_2$ + 50 mM NaH_2PO_4, pH 6.7 to 13 cm past the origin line, approximately 1 to 2 hr (Figure 2.4).

While normals and SA sheets are running, labeled samples are spotted onto a PEI cellulose sheet (D1 development). D1 sheets are run in 80 mL of 2.3 M NaH_2PO_4, pH 5.75, for 16 hr (Figure 2.5). D1 development removes traces of normal nucleotides after the nuclease P1 treatment, as well as residual orthophosphate by pushing them to the wick at the top of the sheet, leaving the [^{32}P] adducted nucleotides behind. D1 sheets are developed on autoradiographic film, and locations of the spots are then drawn on the back of the PEI-cellulose sheets. Spots are then cutout from the D1 PEI-cellulose sheet and transferred to single PEI-cellulose sheets (2D maps) using a strong magnet (Figure 2.6). 2D maps are run vertically in 65 mL of 95% LFU, pH 3.35 + 5% dH_2O (D3 development) to top marked line after being pre-developed in 25 mL of dH_2O to the origin. 2D maps are then checked for transfer, cut at the second line from the top, washed twice in 250 mL of dH_2O for 7 min, dried, and a wick attached to the right side in preparation for the final development (D4 development) (Figure 2.7). For the D4 development, the 2D maps are run horizontally in 65 mL of 90% PTU, pH 8.20 + 10% dH_2O to the top of the wick after being pre-developed in 25 mL of 50% 0.8 M NaH_2PO_4, pH 8.2 + 50% dH_2O to the second line marked from the left side. 2D maps are then checked for separation, cut just below the wick, washed twice in 250 mL of dH_2O for 5 min, dried, and cut for autoradiographic development and imager reading (Figure 2.7). An instant imager is used to calculate CPM per spot.

3.3 Results

A small subset experiment was done using dermal application. The goal of this was to compare back to i.p. application and determine differences. 3x3 (three chemicals, three doses) ANOVAs were preformed on this data, p-values listed in Table 3.2. Relative adduct labeling values (RAL per 10^9 nucleotides) are listed in Table 3.3, with all statistical significance data presented in Tables 3.4 and 3.5. For dermal application in the liver tissue, spot 4, chosen because it has been associated with the BAP-diolepoxide (BPDE) adduct in previous studies, elicited the only significant differences observed (Figure 3.2 and Table 3.4). BAP at the 0.429 mg/g bw and 0.171 mg/g bw doses were significantly higher than NF+BAP at the same doses (RAL of 34.15 ± 3.73 and 34.42 ± 0.64 compared to 33.60 ± 2.36 and 33.24 ± 1.83 per 10^9 nucleotides, Table 3.3). BAP was also significantly larger than the RM at the 0.171 mg/g bw and 0.069 mg/g bw doses. RM was significantly higher than NF+BAP at the 0.429 mg/g bw dose, while NF+BAP was significantly higher than RM at the 0.069 mg/g bw dose. All treatments at the 0.069 mg/g bw dose showed a significant increase from the control in this tissue for both spot 4 and total adducts (Table 3.4). All treatments had the same amount of BAP present at each dose, so it is interesting that the BAP would elicit a larger response alone. Interactions within the mixtures are having some effect on the overall genotoxicity.

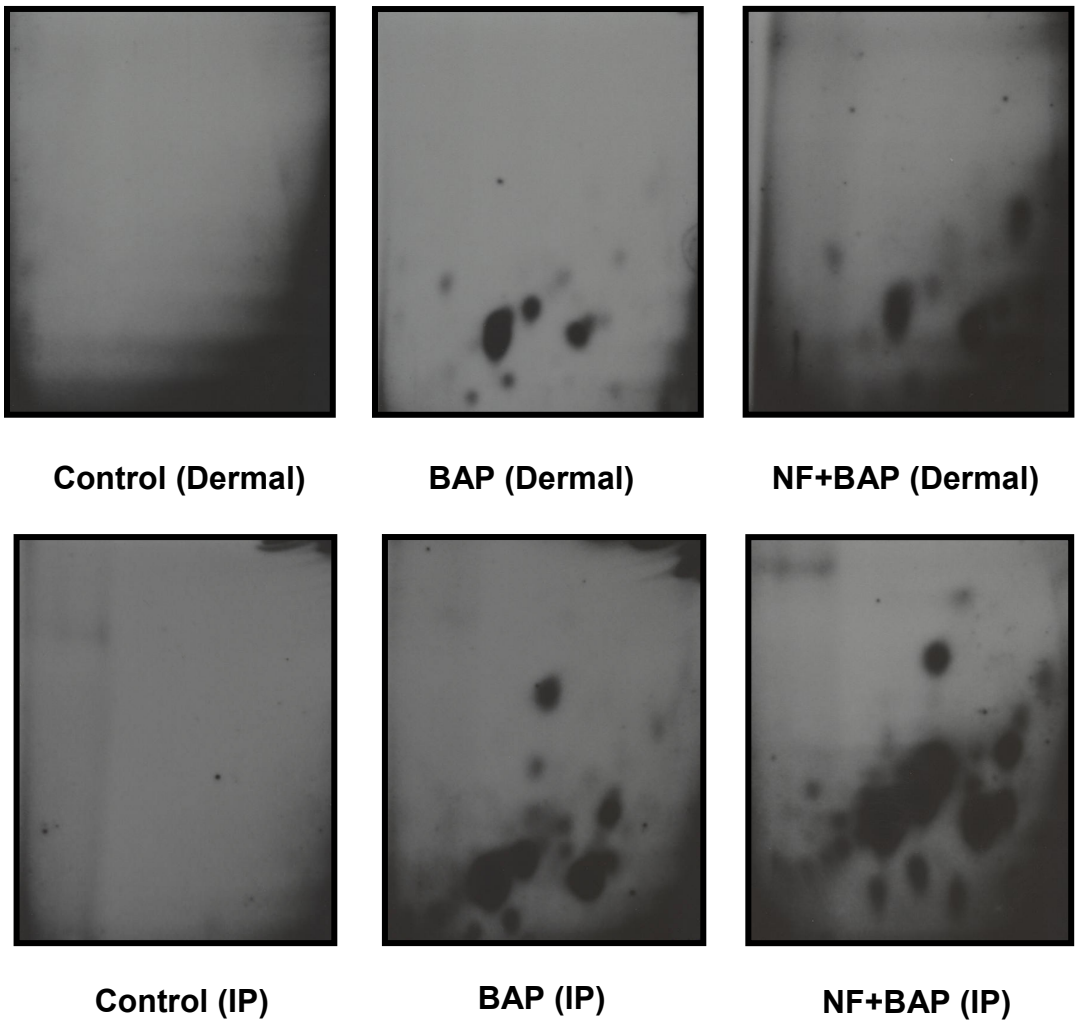

Figure 3.2. Autoradiograms from dermal and intraperitoneal injection (i.p.) exposure of liver tissues, exposure time 1 day.

Table 3.2. P-values for all ANOVAs preformed on contrasts for the dermal application and dermal vs i.p. application analyses (α = 0.05). In the dermal vs i.p. application analysis, a significant three way interaction was observed in all tissues except the forestomach. However, a significant two-way interaction was observed in this tissue as well as in all other tissues.

	Dermal Application		Dermal vs IP Application			
	Chemical:Dose (3x3)		Application:Chemical:Dose (3x3)		Chemical:Dose (3x3)	
Tissue	Total Adducts	Spot 4 Adducts	Total Adducts	Spot 4 Adducts	Total Adducts	Spot 4 Adducts
Liver	0.0001	0.0000	0.0027	0.0004	0.0235	0.0016
Lung	0.0050	0.0090	0.0059	0.0164	0.0001	0.0002
Forestomach	0.0042	0.0000	NS	NS	0.0005	0.0002
Skin	0.0192	0.0108	N/A	N/A	N/A	N/A

NS = Not Significant
N/A = Not Applicable

Table 3.3. Table of DNA adduct levels detected in liver, lung, forestomach and skin of B6CDF1 male mice treated dermally. Data are presented as RAL per 10^9 nucleotides ± SEM.

Mean Total RAL / 10^9 Nucleotides for Skin Application

Tissue	Control	BAP (mg/g bw)		
		0.069	0.171	0.429
Liver	13.24 ± 1.66	24.99 ± 3.04	34.42 ± 0.64	34.15 ± 3.73
Lung	10.13 ± 1.37	21.37 ± 1.87	30.84 ± 3.86	35.06 ± 2.14
Forestomach	7.87 ± 2.52	38.42 ± 5.72	47.80 ± 4.26	37.78 ± 3.32
Skin	7.57 ± 1.03	616.81 ± 99.85	441.92 ± 74.79	640.47 ± 112.09
Mean Spot 4 RAL / 10^9 Nucleotides for Skin Application				
Liver	1.84 ± 0.20	14.68 ± 1.99	13.53 ± 0.42	7.43 ± 0.45
Lung	2.34 ± 0.31	21.00 ± 1.48	17.89 ± 2.20	11.68 ± 0.60
Forestomach	1.10 ± 0.32	17.49 ± 2.03	19.89 ± 1.20	15.10 ± 2.28
Skin	1.55 ± 0.47	426.86 ± 74.26	303.65 ± 52.27	417.36 ± 61.63

Mean Total RAL / 10^9 Nucleotides for Skin Application

Tissue	Control	RM (mg/g bw)		
		0.069	0.171	0.429
Liver	13.24 ± 1.66	23.68 ± 3.37	29.40 ± 2.09	38.80 ± 4.05
Lung	10.13 ± 1.37	9.53 ± 0.67	11.41 ± 3.07	38.94 ± 4.58
Forestomach	7.87 ± 2.52	18.95 ± 2.35	30.96 ± 3.99	60.10 ± 12.34
Skin	7.57 ± 1.03	148.66 ± 20.18	240.44 ± 58.17	492.04 ± 27.77
Mean Spot 4 RAL / 10^9 Nucleotides for Skin Application				
Liver	1.84 ± 0.20	18.14 ± 2.83	8.20 ± 0.98	3.33 ± 0.36
Lung	2.34 ± 0.31	24.31 ± 3.15	6.11 ± 1.54	4.07 ± 0.41
Forestomach	1.10 ± 0.32	26.74 ± 5.19	12.22 ± 1.62	4.74 ± 0.60
Skin	1.55 ± 0.47	322.83 ± 16.21	149.70 ± 38.70	89.39 ± 11.76

Mean Total RAL / 10^9 Nucleotides for Skin Application

Tissue	Control	NF+BAP (mg/g bw)		
		0.069	0.171	0.429
Liver	13.24 ± 1.66	33.62 ± 2.73	33.24 ± 1.83	33.60 ± 2.36
Lung	10.13 ± 1.37	13.55 ± 1	16.81 ± 1.82	19.73 ± 1.12
Forestomach	7.87 ± 2.52	33.88 ± 3.63	53.44 ± 5.26	130.75 ± 18.77
Skin	7.57 ± 1.03	181.04 ± 27.38	224.37 ± 17.76	343.63 ± 70.80
Mean Spot 4 RAL / 10^9 Nucleotides for Skin Application				
Liver	1.84 ± 0.20	6.59 ± 0.39	7.22 ± 0.85	6.26 ± 0.68
Lung	2.34 ± 0.31	10.99 ± 0.68	9.02 ± 1.24	6.45 ± 0.45
Forestomach	1.10 ± 0.32	67.16 ± 10.00	23.69 ± 2.12	11.22 ± 0.86
Skin	1.55 ± 0.47	218.44 ± 47.41	143.56 ± 11.61	108.51 ± 16.86

Table 3.4. Significant confidence intervals for difference in mean total and spot 4 adducts in liver, lung, forestomach and skin of B6C3F1 male mice. For all contrasts computed, the confidence level was 95%. Each tissue had a significant chemical-dose interaction; therefore, data contrasts were computed across dose. P-values listed in Table 3.2.

	BAP x NF+BAP			BAP x RM			RM x NF+BAP		
Tissue	**0.429**	**0.171**	**0.069**	**0.429**	**0.171**	**0.069**	**0.429**	**0.171**	**0.069**
Total DNA Adducts (mg/g bw)									
Liver	NS	NS	NS	NS	NS	NS	NS	NS	NS
Lung	NS	NS	NS	NS	(0.518 , 2.240)	NS	NS	NS	NS
Forestomach	(-2.060 , -0.362)	NS	NS	NS	NS	NS	(-1.790 , -0.092)	NS	NS
Skin	(0.007 , 1.340)	NS	(0.483 , 1.950)	NS	NS	(0.684 , 2.150)	NS	NS	NS
Spot 4 DNA Adducts (mg/g bw)									
Liver	(0.375 , 1.180)	(0.213 , 1.090)	NS	NS	(0.087 , 0.963)	(0.380 , 1.260)	(0.566 , 1.370)	NS	(-1.070 , -0.191)
Lung	NS	NS	NS	NS	(0.535 , 2.670)	NS	NS	NS	NS
Forestomach	(-2.080 , -0.568)	NS	NS	NS	NS	(0.324 , 1.980)	(-1.790 , -0.279)	NS	(-1.710 , -0.056)
Skin	(0.008 , 1.460)	NS	(0.550 , 2.150)	NS	(0.013 , 1.610)	(0.741 , 2.340)	NS	NS	NS

NS = Not Significant

Table 3.5. Significant confidence intervals for difference in mean total and spot 4 adducts compared to control in liver, lung, forestomach and skin in B6C3F1 male mice. For all contrasts computed, the confidence level was 95%. All tissues had a significant chemical-dose interaction; therefore, data contrasts were computed across dose. P-values listed in Table 3.2.

	Total DNA Adducts (0.429mg/g bw)			Spot 4 DNA Adducts (0.429mg/g bw)		
Tissue	**BAP x Control**	**RM x Control**	**NF+BAP x Control**	**BAP x Control**	**RM x Control**	**NF+BAP x Control**
Liver	(0.225 , 1.050)	(0.162 , 0.985)	(0.539 , 1.360)	(0.973 , 1.850)	(0.155 , 1.030)	(0.784 , 1.660)
Lung	NS	NS	NS	(0.571 , 2.710)	NS	NS
Forestomach	(0.969 , 2.830)	(0.278 , 2.140)	(0.864 , 2.720)	(2.010 , 3.670)	(0.856 , 2.510)	(1.740 , 3.400)
Skin	(3.650 , 5.110)	(2.240 , 3.700)	(2.440 , 3.900)	(4.900 , 6.490)	(3.360 , 4.950)	(3.550 , 5.140)

NS = Not Significant

The lung tissue had two significant interactions, one in the total DNA adduct analysis and the other in the spot 4 analysis (Table 3.4). In both significant responses, the BAP was significantly higher than the RM at the 0.171 mg/g bw dose (RAL of 30.84 ± 3.86 and 11.41 ± 3.07 per 10^9 nucleotides for total adducts, Table 3.3). No other response was considered significant in this tissue for dermal application. All treatments were observed to have no significant difference from the control at the 0.069 mg/g bw dose for total adducts (Table 3.4). However, for spot 4 adducts, BAP did elicit a significantly higher response than the control.

In the forestomach, the NF+BAP was observed to be significantly larger than the BAP and RM at the 0.429 mg/g bw dose for total DNA adduct formation (RAL of 130.75 ± 18.77 compared to 37.78 ± 3.32 and 60.10 ±12.34 per 10^9 nucleotides, Tables 3.3 and 3.4). In spot 4 DNA adduct formation, this same response was observed with one difference. NF+BAP was also significantly larger than the RM at the 0.069 mg/g bw dose. All treatments elicit a significantly larger response than the control in this tissue for both total and spot 4 DNA adduct formation at the 0.069 mg/g bw dose (Table 3.5). In this tissue, the NF+BAP elicits larger response than the BAP alone and RM, suggesting unknown interactions are occurring to heighten the response.

Finally, BAP was observed to be significantly higher than NF+BAP at the 0.429 mg/g bw and 0.069 mg/g bw doses in the skin for total DNA adducts formed (RAL of 640.47 ± 112.09 and 616.81 ± 99.85 compared to 343.63 ± 70.80 and 181.04 ± 27.38 per 10^9 nucleotides, Tables 3.3 and 3.4). It was also observed that BAP was significantly higher than the RM at the 0.069 mg/g bw dose. In spot 4, the same responses were observed, along with the BAP also being significantly higher than the RM 0.171 mg/g bw dose. For the control, all treatments at the 0.069 mg/g bw dose were significantly higher than the control in both spot 4 and total DNA adduct formation (Table 3.5). This tissue is the site of application, and is interesting that the BAP alone would elicit larger responses here.

Dermal data was compared to the i.p. application data at time 24 hr. A 3x3 ANOVA was preformed, and all p-values are listed in Table 3.2. A complex three-way

interaction (application-chemical-dose) was found to be significant for all tissues except the forestomach, in which a two-way interaction was significant (chemical-dose). The three-way interaction indicated that none of the factors are significant on their own. Application along with chemical and dose are all connected in the significance. In the two-way interaction, application alone is significant, but only the chemical and dose factors are connected. Interaction plots showing application and chemical-dose interactions for liver are presented in Figure 3.3. There is a significantly different pattern observed based on application and dose and chemical. It is also observed that the i.p. application response is elevated as compared to the dermal response. For BAP dose-response, the dermal levels are observably smaller than those of the i.p. DNA adduct levels (Figure 3.4). When observing each treatment at the 0.429 mg/g bw dose, the same patter for application is again observed, with the NF+BAP eliciting the highest response in the dermal application and the BAP and NF+BAP eliciting similar responses in the i.p. application (Figure 3.5).

Lung total DNA adducts interaction plots for chemical-dose interactions by application are presented in Figure 3.6. Again, a different pattern is observed through the interaction plots based on chemical-dose and application. In the dermal application, BAP and NF+BAP are almost parallel in their response. However, in the i.p. application, BAP begins lower than NF+BAP and then it crosses over at the 0.171 mg/g bw dose to again become parallel to NF+BAP. It is also apparent that the i.p. application is elevated over the dermal application. For the BAP dose-response, plotted in Figure 3.7, it is observed that the dermal application is much lower than the i.p. application. Over all tissues for the 0.429 mg/g bw dose, again it is obvious that the i.p. application is elevated over the dermal application, with apparent differences in patterns (Figure 3.8). In the dermal application, the RM and BAP elicit a similar response, both higher than the NF+BAP. However, in the i.p. application, the NF+BAP clearly elicits a higher response than the RM and BAP.

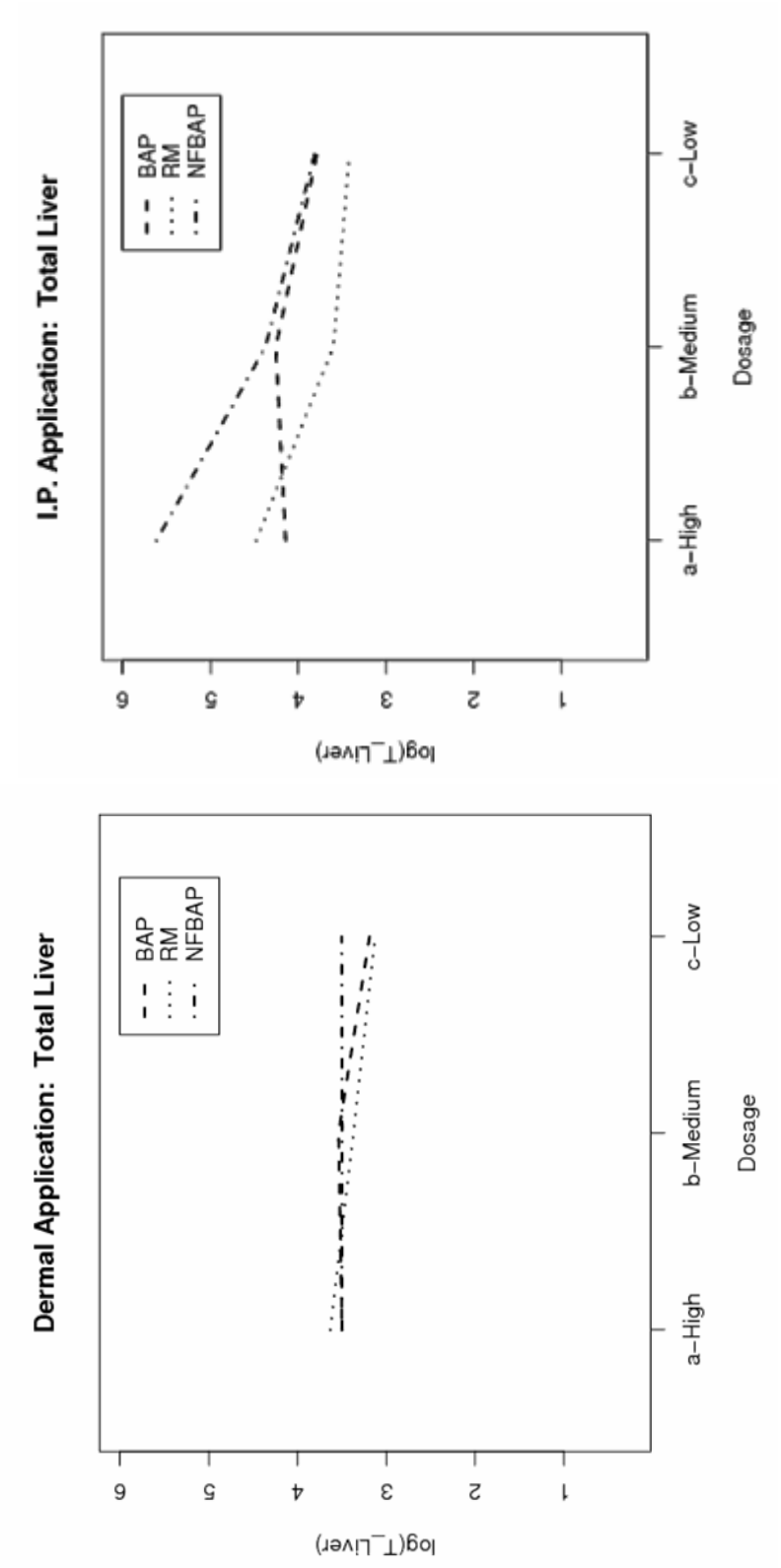

Figure 3.3. Interaction plots of the application-chemical-dose interactions for liver.

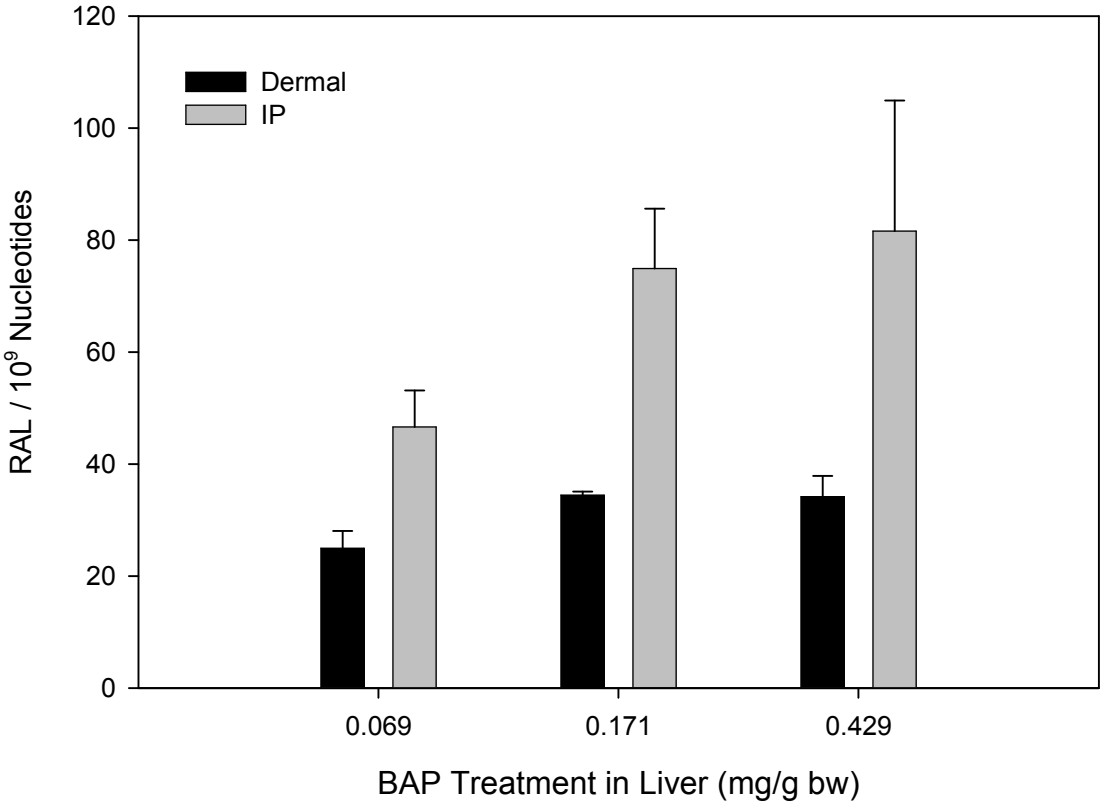

Figure 3.4. Difference between dermal and i.p. application mean total DNA adducts of BAP treatment in liver. Data are presented as RAL per 10^9 nucleotides.

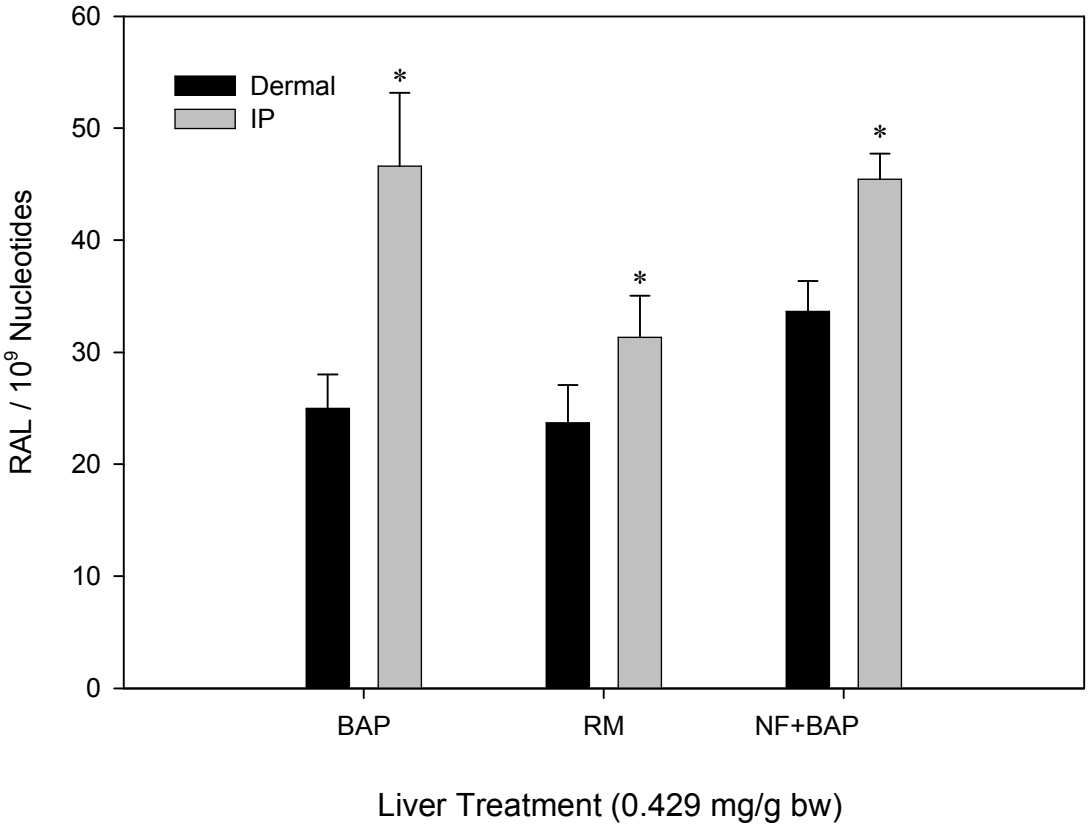

Figure 3.5. Difference between dermal and i.p. application mean total DNA adducts over all treatments in liver. Data are presented as RAL per 10^9 nucleotides. *=Elevated response observed.

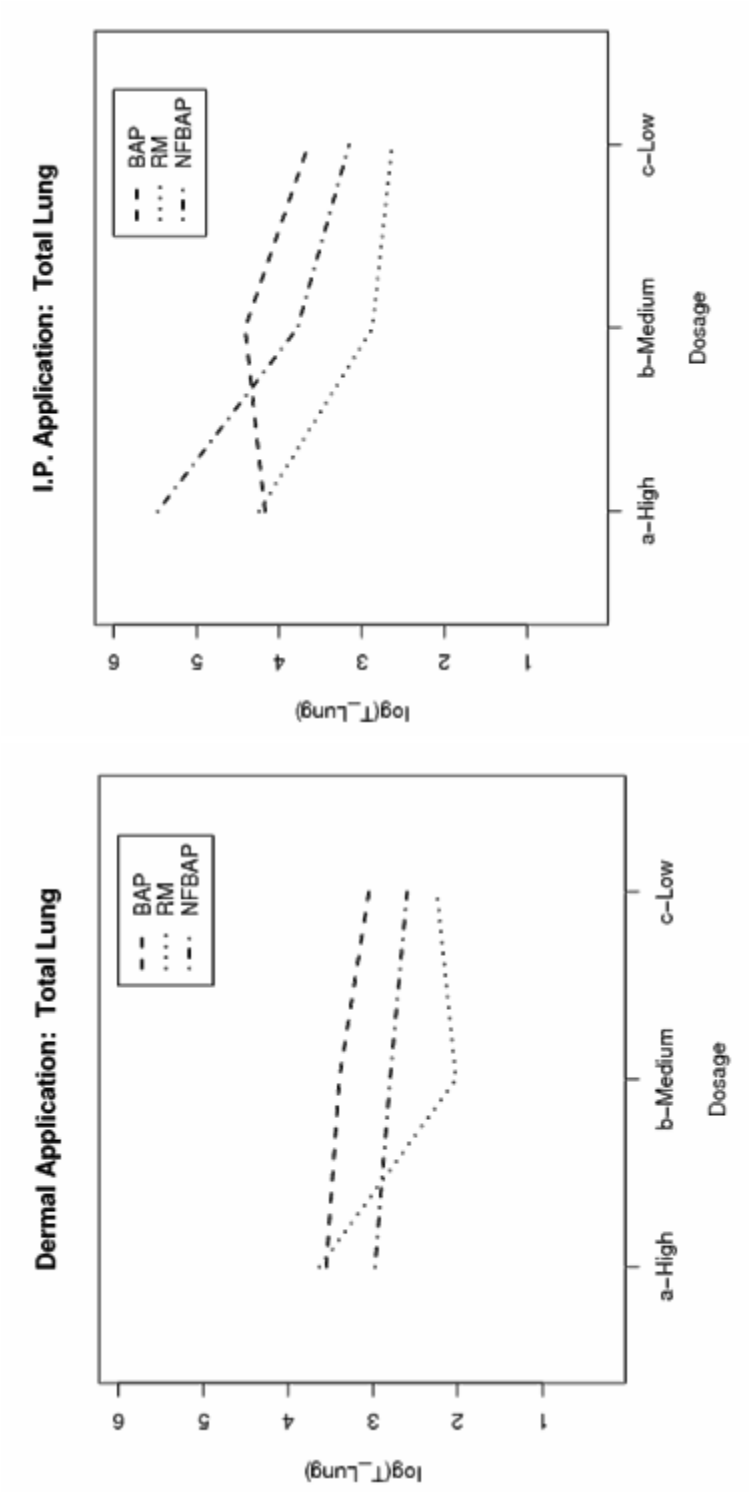

Figure 3.6. Interaction plots of the application-chemical-dose interactions for lung.

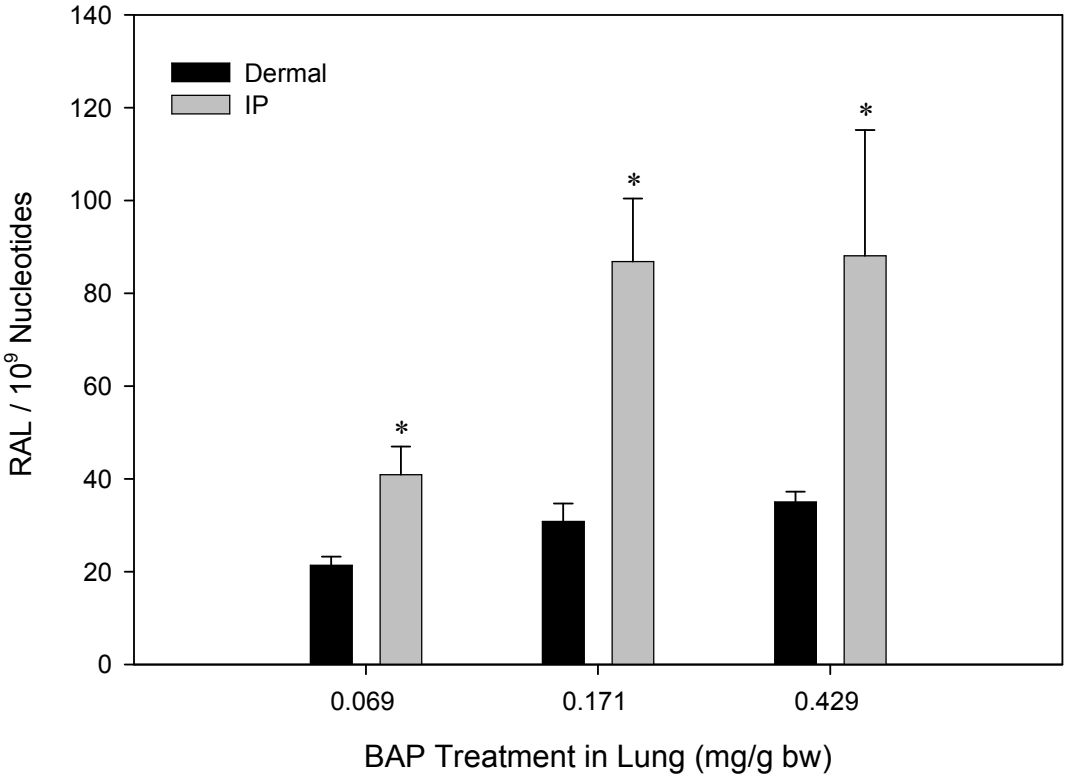

Figure 3.7. Difference between dermal and i.p. application mean total DNA adducts of BAP treatment in lung. Data are presented as RAL per 10^9 nucleotides. *=Elevated response observed.

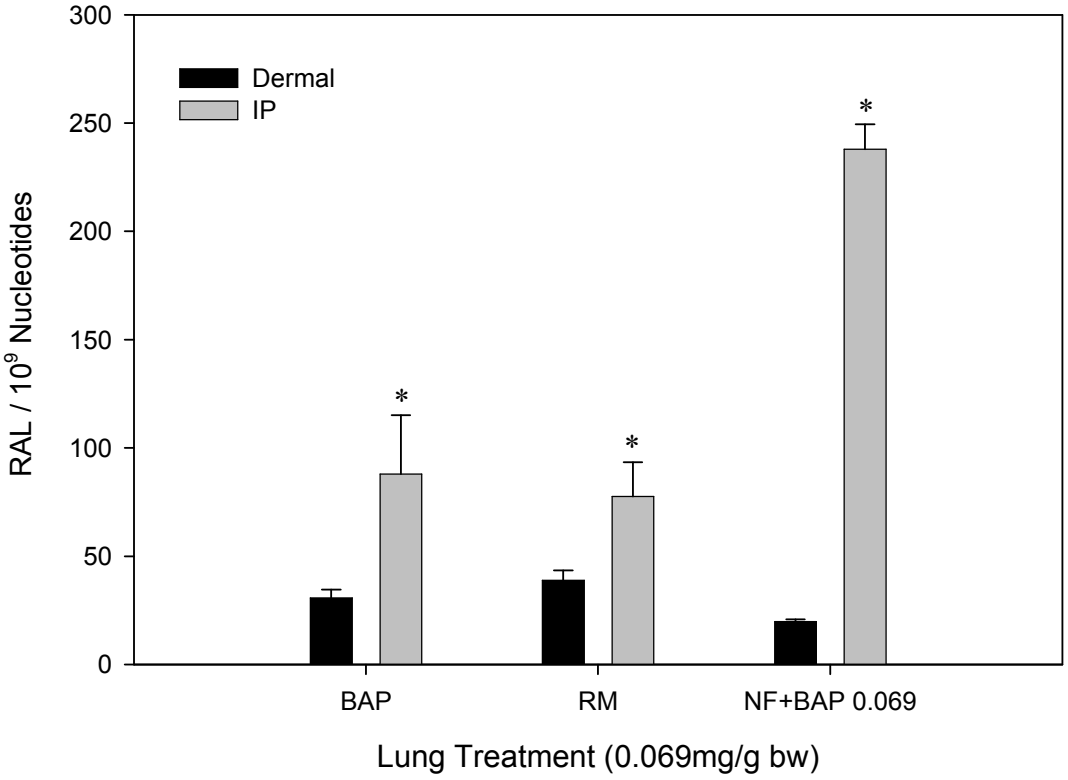

Figure 3.8. Difference between dermal and i.p. application mean total DNA adducts over all treatments in lung. Data are presented as RAL per 10^9 nucleotides. *=Elevated response observed.

Finally, interaction plots for the forestomach dermal and i.p. chemical-dose interactions are presented in Figure 3.9. For the forestomach, only a significant two-way interaction was observed. The same pattern is formed based on the dose-chemical interaction. This pattern is elevated in the i.p. application as compared to the dermal application. In the BAP dose-response for this tissue, this pattern is observed (Figure 3.10). The doses appear to follow the same pattern, just eleveated for the i.p. application. Over all of the chemical treatments, again the same pattern emerges. The BAP shows the lowest response, with RM next above it, and NF+BAP eliciting the highest response in the dermal applications (Figure 3.11). This is the same pattern observed in the i.p. application, just at an elevated level.

A larger experiment was preformed to collect data from the i.p. injection application in three tissues, liver, lung and forestomach over three different time points in the lung and forestomach (1 day, 7 days and 21 days) and four different time points in the liver (1 day, 7 days, 21 days and 280 days). Budget constraints did not allow for all four chemical treatments to be collected at all the time points; therefore, it was decided that the NF would be collected only at two time points (1 day and 21 days). Tissue aliquot constraints prevented the lung and forestomach tissues from being sampled at time 280 days. The DNA adduct data (Table 3.6) shows that NF+BAP was the most genotoxic in all three tissues. Although the NF did not induce a response comparable to the other treatments, it did induce a response that was anywhere from ½ to ¼ as toxic as BAP, eventhough it contains a level of BAP less than 1% the level found in all other treatments. All of the data was compared for differences in DNA adduct frequencies over time among chemical treatment groups, as well as within chemical treatment groups. The BAP treatment groups were contrasted to the NF+BAP and RM treatment groups. These contrasts were done to compare the differences between pure BAP to a

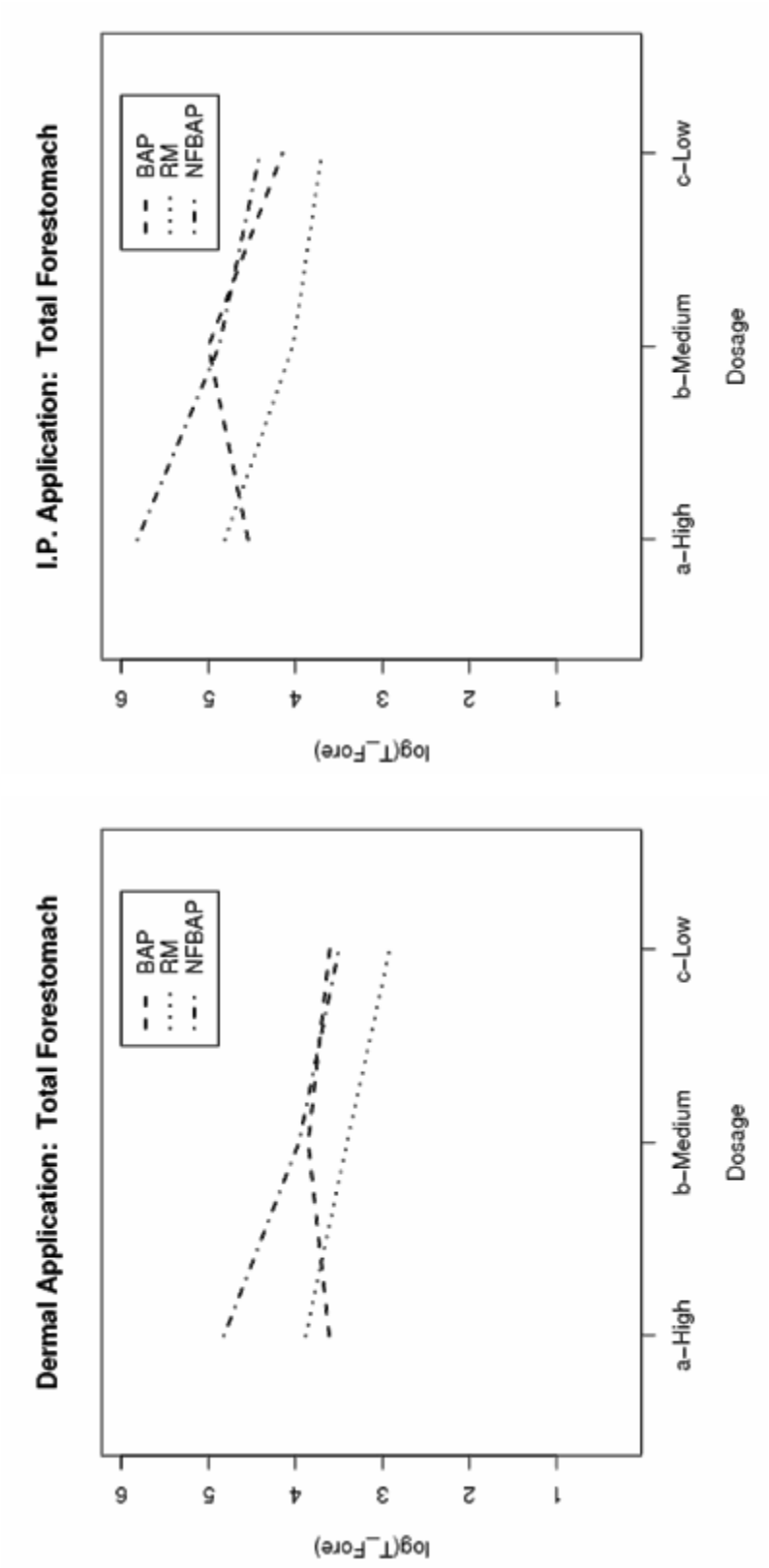

Figure 3.9. Interaction plots of the application-chemical-dose interactions for forestomach.

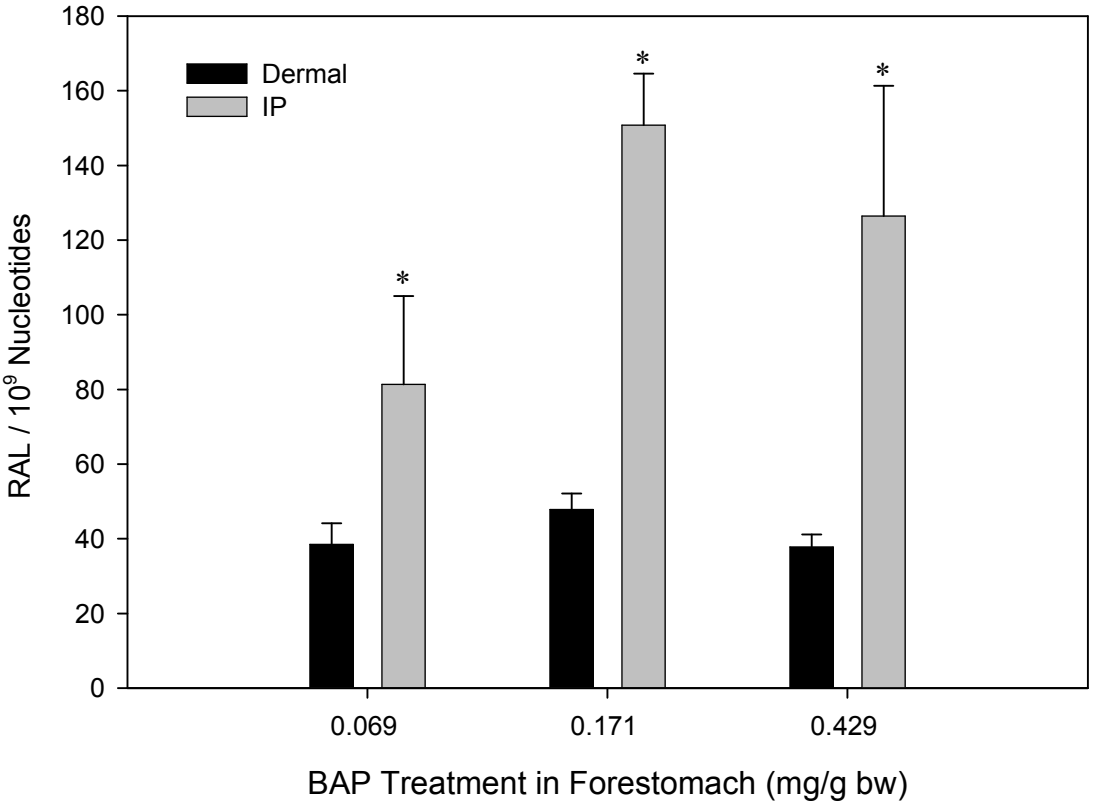

Figure 3.10. Difference between dermal and i.p. application mean total DNA adducts of BAP treatment in forestomach. Data are presented as RAL per 10^9 nucleotides. *=Elevated response observed.

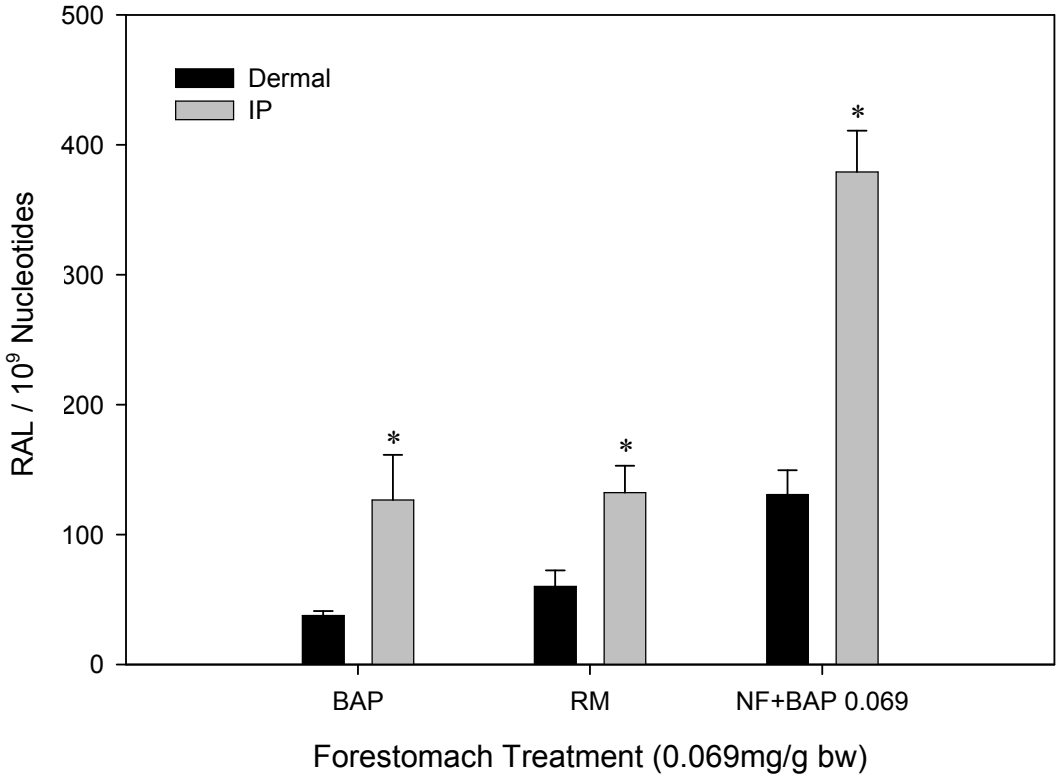

Figure 3.11. Difference between dermal and i.p. application mean total DNA adducts over all treatments in forestomach. Data are presented as RAL per 10^9 nucleotides. *=Elevated response observed.

complex mixture as well as to a mixture of carcinogenic PAHs (all groups containing the same amount of BAP). The RM treatment groups were also contrasted to the NF+BAP treatment groups to compare the differences between a mixture of carcinogenic PAHs to a complex mixture containing the same level of those PAHs. Next, the NF+BAP treatment groups were contrasted to the NF treatment groups to compare the differences between complex mixtures containing high and low levels of BAP. Finally, all chemical treatments were contrasted among themselves to compare the differences over time. All contrasts were built up to the final analysis as described in the materials and methods section. A 4x3x3 (four chemicals, three doses and three times) ANOVA was preformed on the lung and forestomach tissues, while a 4x3x4 (four chemicals, three doses and four times) was preformed on the liver tissue. Both analyses used the log transformed RAL per 10^9 nucleotides. All p-values are listed in Table 3.7.

It is important to note that autoradiograms, presented in Figure 3.12, show a large quantity of background present, especially in the longer time points. This is due to different factors present, including PEI cellulose sheets and I compounds present in older animals. This is most likely one factor that accounts for the increase that is observed at time point 280 days. Controls were contrasted against treatment chemicals to determine statistical relationships (Table 3.8). In the liver tissue, only at days 21 and 280 was the BAP not significantly higher than the control in both total and spot 4 analyses. RM was not significantly higher than the control at day 21 in total and spot 4 analyses, and NF+BAP was not significantly higher than the control at day 280 in total and spot 4 analyses. NF was not significantly higher than the control at days 21 and 280 in the total analyses only. At day 280, RM and NF+BAP were significantly lower than the control in total DNA adducts, as well as RM and NF were significantly lower than the control in the spot 4 DNA adducts. Again, this is most likely due to the large presence of background in the samples. For the lung tissue, all chemicals were significantly higher than the control, except for the NF at 21 days in both the total and spot 4 adduct data. The forestomach tissue, as well, was only not significantly higher than the control in the NF at days 1 and 21 in total and spot 4 adduct analyses.

Table 3.6. Table of DNA adduct levels detected in liver of B6CDF1 male mice. Data are presented as RAL per 10^9 nucleotides ± SEM. N/A = Not Applicable.

		Mean Total RAL / 10^9 Nucleotides in Liver				Mean Spot 4 RAL / 10^9 Nucleotides in Liver			
Chemical	**Dose (mg/g bw)**	**1 Day**	**7 Days**	**21 Days**	**280 Days**	**1 Day**	**7 Days**	**21 Days**	**280 Days**
Control	--	12.51 ± 1.33	10.81 ± 1.42	24.09 ± 4.65	35.41 ± 4.06	1.86 ± 0.18	1.76 ± 0.19	2.62 ± 0.36	4.42 ± 0.37
BAP	0.069	64.62 ± 6.53	24.98 ± 2.19	19.33 ± 1.87	39.44 ± 17.90	21.29 ± 3.93	9.51 ± 1.03	2.94 ± 0.18	4.65 ± 1.94
	0.171	74.88 ± 10.76	74.14 ± 34.77	26.66 ± 3.43	38.69 ± 9.04	37.35 ± 6.02	14.51 ± 1.74	5.63 ± 0.52	5.49 ± 1.48
	0.429	81.57 ± 23.38	61.91 ± 9.15	29.52 ± 3.42	32.46 ± 4.21	40.01 ± 13.49	20.84 ± 3.66	7.86 ± 1.37	4.11 ± 0.17
RM	0.069	31.33 ± 3.70	27.08 ± 3.36	25.52 ± 3.61	16.35 ± 2.61	7.76 ± 1.55	5.24 ± 0.60	3.30 ± 0.27	2.01 ± 0.20
	0.171	42.14 ± 11.17	36.52 ± 4.49	33.83 ± 5.15	17.51 ± 1.93	14.46 ± 5.82	7.08 ± 1.12	6.18 ± 0.61	2.26 ± 0.11
	0.429	94.58 ± 14.94	47.77 ± 5.37	37.62 ± 5.06	20.89 ± 1.42	41.99 ± 8.12	14.27 ± 2.76	9.37 ± 2.23	2.34 ± 0.03
NF+BAP	0.069	45.44 ± 2.30	27.94 ± 1.76	30.41 ± 2.8	10.08 ± 0.70	11.97 ± 0.30	5.74 ± 0.72	5.35 ± 0.55	1.27 ± 0.17
	0.171	85.07 ± 14.46	76.92 ± 6.49	40.29 ± 5.86	16.78 ± 2.81	28.18 ± 7.28	30.62 ± 4.24	9.18 ± 2.19	2.05 ± 0.27
	0.429	276.46 ± 18.97	157.32 ± 41.49	53.52 ± 3.52	20.20 ± 4.65	122.47 ± 6.88	75.76 ± 24.24	13.54 ± 3.37	2.65 ± 0.37
NF	0.069	44.90 ± 5.47	N/A	35.88 ± 3.45	N/A	6.33 ± 0.67	N/A	4.71 ± 0.45	N/A
	0.171	37.62 ± 3.00	N/A	24.16 ± 2.10	N/A	5.76 ± 0.83	N/A	3.50 ± 0.35	N/A
	0.429	39.24 ± 3.46	N/A	32.76 ± 2.98	13.66 ± 1.42	7.76 ± 2.54	N/A	4.35 ± 0.45	1.64 ± 0.28

Table 3.7. ANOVA p-values for all contrasts preformed in the i.p. application analysis ($\alpha = 0.05$). NA = Not Applicable.

	Chemical:Time (4x3x3)		Chemical:Time (5x3 or 5x4)		Chemical:Dose (4x3x3)		Chemcial:Dose:Time (4x3x4)
Tissue	**Total Adducts**	**Spot 4 Adducts**	**Total Adducts**	**Spot 4 Adducts**	**Total Adducts**	**Spot 4 Adducts**	**Spot 4 Adducts**
Liver	0.0000	N/A	0.0000	0.0000	0.0000	N/A	0.0347
Lung	0.0017	0.0003	0.0000	0.0000	0.0000	0.0000	N/A
Forestomach	0.0023	0.0256	0.0154	0.0124	0.0026	0.0050	N/A

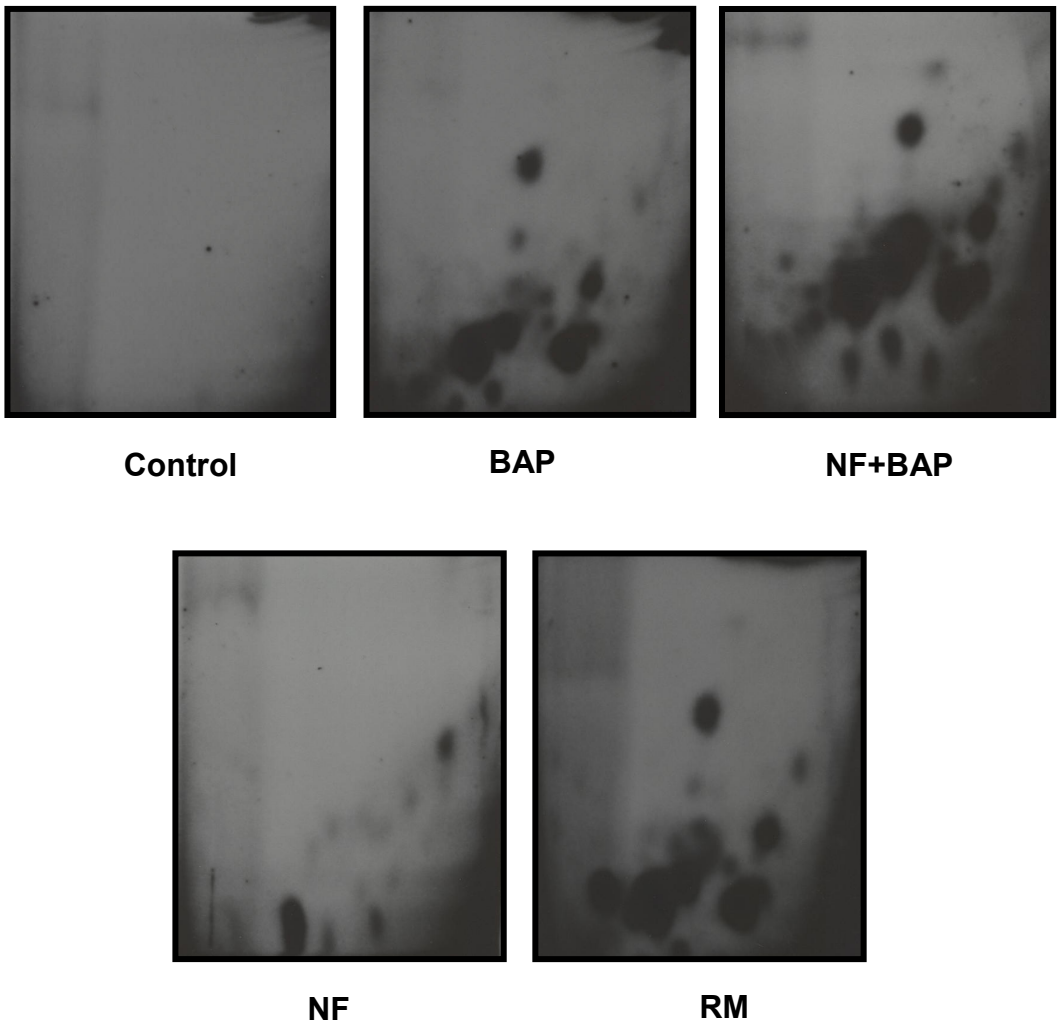

Figure 3.12. Autoradiograms of liver tissues, i.p. exposure time of 1 day.

Table 3.8. Significant confidence intervals for difference in mean total and spot 4 adducts compared to the control in liver, lung, forestomach and skin of B6C3F1 male mice. For all contrasts computed, the confidence level was 95%. Each tissue had a significant chemical-time interaction; therefore, data contrasts were computed across time. P-values listed in Table 3.2.

Total DNA Adducts

	Control x BAP				Control x RM			
Tissue	**1 day**	**7 days**	**21 days**	**280 days**	**1 day**	**7 days**	**21 days**	**280 days**
Liver	(-1.870 , -0.681)	(-1.420 , -0.300)	NS	NS	(-1.500 , -0.312)	(-1.480 , -0.362)	NS	(0.062 , 1.510)
Lung	(-2.650 , -1.570)	(-2.650 , -1.620)	(-1.320 , -0.231)	N/A	(-1.640 , -0.555)	(-1.740 , -0.716)	(-1.250 , -0.224)	N/A
Forestomach	(-2.780 , -1.220)	(-2.870 , -1.400)	(-1.940 , -0.376)	N/A	(-2.330 , -0.765)	(-2.520 , -1.050)	(-1.640 , -0.170)	N/A
	Control x NF+BAP				**Control x NF**			
Tissue	**1 day**	**7 days**	**21 days**	**280 days**	**1 day**	**7 days**	**21 days**	**280 days**
Liver	(-1.900 , -0.707)	(-1.540 , -0.418)	NS	(0.526 , 1.970)	(-1.860 , -0.669)	N/A	NS	NS
Lung	(-2.160 , -1.080)	(-2.140 , -1.110)	(-1.840 , -0.812)	N/A	(-1.510 , -0.422)	N/A	NS	N/A
Forestomach	(-3.040 , -1.480)	(-2.320 , -0.854)	(-1.970 , -0.500)	N/A	NS	N/A	NS	N/A

Spot 4 DNA Adducts

	Control x BAP				Control x RM			
Tissue	**1 day**	**7 days**	**21 days**	**280 days**	**1 day**	**7 days**	**21 days**	**280 days**
Liver	(-2.950 , -1.710)	(-2.270 , -1.100)	NS	NS	(-1.990 , -0.748)	(-1.670 , -0.503)	NS	(0.036 , 1.550)
Lung	(-3.720 , -2.560)	(-3.440 , -2.340)	(-2.030 , -0.865)	N/A	(-2.150 , -0.990)	(-2.330 , -1.240)	(-1.790 , -0.693)	N/A
Forestomach	(-4.250 , -1.990)	(-4.310 , -2.190)	(-3.450 , -1.190)	N/A	(-2.980 , -0.727)	(-3.670 , -1.550)	(-2.670 , -0.548)	N/A
	Control x NF+BAP				**Control x NF**			
Tissue	**1 day**	**7 days**	**21 days**	**280 days**	**1 day**	**7 days**	**21 days**	**280 days**
Liver	(-2.500 , -1.260)	(-1.760 , -0.587)	(-1.320 , -0.146)	NS	(-1.840 , -0.596)	N/A	(-1.200 , -0.026)	(0.498 , 2.010)
Lung	(-2.830 , -1.660)	(-2.770 , -1.670)	(-2.430 , -1.340)	N/A	(-1.480 , -0.315)	N/A	NS	N/A
Forestomach	(-4.360 , -2.100)	(-3.310 , -1.180)	(-3.660 , -1.540)	N/A	NS	N/A	NS	N/A

NS = Not Significant
N/A = Not Applicable

All contrast data for total and spot 4 adducts evaluated in the liver tissue over time is summarized in Tables 3.9, and 3.10. For this tissue, a significant interaction was observed between chemical and time (Table 3.9). Due to this interaction, all contrasts were made using this two-way interaction (Figure 3.13). Overall, all chemicals decrease significantly over time (Figure 3.14). NF+BAP (RAL of 276.46 ± 18.97 per 10^9 nucleotides in 0.429 mg/g bw dose) is significantly higher than RM (RAL of 94.58 ± 14.94 per 10^9 nucleotides in 0.429 mg/g bw dose) and NF (RAL of 39.24 ± 3.46 per 10^9 nucleotides in 0.429 mg/g bw dose) at 1 day, RM at 7 days and finally significantly higher than BAP at 21 days (Table 3.9 and 3.10). A significant interaction between treatment, dose and time was observed for spot 4 (Table 3.11). As there was a significant three-way interaction, all contrasts were made using this three-way interaction (Figure 3.15). In the spot 4 data, NF+BAP is significantly higher than BAP, RM and NF at 1 day, and BAP and RM at 7 days in the 0.429 mg/g bw dose. For the 0.171 mg/g bw dose, NF+BAP is again significantly higher than NF, while BAP is higher than RM at 1 day. At 7 days, NF+BAP is higher than RM. The pattern of the chemical response changes depending upon dose (Figures 3.15 and 3.16). For the high dose, NF+BAP generally elicit the maximum response, while for the medium and low doses BAP generally elicits the maximum response. This could be due to toxicity factors influencing the high dose response.

Table 3.9. Significant confidence intervals for differences in mean total DNA adducts in liver, lung and forestomach tissues across time. For all contrasts computed, the confidence level was 95%. In total adducts, each tissue had a significant chemical-time interaction; therefore, data contrasts were computed across time. P-values listed in Table 3.2.

Confidence Intervals for Differences in Mean Total Adducts in B6C3F1 Male Mouse Tissues: Contrasts for Chemicals Across Time

		BAP x NF+BAP	RM x NF+BAP	NF+BAP x NF	BAP x RM
1 Day	Liver	(-0.973, -0.103)	(-1.203, -0.333)	(0.483, 1.353)	NS
	Lung	NS	(-1.342, -0.428)	(1.094, 2.008)	(0.370, 1.284)
	Forestomach	NS	(-1.439, -0.269)	(1.501, 2.671)	NS
7 Days	Liver	NS	(-1.063, -0.159)	N/A	NS
	Lung	NS	(-1.359, -0.411)	N/A	(0.308, 1.222)
	Forestomach	NS	(-1.376, -0.162)	N/A	(0.024, 1.194)
21 Days	Liver	(-0.941, -0.039)	NS	NS	NS
	Lung	(-1.212, -0.266)	(-1.253, -0.323)	(1.017, 1.981)	NS
	Forestomach	NS	NS	(0.331, 1.565)	NS
280 Days	Liver	(0.261, 1.385)	NS	NS	(0.059, 1.183)
	Lung	N/A	N/A	N/A	N/A
	Forestomach	N/A	N/A	N/A	N/A
		BAP x BAP	**RM x RM**	**NF+BAP x NF+BAP**	**NF x NF**
1 Day to 7 Days	Liver	NS	NS	NS	N/A
	Lung	NS	NS	NS	N/A
	Forestomach	NS	NS	NS	N/A
1 Day to 21 Days	Liver	(0.428, 1.314)	NS	(0.476, 1.362)	NS
	Lung	(0.312, 1.242)	NS	NS	NS
	Forestomach	NS	NS	(0.249, 1.441)	NS
1 Days to 280 Days	Liver	(0.052, 1.058)	(0.443, 1.449)	(1.413, 2.419)	(0.040, 1.548)
	Lung	N/A	N/A	N/A	N/A
	Forestomach	N/A	N/A	N/A	N/A
7 Days to 21 Days	Liver	(0.126, 1.012)	NS	(0.032, 0.950)	N/A
	Lung	(0.255, 1.185)	NS	NS	N/A
	Forestomach	NS	NS	(0.013, 1.247)	N/A
7 Days to 280 Days	Liver	NS	(0.172, 1.178)	(0.971, 2.005)	NS
	Lung	N/A	N/A	N/A	N/A
	Forestomach	N/A	N/A	N/A	N/A
21 Days to 280 Days	Liver	NS	(0.037, 1.043)	(0.488, 1.506)	NS
	Lung	N/A	N/A	N/A	N/A
	Forestomach	N/A	N/A	N/A	N/A

NS = Not Significant
N/A = Data Not Available

Table 3.10. Table of DNA adduct levels detected in lung of B6CDF1 male mice. Data are presented as RAL per 10^9 nucleotides ± SEM. N/A = Not Applicable.

		Mean Total RAL / 10^9 Nucleotides in Lung			Mean Spot 4 RAL / 10^9 Nucleotides in Lung		
Chemical	**Dose (mg/g bw)**	**1 Day**	**7 Days**	**21 Days**	**1 Day**	**7 Days**	**21 Days**
Control	--	4.79 ± 0.64	4.31 ± 0.57	7.71 ± 1.61	1.15 ± 0.15	1.08 ± 0.15	1.76 ± 0.40
BAP	0.069	40.89 ± 6.03	35.28 ± 2.12	13.05 ± 3.96	62.64 ± 20.48	49.66 ± 7.98	21.83 ± 3.07
	0.171	86.81 ± 13.59	61.35 ± 7.83	36.19 ± 7.22	60.55 ± 10.07	36.51 ± 4.18	20.28 ± 4.73
	0.429	88.02 ± 27.13	88.22 ± 13.36	39.26 ± 5.03	28.33 ± 4.64	19.06 ± 1.53	6.99 ± 1.08
RM	0.069	14.19 ± 1.41	14.21 ± 0.76	15.59 ± 2.32	48.58 ± 11.08	31.39 ± 4.73	24.11 ± 3.18
	0.171	21.07 ± 6.42	24.19 ± 3.16	27.20 ± 1.88	10.75 ± 3.87	12.30 ± 1.89	12.78 ± 0.72
	0.429	77.57 ± 15.92	55.72 ± 7.33	44.87 ± 6.03	5.61 ± 0.83	6.26 ± 0.43	5.63 ± 0.67
NF+BAP	0.069	23.64 ± 1.64	19.53 ± 2.27	27.50 ± 3.93	151.65 ± 6.80	129.83 ± 27.13	109.68 ± 51.47
	0.171	48.60 ± 10.60	66.01 ± 14.61	53.71 ± 9.08	27.69 ± 7.65	37.40 ± 8.94	26.51 ± 5.7
	0.429	237.93 ± 11.54	222.73 ± 43.99	147.01 ± 69.34	10.69 ± 0.89	8.92 ± 0.88	10.92 ± 1.94
NF	0.069	12.23 ± 0.59	N/A	6.69 ± 0.49	4.36 ± 0.73	N/A	4.94 ± 0.87
	0.171	11.69 ± 0.56	N/A	12.74 ± 1.73	2.75 ± 0.20	N/A	3.13 ± 0.36
	0.429	16.82 ± 2.08	N/A	18.85 ± 2.51	2.75 ± 0.12	N/A	2.38 ± 0.15

Table 3.11. Significant confidence intervals for difference in mean spot 4 DNA adducts in liver tissue across dose and time. For all contrasts computed, the confidence level was 95%. In spot 4 adducts, each tissue had a significant chemical-dose-time interaction; therefore, data contrasts were computed across dose and time. Spot 4 was chosen because in previous studies it has been shown to correspond with benzo(a)pyrene. P-values listed in Table 3.2.

Confidence Intervals for Differences in Mean Spot 4 Adducts in Liver of B6C3F1 Male Mouse Tissues: Contrasts for Chemicals Across Dose & Time

		BAP x RM	BAP x NF+BAP	RM x NF+BAP	NF+BAP x NF
High Dose (0.429mg/g bw)	1 Day	NS	(-2.532, -0.590)	(-2.165, -0.223)	(1.943, 3.885)
	7 Days	NS	(-2.077, -0.135)	(-2.450, -0.508)	NS
	21 Days	NS	NS	NS	NS
	280 Days	NS	NS	NS	NS
Medium Dose (0.171mg/g bw)	1 Day	(0.267, 2.209)	NS	NS	(0.467, 2.409)
	7 Days	NS	NS	(-2.612, -0.370)	NS
	21 Days	NS	NS	NS	NS
	280 Days	NS	NS	NS	NS
Low Dose (0.069mg/g bw)	1 Day	NS	NS	NS	NS
	7 Days	NS	NS	NS	NS
	21 Days	NS	NS	NS	NS
	280 Days	NS	NS	NS	NS

NS = Not Significant

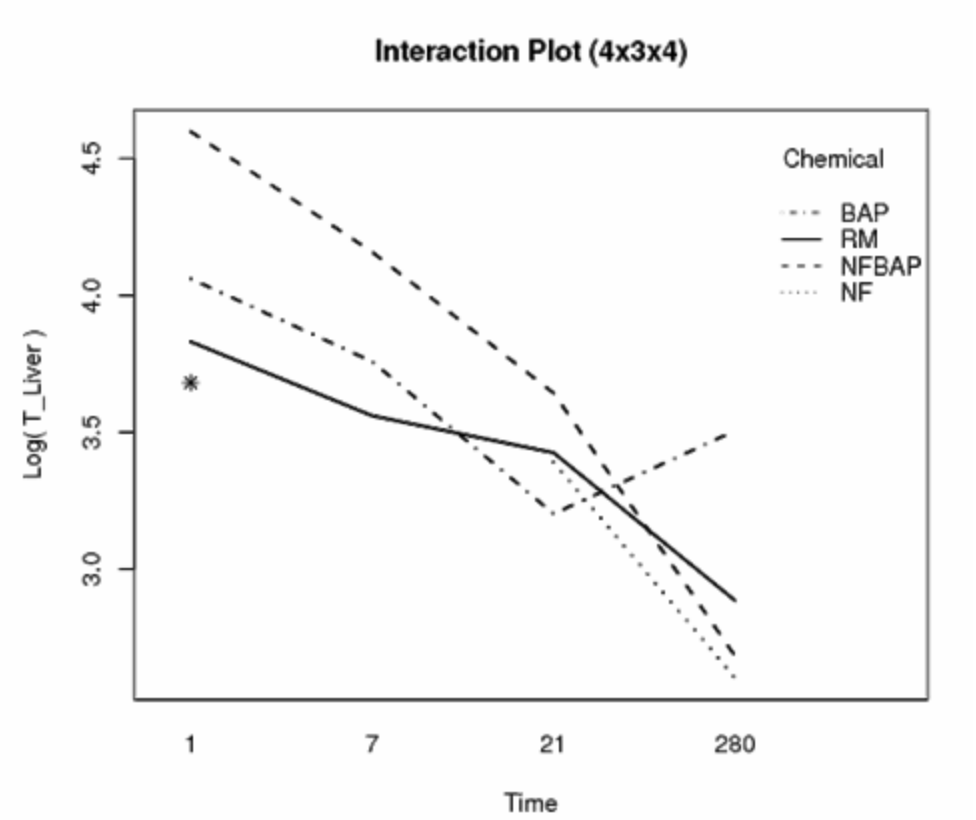

Figure 3.13. 4x3x4 interaction plot for differences in mean total DNA adducts in liver tissue over time. *Represents individual points for NF, a line could not be drawn as points are missing.

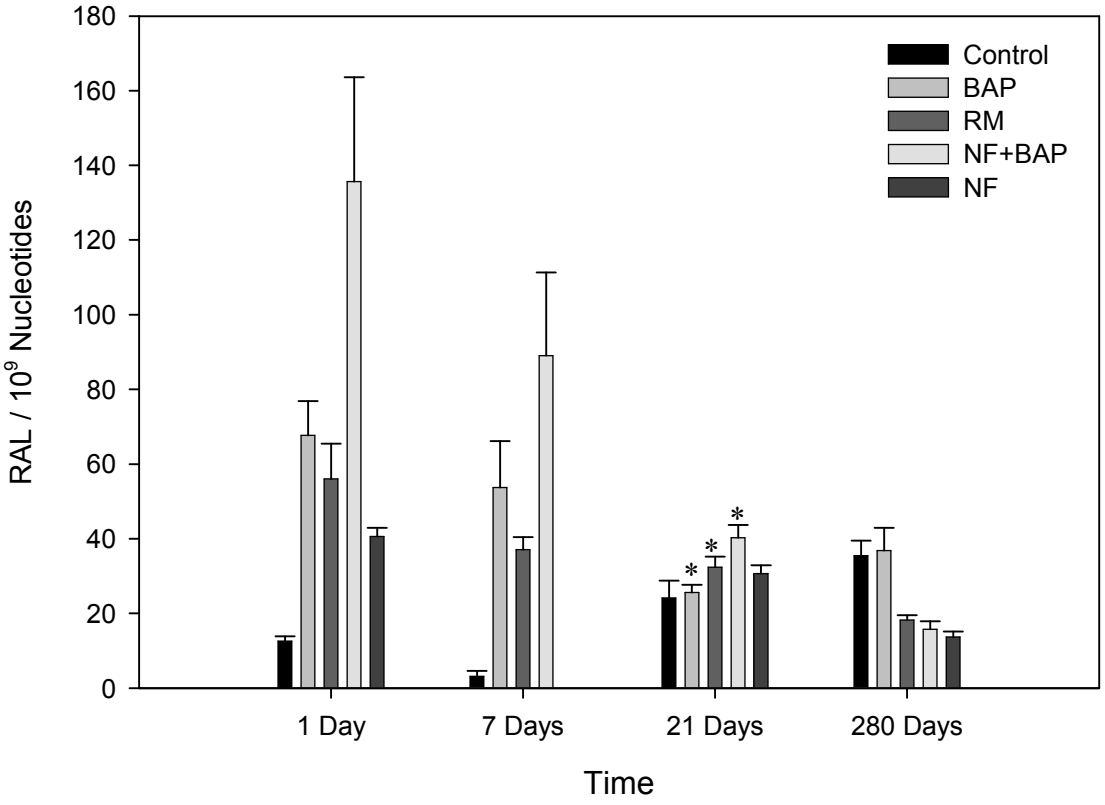

Figure 3.14. Mean total DNA adducts detected in liver tissue for treatments contrasted against time. Data are presented as RAL per 10^9 nucleotides ± SEM. *Significantly lower than day 1.

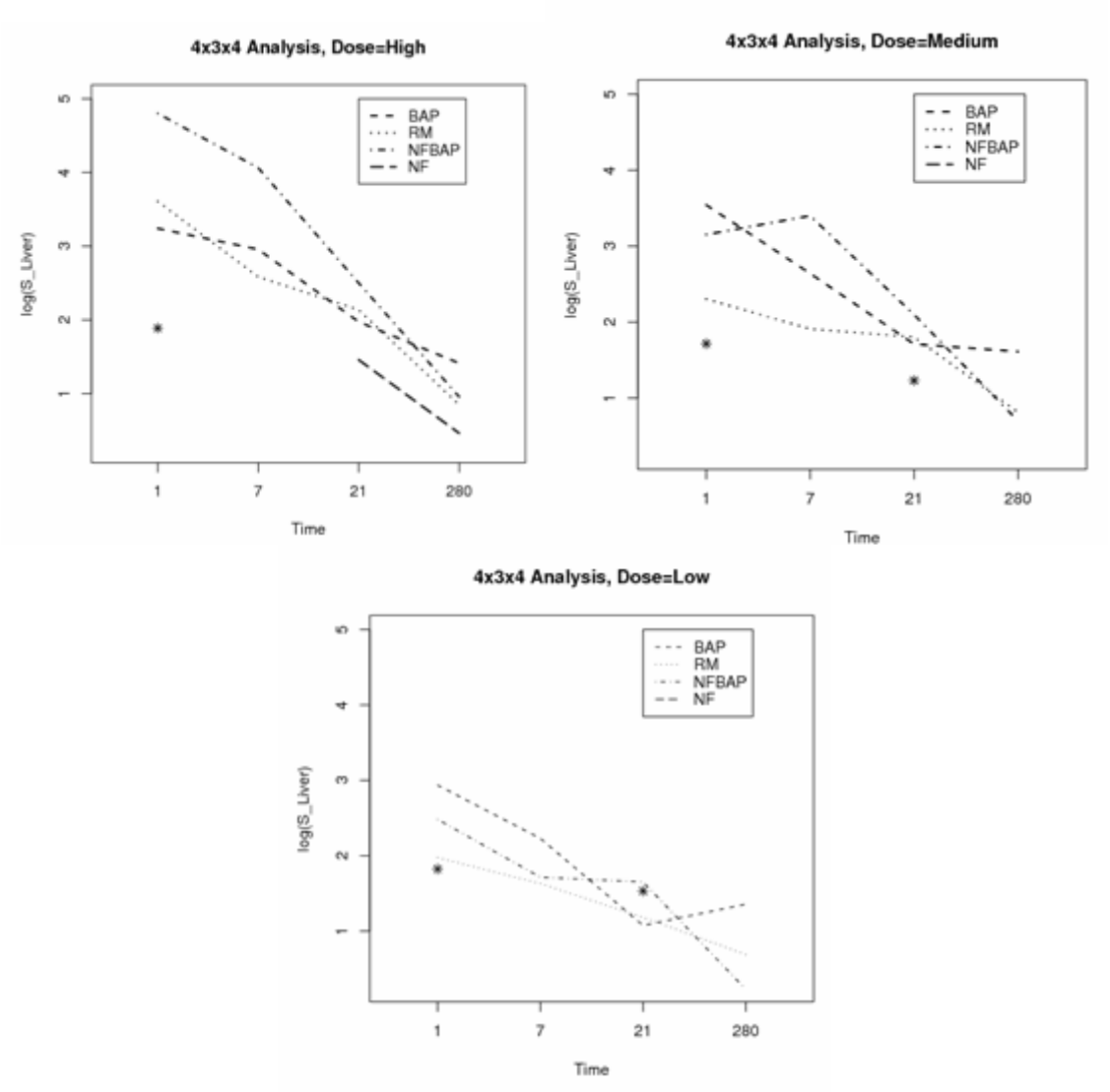

Figure 3.15. 4x3x4 interaction plots for differences in mean spot 4 DNA adducts in liver tissue over dose and time. *Represents individual points for NF, a line could not be drawn as points are missing.

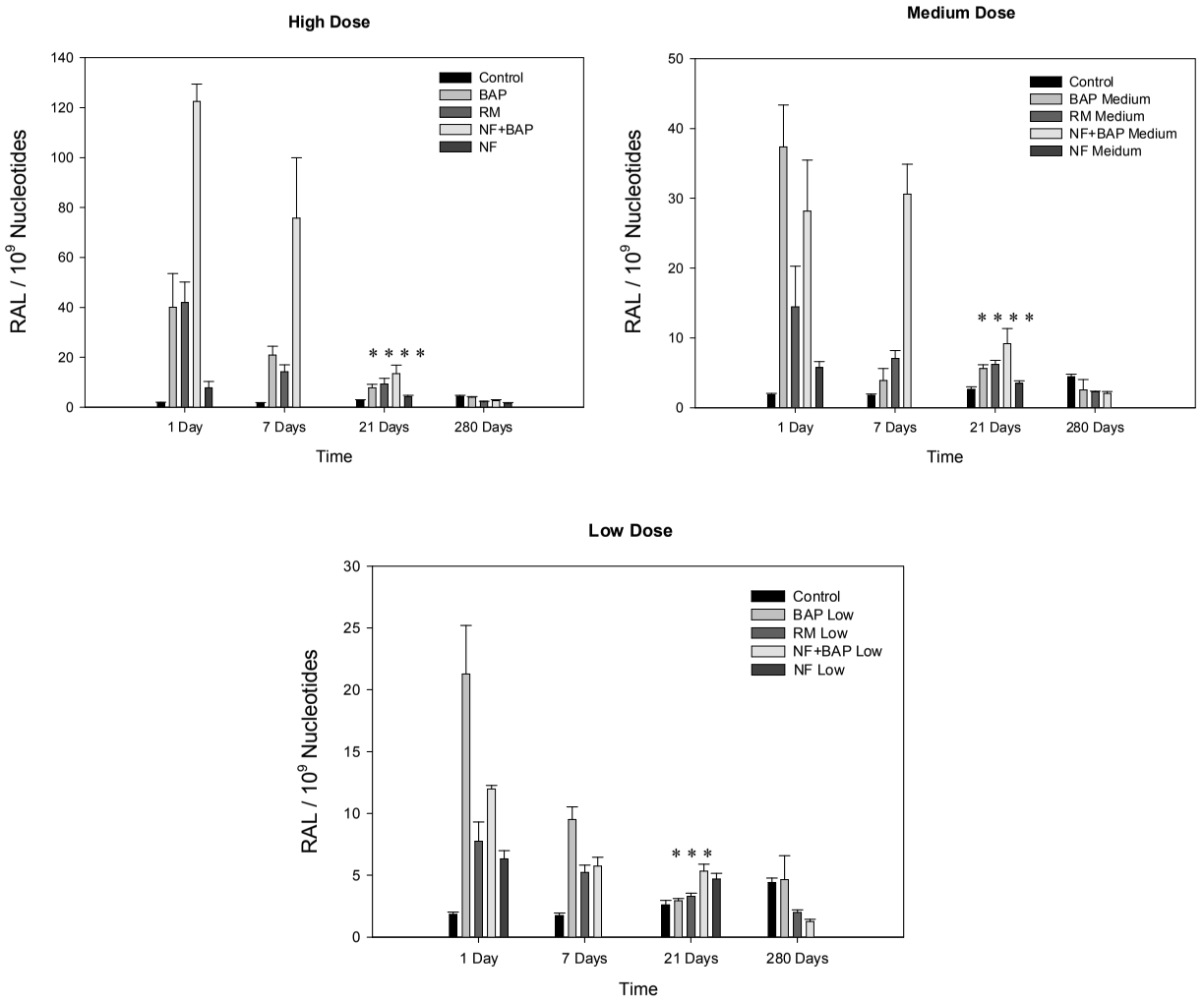

Figure 3.16. Mean spot 4 DNA adducts detected in liver tissue for treatments contrasted against dose and time. Data are presented as RAL per 10^9 nucleotides ± SEM. *Significantly lower than day 1.

Total and spot 4 adducts data for the lung tissue are presented in Table 3.12. A significant interaction between treatment and time was observed in this tissue (Tables 3.7, 3.9 and 3.13). Therefore, all contrasts were made using this two-way interaction, data graphed in Figures 3.17 and 3.18. Both total and spot 4 analyses seem to show similar patterns (Figures 3.19 and 3.20). A more dramatic decrease occurs after day 7 in the RM and NF+BAP fractions, but overall all fractions decrease with time. The NF+BAP and BAP treatments both elicit the highest responses in this tissue (Figures 3.19 and 3.20). It isn't until day 21 that the NF+BAP (RAL of 147.01 ± 69.34 per 10^9 nucleotides) becomes significantly higher than the BAP (RAL of 39.26 ± 5.03 per 10^9 nucleotides) (Table 3.9 and 3.10). Both NF+BAP and BAP are significantly higher than RM, while NF+BAP is higher than NF at 1 day. At day 7 NF+BAP and BAP are significantly higher than RM, and then at day 21 NF+BAP is significantly higher than RM and NF again.

Statistical contrast data for total and spot 4 adducts in the forestomach is presented in Tables 3.9 and 3.12. Once tested, a significant interaction was observed between treatment and time (Table 3.7). Thus, all contrasts were made using this two-way interaction (Figures 3.21 and 3.22). The same interaction pattern is observed in both the total and spot 4 adduct analyses, with the spot 4 being a slightly smaller response (Figures 3.23 and 3.24). After time 7 days, the NF+BAP and BAP both significantly decrease. The NF+BAP and BAP once again are the two chemicals that produce the maximum DNA adduct frequencies (RAL of 305.17 ± 115.88 and 162.40 ± 35.89 per 10^9 nucleotides at time 7 days in the 0.429 mg/g bw dose, Table 3.13). The RM seems to stay at the same level, with no significant change over time. NF+BAP is consistently yields a significantly higher response than RM and NF, while BAP is consistently higher than RM until day 21. At day 21, NF+BAP is significantly higher than RM, NF and BAP. The spot 4 results follow the same pattern as the total results in the forestomach. There is also a fairly consistent pattern observed throughout all tissues.

Table 3.12. Table of DNA adduct levels detected in forestomach of B6CDF1 male mice. Data are presented as RAL per 10^9 nucleotides ± SEM. N/A = Not Applicable.

		Mean Total RAL / 10^9 Nucleotides in Forestomach			Mean Spot 4 RAL / 10^9 Nucleotides in Forestomach		
Chemical	**Dose (mg/g bw)**	**1 Day**	**7 Days**	**21 Days**	**1 Day**	**7 Days**	**21 Days**
Control	--	9.75 ± 3.13	9.27 ± 0.57	15.34 ± 1.92	2.22 ± 1.00	1.90 ± 0.15	1.73 ± 0.22
BAP	0.069	81.36 ± 23.64	79.21 ± 7.57	52.01 ± 11.61	81.64 ± 25.70	106.81 ± 24.73	61.59 ± 9.78
	0.171	150.78 ± 13.79	113.09 ± 12.76	101.72 ± 17.80	104.16 ± 8.68	72.04 ± 9.21	53.39 ± 10.65
	0.429	126.44 ± 34.86	162.40 ± 35.89	112.47 ± 15.59	53.53 ± 16.34	48.41 ± 5.44	21.18 ± 6.50
RM	0.069	44.18 ± 8.80	57.57 ± 8.02	39.98 ± 7.37	63.42 ± 11.79	69.20 ± 26.85	52.37 ± 13.49
	0.171	68.32 ± 21.46	45.18 ± 14.06	82.53 ± 9.27	27.73 ± 12.03	19.30 ± 9.61	36.43 ± 4.68
	0.429	132.16 ± 20.77	109.76 ± 38.44	97.90 ± 18.72	14.12 ± 4.50	27.49 ± 4.99	11.79 ± 4.40
NF+BAP	0.069	82.38 ± 4.41	37.64 ± 11.02	52.80 ± 6.56	186.05 ± 16.89	204.90 ± 79.47	54.11 ± 25.06
	0.171	140.33 ± 22.42	177.61 ± 38.07	77.62 ± 15.98	69.03 ± 14.91	112.26 ± 26.13	42.06 ± 9.45
	0.429	378.93 ± 31.93	305.17 ± 115.88	94.74 ± 35.88	44.57 ± 2.93	16.74 ± 7.01	23.10 ± 2.23
NF	0.069	18.11 ± 1.07	N/A	28.77 ± 3.50	3.39 ± 0.31	N/A	4.03 ± 0.38
	0.171	19.56 ± 1.97	N/A	23.83 ± 3.93	2.83 ± 0.28	N/A	3.91 ± 0.70
	0.429	20.40 ± 1.78	N/A	28.96 ± 4.49	2.54 ± 0.18	N/A	4.21 ± 0.45

Table 3.13. Significant confidence intervals for difference in mean spot 4 DNA adducts in lung and forestomach tissues across time. For all contrasts computed, the confidence level was 95%. In spot 4 adducts, each tissue had a significant chemical-time interaction; therefore, data contrasts were computed across time. Spot 4 was chosen because in previous studies it has been shown to correspond with BAP. P-values listed in Table 3.2.

Confidence Intervals for Differences in Mean Spot 4 Adducts in Lung & Forestomach of B6C3F1 Male Mouse Tissues: Contrasts for Chemicals Across Time

		BAP x NF+BAP	RM x NF+BAP	NF+BAP x NF	BAP x RM
1 Day	Lung	NS	(-1.522, -0.480)	(1.841, 2.883)	(0.666, 1.708)
	Forestomach	NS	(-2.022, -0.484)	(2.552, 4.090)	(0.215, 1.753)
7 Days	Lung	NS	(-1.482, -0.400)	N/A	(0.371, 1.413)
	Forestomach	NS	(-1.723, -0.127)	N/A	(0.167, 1.705)
21 Days	Lung	(-1.178, -0.098)	(-1.338, -0.276)	(1.560, 2.660)	NS
	Forestomach	NS	NS	(1.311, 2.933)	NS
		BAP x BAP	**RM x RM**	**NF+BAP x NF+BAP**	**NF x NF**
1 Day to 7 Days	Lung	NS	NS	NS	N/A
	Forestomach	NS	NS	NS	N/A
1 Day to 21 Days	Lung	(0.531, 1.593)	NS	NS	NS
	Forestomach	NS	NS	(0.104, 1.668)	NS
7 Days to 21 Days	Lung	(0.289, 1.351)	NS	NS	N/A
	Forestomach	NS	NS	NS	N/A

NS = Not Significant
N/A = Data Not Available

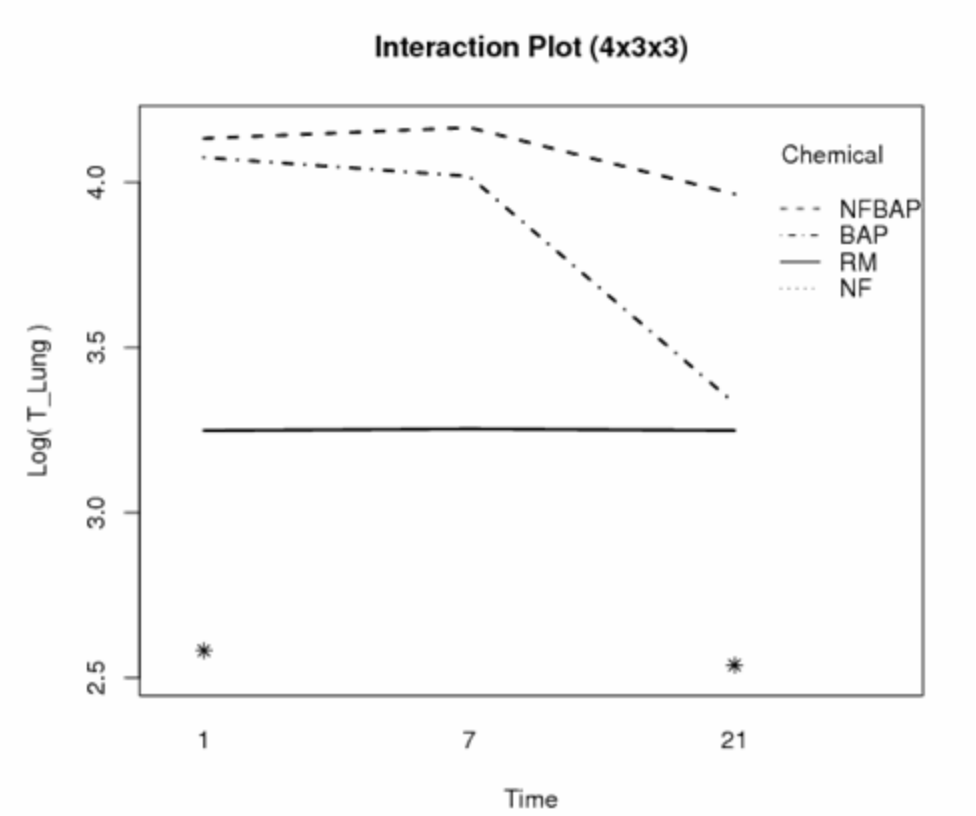

Figure 3.17. 4x3x3 interaction plot for differences in mean total DNA adducts in lung tissue over time. *Represents individual points for NF, a line could not be drawn as points are missing.

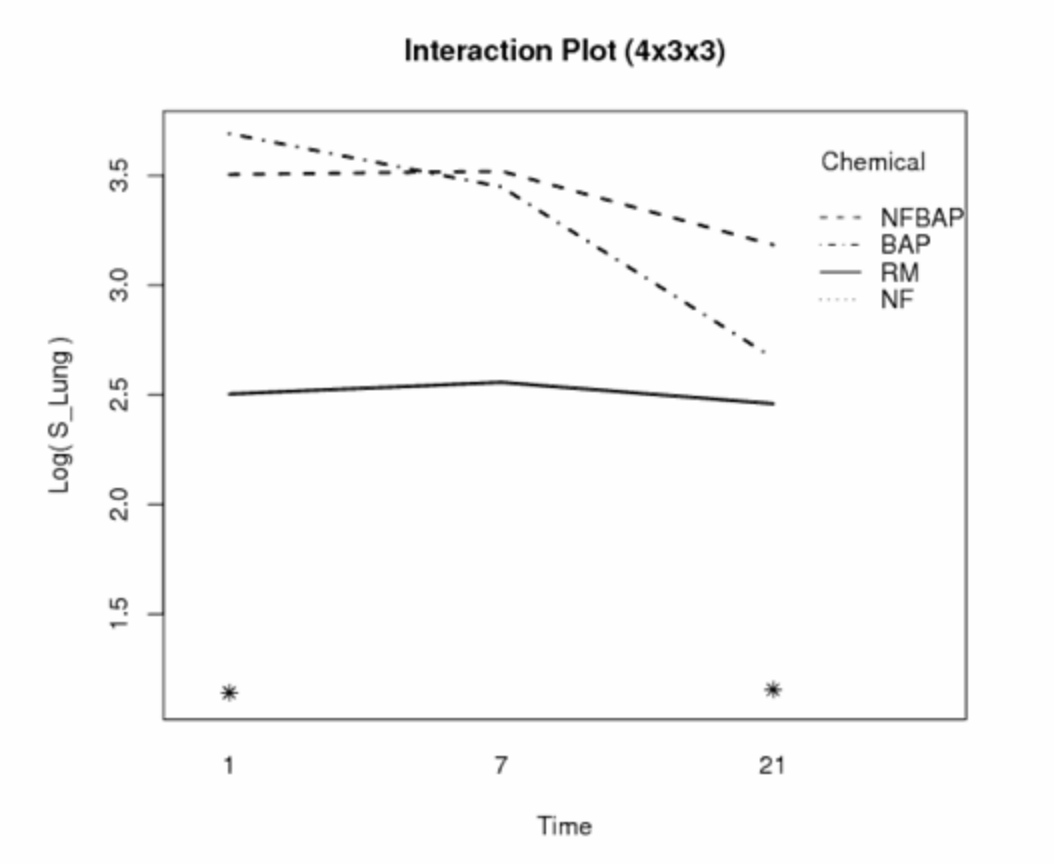

Figure 3.18. 4x3x3 interaction plot for differences in mean spot 4 DNA adducts in lung tissue over time. *Represents individual points for NF, a line could not be drawn as points are missing.

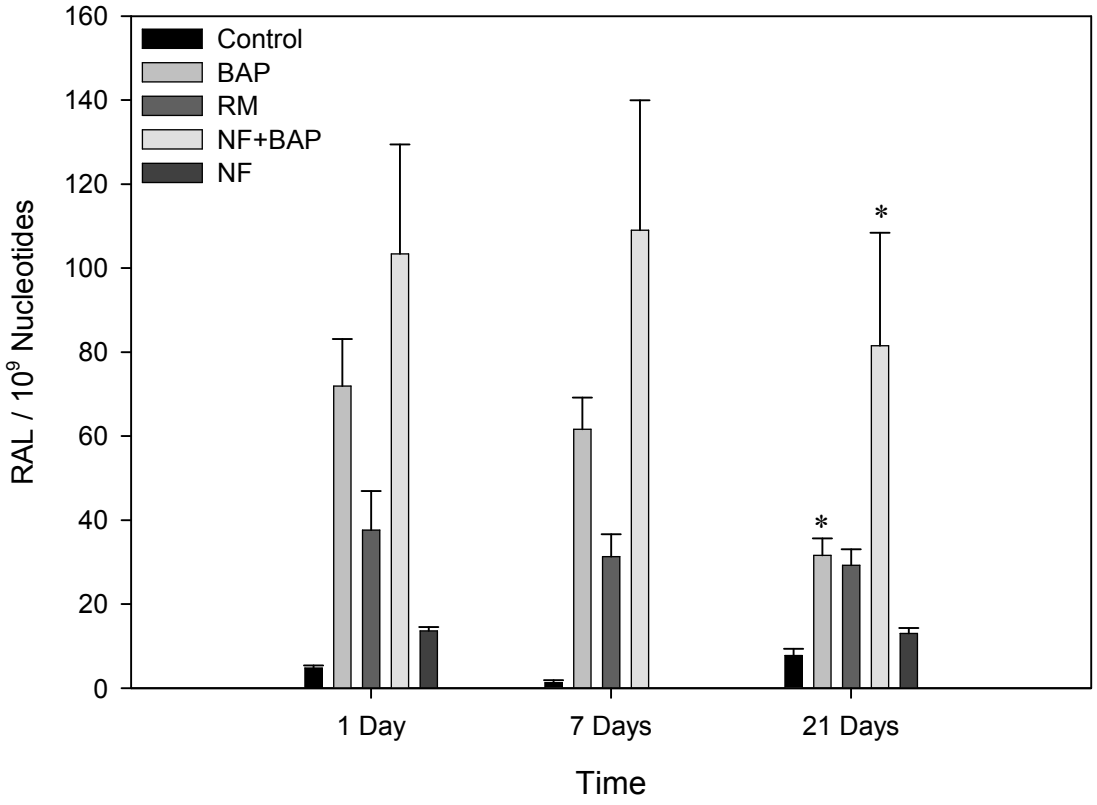

Figure 3.19. Mean total DNA adducts detected in lung tissue for treatments contrasted against time. Data are presented as RAL per 10^9 nucleotides ± SEM. *Significantly lower than day 1.

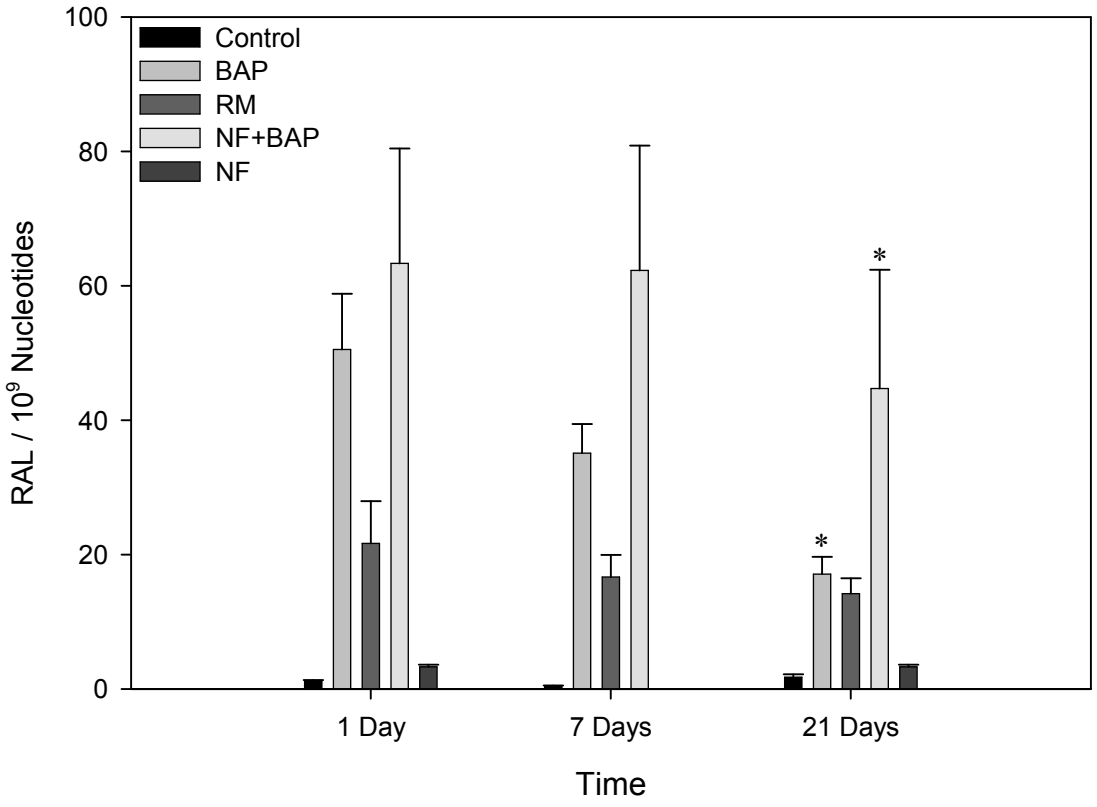

Figure 3.20. Mean spot 4 DNA adducts detected in lung tissue for treatments contrasted against time. Data are presented as RAL per 10^9 nucleotides ± SEM. *Significantly lower than day 1.

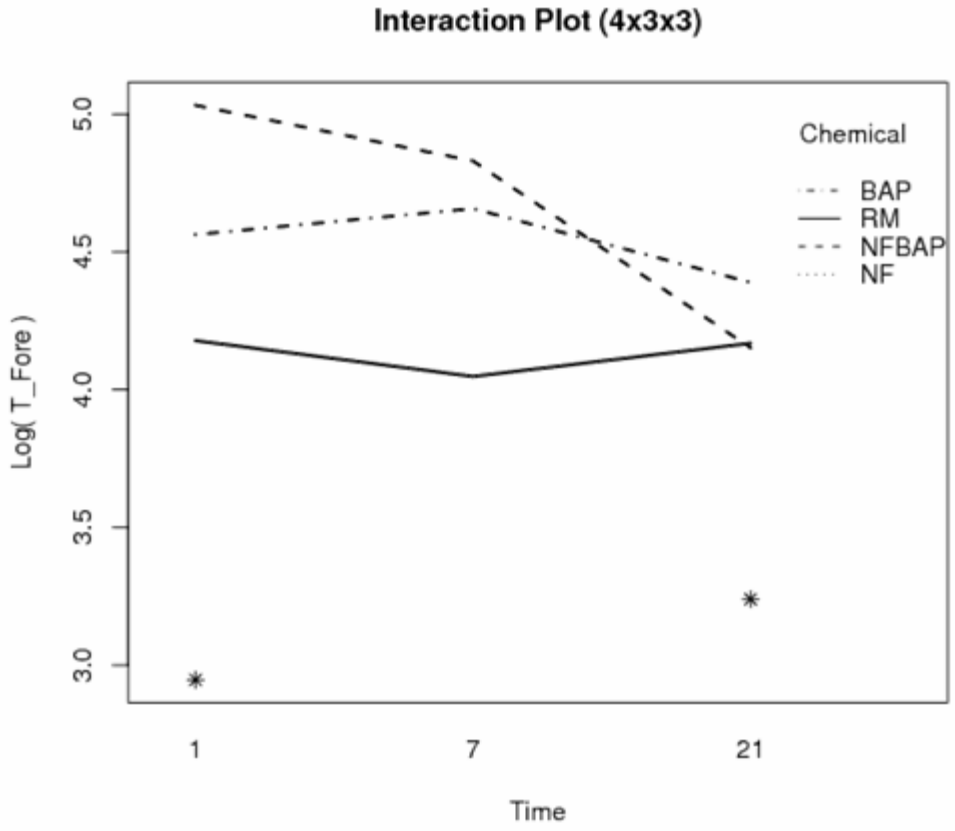

Figure 3.21. 4x3x3 interaction plot for differences in mean total DNA adducts in forestomach tissue over time. * Represents individual points for NF, a line could not be drawn as points are missing.

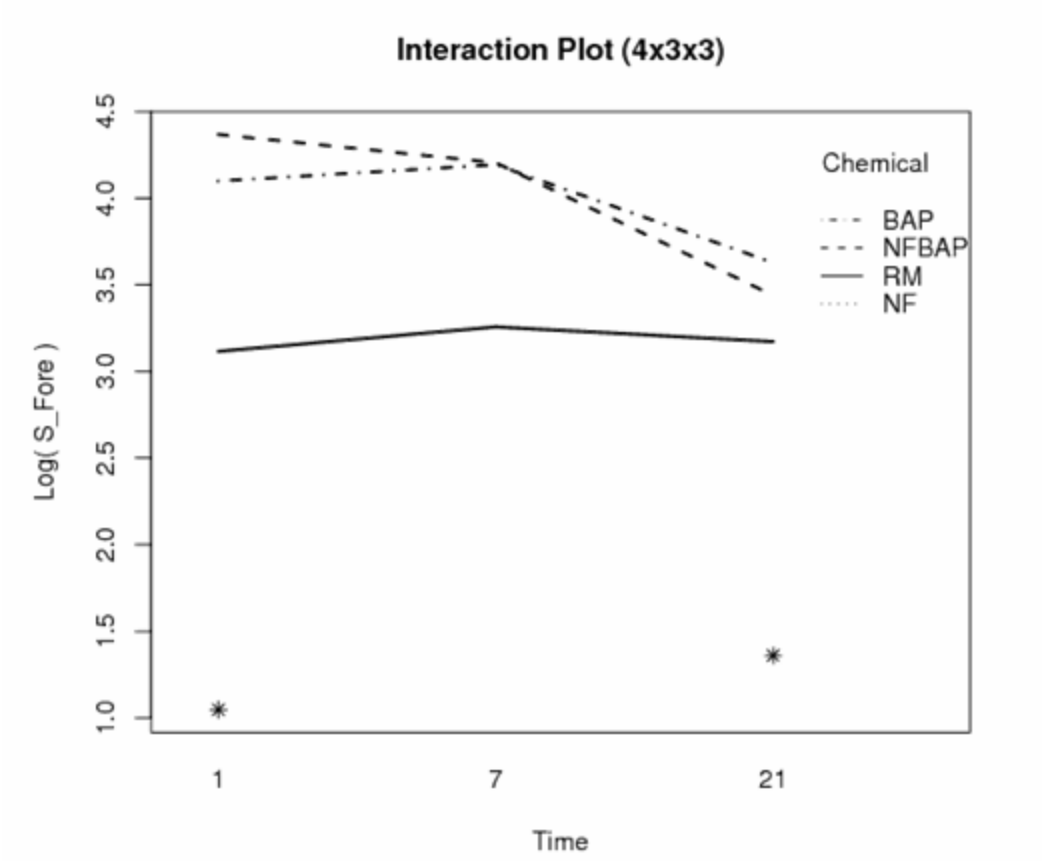

Figure 3.22. 4x3x3 interaction plot for differences in mean spot 4 DNA adducts in forestomach tissue over time. *Represents individual points for NF, a line could not be drawn as points are missing.

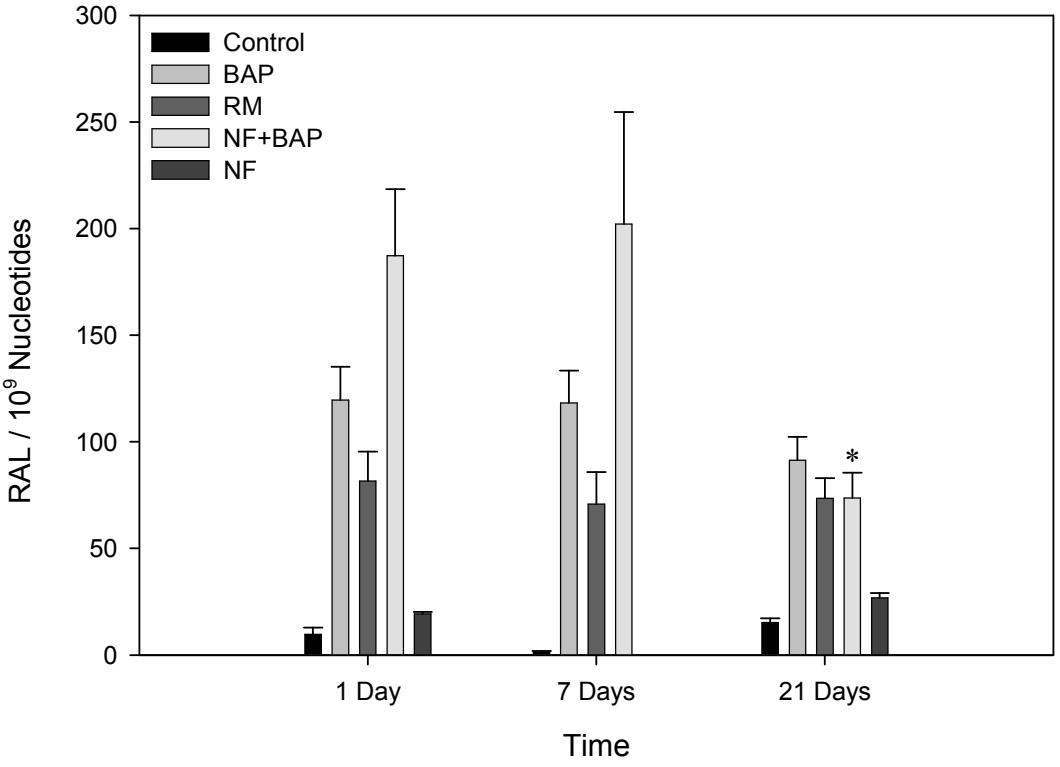

Figure 3.23. Mean total DNA adducts detected in forestomach tissue for treatments contrasted against time. Data are presented as RAL per 10^9 nucleotides ± SEM.

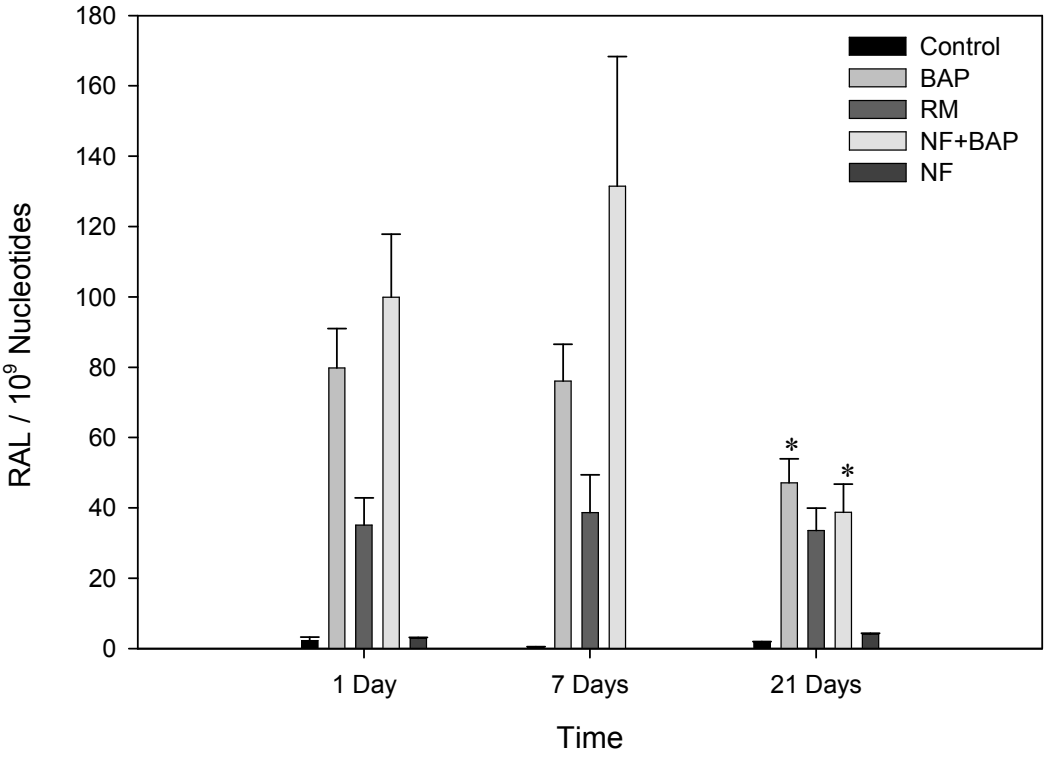

Figure 3.24. Mean spot 4 DNA adducts detected in forestomach tissue for treatments contrasted against time. Data are presented as RAL per 10^9 nucleotides ± SEM. *Significantly lower than day 1.

After the data was analyzed over time, it was then compared among chemical treatments over dose to observe differences between chemical treatment groups, as well as within chemical treatment groups. As before, budget constraints did not allow for all four chemical treatments to be collected at all the time points; therefore, it was decided that the NF would be collected at two time points (1 day and 21 days) instead of all three time points. Tissue aliquot constraints prevented the lung and forestomach tissues from being sampled at time 280 days. The BAP treatment groups were contrasted to the NF+BAP and RM treatment groups. These contrasts were done to compare the differences between pure BAP to a complex mixture as well as to a mixture of

carcinogenic PAHs (all containing the same amount of BAP). The RM treatment groups were also contrasted to the NF+BAP treatment groups to compare the differences between a mixture of carcinogenic PAHs to a complex mixture with the same level of those PAHs. Next the NF+BAP treatment groups were contrasted to the NF treatment groups to compare the differences between complex mixtures containing high and low levels of BAP. Finally, all chemical treatments were contrasted among themselves to compare the differences over dose. All contrasts were built up to the final analysis as described in the materials and methods section. A 4x3x3 (four chemicals, three doses and three times) ANOVA was preformed on the lung and forestomach tissues while a 4x3x4 (four chemicals, three doses and four times) ANOVA was preformed on the liver tissue. Both analyses used the log transformed RAL per 10^9 nucleotides. P-values are reported in Table 3.7.

Contrasts across dose for total adduct analysis in liver are presented in Table 3.14. A significant interaction between treatment and dose was observed in this tissue (Table 3.7). Consequently, all contrasts were made using this two-way interaction, data graphed in Figures 3.25 and 3.26. The interaction plot shows a clear pattern in which all chemicals decrease with dose, except the NF. NF+BAP decreases significantly with dose, and it elicited the highest response of the chemicals (Figure 3.26). NF+BAP is significantly higher than NF, BAP and RM at the 0.429 mg/g bw dose, while it is only significantly higher than NF at the 0.171 mg/g bw dose. BAP is also significantly higher than RM at the 0.171 mg/g bw dose (Table 3.14). A significant dose response is also observed between NF+BAP and BAP.

Table 3.14. Significant confidence intervals for difference in mean total DNA adducts in liver, lung and forestomach tissues across dose. For all contrasts computed, the confidence level was 95%. In total adducts, each tissue had a significant chemical-dose interaction; therefore, data contrasts were computed across dose. P-values listed in Table 3.2.

Confidence Intervals for Differences in Mean Total Adducts in B6C3F1 Male Mouse Tissues: Contrasts for Chemicals Across Dose

		NF+BAP x NF	BAP x NF+BAP	RM x NF+BAP	BAP x RM
High Dose (0.429mg/g bw)	Liver	(0.716, 1.606)	(-1.006, -0.228)	(-1.032, -0.254)	NS
	Lung	(1.85, 2.970)	(-1.630, -0.680)	(-1.700, -0.760)	NS
	Forestomach	(1.422, 2.864)	NS	(-1.298, -0.088)	NS
Medium Dose (0.171mg/g bw)	Liver	(0.097, 1.023)	NS	NS	(0.023, 0.789)
	Lung	(0.908, 1.980)	NS	(-1.310, -0.350)	(0.442, 1.370)
	Forestomach	(0.989, 2.357)	NS	(-1.287, -0.053)	(0.125, 1.313)
Low Dose (0.069mg/g bw)	Liver	NS	NS	NS	NS
	Lung	(0.258 ,1.290)	NS	(-0.964 ,-0.038)	(0.187 ,1.130)
	Forestomach	(0.279, 1.607)	NS	NS	NS
		BAP x BAP	**RM x RM**	**NF+BAP x NF+BAP**	**NF x NF**
High to Medium Dose (0.429 - 0.171mg/g bw)	Liver	NS	NS	(0.207, 1.007)	NS
	Lung	NS	(0.434, 0.897)	(0.812, 1.790)	NS
	Forestomach	NS	NS	NS	NS
High to Low Dose (0.429 - 0.069mg/g bw)	Liver	(0.020, 0.798)	(0.179, 0.945)	(0.777, 1.555)	NS
	Lung	(0.282, 1.230)	(0.874 ,1.800)	(1.590 ,2.540)	NS
	Forestomach	(0.011, 1.221)	(0.233, 1.421)	(0.635, 1.845)	NS
Medium to Low Dose (0.171 - 0.069mg/g bw)	Liver	(0.045, 0.823)	NS	(0.164, 0.954)	NS
	Lung	(0.214, 1.160)	NS	(0.284 ,1.250)	NS
	Forestomach	NS	NS	(0.030, 1.264)	NS

NS = Not Significant

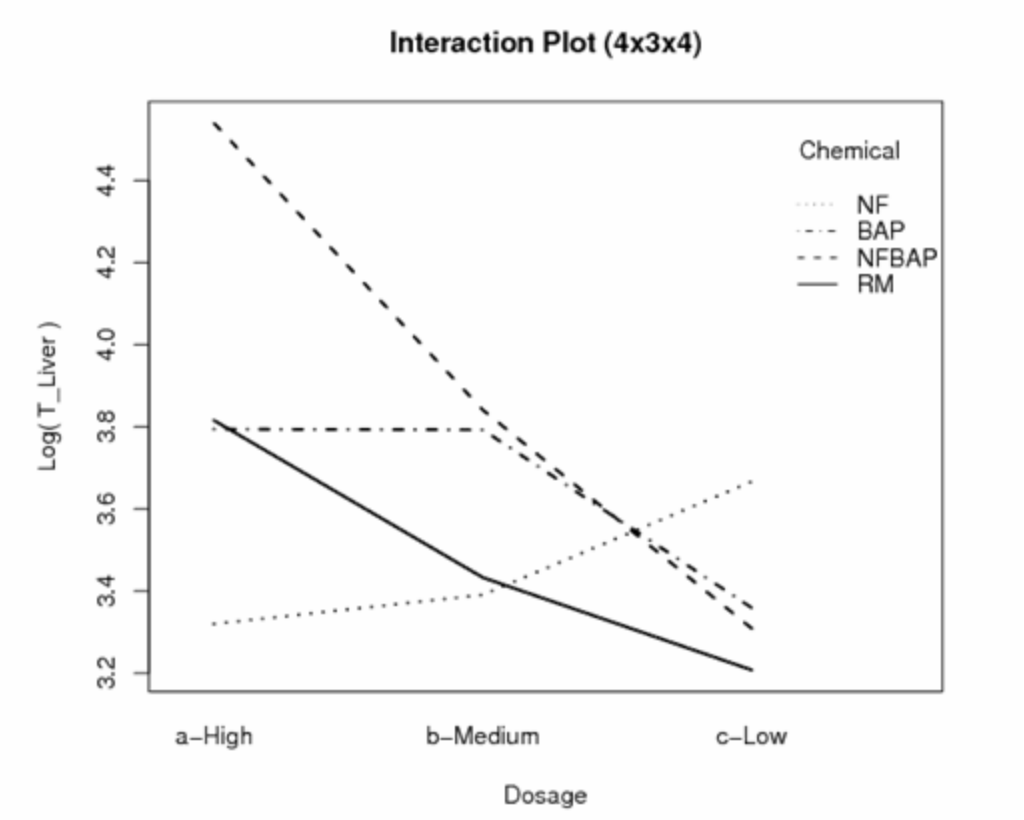

Figure 3.25. 4x3x4 interaction plot for differences in mean total DNA adducts in liver tissue over dose.

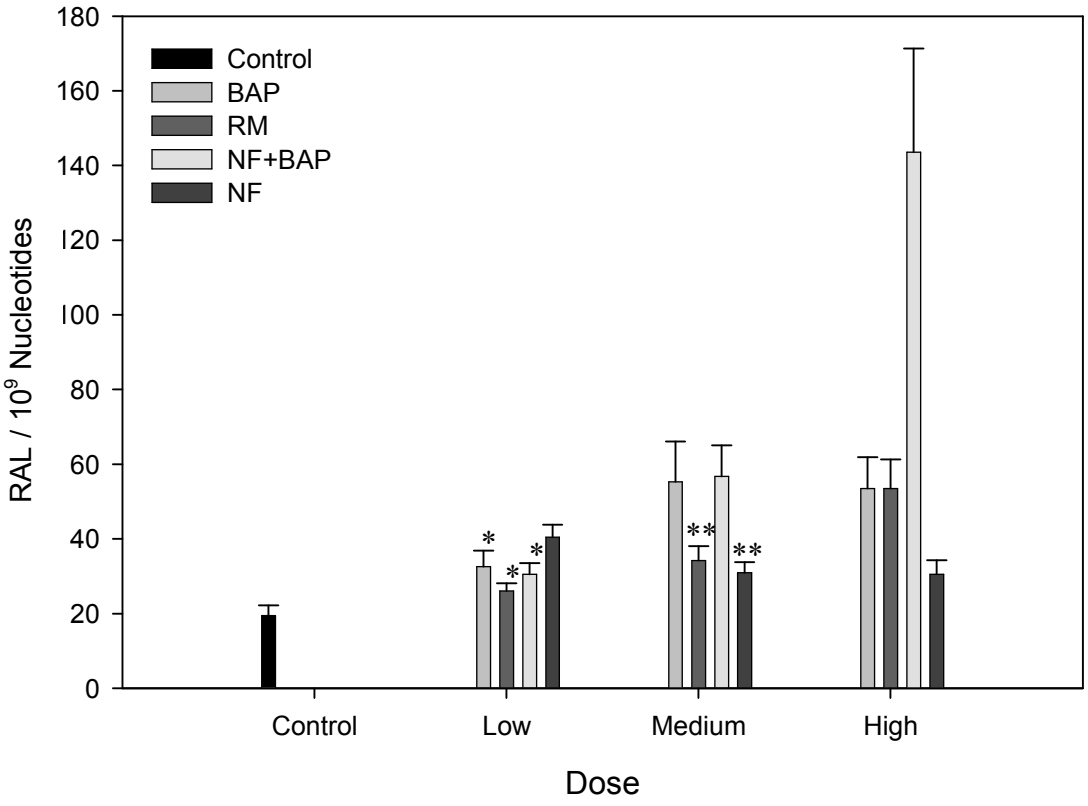

Figure 3.26. Mean total DNA adducts detected in liver tissue for treatments contrasted against dose. Data are presented as RAL per 10^9 nucleotides ± SEM. *Low dose significantly lower than high dose; **medium dose significantly lower than high dose.

All contrasts for total and spot 4 adducts evaluated in lung tissue are summarized in Tables 3.14 and 3.15. When these analyses were run, a significant interaction was observed between treatment and dose (Table 3.7). Therefore, all contrasts were made using this two-way interaction, data graphed in Figurs 3.27 and 3.28. The total and spot 4 data follow the same pattern, with the total adducts being more elevated. All chemicals decrease with dose, and we see the same cross effect here where the NF+BAP begins by eliciting the maximum response, and then the BAP ends up eliciting a slightly higher response than the NF+BAP (Figures 3.29 and 3.30). The NF+BAP starts as being significantly higher than the BAP, RM and NF at the 0.429 mg/g bw dose. After that,

the NF+BAP and BAP are not significantly different. This tissue follows the same pattern as the liver, except that at the 0.069 mg/g bw dose, NF+BAP is significantly higher than RM and NF, while BAP is significantly higher than RM (Tables 3.14 and 3.15). A dose response is also observed within all chemicals.

Table 3.15. Significant confidence intervals for difference in mean spot 4 DNA adducts in lung and forestomach tissues across dose. For all contrasts computed, the confidence level was 95%. In spot 4 adducts, each tissue had a significant chemical-dose interaction; therefore, data contrasts were computed across dose. Spot 4 was chosen because in previous studies it has been shown to correspond with BAP. P-values listed in Table 3.2.

Confidence Intervals for Differences in Mean Spot 4 Adducts in Lung & Forestomach of B6C3F1 Male Mouse Tissues: Contrasts for Chemicals Across Dose

		NF+BAP x NF	BAP x NF+BAP	RM x NF+BAP	BAP x RM
High Dose	Lung	(2.580, 3.864)	(-1.668, -0.590)	(-1.793, -0.715)	NS
(0.429mg/g bw)	Forestomach	(2.489, 4.383)	NS	(-1.591, -0.003)	NS
Medium Dose	Lung	(1.602, 2.822)	NS	(-1.458, -0.360)	(0.619, 1.677)
(0.171mg/g bw)	Forestomach	(1.991, 3.789)	NS	(-1.834, -0.214)	(0.444, 2.004)
Low Dose	Lung	(0.794, 1.978)	NS	(-1.114, -0.056)	(0.435, 1.513)
(0.069mg/g bw)	Forestomach	(1.223, 2.967)	NS	NS	(0.091, 1.679)
		BAP x BAP	**RM x RM**	**NF+BAP x NF+BAP**	**NF x NF**
High to Medium Dose	Lung	NS	(0.534, 1.592)	(0.850, 1.966)	NS
(0.429 - 0.171mg/g bw)	Forestomach	NS	(0.142, 1.702)	NS	NS
High to Low Dose (0.429	Lung	(0.302, 1.380)	(1.161, 2.219)	(1.820, 2.898)	NS
- 0.069mg/g bw)	Forestomach	NS	(0.562, 2.122)	(0.678, 2.266)	NS
Medium to Low Dose	Lung	(0.262, 1.340)	(0.098, 1.156)	(0.402, 1.500)	NS
(0.171 - 0.069mg/g bw)	Forestomach	NS	NS	NS	NS

NS = Not Significant

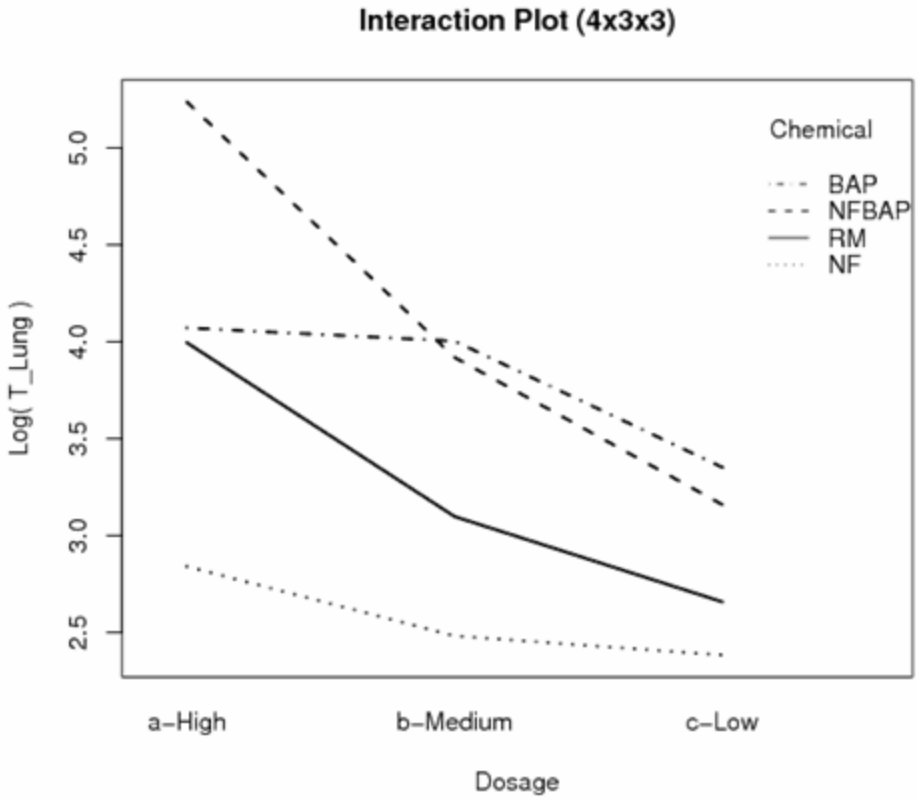

Figure 3.27. 4x3x3 interaction plot for differences in mean total DNA adducts in lung tissue over dose.

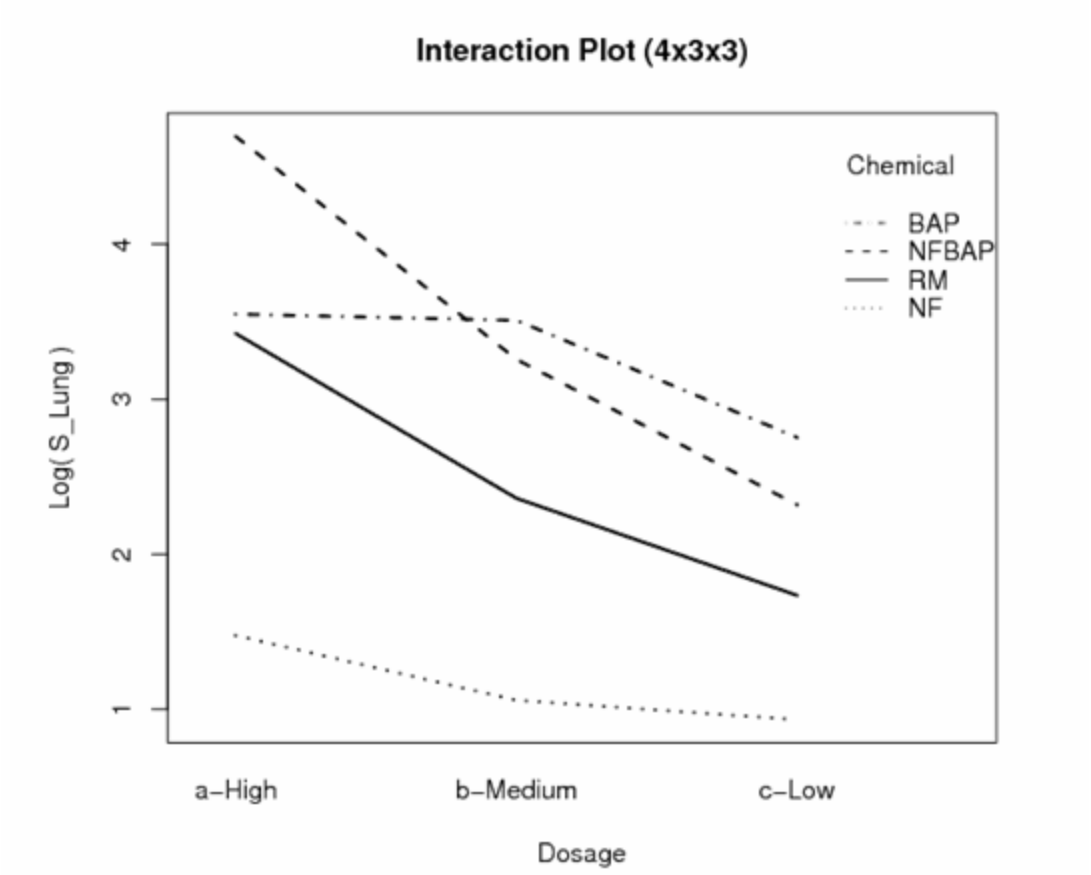

Figure 3.28. 4x3x3 interaction plot for differences in mean spot 4 DNA adducts in lung tissue over dose.

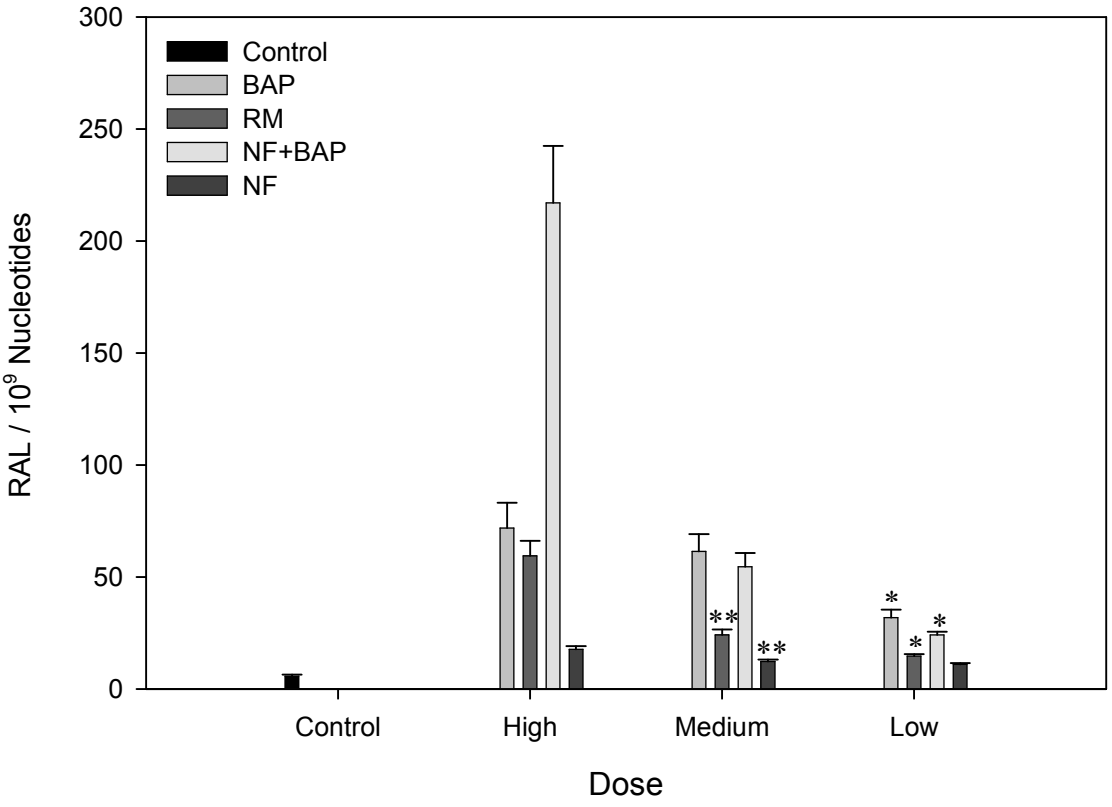

Figure 3.29. Mean total DNA adducts detected in lung tissue for treatments contrasted against dose. Data are presented as RAL per 10^9 nucleotides ± SEM. *Low dose significantly lower than high dose; **medium dose significantly lower than high dose.

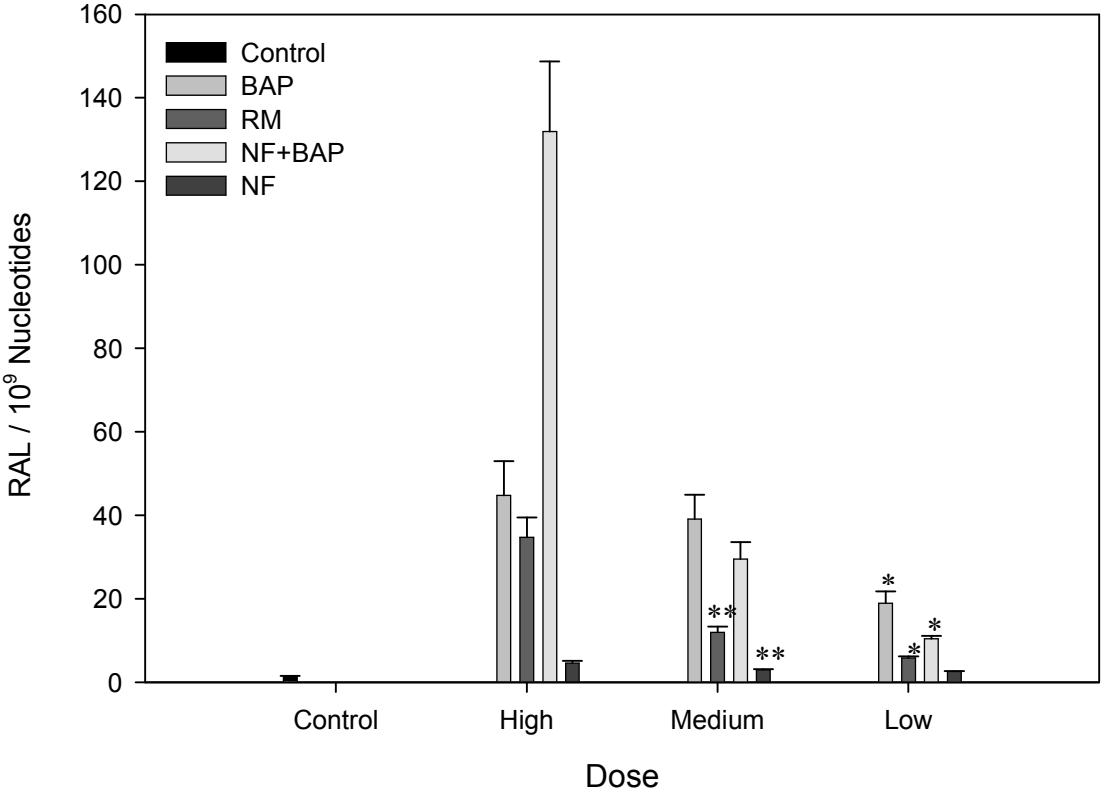

Figure 3.30. Mean spot 4 DNA adducts detected in lung tissue for treatments contrasted against dose. Data are presented as RAL per 10^9 nucleotides ± SEM. *Low dose significantly lower than high dose; **medium dose significantly lower than high dose.

Data contrasts showing total and spot 4 adduct levels evaluated in forestomach tissue are reported in Tables 3.14 and 3.15. After the data was run, a significant interaction was observed between treatment and dose (Table 3.7). Thus, all contrasts were made using this two-way interaction (Figure 3.31 and 3.32). Once again, a similar pattern is observed between total and spot 4 adduct analyses. All chemicals decrease significantly with dose, except the NF, which decreases slightly. The NF+BAP has elicited the maximum response at the 0.429 mg/g bw dose, whereas after that, the NF+BAP and BAP elicit a very similar level of adducts (Figures 3.33 and 3.34). The

forestomach follows the same exact pattern as the lung for significance between chemicals. A dose-response is observed for the RM, NF+BAP and BAP in the total analysis, with BAP not included in the spot 4 analysis (Table 3.14 and 3.15).

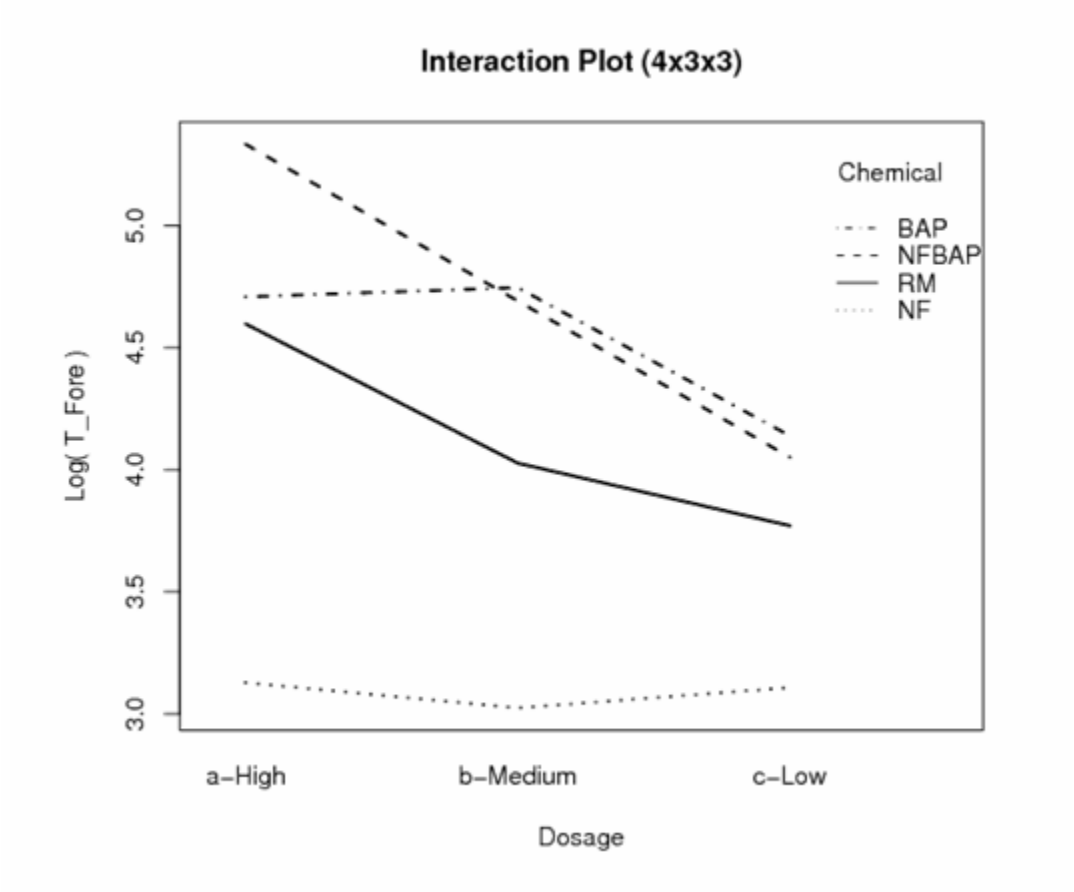

Figure 3.31. 4x3x3 interaction plot for differences in mean total DNA adducts in forestomach tissue over dose.

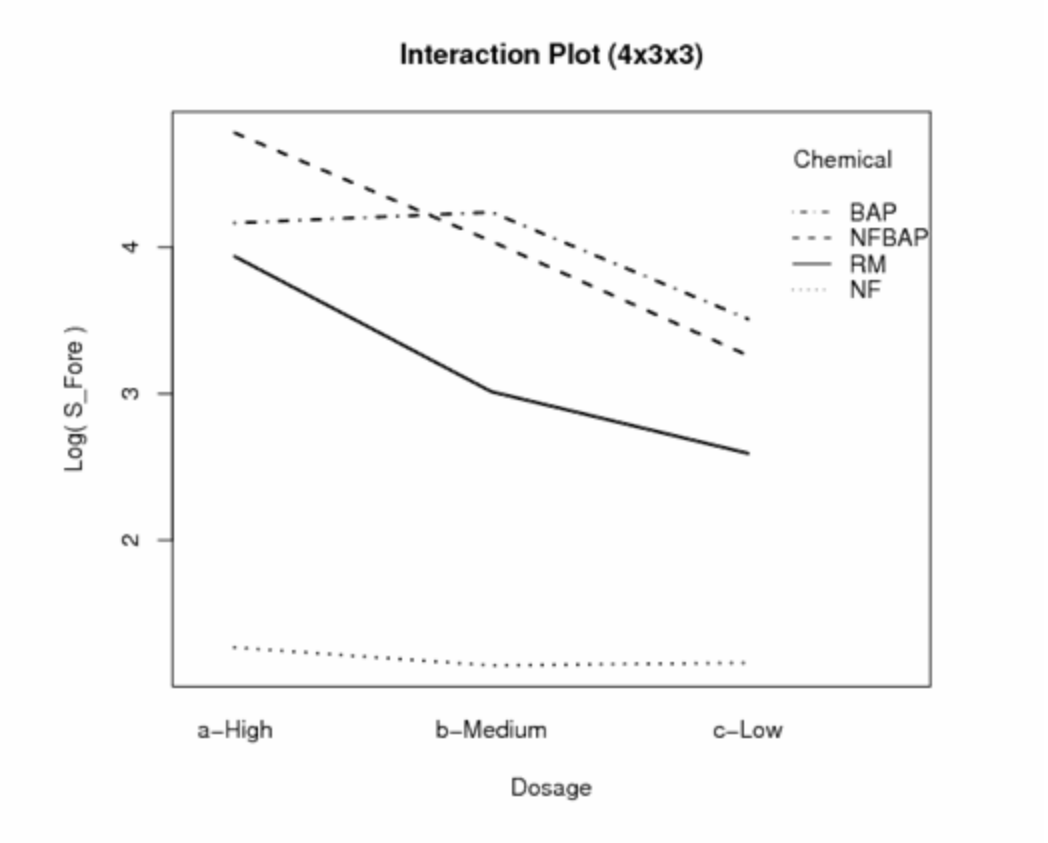

Figure 3.32. 4x3x3 interaction plot for differences in mean spot 4 DNA adducts in forestomach tissue over dose.

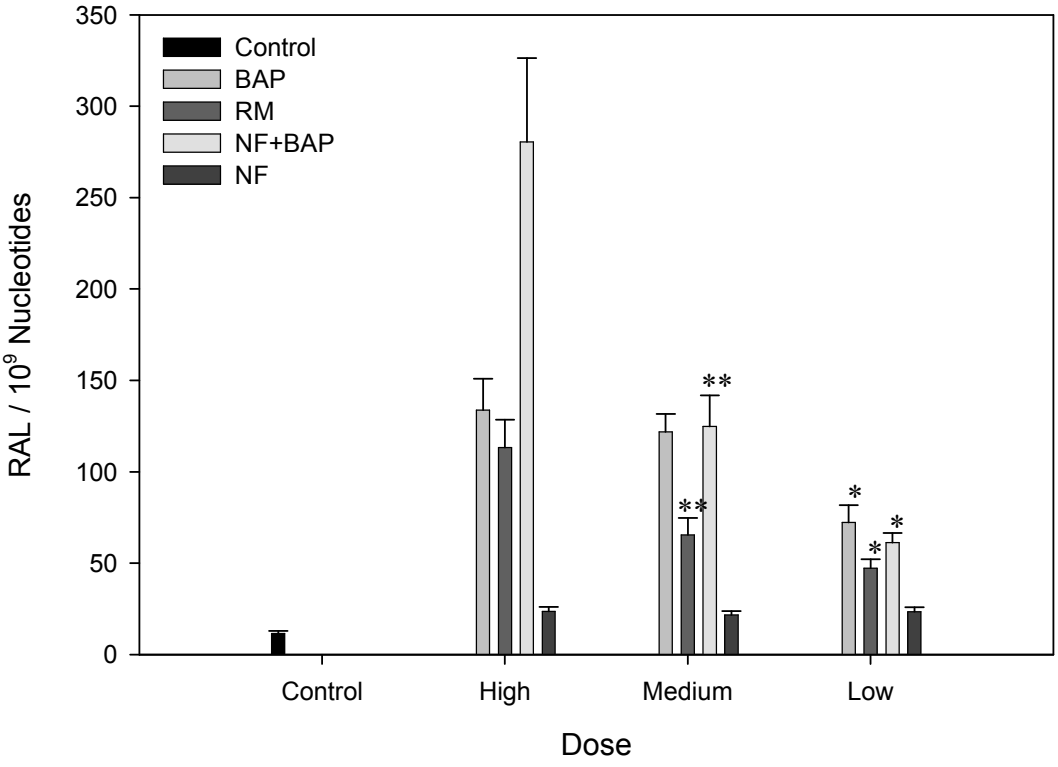

Figure 3.33. Mean total DNA adducts detected in forestomach tissue for treatments contrasted against dose. Data are presented as RAL per 10^9 nucleotides ± SEM. *Low dose significantly lower than high dose; **medium dose significantly lower than high dose.

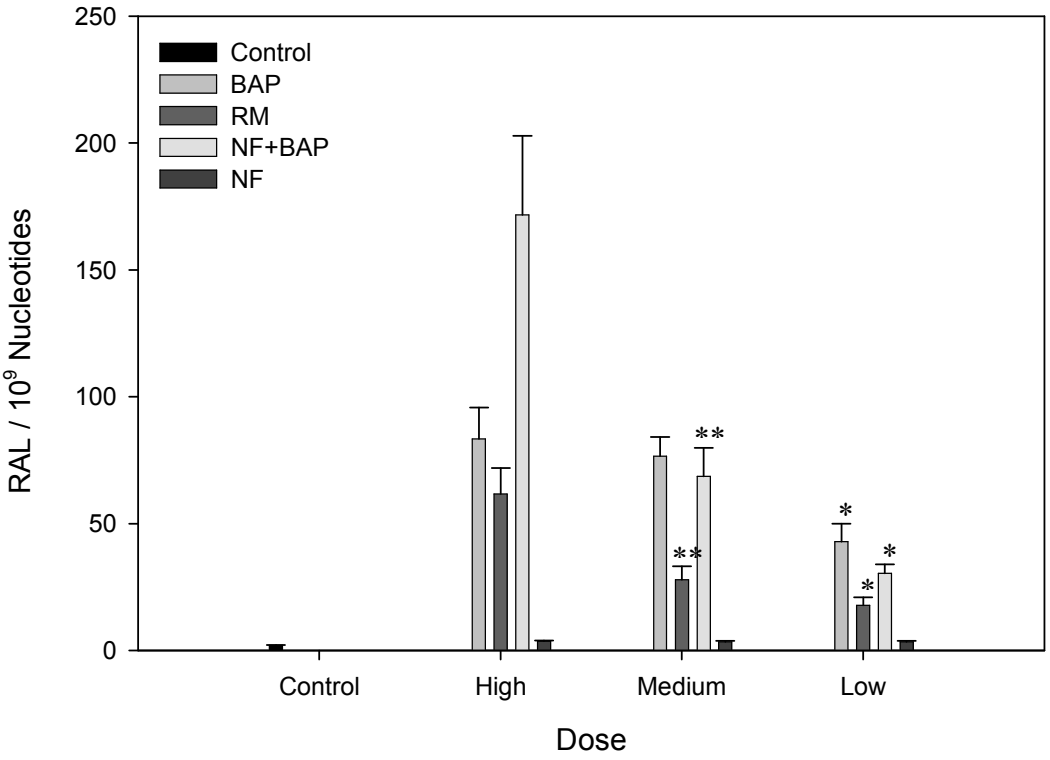

Figure 3.34. Mean spot 4 DNA adducts detected in forestomach tissue for treatments contrasted against dose. Data are presented as RAL per 10^9 nucleotides $\pm$ SEM. *Low dose significantly lower than high dose; **medium dose significantly lower than high dose.

3.4 Discussion

The results of the current experiment are comparable to those observed in Chapter II. The intraperitoneal (i.p.) injection application DNA adduct levels were observed to be greater than the dermal application DNA adduct levels. The difference, for most of the tissues, reflects differences in application method, chemical treatment and dose. Pharmacokinetics plays an important role in determining the fate of a chemical once it has been introduced into a biological system. There are multiple mechanisms which occur when an exogenous compound enters a cell. One of the most important factors in how a compound will act is the route of exposure. In most instances, dermal application will not elicit as large a response as a more direct route of administration due to absorption. Chemicals cannot cross through the epidermis easily, which explains why DNA adduct levels are lower with the dermal application. This would account for the NF+BAP treatment eliciting a larger response via i.p. injection. When you have route of exposure in the intraperitoneal cavity, absorption of the chemical is made easier due to direct access to capillaries. Once the chemicals have been adsorbed, distribution and metabolism become more important. These factors can be influenced by chemical, as well as by route of exposure and dose. Comparing the two routes of exposure for this research was important for determining differences that would be observed in the chemical responses based on administration. The ultimate goal of the comparison was to determine if i.p. injection administration would be a comparable route of exposure to dermal application.

The first step was to compare all low dose samples were to the controls. This ensures that responses of treatments were significant over the control samples, while also ensuring the controls are not having an effect on the responses observed. It was observed that all chemicals were either significantly larger than the control, or not significantly different from the control. It was also observed that after 21 days controls did increase. This is due to the detection of I-compounds. As animals age, a linear correlation can be seen with respect to an increase in I-compound. I-compounds are indigenous compounds in the organism which will bind with DNA and form DNA

adducts. Results from the 280 day time point are difficult to interpret due to the high presence of I-compounds.

Comparison between routes of exposure was the next big step. It was observed that there were slight differences between route of administration and response of the treatment. BAP responses via dermal application are smaller than responses via i.p. injection. It was also observed that there was a difference in dose-response based on route of exposure. Dermal doses showed smaller responses than those from i.p. injection. This chemical-dose-application interaction suggests that it is very important to determine optimal dose and application methods for the chemicals to be tested. However, for testing complex mixtures this becomes a difficult task, as these interactions can be very different for each chemical within the mixture. Overall, it was observed that i.p. injection as a route of exposure elicited larger responses than dermal application. This route of exposure, which allows for a more direct absorption of the chemicals, is more efficient for the type of testing this research is conducting.

All samples administered via i.p. injection were compared, and similar responses were observed over all three tissues collected (liver, lung, forestomach). A similar response among tissues is an important observation. When all tissues tested have similar responses, a presidence is set for that chemical-dose-application. Future studies will be able to focus more attention on the target organ based on this observation. The NF+BAP treatment elicited the maximum response at the high dose (0.429 mg/g bw) for all tissues. BAP and NF+BAP appear to be closely parallel in their responses. A dose response was observed with the NF+BAP treatment, while the BAP treatment showed a dose response between the intermediate dose and the low dose. It was shown that absorption is more efficient via this route of exposure; therefore, results at the high dose for BAP could be attributed to a cytotoxic response from distribution in the cells, which would explain why the intermediate dose elicited a stronger response than the high dose.

DNA adducts in general do not persist for long periods of time. After approximately a week, a decrease in DNA adducts present should be observed. However, there are instances were chemicals to persist in the form of DNA adducts. Therefore, it is important to characterize this persistence with these treatments. All i.p. injection samples were compared over time for persistence. Over time, it was observed that adduct levels decreased. However, DNA adducts did persist shortly. The BAP and NF+BAP responses persisted from 1 day to 7 days, and then began to decrease. The RM and NF responses however persisted relatively at the same level from 1 day to 21 days. The responses to these chemicals were lower than those of the NF+BAP and BAP responses, which could account for the apparent persistence of their DNA adduct levels.

The next stage of this research is the long-term tumorigenicity study, modeled after Rodriguez et al. 1997. Rodriguez et al. (1997) exposed infant male mice to BAP or manufactured gas plant residues via i.p. injection. This research has demonstrated that the most efficient method of treatment application is via i.p. injection. This route of administration allows for more rapid absorption of PAHs, and therefore a more complete genotoxic response. Based on the present results it is expected that the highest tumor incidence would be seen in the NF+BAP treatment.

CHAPTER IV
RELATIONSHIP BETWEEN DNA ADDUCT AND TUMOR FORMATION IN INFANT MALE MICE

4.1 Introduction

In the United States, cancer is the cause of 1 in four deaths (Jemal et al. 2004). In the years from 1999 to 2000, approximately 13 million adults had been diagnosed with cancer (CDC 2003a). In 2003 nearly 1.3 million new cancer cases were diagnosed (CDC 2003b). Cancer can be caused by various agents including environmental and occupational exposures, household use of chemicals and genetic predispositions. Smoking and exposure to environmental tobacco smoke has been associated with cancer in the lung, bronchus, larynx, bladder, cervix and oral mucosa (Lee et al. 2006; Phillips 1997; Yach and Wipfli 2006) . A study by Boffetta (2006) on human cancer due to environmental pollutants concludes that in Europe 10.7% of lung cancers are due to urban air pollution. A connection between second-hand smoking and lung cancer has also been suggested, with an incidence of approximately 1.6%. Excess rates of cancer have also been associated with exposure to asbestos, arsenic, nickel and chromium (Case 2006; Kuo et al. 2006; Smith et al. 2006). Occupational exposure to chemicals such as PAHs has been associated with cancer in liver, lung, and stomach (Binkova and Sram 2004; Karlehagen et al. 1992; Vyskocil et al. 2004).

Occupational exposure to PAHs has been a concern since 1775, when Sir Percival Pott discovered a link between chimney sweeps and scrotal cancer. Numerous epidemiological studies have been conducted with regards to PAH exposure (Lloyd 1971; Maclure and MacMahon 1980; Mazumdar et al. 1975; Redmond et al. 1976; Wynder and Hoffmann 1967). ^{32}P-postlabeling can be a useful tool in the biomonitoring of exposure to genotoxic and carcinogenic compounds (Phillips 1997; Randerath et al. 1992). Pauisieux et al. (1991) did a study on selectivity of p53 genes. They found that p53 nucleotide “hot spots” in the lung and liver are preferred targets for BAP in the environment. Epidemiological studies are the best way to observe effects from exposure

to chemical mixtures in humans (Krewski and Thomas 1992). Vyskocil et al. (2004) did a risk assessment on lung cancer and environmental exposure to PAHs. They found that toxicity gradients based on animals studies for BAP were a magnitude higher than those that were based on BAP levels measured in the years studied. Their approach is that risk assessment and epidemiology should be used jointly, in order to reduce uncertainty factors associated with risk assessments. Wong and Harris (2005) did a retrospective occupational cohort study of workers at 11 wood-treating facilities. They looked at mortality due to malignant and non-malignant effects. Even though significant numbers of liver and lung cancers were observed, along with a multitude of other cancers, they found that mortality could not be linked to exposure at the facilities. Kerr et al. (2000) conducted a study of parental occupational exposures and neuroblastoma probability in their children. They found that maternal and paternal parents occupationally exposed to creosote (OR of 1.3 and 2.4 respectively) and coal tar (OR of none and 4.1 respectively) would have and increased probability for neuroblastoma to present in their children under the age of 15. Jean Brender et al. (2003) did a study on health risks associated with a residential population living in community near an old wood preserving site. In this study, she observed that there was a definite effect on health for residents in close proximity to a site that was contaminated with PAHs. There was an increased incidence of skin rashes, chronic bronchitis, premature births and low birth weights. However, higher rates of cancer had not been observed at this time. All of these epidemiological studies give insight into effects complex PAH mixtures have on humans. However, without toxicity testing, there is no absolute data on how chemicals react inside a biological system, and the amount of damage they may cause.

PAHs, especially BAP, have been extensively studied using animals as models to determine carcinogenic potential. One of the many models used is the ^{32}P-postlabeling assay. This assay has shown that complex PAH mixtures cause DNA aberrations, and as a result are potentially carcinogenic (Gupta et al. 1982; Hemminki et al. 2000; Lu et al. 1986; Randerath et al. 1981; Randerath et al. 1985; Randerath et al. 1996). However, it is not known if DNA adducts will definitely produce tumors *in vivo*. The best way to

determine tumorigenicity, is to use an animal model. Vesselinovitch et al. (1975a) carried out an extensive tumor study with B6C3F1 and C3AF strains of mice exposed to BAP. Mice were exposed at different ages in order to determine the effect that BAP had at different ages. The B6C3F1 mouse was the hardier of the two strains, as well as more susceptible to liver tumors. Mice dosed in infancy tended to be smaller in weight and not live as long as those dosed in adulthood. This is an important study, from it came a good liver model to determine tumor formation from PAH exposure. Rodriguez et al. (1997) modified this study for manufactured gas plant residues. They found that consistent dose-response relationships could not be obtained with the chemicals he used. However, tumor incidence was collected, and suggested that this is a good model to use for relatively quick carcinogenicity analysis of chemicals exposure. Culp et al. (2000) did a similar study on DNA adduct measurements and tumor mutation with B6C3F1 female mice. This study used a complex mixture of coal tar that was fed to the animals. This study found that the forestomach had high levels of tumor incidence. Suggesting that BAP (or similar PAHs) in coal tar mixtures are mostly responsible for the forestomach tumor induction. Von Tungeln et al. (1999) carried out a tumorigenicity study of nitropolycyclic aromatic hydrocarbons in neonatal B6C3F1 male mice. It was observed in this study that *in vitro* assays, while providing vital information on chemicals, are actually poor predictors of the tumorigenic potential of those chemicals. It was their assumption that liver tumors were induced by the nitro-PAHs from PAH-like metabolism. The *in vivo* infant male mouse model is highly versatile. Reynolds et al. (2004) conducted a study using this model to detect DNA damage-induced changes in the liver. They concluded that this model not only can detect tumor formation, but can be used for studying hepatocyte proliferation, p53 observations, and gene expression changes. The use of the model to look at these and other parameters is important, as it is more reliable than *in vitro* data. Tumor studies are expensive, and alternative *in vivo* studies such as the ^{32}P-postlabeling assay are ideal.

^{32}P-postlabeling is a sensitive method for determining DNA adduct formation in tissues from animals that have been treated with chemicals or chemical mixtures

(Phillips 1997; Randerath et al. 1984; Reddy 2000; Williams et al. 1996). This assay has shown that DNA damage does in fact occur with certain chemicals. In fact, this assay has been essential in showing that previously thought non-genotoxic chemicals did actually bind to and alter DNA (Phillips 1997). It has been shown in previous studies that DNA binding activity of certain mixtures does in fact correlate with mutagenic/carcinogenic activity (Phillips 1997).

The USEPA published "Guidelines for the Health Risk Assessment of Chemical Mixtures" in 1986. These guidelines should be used when trying to assess the risk a mixture (more than one chemical) posses. There are three approaches that can be used, based on mixture composition, the chronic or subchronic exposure approach, the sufficiently similar approach and the toxic or carcinogenic properties approach. The chronic or subchronic exposure approach is the most accurate and preferred approach for assessing mixtures. This approach is used when data is available for the mixture of concern. When using this approach, the procedures for single compounds can be adopted for both systemic toxicants and carcinogens. However, the dose-response is not the same for single compounds as compared to mixtures, and this should be taken into consideration. The sufficiently similar approach is used when there is no data available on the mixture of concern, but a similar mixture does have data available. It is important when using this approach that dissimilarity of the mixtures be taken into consideration. Finally, toxic or carcinogenic properties can be used when data is not available on the mixture of concern as well as any reasonably similar mixtures. The toxic or carcinogenic properties of the individual components of the mixture may then be evaluated for the risk assessment. Dose additivity is often assumed for systemic toxicants, but is not the most biologically plausible approach. However, this approach predicts reasonably well the risk assessment of mixtures. Risk assessment should be tailored to the mixture of concern, taking into account the many levels of complexity a mixture poses. It is important to study mixtues as a whole, and as fractions of the whole, in order to obtain a better understanding of the risks posed by exposure to mixtures.

This study was conducted to test two hypotheses related to complex PAH mixtures. The first hypothesis is that the frequency of DNA adducts in tissues of mice treated with BAP or complex mixtures containing the same amount of BAP will correlate with the incidence of tumors in animals receiving comparable treatments. The second hypothesis is that the incidence of tumors in animals treated with BAP, or complex mixtures containing equal amounts of BAP, will not be significantly different. The data from these experiments provides useful information for understanding the impact of mixture interactions on BAP carcinogenicity.

4.2 Materials and Methods

4.2.1 Sample Collection and Extraction

Methods on sample collection and extraction were previously described in Chapter II.

4.2.2 Chemicals and Materials

The following chemicals were purchased from EM Science (Gibbstown, NJ): methylene chloride (ACS reagent grade, 99.5% pure), isopropyl alcohol (HPLC grade) and acetone (ACS reagent grade, 99.5% pure). Pentachlorophenol (98% pure), benz(a)anthracene (99% pure), chrysene (98% pure), benzo(b)fluoranthene 98% pure), benzo(k)fluoranthene (98% pure), benzo(a)pyrene (97% pure), dibenz(a,h)anthracene (200µg/mL in CH_2Cl_2), guanidine HCl (99+% pure), and trizma base (99%) were purchased from the Sigma-Aldrich Group (St. Louis, MO). Indeno(1,2,3-c,d)pyrene (1000µg/mL in CH_2Cl_2) was purchased from Absolute Standards (Hamden, CT). The following were purchased from QIAGEN Sciences, Inc (Germantaown, MD): QIAGEN Genomic-tip 100/G and RNase A (17500 U). Proteinase K (recombinant, PCR grade, lyphilizate) was purchased from Roche Diagnostics (Indianapolis, IN). Tween-20 (enzyme grade) was purchased from Fisher Scientific (Pittsburgh, PA). Acide MOPS 3-

(N-morpholino) propane sulfonique (Molecular Biology Grade) was purchased from VWR International (Batavia, IL). The following chemicals were purchased from EMD Biosciences, Inc. (San Diego, CA): $Na_2EDTA \bullet 2H_2O$, triton X-100, and NaCl (ACS grade).

4.2.3 Animals

All animals were obtained from Harlan (Houston, TX). Strains used were B6C3F1/Hsd male mice, 21 days old, 7 to 11 g. These mice are inbred hybrid agouti offspring of a cross between a C57BL/6Nhsd inbred female mouse and a C3H/HeNHsd inbred male mouse. Mice were shipped via Harlan truck in filtered shipping containers. Mice are housed in a barrier facility, 3 mice per filtered cage. Mice were fed ad libitum using sterilized food provided by the facility. Water was also ad libitum, using filtered and sterilized water provided by the facility.

4.2.4 Statistics

Statistics were carried out by a Graduate Student in the Department of Statistics at Texas A&M University using SAS software. Mortality was computed using a logistic regression, with odd ratios computed for chemical and dose combinations. Among each tissue, all tissues combined as well as liver tissue alone were the only groups with enough tumors to warrant analysis using logistic regression. The first analysis run only included treatments that had a low, medium and high dose range (this excluded the NF and control). Odds ratios were computed for all chemical-dose combinations. Next, a logistic regression was run on only high dose treatments (this excluded all medium and low doses, and the control). Odds ratios were computed for all chemical-chemical combinations. The final analysis included all treatments, all doses and the control in a logistic regression. Odds ratios were run for chemical-control as well as chemical-chemical combinations.

4.2.5 Extraction and Fractionation of a Complex Chemical Mixture

4.2.5.1 Extraction

As previously described in Chapters II and III, the WPW was a pure oil, and therefore no extraction was necessary.

4.2.5.2 Fraction Selection

As stated in Chapter III, the neutral fraction isolated for Specific Aim I was chosen to be evaluated for Specific Aim II in Chapter III. The neutral fraction will also be evaluated in this chapter for Specific Aim III. The neutral fraction is the elutant which isolated mostly PAHs from the parent complex mixture. The fractionation procedure was previously described in Chapter II. This fraction was tested against BAP and a reconstituted mixture in Specific Aims II and III.

4.2.5.3 Preparation of a Reconstituted Mixture

Methods for preparation of a reconstituted mixture (RM) were previously described in Chapter II. Table 4.1 lists the amount of PAHs present per treatment for the high dose (0.429 mg/g bw).

Table 4.1. Comparison of PAHs present across treatments for the high dose (0.429 mg/g bw).

	Amount of PAH per High Dose (ug/mouse)							
Treatment	**PCP**	**BaA**	**Chrysene**	**BbF**	**BkF**	**BAP**	**IP**	**DA**
BAP	--	--	--	--	--	**3.75E+02**	--	--
RM	6.80E+00	3.90E+00	4.80E+00	2.10E+00	1.30E+00	**3.75E+02**	6.00E-01	1.00E-01
NF+BAP	6.10E+00	5.30E+00	5.30E+00	2.10E+00	1.30E+00	**3.75E+02**	7.00E-01	1.00E-01
NF	6.10E+00	5.30E+00	5.30E+00	2.10E+00	1.30E+00	**1.70E+00**	7.00E-01	1.00E-01

4.2.6 *In Vivo* Bioassays

4.2.6.1 DNA Adducts in Mice, Topical Application

DNA adducts were quantified in B6C3F1 21 day-old male mice exposed topically to 150µl of sample (in CH_2Cl_2) at does of 3, 1.2, and 0.48mg/mouse for 24 hr. Dosing procedures were followed as previously described by Reddy and Randerath (1986). A brief description follows. Mice were weighed and sorted into groups, 5 mice per group, so that average group weights were approximately equal. The backs of the mice were then shaved, and left for 24 hr. After 24 hr, the mice were shaved again, allowing the chemicals to be applied directly to the skin. Mice were then reweighed, groups adjusted accordingly, and any nicked mice were removed. A total of 10 groups were treated, including a control group. Topical application was applied to the shaved skin via capillary tubes, and mice were left for 24 hr. Three groups were tested, BAP, RM and NF+BAP. Each group was tested for dose-response with 3, 1.2, and 0.48 mg/mouse doses. Mice were sacrificed after 24 hr, and the exposed skin, lung, and liver were collected and stored at -80°C.

4.2.6.2 Infant Male Mouse Model

Tumor incidence in infant B6C3F1 male mice was first described by Vesselinovitch et al. (1975a) and Vesselinovitch et al. (1975b), and later modified for complex mixtures by Rodriguez et al. (1997). For this study, tumor incidence and DNA adducts were evaluated in infant male B6C3F1 mice by using the protocol described by Rodriguez et al. (1997). Briefly, 21 day old male B6C3F1 mice were injected intraperitoneally one time with sample or control. The sample was dissolved in 50:50 DMSO:Corn oil. A total of 24 groups of mice were treated. For ice with a 280 day endpoint (tumor mice), there were 10 treated groups with 20 mice per group (Control, BAP, reconstituted mixture, and neutral fraction + BAP) and one treated group having 10 mice per group (neural fraction). BAP, reconstituted mixture and neutral fraction + BAP had three groups each, one for each dose concentration. Neutral fraction was dosed at the highest concentration only. Mice with a 1 day, 7 day and 21 day endpoint (DNA

adduct mice), there were 13 treated groups with 15 mice per group (5 mice per sample endpoint). Groups included control, BAP, reconstituted mixture, neutral fraction + BAP, and neutral fraction. All treatments had three groups dosed with the dose-response concentrations. Dose concentrations administered to the mice included 0.429, 0.171, and 0.069 mg/g body weight in a volume of 7.14 µL vehicle/g body weight. Control was administered as a volume of 7.14 µL vehicle/g body weight. Before treatment administration, mice were taken from their mothers and weighed. After weight was determined, mice were injected according to dosing chart (Table 4.2). After intraperitoneal injection, tumor mice were watched daily for 3 months, and then bi-weekly until the 280 day endpoint. DNA adduct mice were watched daily until the endpoints of 1 day, 7 days and 21 days were reached. For DNA adduct mice, lung, liver and forestomach were collected and stored at -80°C. For tumor mice, lung, liver and forestomach were collected and immediately put into 10% formalin. A small piece of liver was collected from the first three mice of each group and stored at -80°C for DNA adduct testing.

Table 4.2. Intraperitoneal injection dose chart listing the volume of sample (mL) given based on the weight of the mouse (g). Volume dose was based on mouse receiving approximately 0.429, 0.171, and 0.069 mg of sample per g body weight in a 7.14 µL vehicle per g of body weight dose. Dose-response concentrations were calculated and mixed prior to dosing.

Weight (g)	Dose Volume (mL)
5.0 - 6.5	40
6.6 - 7.7	50
7.8 - 9.1	60
9.2 - 10.5	70
10.6 - 11.9	80
12.0 - 13.3	90

4.2.6.3 ^{32}P-Postlabeling

Methods previously described in chapters II and III.

4.2.6.4 Histology

Tissues were collected according to the Veterinary Integrated Biosciences departmental Histology Lab requirements. Samples were taken from the animal immediately after sacrifice. Tissues were then cut to be approximately the same size, taking the piece that is most abnormal in appearance. Samples collected include liver, lung, forestomach and tumors (if large ones present). Tissues were placed in a histology cassette, and then put in a container of 10% neutral buffered formalin for 7 days at 2°C. Ten % neutral buffered formalin (100 mL formaldehyde (37-40%), 900 mL distilled water, 4 g monobasic sodium phosphate, and 6.5 g dibasic sodium phosphate) is the recommended solution for fixation, as the pH 6.8 and relatively sTable. After fixation, tissues were transferred to 70% ethanol, and kept at 2°C until sent for processing at the Texas A&M Univeristy Veterinary Integrative Biosciences (VIBS) Histology Lab.

A description of methods used at the VIBS Histology Lab follows. Tissues were processed in a tissue processor based on size of tissues. The main purpose of the embedding is to exchange the unbound water within the tissue to paraffin—dehydrate the tissues. The cycle for this process is: 70% ETOH, 80% ETOH two times, 89% ETOH two times, absolute alcohol two times, Pro-Par (clearing reagent) three times, and paraffin four times. Pro-par is a clearing reagent that is used because it is miscible with alcohol and paraffin, whereas the alcohol alone is not miscible with paraffin. The paraffin is run four times because the first run is always contaminated with Pro-Par. Once the tissue is done with the processing step, it is filled with paraffin. The tissue is then embedded on the cassette. The tissue is covered with paraffin to form a block wich will hold it steady while it is being sliced. Tissues are then sliced at 4-5 μm. After tissues were sliced, they underwent H&E staining. The paraffin is then removed from the slices via the following cycle: Pro-Par three times, absolute alcohol two times, 95% ETOH two times, 70% ETOH one time, tap water one time, and deionized water one

time. Haematoxylin is then added to the slide for 5 min, to stain the nuclei. The slice is then rinsed with tap water, and then with acid alcohol (0.5% HCl in 70% ETOH). The acid alcohol removes any extra haematoxylin from the slice. Lithium carbonate (0.5% lithium carbonate in deionized water) is added to the slice. This step changes the pH of the nuclei, which in turn makes the stain a blue color. The slice is then rinsed with tap water, and then 80% ETOH, followed by the addition of Eosin Y + Phloxine stain. This will stain the cytoplasm (a light pink), muscle and connective tissue (a darker pink), and blood cells (magenta). The slice is then rinsed with 95% ETOH two times, absolute alcohol two times, and Pro-Par four times. These final rinses are done because Pro-Par is miscible with the mounting media. The cover slip is mounted via mounting media, and the slides are ready.

All tissue slides were packaged and hand delivered to a trained pathologist at the Baylor College of Dentistry in Dallas, TX. She viewed each slide and made a diagnosis based on her knowledge in pathology. She determined tumor presence, and type (malignant or benign) within each tissue (three slides per tissue).

4.3 Results

4.3.1 Mortality

Mortality information was collected during the duration of the study. Incidence of mortality by chemical and dose is presented in Table 4.3. Information was not obtained for all animals to distinguish mortality due to acute toxicity or organ failure from mortalities caused by tumor formation. NF+BAP had the largest incidence of mortality at the high dose (75%), with the NF having the second largest incidence of mortality at the high dose (46%). BAP and RM follow with mortalitly incidences of 27% and 14%. Most mice that did not survive to the end point came from the high doses of each chemical (Figure 4.1). Odds ratios for mortality, Table 4.4, confirm that the high dose (0.429 mg/g bw) has a probability of causing premature death 11.2 times that of the low dose (0.069 mg/g bw), and 3.7 times that of the medium dose (0.171 mg/g bw) (Table 4.4).

Table 4.3. Mortality and survival of B6C3F1 male mice treated with BAP and complex chemical mixtures containing BAP. Mortality is a measure of animals found dead or euthanized due to poor health status prior to the 280 day end point. RM = reconstituted mixture; NF+BAP = neutral fraction plus BAP, NF = neutral fraction.

Chemical	Dose	Fatalities		Survivals		Totals
Control	--	1	(5%)	19	(95%)	20
BAP (mg/g bw)	0.429	6	(27%)	16	(73%)	22
	0.171	3	(14%)	19	(86%)	22
	0.069	0	(0%)	20	(100%)	20
RM (mg/g bw)	0.429	4	(14%)	24	(86%)	28
	0.171	2	(8%)	24	(92%)	26
	0.069	0	(0%)	26	(100%)	26
NF+BAP (mg/g bw)	0.429	15	(75%)	5	(25%)	20
	0.171	5	(25%)	15	(75%)	20
	0.069	3	(15%)	17	(85%)	20
NF (mg/g bw)	0.429	6	(46%)	7	(46%)	13
Totals		**45**	**(19%)**	**192**	**(81%)**	**237**

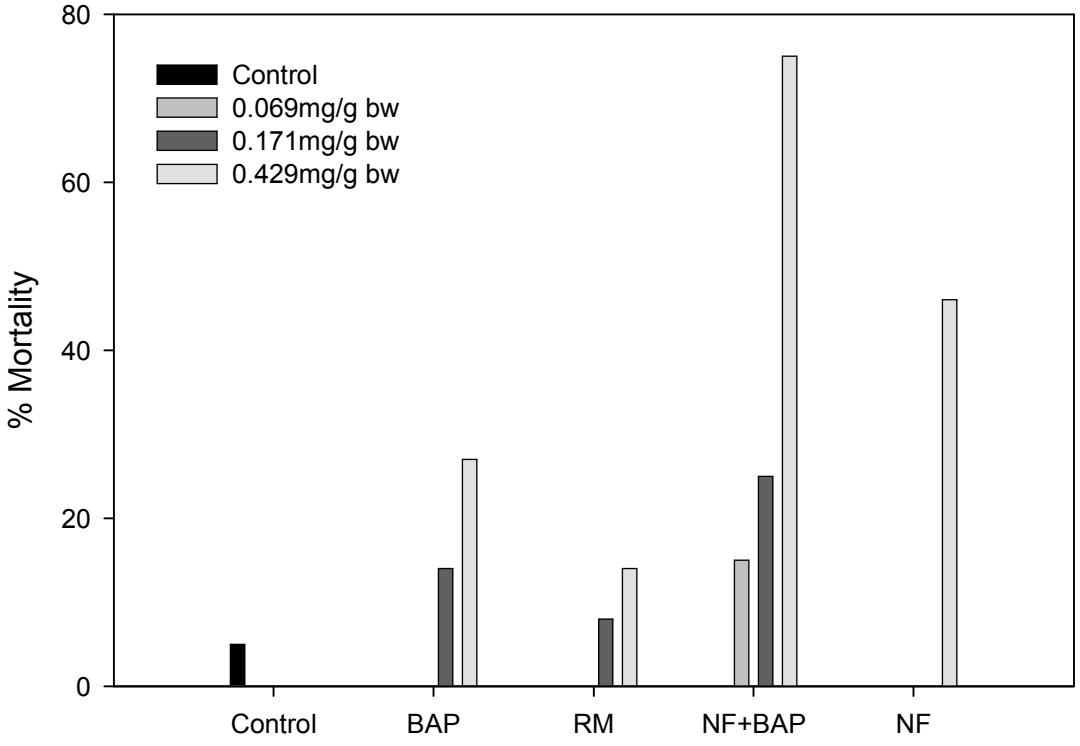

Figure 4.1. Percent mortality in each treatment group prior to 280 days.

Table 4.4. Odds ratios for mortality from chemical and dose treatments in B6C3F1 male mice treated with BAP and complex chemical mixtures containing BAP. Odds ratios represent the probability of one factor causing mortality over the other factor.

Odds Ratios

			Mortality	
Factor 1	**vs**	**Factor 2**	**OR**	**(95% CI)**
0.429	x	0.069	11.2	(3.6, 35.3)
0.429	x	0.171	3.7	(1.5, 8.8)
0.171	x	0.069	3.1	(0.9, 10.1)
NF+BAP	x	BAP	4.4	(1.8, 11.0)
BAP	x	RM	2.0	(0.7, 5.6)
NF+BAP	x	RM	8.7	(3.3, 23.6)

4.3.2 Tumor Incidence

Upon dissection of the mice that survived to the 280 day end point, gross tumor formation was observed. All observable gross tumors are reported in Table 4.5. The liver tissue is the one tissue that had the most gross tumors. The RM low dose (0.069 mg/g bw) showed the largest incidence of gross tumor formation (38% overall). The second highest frequency of gross tumors was seen in the BAP medium dose treatment group (0.171 mg/g bw), at 32%. Overall, NF+BAP showed a dose-response when graphed (Figure 4.2). BAP increases at the medium dose (0.171 mg/g bw), while RM decreases at the same dose. BAP and RM appear to show opposite gross tumor incidence. Each treatment (BAP, reconstituted mixture, neutral fraction plus BAP and neutral fraction), except the control, had some level of gross tumor formation observed.

Table 4.5. Incidence of visible tumors in B6C3F1 male mice treated with BAP or complex chemical mixtures containing BAP. Values represent number of animals in each treatment group with tumors visible upon dissection at day 280 and total number of animals (values in parentheses are percentages).

Chemical	Dose	Total Incidence	Liver Incidence
Control	--	0/19 (0%)	0/19 (0%)
BAP (mg/g bw)	0.429	1/16 (6%)	1/16 (6%)
	0.171	6/19 (32%)	4/19 (21%)
	0.069	4/20 (20%)	4/20 (20%)
RM (mg/g bw)	0.429	4/26 (15%)	4/26 (15%)
	0.171	1/24 (4%)	1/24 (4%)
	0.069	10/26 (38%)	9/26 (35%)
NF+BAP (mg/g bw)	0.429	1/8 (13%)	1/8 (13%)
	0.171	4/17 (24%)	4/17 (24%)
	0.069	2/18 (11%)	2/18 (25%)
NF (mg/g bw)	0.429	1/8 (13%)	1/8 (13%)

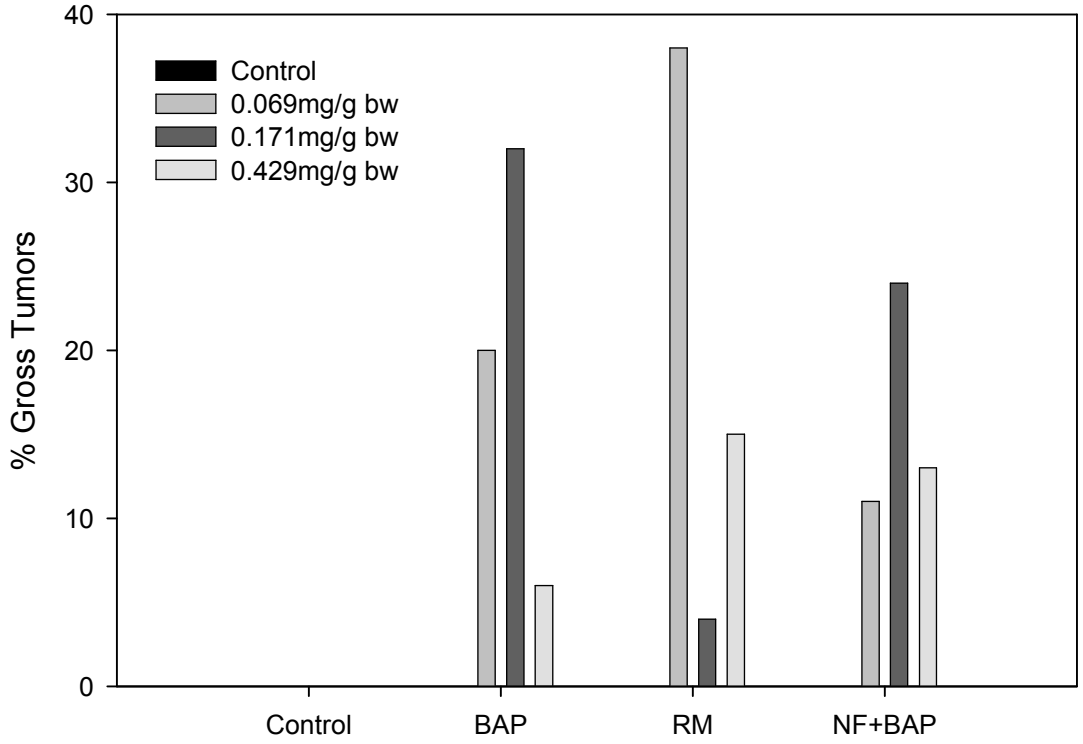

Figure 4.2. Percent of animals in each treatment group exhibiting tumors that were visible (without magnification) upon dissection. Percentages are calculated as number of total tumors divided by total number of animals in each dose and group.

Histopathologic observation of the tissue slices, along with the gross tumor incidence are added together to give the tumor incidence. Overall tumor incidence, as well as liver tumor incidence was determined. For overall tumor incidence, data reported in Table 4.6, NF+BAP at the high dose (0.429 mg/g bw) had the largest incidence (75%). BAP at the medium dose (0.171 mg/g bw) had the second largest incidence (63%), with RM low dose (0.096 mg/g bw) next with 46%. The trend seen in gross tumor incidence is also apparent in the overall tumor incidence (Figure 4.3). Tumors were classified as either benign or malignant in Table 4.7. Most tumors observed were benign, with the RM and NF+BAP high dose (0.429 mg/g bw) treatments showing 4% and 13% respectively.

Table 4.6. Overall tumor incidence (gross and microscopic) in B6C3F1 male mice treated with BAP and complex chemical mixtures containing BAP. Data represent total number of animals with tumors (gross and microscopic) in each treatment group and percentage of animals with tumors.

Treatment	Dose	Tumor Incidence
Control	--	1 (5%)
BAP (mg/g bw)	0.429	7 (44%)
	0.171	12 (63%)
	0.069	6 (30%)
RM (mg/g bw)	0.429	11 (42%)
	0.171	3 (13%)
	0.069	12 (46%)
NF+BAP (mg/g bw)	0.429	6 (75%)
	0.171	8 (47%)
	0.069	6 (33%)
NF (mg/g bw)	0.429	1 (13%)

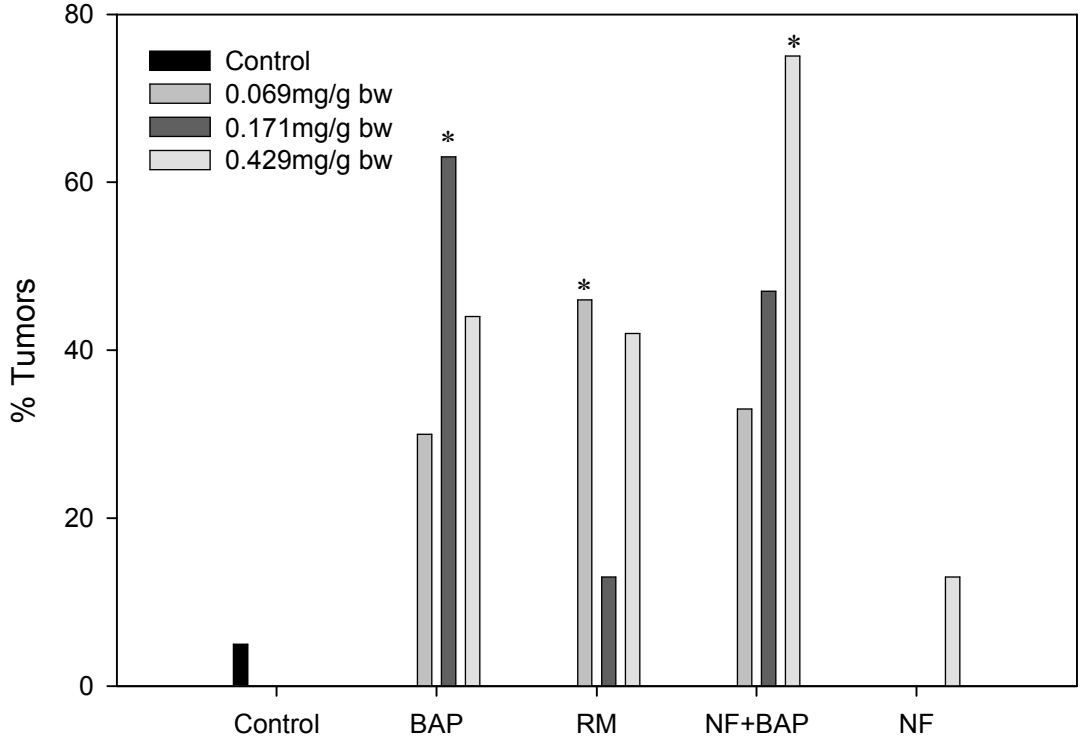

Figure 4.3. Overall tumor incidence (gross and microscopic) in infant mice treated with BAP or complex mixtures. Percentage represents total animals in each treatment group with at least one tumor divided by total animals in that group. *Highest probability in this group at this dose of developing a tumor.

Table 4.7. Histologic classification of tumors observed in B6C3F1 infant mice treated with BAP or complex PAH mixtures. Data are presented as total number of animals with benign or malignant tumors within each treatment group and total animals in group; values in parenthesis are percentage of animals in group with benign or malignant tumors.

Treatment	Dose	Benign		Malignant	
Control	--	1/19	5%	0/19	0%
BAP (mg/g bw)	0.429	7/16	44%	0/16	0%
	0.171	13/19	68%	0/19	0%
	0.069	6/20	30%	0/20	0%
RM (mg/g bw)	0.429	10/26	38%	1/26	4%
	0.171	3/24	13%	0/24	0%
	0.069	13/26	50%	0/26	0%
NF+BAP (mg/g bw)	0.429	5/8	63%	1/8	13%
	0.171	6/17	35%	0/17	0%
	0.069	5/18	28%	0/18	0%
NF (mg/g bw)	0.429	1/8	13%	0/8	0%

Overall tumor incidence is reported with bulky DNA adduct relative adduct labeling (RAL) per 10^9 nucleotides values in Table 4.8. NF+BAP has the largest incidence of tumors overall in the high dose (0.249 mg/g bw) (Table 4.9a), while the DNA adduct frequencies are highest in the high dose (0.249 mg/g bw) for each tissue. The largest incidence of overall tumor in BAP was in the middle dose (0.171 mg/g bw) (Table 4.9b), while the DNA adduct frequencies were highest in the high and middle doses (0.429 and 0.171 mg/g bw). For RM, the largest tumor incidence was in the low dose (0.069 mg/g bw) (Table 4.9c), while the highest frequency of DNA adducts was in the high dose (0.429 mg/g bw) of all tissues. It would appear that the ^{32}P-postlabeing assay is a good predictor of potential tumor incidence for NF+BAP and BAP, but not as good of a predictor for RM. When comparing the ^{32}P-postlbeling assay to tumor incidence (Figures 4.4, 4.5 and 4.6), it is apparent that a clear relationship cannot be deciphered. With the high dose, the larger the RAL value, the higher percentage of tumors formed (Figure 4.4). the same trend can be seen in the intermediate dose, with the exception of BAP (Figure 4.5). For the low dose, it appears that the larger the RAL value, the smaller the percent tumor formation (Figure 4.6). Therefore, while ^{32}P-postlabeling is a good indication of the tumor forming potential of a chemical, a correlation cannot be made with respect to actual percentage tumor formation.

Table 4.8. Comparison of overall tumor incidence in each treatment group and relative DNA adduct levels in various tissues. Tumor incidence is a measure of total tumors formed in each animal (gross and microscopic). Tumor data is presented as total number of tumors per group divided by total number animals that survived to 280 day end point (percentage). Bulky DNA adduct formation was measured in mice treated with a one-time injection exposure time of 24 hr. Adduct data is presented as RAL per 10^9 nucleotides ± SEM.

				Liver	Lung	Forestomach	
Chemical	**Dose**	**Tumor Present**		**RAL / 10^9 Nucleotides**	**RAL / 10^9 Nucleotides**	**RAL / 10^9 Nucleotides**	**Totals**
Control	--	1	(5%)	12.51 ± 1.33	4.79 ± 0.64	9.75 ± 3.13	19
BAP (mg/g bw)	0.429	7	(44%)	81.57 ± 23.38	88.02 ± 27.13	126.44 ± 34.86	16
	0.171	12	(63%)	74.88 ± 10.76	86.81 ± 13.59	150.78 ± 13.79	19
	0.069	6	(30%)	64.62 ± 6.53	40.89 ± 6.03	81.36 ± 23.64	20
RM (mg/g bw)	0.429	11	(42%)	94.58 ± 14.94	77.57 ± 15.92	132.16 ± 20.77	26
	0.171	3	(13%)	42.14 ± 11.17	21.07 ± 6.42	68.32 ± 21.46	24
	0.069	12	(46%)	31.33 ± 3.70	14.19 ± 1.41	44.18 ± 8.80	26
NF+BAP (mg/g bw)	0.429	6	(75%)	276.46 ± 18.97	237.93 ± 11.54	378.93 ± 31.93	8
	0.171	8	(47%)	85.07 ± 14.46	48.60 ± 10.60	140.33 ± 22.42	17
	0.069	6	(33%)	45.44 ± 2.30	23.64 ± 1.64	82.38 ± 4.41	18
NF (mg/g bw)	0.429	1	(13%)	44.90 ± 5.47	12.23 ± 0.59	18.11 ± 1.07	8

Table 4.9a. Tumor incidence and DNA adduct formation in various tissues isolated from infant male B6C3F1 mice administered high dose BAP or complex mixture (RM, NF+BAP, NF).

	% Animals with Tumors			RAL / 10^9 nucleotides ± SEM		
Treatment	Liver	Lung	Forestomach	Liver	Lung	Forestomach
BAP	31	13	0	81.57 ± 23.38	88.02 ± 27.13	126.44 ± 34.86
RM	31	8	4	94.58 ± 14.94	77.57 ± 15.92	132.16 ± 20.77
NF+BAP	50	13	13	276.46 ± 18.97	237.93 ± 11.54	378.93 ± 31.93
NF	13	0	0	44.90 ± 5.47	12.23 ± 0.59	18.11 ± 1.07

Table 4.9b. Tumor incidence and DNA adduct formation in various tissues isolated from infant male B6C3F1 mice administered medium dose BAP or complex mixture (RM, NF+BAP).

	% Animals with Tumors			RAL / 10^9 nucleotides ± SEM		
Treatment	Liver	Lung	Forestomach	Liver	Lung	Forestomach
BAP	58	11	0	74.88 ± 10.76	86.81 ± 13.59	150.78 ± 13.79
RM	13	0	0	42.14 ± 11.17	21.07 ± 6.42	68.32 ± 21.46
NF+BAP	35	0	0	85.07 ± 14.46	48.60 ± 10.60	140.33 ± 22.42

Table 4.9c. Tumor incidence and DNA adduct formation in various tissues isolated from infant male B6C3F1 mice administered low dose BAP or complex mixture (RM, NF+BAP).

	% Animals with Tumors			RAL / 10^9 nucleotides ± SEM		
Treatment	Liver	Lung	Forestomach	Liver	Lung	Forestomach
BAP	25	5	0	64.62 ± 6.53	40.89 ± 6.03	81.36 ± 23.64
RM	42	4	4	31.33 ± 3.70	14.19 ± 1.41	44.18 ± 8.80
NF+BAP	28	0	0	45.44 ± 2.30	23.64 ± 1.64	82.38 ± 4.41

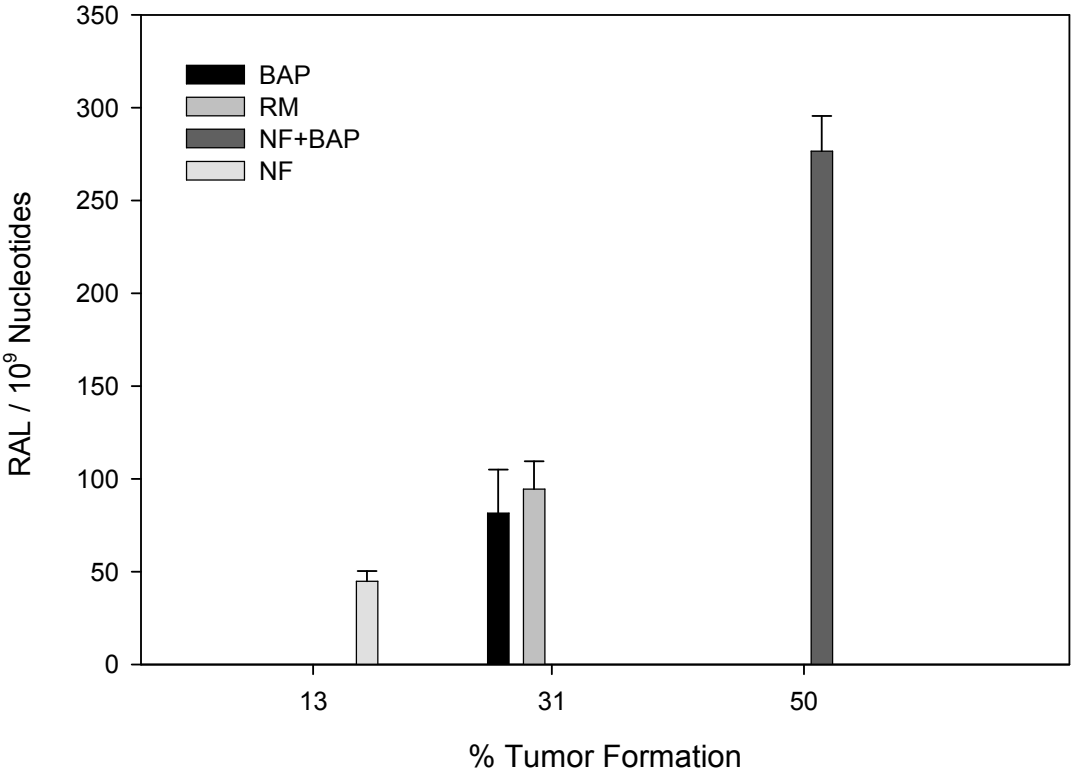

Figure 4.4. Relationship between the formation of DNA adducts (24 hr after exposure) and tumor formation (after 280 days) in liver from male B6C3F1 infant mice administered high dose of BAP (0.429 mg/g bw), RM, NF+BAP and NF.

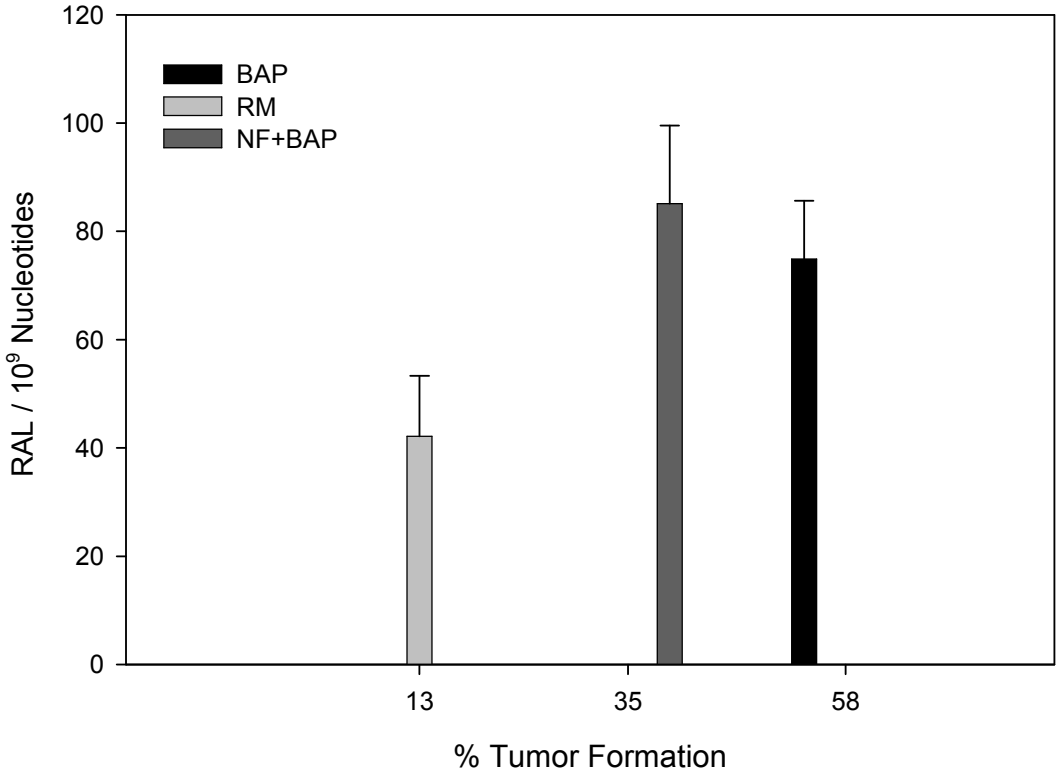

Figure 4.5. Relationship between the formation of DNA adducts (24 hr after exposure) and tumor formation (after 280 days) in liver from male B6C3F1 infant mice administered optimal dose of BAP (0.171 mg/g bw), RM and NF+BAP.

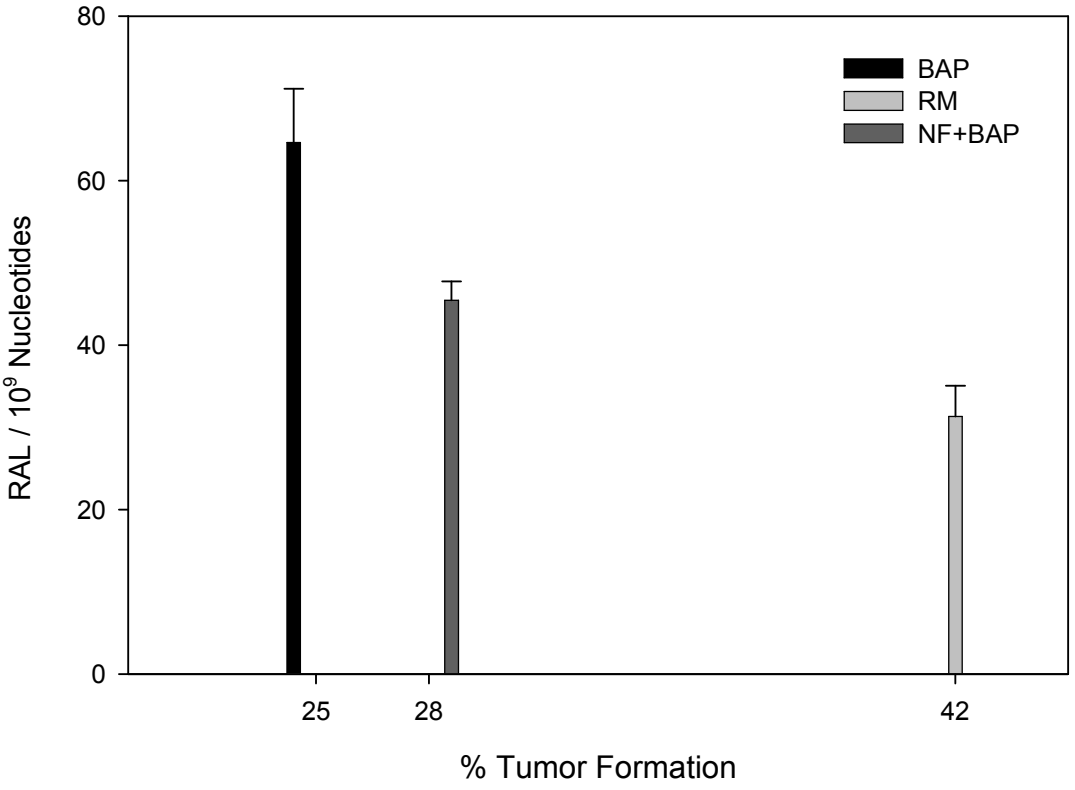

Figure 4.6. Relationship between the formation of DNA adducts (24 hr after exposure) and tumor formation (after 280 days) in liver from male B6C3F1 infant mice administered low dose of BAP (0.069 mg/g bw), RM, NF+BAP and NF.

Odds ratios for overall tumor incidence can confirm that BAP medium dose (0.171 mg/g bw) is 4.0 times more probable to produce tumors than in the low dose (0.069 mg/g bw) (Table 4.10). The high dose (0.429 mg/g bw) is 5.1 times more probable to produce tumor formation than the medium dose (0.171 mg/g bw) for the RM. Liver tumor incidence odds ratios follow the same trend as overall tumor incidence (Table 4.10). The overall trend of these odd ratios can be seen in Figures 4.7 and 4.8. NF+BAP tumor incidence decreases with dose. BAP increases from the high (0.429 mg/g bw) to the medium (0.171 mg/g bw) dose, while the RM decreases from the high (0.429 mg/g

bw) to the medium (0.171 mg/g bw) and visa versa from the medium (0.171 mg/g bw) to the low (0.069 mg/g bw) doses. Both the overall and the liver tumor incidence probability trends are similar. The liver is the target organ for tumor formation in this study, which would account for the similarities between overall and liver tumor trends. Odds ratios for the effect of the treatment for overall and liver are listed in Table 4.11. This data confirms that the chemical treatments have a higher probability of causing tumors than the control. This is an expected observation.

Table 4.10. Total risk of developing a tumor, as measured by odds ratios, in B6C3F1 infant male mice treated with BAP or complex mixtures. Odds ratios were calculated as the probability of one chemical causing tumor presence over the other chemical.

			Overall Tumor Presence		Liver Tumor Presence	
Chemical 1	**vs**	**Chemical 2**	**OR**	**(95% CI)**	**OR**	**(95% CI)**
BAP 0.429	x	BAP 0.069	1.8	(0.5, 7.2)	1.4	(0.3, 5.9)
BAP 0.429	x	BAP 0.171	0.5	(0.1, 1.8)	0.3	(0.1, 1.3)
BAP 0.171	x	BAP 0.069	4.0	(1.1, 15.2)	4.1	(1.1, 16.1)
RM 0.429	x	RM 0.069	0.9	(0.3, 2.6)	0.6	(0.2, 1.9)
RM 0.429	x	RM 0.171	5.1	(1.2, 21.6)	3.1	(0.7, 13.5)
RM 0.171	x	RM 0.069	0.2	(0.0, 0.7)	0.2	(0.0, 0.8)
NF+BAP 0.429	x	NF+BAP 0.069	6.0	(0.9, 39.2)	2.6	(0.5, 14.6)
NF+BAP 0.429	x	NF+BAP 0.171	3.4	(0.5, 21.7)	1.8	(0.3, 10.1)
NF+BAP 0.171	x	NF+BAP 0.069	1.8	(0.5, 7.0)	1.4	(0.3, 5.9)
NF+BAP 0.429	x	BAP 0.429	3.9	(0.6, 25.3)	2.2	(0.4, 12.6)
BAP 0.429	x	RM 0.429	1.1	(0.3, 3.7)	1.0	(0.3, 3.9)
NF+BAP 0.429	x	RM 0.429	4.1	(0.7, 24.2)	2.3	(0.4, 11.3)
BAP 0.171	x	NF+BAP 0.171	1.9	(0.5, 7.3)	2.5	(0.7, 9.7)
BAP 0.171	x	RM 0.171	12.0	(2.6, 55.3)	9.6	(2.1, 43.7)
NF+BAP 0.171	x	RM 0.171	6.2	(1.3, 29.0)	3.8	(0.8, 18.3)
NF+BAP 0.069	x	BAP 0.069	1.2	(0.3, 4.6)	1.2	(0.3, 4.9)
RM 0.069	x	BAP 0.069	2.0	(0.6, 6.8)	2.2	(0.6, 7.9)
RM 0.069	x	NF+BAP 0.069	1.7	(0.5, 6.0)	1.9	(0.5, 6.9)

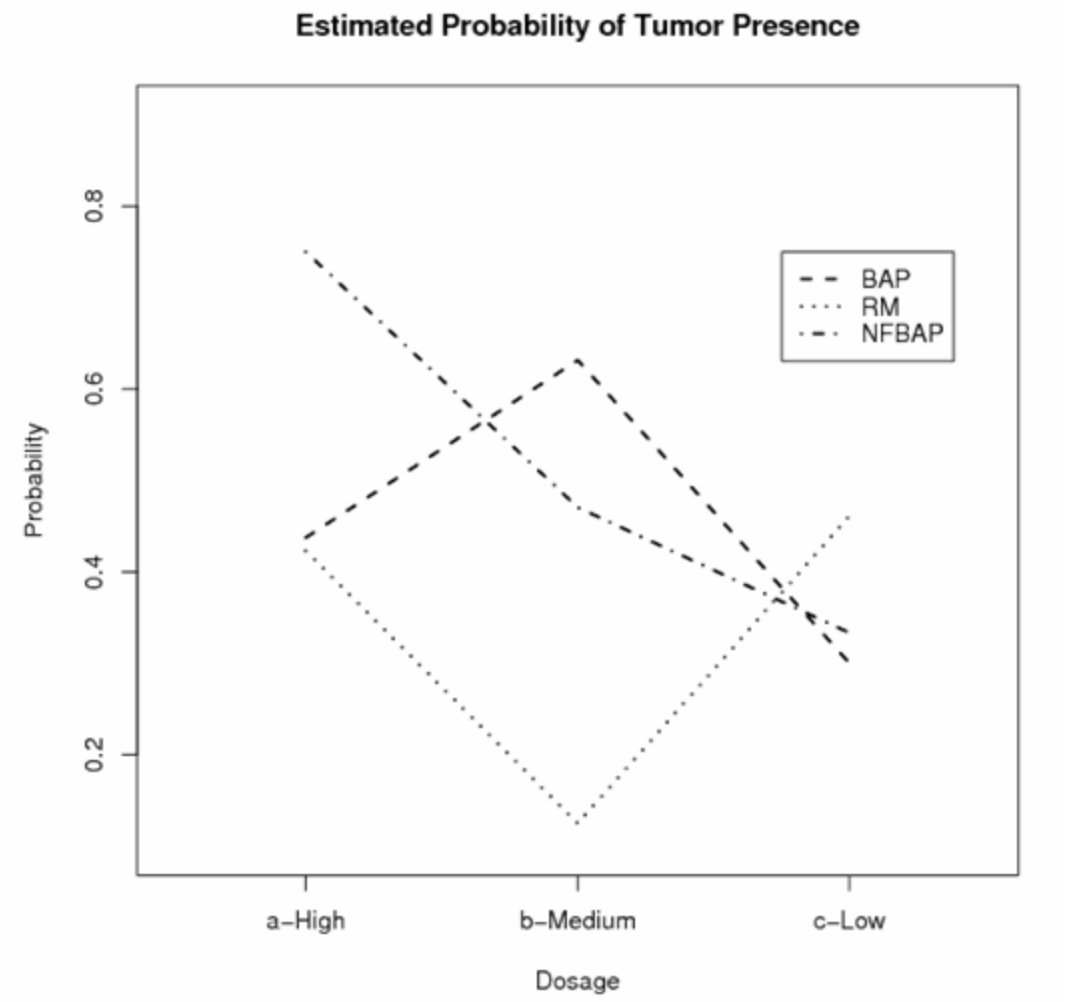

Figure 4.7. Overall probability of developing a tumor in B6C3F1 male mice treated with BAP or complex mixtures containing the same level of BAP. Probability is a statistically estimated value for all tissues.

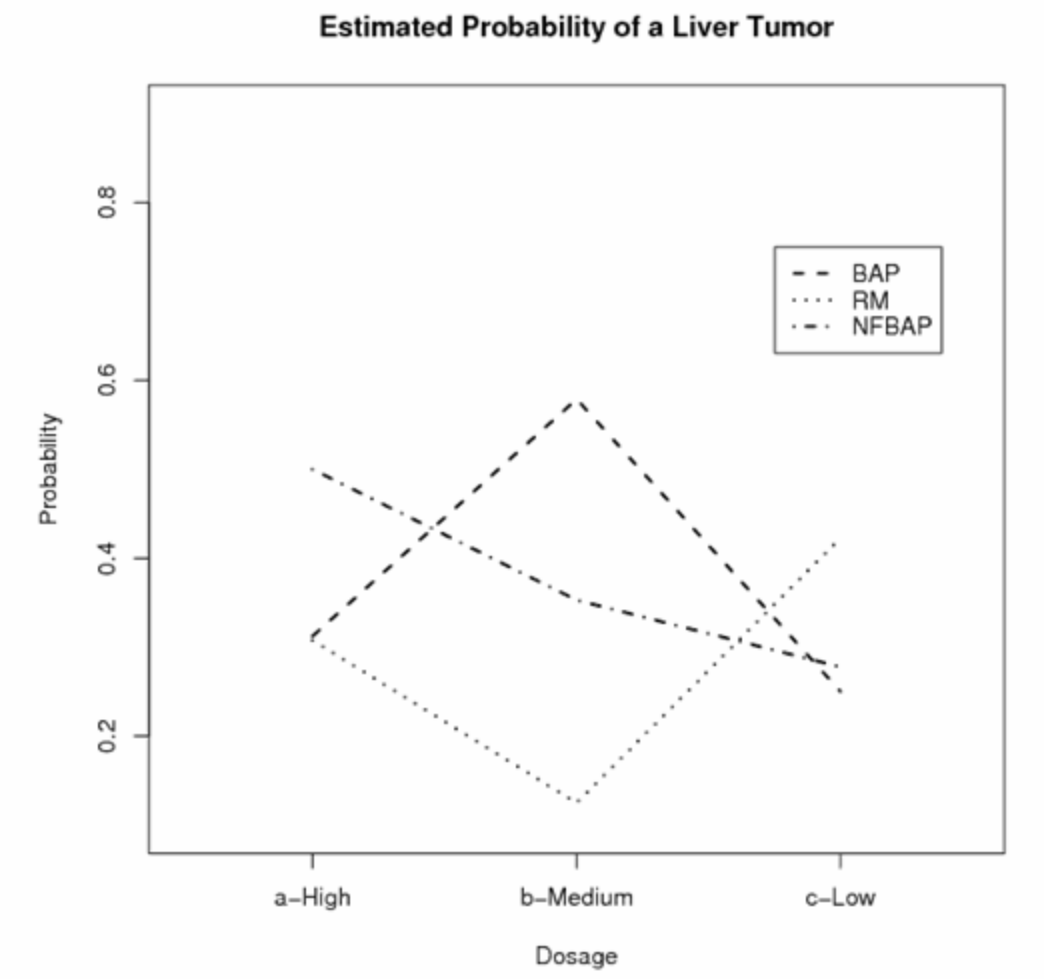

Figure 4.8. Probability of developing a liver tumor in B6C3F1 male mice treated with BAP or complex mixtures containing the same level of BAP. Probability is shown for each chemical and dose treatment. Probability is a statistically estimated value for all tissues.

Table 4.11. Risk of tumor formation, total and liver, in B6C3F1 infant male mice treated with BAP or a complex mixture. Risk is presented as an odds ratio calculated as the probability of one chemical causing tumor formation compared to the control.

			Total Tumors		Liver Tumors	
Chemical 1	**vs**	**Chemical 2**	**OR**	**(95% CI)**	**OR**	**(95% CI)**
BAP 0.429	x	Control	14.0	(1.5, 131.7)	18.7	(0.9, 369.1)
BAP 0.171	x	Control	30.8	(3.4, 283.5)	52.8	(2.8, >999.9)
BAP 0.069	x	Control	7.7	(0.8, 71.6)	13.8	(0.7, 269.9)
RM 0.429	x	Control	13.2	(1.5, 114.2)	17.9	(1.0, 332.9)
RM 0.171	x	Control	2.6	(0.2, 26.9)	6.3	(0.3, 130.8)
RM 0.069	x	Control	15.4	(1.8, 133.1)	28.9	(1.6, 530.5)
NF+BAP 0.429	x	Control	54.0	(4.1, 706.3)	39.0	(1.8, 862.4)
NF+BAP 0.171	x	Control	16.0	(1.7, 148.3)	22.0	(1.1, 428.4)
NF+BAP 0.069	x	Control	9.0	(1.0, 84.4)	15.9	(0.8, 311.8)
NF 0.429	x	Control	2.6	(0.1, 47.0)	7.8	(0.3, 213.5)

Tumor incidence was also calculated for the liver, as that was the tissue that had the highest amount of tumor formation. Liver tumor incidence is reported in Table 4.12. The same trend that was seen in the overall tissues are seen in the liver tissue as well. Liver tumor classification is listed in Table 4.13. No malignant tumors were observed in the liver tissue, as mentioned above. Liver tumor incidence is reported with liver DNA adduct frequency in Table 4.14. As with the overall tumor incidence and DNA adduct formation, a similar trend is observed in the liver. The over all trend from liver tumor incidence can be seen in Figure 4.9. Again, the same trend that has been seen in the gross tumors and overall tumor incidences is observed here as well. In Figure 4.10, all chemical treatments that contain the same level of BAP are graphed together. The RM and BAP treatments show opposite tumor incidence, while the NF+BAP show a slight dose-response. Even though these chemicals have the same levels of BAP, there are unknown interactions occurring which account for the different patterns, interactions that could be inhibitory, synergistic, etc. NF+BAP and NF, chemical treatments that have the same composition, except for BAP, are graphed in Figure 4.11. NF+BAP is clearly eliciting a higher tumor incidence in liver than NF. The difference between these two mixtures is the concentration of BAP. A larger concentration of BAP is apparently enhancing the potency of the neutral fraction, possibly through synergism, potentiation, etc.

Table 4.12. Frequency of liver tumors (gross and microscopic) detected in B6C3F1 infant male mice treated with BAP or complex mixtures. Data are presented as total number of animals within each treatment group with liver tumors over total animals in group. Values in parenthesis are percentage of animals with tumors at day 280.

Chemical	Dose	Tumor Present	
Control	--	0	(0%)
BAP (mg/g bw)	0.429	5	(31%)
	0.171	11	(58%)
	0.069	5	(25%)
RM (mg/g bw)	0.429	8	(31%)
	0.171	3	(13%)
	0.069	11	(42%)
NF+BAP (mg/g bw)	0.429	4	(50%)
	0.171	6	(35%)
	0.069	5	(28%)
NF (mg/g bw)	0.429	1	(13%)

Table 4.13. Histologic classification of liver tumors in B6C3F1 male mice treated with BAP or complex mixtures containing BAP. Data are presented as total number of tumors per group divided by total number animals that survived to 280 day end point (percentage).

		Typing at 280 Days Post Exposure			
Chemical	Dose	Benign		Malignant	
Control	--	0/19	0%	0/19	0%
BAP (mg/g bw)	0.429	5/16	31%	0/16	0%
	0.171	11/19	58%	0/19	0%
	0.069	5/20	25%	0/20	0%
RM (mg/g bw)	0.429	8/26	31%	0/26	0%
	0.171	3/24	13%	0/24	0%
	0.069	11/26	42%	0/26	0%
NF+BAP (mg/g bw)	0.429	4/8	50%	0/8	0%
	0.171	6/17	35%	0/17	0%
	0.069	5/18	63%	0/18	0%
NF (mg/g bw)	0.429	1/8	13%	0/8	0%

Table 4.14. Liver tumor incidence and bulky DNA adduct formation in B6C3F1 male mice treated with BAP and complex mixtures containing BAP. Tumor incidence is a measure of total tumors formed in the liver of each animal (gross and microscopic). Data is presented as total number of tumors per group divided by total number animals that survived to 280 day end point (percentage). Bulky DNA adduct formation was measured in mice treated with a one-time injection exposure time of 24 hr. Data is presented as RAL per 10^9 nucleotides ± SEM.

Chemical	Dose	Tumor Present		RAL / 10^9 Nucleotides	Totals
Control	--	0	(0%)	12.51 ± 1.33	19
BAP (mg/g bw)	0.429	5	(31%)	81.57 ± 23.38	16
	0.171	11	(58%)	74.88 ± 10.76	19
	0.069	5	(25%)	64.62 ± 6.53	20
RM (mg/g bw)	0.429	8	(31%)	94.58 ± 14.94	26
	0.171	3	(13%)	42.14 ± 11.17	24
	0.069	11	(42%)	31.33 ± 3.70	26
NF+BAP (mg/g bw)	0.429	4	(50%)	276.46 ± 18.97	8
	0.171	6	(35%)	85.07 ± 14.46	17
	0.069	5	(28%)	45.44 ± 2.30	18
NF (mg/g bw)	0.429	1	(13%)	44.90 ± 5.47	8

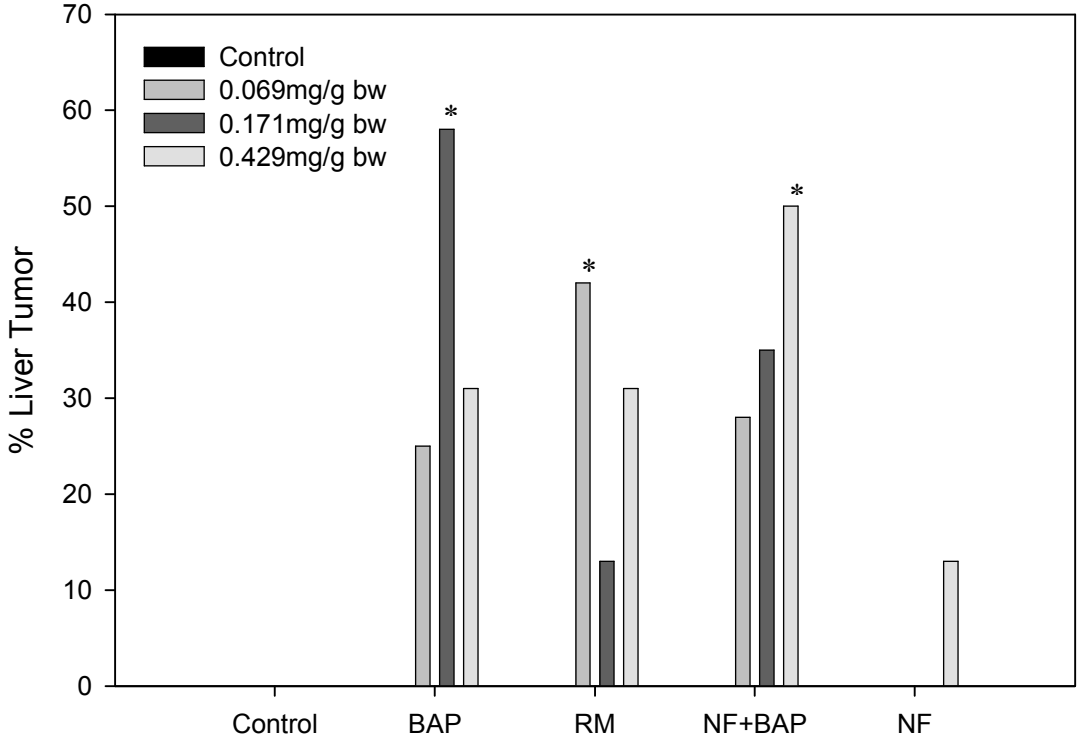

Figure 4.9. Percent tumor formation in the liver for each treatment and dose. Percentages are calculated as number of total tumors divided by total number of animals in each dose and group. *Highest probability in this group at this dose of developing a tumor.

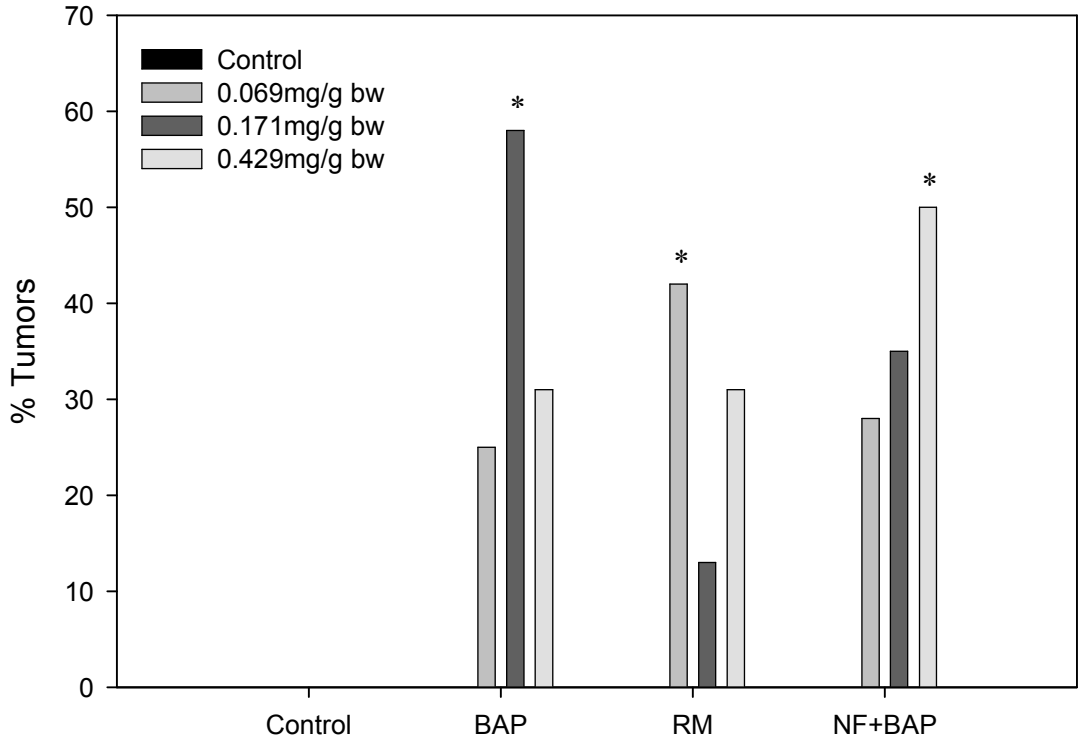

Figure 4.10. Percent tumor formation in the liver for treatments which contain the same level of BAP. Percentages are calculated as number of total tumors divided by total number of animals in each dose and group. *Highest probability in this group at this dose of developing a tumor.

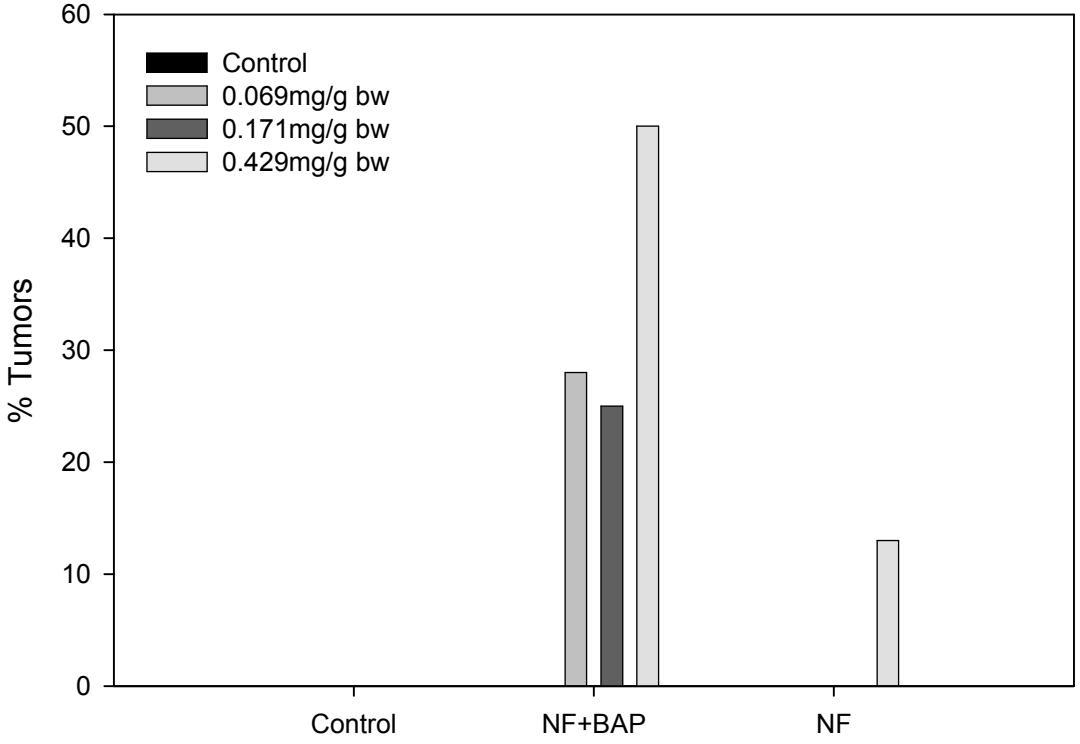

Figure 4.11. Percent tumor formation in the liver for treatments which contain different levels of BAP. Percentages are calculated as number of total tumors divided by total number of animals in each dose and group.

4.4 Discussion

This research was modeled after a long-term tumor study for animals receiving one of four treatments. For the current experiment, the four treatments consisted of BAP, RM, NF+BAP and NF. All treatments were administered via i.p. injection. DNA adducts were measure after 24 hr in mice. In a separate group of animals tumor formation was monitored for 280 days. As is standard practice for cancer studies, threatments were administered at a maximum tolerable dose.

Primary toxicity was observed in the NF+BAP and NF treatments. Although some toxicity was observed in animals administered RM and BAP treatments, fatalites were less than those observed in the other treatments. Among the animals that did not survive to 280 days, the majority of them had aggressive tumor formation. Gross tumors were observed in all treatment goups. The highest gross tumor frequency was observed in the RM treatment receiving the lowest dose, whereas total tumors were highest in the high dose NF+BAP treatment. It is possible that more visible tumors were present on the outside of the organs with regard to the RM treatment. Another explanation would be that we did not take enough slices to discover all tumors present. Only three slices were taken per tissue for this research due to time and monetary constraints. Animals receiving treatment with BAP, RM or NF+BAP received equivalent amounts of BAP. However, tumor incidence observed in these treatment goups was different. A consistent dose response relationship from low to high dose for tumor incidence was observed in the NF+BAP treatment. The high dose NF+BAP treatment also produced the highest overall tumor indcidence. For animals administered only BAP, the optimal dose for tumor incidence was the intermediate dose. Whereas for animals administered the RM treatment, the low and the high dose induced the highest tumor incidence, while the intermediate dose induce approximately a three fold decrease in tumor incidence. These differences appear to reflect ineractions of the seven components of the RM and the unknown number of components of the NF+BAP treatment. The increase in response from the high dose to the intermediate dose for the BAP treatment could be due to a cytotoxic effect from the high dose. At the same dose of BAP there were six tumors

in the BAP treatment group, whereas the group that received the RM treatment exhibited only one tumor. There are several explanations surrounding this. One would be that we don't have the full picture with only interpreting three slices per tissue. Another would be that there is some inhibitory interaction occurring between the eight chemicals present. However, at the lowest dose animals receiving only BAP exhibited 20% tumor incidence, while those receiving the RM treatment exhibited a tumor incidence of 38%. Rodriguez et al. (1997) observed primarily liver tumors as well. While Rodriguez et al. (1997) observed tumor incidence in BAP, they did not observe tumor incidence for the manufactured gas plant residue (MGPR). In this research, we also primarily observed liver tumors, with smaller numbers of tumors seen in the forestomach and lung. This is a liver model, which would account for the smaller numbers seen in the other organs. However, even though we also observed tumor formation after exposureto BAP, we also observed tumor formation avter exposure to NF+BAP. These two studes are similar, however the makeup of the mixtures tested has resulted in different outcomes. Metabolism and distribution have played a ey role in this part of this research. Since liver is the target organ in this model, metabolism seems to be more important. Interactions by chemicals in the mixtures are influencing metabolism, which in turn is influencing genotoxicity. For instance, PAH is possibly inhibiting phase I and phase II enzymes while NF+BAP is enhancing these enzymes at the high dose. However, at the low dose, these two treatments are approximately equal. There are multiple interactions occurring which need to be dissected further. There are interactions with metabolic enzymes occurring, as well as dose specific interactions and chemical interactions within the mixtures.

A relationship between DNA adducts and tumor formation was difficult to delineate. For selected treatments, however, a relationship was seen between adduct levels and tumor formation. BAP had an increased response at the intermediate dose, preceded and followed by a lower response. This suggests that the high dose may have been cytotoxic, while the intermediate dose was optimal for a response. At this optimal treatment dose for BAP (0.171 mg/g bw), the tumor incidence was 58% and the RAL

was approximately 75 per 10^9 nucleotides. At the same treatment dose for the RM, tumor incidence was reduced to 13% and the RAL was reduced to approximately 42 per 10^9 nucleotides. Similarly, at the highest treatment dose the RM induced tumors in 31% of animlas and RAL was 95 per 10^9 nucleotides. The NF+BAP induced approximately an approximate two fold increase in tumor incidence and six fold increase in DNA adduct formation.

Overall, the data demonstrates that the NF+BAP treatment is the most genotoxic and carcinogenic mixture tested. Even though all three treatments (BAP, RM and NF+BAP) have the same amount of BAP present, there were appreciable differences in the incidence of tumors formed due to interactions of the constituents within the mixtures. Although a consistent relationship was not observed between DNA adducts and tumor incidence, there were possible relationships between certain treatments, which could not be confirmed statistically. It is possible that a relationship between DNA adduct formation is more apparent with tumor formation when cytotoxicity does not play a role. Based on the data from this research, DNA adducts are a good measure of the tumorigenic potential of complex mixtures, especially when cytotoxicity does not influence the response. Both inhibitory and enhanced responses were ultimately observed in the RM and NF+BAP treatments, respectively. At the same level of BAP, NF+BAP and BAP both elicited very different responses. NF+BAP induced significantly more tumors than BAP, which has implications for risk assessment. It is very important to understand these interactions, so that risk assessment of these types of chemicals may be improved in the future.

CHAPTER V
SUMMARY

The research in this dissertation was conducted to investigate the genotoxic and carcinogenic interactions of the components of fractions isolated from WPW oil. The WPW was used in this study as a representative complex mixture of PAHs and PCAs. Chemical analysis of the WPW identified a variety of compounds including low and high molecular weight PAHs, pentachlorophenol and smaller concentrations of PCDDs. These compounds are ubiquitous in the environment, and pose a threat to humans and ecological receptors that may be exposed to contaminated media. Current regulatory guidelines recommend that the risk of a complex mixture is estimated assuming additive interactions. However, mixture interactions may enhance or inhibit component toxicity and genotoxicity. These studies were conducted to investigate the interactions of several fractions isolated from a WPW. Data were obtained to investigate the genotoxicity of the isolated fractions in microbial mutagenicity assays, as well as in an animal model using 32P-postlabeling. The results obtained from short-term bioassays were compared with the results from a 40-week tumor study using a juvenile mouse model. These studies were conducted to investigate the hypothesis that the isolation of high molecular weight PAHs from the complex WPW mixture will allow increased expression of genotoxicity *in vitro* and *in vivo*.

This research included chemical separation and fractionation of a complex WPW mixture, analysis of chemical components and genotoxicity using microbial cell cultures and animal models, and for a limited number of samples evaluation of carcinogenic potential in an infant mouse model. The complex oily WPW waste was initially fractionated into acid, base and neutral fractions using liquid-liquid separations. An aliquot of the neutral fraction was further separated using column chromatography into two fractions enriching the high molecular weight PAHs and the PCDDs. The acid fraction was found to contain the highest concentration of pentachlorophenol, the neutral fraction isolated the high and low molecular weight PAH compounds, and the base

fraction retained a smaller amount of pentachlorophenol with PAH concentrations below detection limits. Two fractions were isolated from the neutral fraction. The PAH fraction contained primarily high molecular weight carcinogenic PAHs (i.e., BAP, IP, and DA), while the PCDD fraction contained the maximum levels of carcinogenic PAHs.

A series of short-term bioassays were then conducted to investigate potential interactions of the components of the various fractions isolated from the WPW. In the *Salmonella* microsome assay, the base fraction induced the maximum genotoxic response. It is unclear which components of this fraction were genotoxic. PAH concentrations in the base fraction were generally below levels of detection. Thus, it is assumed that nitrogen containing hydrocarbons may have produced the mutagenic response observed in this bioassay. The PAH and crude extract also induced a positive mutagenic response in *Salmonella*, while the neutral fraction induced a weak positive response (i.e., a doubling of revertants at only one dose). In the *E. coli* assay, the acid fraction induced more than a 20-fold increase in plaque formation. The base fraction also induced a weak positive response, possibly due to residual pentachlorophenol in this fraction.

These fractions were also applied to the skin of CD-1 mice to measure the induction of DNA adducts. For comparative purposes, a reconstituted mixture was synthesized to match the levels of eight class B2 carcinogens found in the neutral fraction (benzo(a)pyrene, benz(a)anthracene, benzo(b)fluoranthene, benzo(k)fluoranthene, chrysene, dibenz(a,h)anthracene, indeno(1,2,3-cd)pyrene and pentachlorophenol). All fraction constituents were confirmed via GC/MS (the levels of sixty PAHs were tested, as well as the levels of PCDDs and PCDFs in the PCDD fraction). Following dermal application, most fractions induced the maximum level of genotoxic damage in lung tissue, with the lowest frequency of adduct observed in liver. The exception to this, was the PAH fraction which induced the highest level of DNA adducts in liver. The PAH fraction induced a RAL level of 383 per 10^9 nucleotides in the liver, 306 per 10^9 nucleotides in the lung, and 109 per 10^9 nucleotides in skin. It was

also observed that the overall pattern of bulky DNA adducts were similar for the RM and NF. The autoradiogram for the RM showed multiple distinct spots, apparently reflecting the seven carcinogenic PAHs present in this mixture. Whereas the NF, containing comparable levels of the seven carcinogenic PAHs exhibited less distinct spots from the bulky adducts suggesting that PAH interactions may have modified PAH metabolism. Based on results from the short-term bioassay, the NF and RM were selected for a long term tumor study.

Prior to the long term study, an *in vivo* study was conducted to compare the persistence of DNA adducts from various fractions. In addition, the level of adducts induced from dermal exposure was compared to adduct levels following intraperitoneal injection of various fractions. It is assumed that the persistence of DNA adducts induced by genotoxic chemicals can have an influence on potential carcinogenic outcomes. This study was modeled after a previously published infant male mouse model (Rodriguez et al. 1997). Based on the previous study, three doses of BAP were selected (0.429, 0.171 and 0.069 mg/g body weight (bw)). The NF and RM were amended with BAP so that animals would receive the same BAP concentration as was administered in the BAP alone treatment groups. All mice were injected intraperitoneally (i.p.) one time at 21 days of age. Mice were euthanized after 1, 7, 21, and 280 days (280 for liver only). In addition, mice were treated topically once with a dose of 3, 1.2 and 0.48 mg/mouse (the dose used in the standard complex mixture protocol for ^{32}P-postlabeling). These mice were euthanized 1 day following treatment. Mice administered complex mixture via dermal application mice showed a different pattern of DNA adduct frequencies than mice administered the mixtures via i.p. injection. Overall, the BAP treatment elicited a higher DNA adduct frequency than the NF+BAP and the RM treatments for the dermal application. The reason for this is adsorption and distribution. The NF+ABP and RM treatments contain structurally larger compounds than BAP alone. Larger compounds have a diffictult time passing through barriers. For mice sacrificed one day following i.p. application, the NF+BAP fraction induced a relative adduct level of 276 per 10^9 nucleotides, while BAP induced 82 PER 10^9 nucleotides. The chemical-dose-

application interactions were not significantly different in the forestomach for treatment groups administered the fractions by i.p. and dermal application. However, for the liver and lung there were significant chemical-dose-application interactions observed from dermal and i.p. treatments.

The persistence of DNA adducts were measured in animals treated with the three mixtures or BAP. At the high treatment dose, the NF+BAP group exhibited higher adduct frequencies than was observed for the other treatments. However, at the medium and low dose, the BAP treatment elicited the highest adduct frequencies. This appears to indicate that the intermediate dose was optimal for BAP. It was also observed that the DNA adduct pattern in tissues from animals receiving the NF treatment was similar to the pattern for animal receiving the RM treatment. For BAP, RM and NF+BAP treatment, DNA adduct frequencies in liver exhibited a consistent decrease over time. After 21 days, adduct frequencies in liver from animals receiving each of these treatments was reduced by approximately 70%. Whereas for animals receiving the NF treatment, DNA adduct frequencies after 21 days were reduced by less than 20%. This indicates that this treatment was more persistent than the other treatments. Perhaps the lower levels of BAP allowed for a slower response from the metabolizing enzymes, enableing the NF to persist longer than the other treatments.

The ability of the four treatments, BAP and the three complex mixtures, to induce the formation of tumors was investigated using the infant mouse model following a protocol used by Rodriguez et al. (1997). Measurement of the ability of the pure compound and complex mixtures to induce tumor formation is important in the overall understanding of the interactions that occur within these and similar mixtures. In comparison to a 40-week tumor study, ^{32}P-postlabeling is a less costly and more efficient method for screening the genotoxic potential of chemicals and chemical mixtures. However, the ability of this assay to predict potential tumor formation for chemical mixtures has not been studied in depth. Therefore, comparing the frequency of DNA adduct formation to tumor induction will assist in understanding the utility of the short-term protocol.

Prior to the 280 day end point, several mice were euthanized due to illness or tumor formations that affected the animals' health. Mortality incidence was highest (75%) in animals receiving the NF+BAP treatment, while the NF produced a mortality rate of 46%. Upon dissection, gross tumors were observed on the organs of the animals. The highest gross tumor incidence, 38%, was observed in animals receiving the low dose RM treatment. Tissues were classified as benign or malignant based on histopathologic observations. Total incidence of tumor formation was calculated as gross plus microscopic for each tissue. For all tissues combined, the highest incidence of tumors included 75% for the NF+BAP treatment high dose, 63% in the BAP treatment medium dose and 46% in the RM low dose. Note that the concentration of BAP administered was the same across these three treatment groups, although the optimal dose for tumor formation was different. This suggests that component interactions influenced the optimal treatment dose for induction of tumors. As was observed in the Rodriguez et al. (1997) study, histologic classification confirmed that most of the tumors were benign. While most of the tumors observed were bening at the stage they were collected, there is a potential for a malignancy to form from the benign tumor. Malignant tumors were observed in animals receiving high dose RM treatment (4%) and NF+BAP treatment (13%). All tumors observed in liver tissue were benign.

The relationship between DNA adduct frequencies and tumor incidence was inconsistent. For select treatments and dosages, there did appear to be a relationship between DNA adduct and tumor formation. The optimal (intermediate) treatment dose for BAP induced a tumor incidence of 58% and a relative adduct level of 75 per 10^9 nucleotides. The same dose for the RM treatment induced a tumor incidence of 13%, and a RAL of 42 per 10^9 nucleotides. For the high dose of the RM in liver, the tumor incidence was 31% and the RAL 95 per 10^9 nucleotides; and, for the NF+BAP the tumor incidence was 50% and DNA adduct formation 276 per 10^9 nucleotides. The NF+BAP treatment induced the highest tumor frequency at the high dose, and DNA adduct frequencies were also highest at this dose. The data suggest that there is a relationship between the formation of DNA adducts and tumors, however this relationship is not a

very accurate one with an unknown mechanism. While there may not be a direct correlation between adduct formation and tumors, measurement of elevated adduct frequencies does appear to reflect an increased risk of cancer.

Complex chemical mixtures are ubiquitous in the human diet and the environment. These mixtures are also of concern at wood treating plants. There are 26 wood treatment sites on the National Priorities List (NPL) in the United States. There are 749 additional sites on the NPL which list PAH mixtures as contaminants of concern. In order to develop improved methods to rank and remediate these sites, it is important to obtain information to understand how chemical mixtures interact. The conclusions of this research include:

1. Fractionation of complex mixture is capable of isolating genotoxic components and specific chemical classes, although compound separation frequently overlaps.
2. Mixture isolates were genotoxic in short-term bioassays. The *Salmonella* bioassay was capable of detecting genotoxic PAHs and the *E. coli* bioassay was sensitive to pentachlorophenol in the complex mixture. These results were not very predictive of the ^{32}P-postlabeling results.
3. DNA adduct formation was higher when mixtures were administered by intraperitoneal application than by dermal application.
4. DNA adducts levels were generally reduced over time. However, adduct levels for certain treatment groups did persist for longer periods of time.
5. Tumor formation could not be predicted by the concentration of BAP alone. Component interactions appear to have affected the carcinogenic potential of the complex mixtures. It is important to determine how dose influences these chemicals to cause cancer.

Future studies are warranted on determining the mechanism of these interactions, and how this affects the carcinogenic outcomes. The data indicate that the liver is the target organ for PAH carcinogenesis in the infant mouse model. DNA adducts correlate most closely with tumor formation in this organ. Future studies would benefit from a

larger number of animals per treatment group, and a smaller number of treatment doses. Based on the statistical evaluation of the data, it is recommended that two doses and a single tissue be the focus of additional investigations into the carcinogenic interactions of complex mixtures.

REFERENCES

Agency for Toxic Substances and Disease Registry (ATSDR). 2002. Toxicological profile for creosote. Atlanta, GA:ATSDR. http://www.atsdr.cdc.gov/toxpro2.html.

Agency for Toxic Substances and Disease Registry (ATSDR). 2001. Toxicological profile for pentachlorophenol. Atlanta, GA:ATSDR. http://www.atsdr.cdc.gov/toxpro2.html.

Agency for Toxic Substances and Disease Registry (ATSDR). 1998. Toxicological profile for chlorinated dibenzo-*p*-dioxins (CDDs). Atlanta, GA:ATSDR. http://www.atsdr.cdc.gov/toxpro2.html.

Agency for Toxic Substances and Disease Registry (ATSDR). 1995. Toxicological profile for polycyclic aromatic hydrocarbons (PAHs). Atlanta, GA:ATSDR. http://www.atsdr.cdc.gov/toxpro2.html.

Agency for Toxic Substances and Disease Registry (ATSDR). 1994. Toxicological profile for chlorodibenzofurans (CDFs). Atlanta, GA:ATSDR. http://www.atsdr.cdc.gov/toxpro2.html.

Ahlborg UG, Thunber TM. 1980. Chlorinated phenols: occurrence, toxicity, metabolism, and environmental impact. Crit Rev Toxicol 7(1):1-35.

Ahlborg UG, Lindgren JE, Mercier M. 1974. Metabolism of pentachlorophenol. Arch Toxicol 32:271-81.

Ames BN, McCann J, Yamasaki E. 1975. Methods for detecting carcinogens and mutagens with the *Salmonella*/mammalian-microsome mutagenicity test. Mutat Res 31(6):347-64.

Anderson ME, Conolly RB. 1998. Mechanistic modeling of rodent liver tumor promotion at low levels of exposure: an example related to dose-response relationships for 2,3,7,8-tetrachlorodibenzo-*p*-dioxin. Hum Exp Toxicol 17:683-90.

Asp S, Riihimaki V, Hernberg S, Pukkala E. 1994. Mortality and cancer morbidity of Finnish chlorophenoxy herbicide applicators: an 18-year prospective follow-up. Am J Ind Med 26(2):243-53.

Barrett JC. 1995. Mechanisms for species differences in receptor-mediated carcinogenesis. Mutat Res 333(1-2):189-202.

Barrett JC. 1993. Mechanisms of multistep carcinogenesis and carcinogen risk assessment. Environ Health Perspect 100:9-20.

Becher H, Flesch-Janys D, Kauppinen T. 1996. Cancer mortality in German male workers exposed to phenoxy herbicides and dioxins. Cancer Causes Control 7:312-21.

Bertazzi PA, Zocchetti C, Guercilena S. 1997. Dioxin exposure and cancer risk: a 15-year mortality study after the "Seveso accident". Epidemiology 8:646-52.

Bertrand JP, Chau N, Patris A, Mur JM, Pham QT, Moulin JJ, Morviller P, Auburtin G, Figueredo A, Martin J. 1987. Mortality due to respiratory cancers in the coke oven plants of the Lorraine coalmining industry (Houilleres du Bassin de Lorraine). Br J Ind Med 44(8):559-65.

Bevenue A, Emerson ML, Casarett LJ. 1968. A sensitive gas chromatographic method for the determination of pentachlorophenol in human blood. J Chromatogr 38:467-72.

Biancifiori C, Caschera F. 1962. The relation between pseudopregnancy and the chemical induction by four carcinogens of mammary and ovarian tumours in BALB/c mice. Br J Cancer 16:722-30.

Binkova B, Sram RJ. 2004. The genotoxic effect of carcinogenic PAHs, their artificial and environmental mixtures (EOM) on human diploid lung fibroblasts. Mutat Res 547:109-21.

Boffetta P. 2006. Human cancer from environmental pollutants: the epidemiological evidence. Mutat Res 608(2):157-62.

Booth ED, Loose RW, Watson WP. 1999. Effects of solvent on DNA adduct formation in skin and lung of CD1 mice exposed cutaneously to benzo(a)pyrene. Arch Toxicol 73(6):316-22.

Borm PJ. 2002. Particle toxicology: from coal mining to nanotechnology. Inhal Toxicol 14(3):311-24.

Boysen G, Hecht SS. 2003. Analysis of DNA and protein adducts of benzo(a)pyrene in human tissues using structure-specific methods. Mutat Res 543(1):17-30.

Braun WH, Blau GE, Chenoweth MB. 1979. The metabolism/pharmacokinetics of pentachlorophenol in man, and a comparison with the rat and monkey. In Deichmann WE, ed. Toxicology and occupational medicine. New York:Elsevier, 289-96.

Breathnach CS. 1987. Biographical sketch: Orfila. Ir Med J 80(3):99.

Brender JD, Zhan FB, Suarez L, Langlois PH, Moody K. 2006. Maternal residential proximity to waste sites and industrial facilities and oral clefts in offspring. J Occup Environ Med 48(6):565-72.

Brender JD, Pichette JL, Suarez L, Hendricks KA, Holt M. 2003. Health risks of residential exposure to polycyclic aromatic hydrocarbons. Arch Environ Health 58(21):111-8.

Brown P, Clapp R. 2002. Looking back on Love Canal. Public Health Rep 117(2):95-8.

Brune H, Deutsch-Wenzel RP, Habs M, Ivankovic S, Schmahl D. 1981. Investigation of the tumorigenic response to benzo(a)pyrene in aqueous caffeine solution applied orally to Sprague-Dawley rats. J. Cancer Res Clin Oncol 102(2):153-7.

Buening MK, Levin W, Karle JM. 1979. Tumorigenicity of bay region epoxides and other derivatives of chrysene and phenanthrene in newborn mice. Cancer Res 39:5063-8.

Bullman TA, Kang HK. 1994. The effects of mustard gas, ionizing radiation, herbicides, trauma, and oil smoke on US military personnel: the results of veteran studies. Annu Rev Public Health 15:69-90.

Carson R. 1962. Silent spring. New York:Houghton Mifflin Company.

Case BW. 2006. Asbestos, smoking, and lung cancer: interaction and attribution. Occup Environ Med 63(8):507-8.

Centers for Disease Control and Prevention (CDC). 2003a. National Center for Health Statistics data on cancer. Atlanta, GA:CDC. http://www.cdc.gov/cancer.

Centers for Disease Control and Prevention (CDC). 2003b. Fact sheet: comprehensive cancer control. Atlanta, GA:CDC. http://www.cdc.gov/cancer.

Chou PP, Bailey JL. 1986. Liquid chromatographic determination of urinary pentachlorophenol. Clin Chem 32:1026-8.

Chu KC, Patel KM, Lin AH, Tarone RE, Linhart MS, Dunkel VC. 1981. Evaluating statistical analyses and reproducibility of microbial mutagenicity assays. Mutat Res 85(3):119-32.

Ciganek M, Neca J, Adamec V, Janoskek J, Machala M. 2004. A combined chemical and bioassay analysis of traffic-emitted polycyclic aromatic hydrocarbons. Sci Total Environ 334-335:141-8.

Cole P, Trichopoulos D, Pastides H, Starr T, Mandel JS. 2003. Dioxin and cancer: a critical review. Regul Toxicol Pharmacol 38:378-88.

Cook JW, Hewett CL, Hieger I. 1933. The isolation of a cancer-producing hydrocarbon from coal tar: parts I, II, and III. J Chem Soc 395-405.

Culp SJ, Warbritton AR, Smith BA, Li EE, Beland FA. 2000. DNA adduct measurements, cell proliferation and tumor mutation induction in relation to tumor formation in B6C3F1 mice fed coal tar or benzo(a)pyrene. Carcinogenesis 21(7):1433-40.

Culp SJ, Gaylor DW, Sheldon WG, Goldstein LS, Beland FA. 1998. A comparison of the tumors induced by coal tar and benzo(a)pyrene in a 2-year bioassay. Carcinogenesis 19(1):117-24.

Dahlgren J, Warshaw R, Thornton J, Anderson-Mahoney CP, Takhar H. 2003. Health effects on nearby residents of a wood treatment plant. Environ Res 92(2):92-8.

DeMarini DM, Brooks HG, Parkes DG. 1990. Induction of prophage lambda by chlorophenols. Environ Mol Mutagen 15(1):1-9.

Demers PA, Davies HW, Friesen MC, Hertzman C, Ostry A, Hershler R, Teschke K. 2006. Cancer and occupational exposure to pentachlorophenol and tetrachlorophenol (Canada). Cancer Causes Control 17(6):749-58.

Donnelly KC, Claxton LD, Huebner HJ, Capizzi JL. 1998. Mutagenic interactions of model chemical mixtures. Chemosphere 37(7):1253-61.

Donnelly KC, Brown KW, Kampbell D. 1987. Chemical and biological characterization of hazardous industrial waste. I. Prokaryotic bioassays and chemical analysis of a wood-preserving bottom-sediment waste. Mutat Res 180(1):31-42.

Drummond I, Van Roosmalen PB, Kornicki M. 1982. Determination of total pentachlorophenol in the urine of workers. Int Arch Occup Environ Health 50:321-7.

Edgerton TR, Moseman RF, Linder RE. 1979. Multi-residue method for the determination of chlorinated phenol metabolites in urine. J Chromatogr 170:331-42.

Eriksson M, Hardell L, Adami HO. 1990. Exposure to dioxins as a risk factor for soft tissue sarcoma: a population-based case-control study. J Natl Cancer Inst 82:486-90.

Falahatpisheh M, Kerzee J, Metz R, Donnelly K, Ramos K. 2004. Inducible cytochrome P450 activities in renal glomerular mesangial cells: biochemical basis for antagonistic interactions among nephrocarcinogenic polycyclic aromatic hydrocarbons. J Carcinog 3(1):12-9.

Farber E, Sarma DS. 1987. Hepatocarcinogenesis: a dynamic cellular perspective. Lab Invest 56(1):4-22.

Fattore E, Trossvik C, Hakansson H. 2000. Relative potency values derived from hepatic vitamin A reduction in male and female Sprague-Dawley rats following subchronic dietary exposure to individual polychlorinated dibenzo-*p*-dioxin and dibenzofuran congeners and a mixture thereof. Toxicol Appl Pharmacol 165(3):184-94.

Fay RM, Feron VJ. 1996. Complex mixtures: hazard identification and risk assessment. Food Chem Toxicol 34(11-12):1175-6.

Feron VJ, Groten JP, Jonker D, Cassee FR, van Bladeren PJ. 1995. Toxicology of chemical mixtures: challenges for today and the future. Toxicology 105(2-3):415-27.

Finley BL, Connor KT, Scott PK. 2003. The use of toxic equivalency factor distributions in probabilistic risk assessments for dioxins, furans, and PCBs. J Toxicol Environ Health A 66:533-50.

Fletcher N, Hanberg A, Hakansson H. 2001. Hepatic vitamin a depletion is a sensitive marker of 2,3,7,8-tetrachlorodibenzo-*p*-dioxin (TCDD) exposure in four rodent species. Toxicol Sci 62(1):166-75.

Franc MA, Pohjanvirta R, Tuomisto J, Okey AB. 2001a. *In vivo* up-regulation of aryl hydrocarbon receptor expression by 2,3,7,8-tetrachlorodibenzo-*p*-dioxin (TCDD) in a dioxin-resistant rat model. Biochem Pharmacol 62(12):1565-78.

Franc MA, Pohjanvirta R, Tuomisto J, Okey AB. 2001b. Persistent, low-dose 2,3,7,8-tetrachlorodibenzo-*p*-dioxin exposure: effect on aryl hydrocarbon receptor expression in a dioxin-resistance model. Toxicol Appl Pharmacol 175(1):43-53.

Gaylor DW, Culp SJ, Goldstein LS, Beland FA. 2000. Cancer risk estimation for mixtures of coal tars and benzo(a)pyrene. Risk Anal 20(1):81-5.

Gennings C. 1995. An efficient experimental design for detecting departure from additivity in mixtures of many chemicals. Toxicology 105(2-3):189-97.

Godschalk RW, Maas LM, Kleinjans JC, Van Schooten FJ. 1998. Influences of DNA isolation and RNA contamination on carcinogen-DNA adduct analysis by ^{32}P-postlabeling. Environ Mol Mutagen 32(4):344-50.

Green LM. 1991. A cohort mortality study of forestry workers exposed to phenoxy acid herbicides. Br J Ind Med 48(4):234-8.

Grimmer G, Jacob J, Dettbarn G. 1997. Determination of urinary metabolites of polycyclic aromatic hydrocarbons (PAH) for the risk assessment of PAH-exposed workers. Int Arch Occup Environ Health 69:231-9.

Groten JP, Feron VJ, Suhnel J. 2001. Toxicology of simple and complex mixtures. Trends Pharmacol Sci 22(6):316-22.

Gupta RC, Reddy MV, Randerath K. 1982. ^{32}P-postlabeling analysis of non-radioactive aromatic carcinogen--DNA adducts. Carcinogenesis 3(9):1081-92.

Hardell L, Eriksson M, Degerman A. 1994. Exposure to phenoxyacetic acids, chlorphenols, or organic solvents in relation to histopathology, stage, and anatomical localization of non-Hodgkin's lymphoma. Cancer Res 54:2386-9.

Harvey RG. 1997. Polycyclic aromatic hydrocarbons. New York:Wiley, VCH.

Harvey RG. 1991. Polycyclic aromatic hydrocarbons: chemistry and carcinogenicity. Cambridge, United Kingdom:Cambridge University Press.

Heinrich U, Pott F, Mohr U, Fuhst R, Konig J. 1986. Lung tumours in rats and mice after inhalation of PAH-rich emissions. Exp Pathol 29(1):29-34.

Hemminki K, Koskinen M, Rajaniemi H, Zhao C. 2000. DNA adducts, mutations, and cancer 2000. Regul Toxicol Pharmacol 32(3):264-75.

Hemminki K. 1993. DNA adducts, mutations and cancer. Carcinogenesis 14(10):2007-12.

Hoffmann D, Wynder EL. 1966. On the carcinogenic activity of dibenzopyrenes. Zeitschrift fur Krebsforschung (Germany) 68:137-49.

Holler JS, Fast DM, Hill RH. 1989. Qualification of selected herbicides and chlorinated phenols in urine by using gas chromatography/mass spectrometry. J Anal Toxicol 13:152-7.

Hooiveld M, Heederil DJ, Kogevinas M. 1998. Second follow-up of a Dutch cohort occupationally exposed to phenoxy herbicides, chlorophenols, and contaminants. Am J Epidemiol 147:891-901.

Houk VS, Claxton LD. 1986. Screening complex hazardous wastes for mutagenic activity using a modified version of the TLC/*Salmonella* assay. Mutat Res 169(3):81-92.

Institute of Medicine (IOM). 2003. Dioxins and dioxin-like compounds in the food supply: strategies to decrease exposure. Washington, DC:The National Academies Press.

International Agency for Research on Cancer (IARC). 2004. IARC monographs on the evaluation of carcinogenic risks to humans. Lyon, France:IARC. http://monographs.iarc.fr/.

International Agency for Research on Cancer (IARC). 1998a. Monographs on the evaluation of carcinogenic risks to humans: polynuclear aromatic compounds, part 4, bitumens, coal-tars and derived products, shale-oils and soots. Lyon, France:IARC. http://monographs.iarc.fr/ENG/Monographs/vol35/volume35.pdf.

International Agency for Research on Cancer (IARC). 1998b. Monographs on the evaluation of carcinogenic risks to humans: tobacco smoking. Lyon, France:IARC. http://monographs.iarc.fr/ENG/Monographs/vol38/volume38.pdf.

Jakszyn PG, Ibanez R, Pera G, Agudo A, Garcia-Closas R, Amiano P, Luquin E, Gonzalez CA. 2004. Food content of potential carcinogens. Barcelona, Spain:Catalan Institute of Oncology.

Jappinen P, Pukkala E, Tola S. 1989. Cancer incidence of workers in a Finnish sawmill. Scand J Work Environ Health 15:18-23.

Jarvholm B, Lillienberg L, Sallsten G, Thiringer G, Axelson O. 1981. Cancer morbidity among men exposed to oil mist in the metal industry. J Occup Med 23(5):333-7.

Jelinsky SA, Liu T, Geacintov NE, Loechler EL. 1995. The major, N^2-Gua adduct of the (+)-*anti*-benzo(a)pyrene diol epoxide is capable of inducing G-->A and G-->C, in addition to G-->T, mutations. Biochem 34(41):13545-53.

Jemal A, Clegg LX, Ward E, Ries LA, Wu X, Jamison PM, Wingo PA, Howe HL, Anderson RN, Edwards BK. 2004. Annual report to the nation on the status of cancer, 1975-2001, with a special feature regarding survival. Cancer 101(1):3-27.

Johnsen AR, Lipthay JR, Reicchenberg R, Sorensen SJ, Andersen O, Christensen P, Binderup ML, Jacobsen CS. 2006. Biodegradation, bioaccessibility, and genotoxicity of diffuse polycyclic aromatic hydrocarbon (PAH) pollution at a motorway site. Environ Sci Technol 40:3293-8.

Johnson BL, DeRosa CT. 1995. Chemical mixtures released from hazardous waste sites: implications for health risk assessment. Toxicology 105(2-3):145-56.

Jorens PG, Schepens PJ. 1993. Human pentachlorophenol poisoning. Hum Exp Toxicol 12(6):479-95.

Juhl U, Witte I, Butte W. 1985. Metabolism of pentachlorophenol to tetrachlorohydroquinone by human liver homogenate. Bull Environ Contam Toxicol 35:596-601.

Karlehagen S, Andersen A, Ohlson CG. 1992. Cancer incidence among creosote-exposed workers. Scand J Work Environ Health 18:26-9.

Kerr MA, Nasca PC, Mundt KA, Michalek AM, Baptiste MS, Mahoney MC. 2000. Parental occupational exposures and risk of neuroblastoma: a case-control study (United States). Cancer Causes Control 11:635-43.

Klaassen CD. 2001. Casarett and Doull's Toxicology: the basic science of poisons. New York:McGraw-Hill.

Knize MG, Salmon CP, Felton JS. 2003. Mutagenic activity and heterocyclic amine carcinogens in commercial pet foods. Mutat Res 539(1-2):195-201.

Koch-Weser J, Schechter PJ. 1978. Schmiedeberg in Strassburg 1872-1918: the making of modern pharmacology. Life Sci 22(13-15):1361-71.

Kogevinas M, Becher H, Benn T. 1997. Cancer mortality in workers exposed to phenoxy herbicides, chlorophenols, and dioxins. Am J Epidemiol 145:1061-75.

Krewski D, Thomas RD. 1992. Carcinogenic mixtures. Risk Anal 12(1):105-13.

Kuehl DW, Dougherty RC. 1980. Pentachlorophenol in the environment. Evidence for its origin from commercial pentachlorophenol by negative chemical ionization mass spectrometry. Environ Sci Tech 14:447-9.

Kulhanek A, Trapp S, Sismilich M, Janku J, Zimova M. 2005. Crop-specific human exposure assessment for polycyclic aromatic hydrocarbons in Czech soils. Sci Total Environ 339(1-3):71-80.

Kuo CY, Wong RH, Lin JY, Lai JC, Lee H. 2006. Accumulation of chromium and nickel metals in lung tumors from lung cancer patients in Taiwan. J Toxicol Environ Health A 69(14):1337-44.

Langman LJ, Kapur BM. 2006. Toxicology: then and now. Clin Biochem 39(5):498-510.

Larsen RV, Kirsch LE, Shaw SM. 1972. Excretion and tissue distribution of uniformly labeled (^{14}C)-pentachlorophenol in rats. J Pharmacol Sci 61:2004-6.

LaVoie EJ, Braley J, Rice JE. 1987. Tumorigenic activity of non-altemant polynuclear aromatic hydrocarbons in newborn mice. Cancer Let 34:15-20.

Lee DJ, Fleming LE, Leblanc WG, Arheart KL, Chung-Bridges K, Christ SL, Caban AJ, Pitman T. 2006. Occupation and lung cancer mortality in a nationally representative U.S. cohort: the National Health Interview Survey (NHIS). J Occup Environ Med 48(8):823-32.

Lloyd JW. 1971. Long-term mortality study of steelworkers. V. Respiratory cancer in coke plant workers. J Occup Med 13(2):53-68.

Loertscher JA, Lin TM, Peterson RE, Allen-Hoffmann BL. 2002. *In utero* exposure to 2,3,7,8-tetrachlorodibenzo-*p*-dioxin causes accelerated terminal differentiation in fetal mouse skin. Toxicol Sci 68(2):465-72.

Lu LJ, Disher RM, Reddy MV, Randerath K. 1986. ^{32}P-postlabeling assay in mice of transplacental DNA damage induced by the environmental carcinogens safrole, 4-aminobiphenyl, and benzo(a)pyrene. Cancer Res 46(6):3046-54.

Lubet RA, Connelly GM, Nebert DW. 1983. Dibenz(a,h)anthracene-induced subcutaneous tumors in mice. Strain sensitivity and the role of carcinogen metabolism. Carcinogenesis 4:513-7.

Maclure KM, MacMahon B. 1980. An epidemiologic perspective of environmental carcinogenesis. Epidemiol Rev 2:19-48.

Majtan T, Bukovska G, Timko J. 2004. DNA microarrays--techniques and applications in microbial systems. Folia Microbiol (Praha) 49(6):635-64.

Malkin R, Kiefer M, Tolos W. 1996. 1-Hydroxypyrene levels in coal-handling workers at a coke oven. J Occup Environ Med 38(11):1141-4.

Malling HV. 1971. Dimethylnitrosamine: formation of mutagenic compounds by interaction with mouse liver microsomes. Mutat Res 13(4):425-9.

Mann RD. 1993. Famous names in toxicology. Paracelsus--born 500 years ago. Adverse Drug React Toxicol Rev 12(2):81-2.

Marr LC, Grogan LA, Wohrnschimmel H, Molina L, Molina MJ. 2004. Vehicle traffic as a source of particulate polycyclic aromatic hydrocarbon exposure in the Mexico City metropolitain area. Environ Sci Technol 38(9):2584-92.

Maron DM, Ames BN. 1983. Revised methods for the *Salmonella* mutagenicity test. Mutat Res 113(3-4):173-215.

Mazumdar S, Lerer T, Redmond CK. 1975. Long-term mortality study of steelworkers. IX. Mortality patterns among sheet and tin mill workers. J Occup Med 17(12):751-5.

McCann J, Choi E, Yamasaki E, Ames BN. 1975. Detection of carcinogens as mutagens in the *Salmonella*/microsome test: assay of 300 chemicals. Proc Natl Acad Sci USA 72:5135-9.

Melber C, Kielhorn J, Mangelsdorf I. 2004. Concise international chemical assessment document 62: coal tar creosote. Geneva, Switzerland:World Health Organization.

Miller EC. 1978. Some current perspectives on chemical carcinogenesis in humans and experimental animals: presidential address. Cancer Res 38:1479-96.

Miller JA, Miller EC. 1971. Chemical carcinogenesis: mechanisms and approaches to its control. J Natl Cancer Inst 47(3):V-XIV.

Monosson E. 2005. Chemical mixtures: considering the evolution of toxicology and chemical assessment. Environ Health Perspect 113(4):383-90.

Moorthy B, Sriram P, Randerath K. 1994. Chemical structure- and time-dependent effects of polycyclic aromatic hydrocarbon-type inducers on rat liver cytochrome P450, DNA adducts, and I-compounds. Fundam Appl Toxicol 22(4):549-60.

Morabia A. 2006. Claude Bernard was a 19th century proponent of medicine based on evidence. J Clin Epidemiol 59(11):1150-4.

Mueller JG, Middaugh DP, Lantz SE, Chapman PJ. 1991. Biodegradation of creosote and pentachlorophenol in contaminated groundwater: chemical and biological assessment. Appl Environ Microbiol 57(5):1277-85.

Mueller JG, Chapman PJ, Pritchard PH. 1989. Creosote-contaminated sites: their potential for bioremediation. Environ Sci Technol 23(10):1197-201.

Nakayama T, Kurosawa Y, Furui S, Kerman K, Kobayashi M, Rao SR, Yonezawa Y, Nakano K, Hino A, Yamamura S, Takamura Y, and Tamiya E. 2006. Circumventing air bubbles in microfluidic systems and quantitative continuous-flow PCR applications. Anal Bioanal Chem 386(5):1327-33.

Neal J, Rigdon, RH. 1967. Gastric tumors in mice fed benzo(a)pyrene--a quantitative study. Tex Rep Biol Med 25(4):553-7.

Needham LL, Cline RE, Head SL. 1981. Determining pentachlorophenol in body fluids by gas chromatography after acetylation. J Anal Toxicol 5:283-6.

Nesnow S, Ross JA, Stoner GD, Mass MJ. 1995. Mechanistic linkage between DNA adducts, mutations in oncogenes and tumorigenesis of carcinogenic environmental polycyclic aromatic hydrocarbons in strain A/J mice. Toxicology 105(2-3):403-13.

Nygren M, Hansson M, Sjastram M. 1988. Development and validation of a method for determination of PCDDs and PCDFs in human blood plasma: a multivariate comparison of blood and adipose tissue levels between Vietnam veterans and matched controls. Chemosphere 17:1663-92.

Ohe T, Watanabe T, Wakabayashi K. 2004. Mutagens in surface waters: a review. Mutat Res 567(2-3):109-49.

Ohe T. 1979. Pentachlorophenol residues in human adipose tissue. Bull Environ Contam Toxicol 22:287-92.

Otteneder M, Lutz WK. 1999. Correlation of DNA adduct levels with tumor incidence: carcinogenic potency of DNA adducts. Mutat Res 424:237-47.

Perez S, Reifferscheid G, Eichhorn P, Barcelo D. 2003. Assessment of the mutagenic potency of sewage sludges contaminated with polycyclic aromatic hydrocarbons by an ames sludges for fluctuation assay. Environ Toxicol Chem 22(11):2576-84.

Phillips DH. 1997. Detection of DNA modifications by the ^{32}P-postlabelling assay. Mutat Res 378(1-2):1-12.

Pitot HC, Goldsworthy T, Campbell HA. 1980. Quantitative evaluation of the promotion by 2,3,7,8-tetrachlorodibenzo-*p*-dioxin of hepatocarcinogenesis from diethylnitrosamine. Cancer Res 40:3616-20.

Poland A, Kimbrough RD. 1984. Brandbury report 18: biological mechanisms of dioxin action. Cold Spring Harbor, NY:Cold Spring Harbor Laboratory.

Poland A, Palen D, Glover E. 1982. Tumour promotion by TCDD in skin of HRS/J hairless mice. Nature 300(5889):271-3.

Pott P. 1775. Chirurgical observations relative to the cataract, the polypus of the nose, the cancer of the scrotum, the different kinds of ruptures, and the mortification of the toes and feet. London, United Kingdom:Hawkes, Clark and Collins. Based on information from English Short Title Catalogue, accessed from Eighteenth Century Collections Online by the Gale Group. http://galenet.galegroup.com.ezproxy.tamu.edu:2048/servlet/ECCO.

Puisieux A, Lim S, Groopman J, Ozturk M. 1991. Selective targeting of p53 gene mutational hotspots in human cancers by etiologically defined carcinogens. Cancer Res 51(22):6185-9.

Purchase IF, Longstaff E, Ashby J, Styles JA, Anderson D, Lefevre PA, Westwood FR. 1976. Evaluation of six short term tests for detecting organic chemical carcinogens and recommendations for their use. Nature 264(5587):624-7.

Ramesh A, Knuckles ME. 2006. Dose-dependent benzo(a)pyrene (B(a)P)-DNA adduct levels and persistence in F-344 rats following subchronic dietary exposure to B(a)P. Cancer Lett 240(2):268-78.

Ramesh A, Walker SA, Hood DB, Guillen MD, Schneider K, Weyand EH. 2004. Bioavailability and risk assessment of orally ingested polycyclic aromatic hydrocarbons. Int J Toxicol 23(5):301-33.

Randerath K, Randerath E, Zhou GD, Donghui L. 1999. Bulky endogenous DNA modifications (I-compounds)-possible structural origins and functional implications. Mutat Res 424:183-94.

Randerath K, Zhou GD, Randerath E, Safe SH, Donnelly KC. 1997. Comparative ^{32}P-postlabeling analysis of exogenous and endogenous DNA adducts in mouse skin exposed to a wood-preserving waste extract, a complex mixture of polycyclic and polychlorinated chemicals. Environ Mol Mutagen 29(4):372-8.

Randerath E, Zhou GD, Donnelly KC, Safe SH, Randerath K. 1996. DNA damage induced in mouse tissues by organic wood preserving waste extracts as assayed by ^{32}P-postlabeling. Arch Toxicol 70(11):683-95.

Randerath E, Watson WP, Zhou GD, Chang J, Randerath K. 1995. Intensification and depletion of specific bulky renal DNA adducts (I-compounds) following exposure of male F344 rats to the renal carcinogen ferric nitrilotriacetate (Fe-NTA). Mutat Res 341(4):265-79.

Randerath K, Zhou GD, Donnelly KC, Safe SH, Randerath E. 1994. DNA damage induced by wood preserving waste extracts *in vitro* without metabolic activation, as assayed by ^{32}P-postlabeling. Cancer Lett 83(1-2):123-8.

Randerath K, Randerath E. 1994. ^{32}P-postlabeling methods for DNA adduct detection: overview and critical evaluation. Drug Metab Rev 26(1-2):67-85.

Randerath K, Li D, Nath R, Randerath E. 1992. Exogenous and endogenous DNA modifications as monitored by ^{32}P-postlabeling: relationships to cancer and aging. Exp Gerontol 27(5-6):533-49.

Randerath K, Putman KL, Randerath E, Mason G, Kelley M, Safe S. 1988. Organ-specific effects of long term feeding of 2,3,7,8-tetrachlorodibenzo-*p*-dioxin and 1,2,3,7,8-pentachlorodibenzo-*p*-dioxin on I-compounds in hepatic and renal DNA of female Sprague-Dawley rats. Carcinogenesis 9(12):2285-9.

Randerath K, Reddy V, Disher RM. 1986. Age- and tissue-related DNA modifications in untreated rats: detection by ^{32}P-postlabeling assay and possible significance for spontaneous tumor induction and aging. Carcinogenesis 7(9):1615-7.

Randerath K, Randerath E, Agrawal HP, Reddy MV. 1984. Biochemical (postlabeling) methods for analysis of carcinogen-DNA adducts. IARC Sci Pub 59:217-31.

Randerath K, Reddy MV, Gupta RC. 1981. ^{32}P-labeling test for DNA damage. Proc Natl Acad Sci USA 78(10):6126-9.

Rappe C, Kjeller LO, Bruckmann P, Hackhe KH. 1988. Identification and quantification of PCDDs and PCDFs in urban air. Chemosphere 17(1):3-20.

Reddy MV. 2000. Methods for testing compounds for DNA adduct formation. Regul Toxicol Pharmacol 32(3):256-63.

Reddy MV, Randerath K. 1986. Nuclease P1-mediated enhancement of sensitivity of ^{32}P-postlabeling test for structurally diverse DNA adducts. Carcinogenesis 7(9):1543-51.

Reddy MV, Gupta RC, Randerath E, Randerath KR. 1984. ^{32}P-postlabeling test for covalent DNA binding of chemicals *in vivo*: application to a variety of aromatic carcinogens and methylating agents. Carcinogenesis 5(2):231-43.

Redmond CK, Strobino BR, Cypess RH. 1976. Cancer experience among coke by-product workers. Ann NY Acad Sci 271:102-15.

Ress NB, Donnelly KC, George SE. 2002. The effect of pentachlorophenol on DNA adduct formation in p53 wild-type and knockout mice exposed to benzo(a)pyrene. Cancer Lett 178(1):11-7.

Reynolds R, Witherspoon S, Fox T. 2004. The infant mouse as an *in vivo* model for the detection and study of DNA damage-induced changes in the liver. Mol Carcinog 40(1):62-72.

Rice JE, Hosted TJ, DeFloria MC. 1986. Tumor-initiating activity of major *in-vivo* metabolites of indeno(1,2,3-cd)pyrene on mouse skin. Carcinogenesis 7(10):1761-4.

Rockette HE, Redmond CK. 1976. Long-term mortality study of steelworkers. J Occup Med 18(8):541-5.

Rodriguez LV, Dunsford HA, Steinberg M, Chaloupka KK, Zhu L, Safe S, Womack JE, Goldstein LS. 1997. Carcinogenicity of benzo(a)pyrene and manufactured gas plant residues in infant mice. Carcinogenesis 18(1):127-35.

Roemer E, Stabbert R, Rustemeier K, Veltel DJ, Meisgen TJ, Reininghaus W, Carchman RA, Gaworski CL, Podraza KF. 2004. Chemical composition, cytotoxicity and mutagenicity of smoke from US commercial and reference cigarettes smoked under two sets of machine smoking conditions. Toxicology 195(1):31-52.

Roffey R, Tegnell A, Elgh F. 2002. Biological warfare in a historical perspective. Clin Microbiol Infect 8(8):450-4.

Rossman TG, Molina M, Meyer LW. 1984. The genetic toxicology of metal compounds: I. induction of lambda prophage in *E. coli* WP2s(lambda). Environ Mutagen 6(1):59-69.

Safe S. 1990. Polychlorinated biphenyls (PCBs), dibenzo-*p*-dioxins (PCDDs), dibenzofurans (PCDFs), and related compounds: environmental and mechanistic considerations which support the development of toxic equivalency factors (TEFs). Crit Rev Toxicol 21(1):51-88.

Sai-Kato K, Umemura T, Takagi A. 1995. Pentachlorophenol-induced oxidative DNA damage in mouse liver and protective effect of antioxidants. Food Chem Toxicol 33:877-82.

Samanta SK, Singh OV, Jain RK. 2002. Polycyclic aromatic hydrocarbons: environmental pollution and bioremediation. Trends Biotechnol 20(6):243-8.

Schonwalder C, Olden K. 2003. Environmental health moves into the 21st century. Int J Hyg Environ Health 206(4-5):263-7.

Seagrave J, Gigliotti A, McDonald JD, Seilkop SK, Whitney KA, Zielinska B, Mauderly JL. 2005. Composition, toxicity, and mutagenicity of particulate and semivolatile emissions from heavy-duty compressed natural gas-powered vehicles. Toxicol Sci 87(1):232-41.

Seiler JP. 1991. Pentachlorophenol. Mutat Res 257:27-47.

Shampo MA, Kyle RA. 1987. Francois Magendie: early French physiologist. Mayo Clin Proc 62(5):412.

Shishu, Kaur IP. 2003. Inhibition of mutagenicity of food-derived heterocyclic amines by sulforaphane--a constituent of broccoli. Indian J Exp Biol 41(3):216-9.

Sinclair U. 2003. The jungle. New York:Barnes & Noble Books.

Smith AH, Marshall G, Yuan Y, Ferreccio C, Liaw J, von Ehrenstein O, Steinmaus C, Bates MN, Selvin S. 2006. Increased mortality from lung cancer and bronchiectasis in young adults after exposure to arsenic *in utero* and in early childhood. Environ Health Perspect 114(8):1293-6.

Solt DB, Farber E. 1976. New principle for the analysis of chemical carcinogenesis. Nature 263:702.

Steenland K, Piacitelli L, Deddens J, Fingerhut M, Chang LI. 1999. Cancer, heart disease, and diabetes in workers exposed to 2,3,7,8-tetrachlorodibenzo-*p*-dioxin. J Natl Cancer Inst 91(9):779-86.

Steiner PE, Falk HL. 1951. Summation and inhibition effects of weak and strong carcinogenic hydrocarbons: 1,2-benzanthracene, chrysene, 1,2,5,6-dibenzanthracene and 20-methylcholanthrene. Cancer Res 11:56-63.

Sugimura T, Wakabayashi K, Nakagama H, Nagao M. 2004. Heterocyclic amines: mutagens/carcinogens produced during cooking of meat and fish. Cancer Sci 95(4):290-9.

Tennant RW, Margolin BH, Shelby MD, Zeiger E, Haseman JK, Spalding J, Caspary W, Resnick M, Stasiewicz S, Anderson B and others. 1987a. Prediction of chemical carcinogenicity in rodents from *in vitro* genetic toxicity assays. Science 236(4804):933-41.

Tennant RW, Spalding JW, Stasiewicz S, Caspary WD, Mason JM, Resnick MA. 1987b. Comparative evaluation of genetic toxicity patterns of carcinogens and noncarcinogens: strategies for predictive use of short-term assays. Environ Health Perspect 75:87-95.

Teuschler LK, Hertzberg RC. 1995. Current and future risk assessment guidelines, policy, and methods development for chemical mixtures. Toxicology 105(2-3):137-44.

Umemura T, Sai-Kato K, Takagi A. 1996. Oxidative DNA damage and cell proliferation in the livers of B6C3F1 mice exposed to pentachlorophenol in their diet. Fundam Appl Toxicol 30:285-9.

Uno S, Dalton TP, Derkenne S, Curran CP, Miller ML, Shertzer HG, Nebert DW. 2004. Oral exposure to benzo(a)pyrene in the mouse: detoxication by inducible cytochrome P450 is more important than metabolic activation. Mol Pharmacol 65(5):1225-37.

Uno S, Dalton TP, Shertzer HG, Genter MB, Warshawsky D, Talaska G, Nebert DW. 2001. Benzo(a)pyrene-induced toxicity: paradoxical protection in Cyp1a1(-/-) knockout mice having increased hepatic BaP-DNA adduct levels. Biochem Biophys Res Commun 289(5):1049-56.

United States Code (USC). 1980. Title 42--the public health and welfare: 103 (9601-9675) comprehensive environmental response, compensation and liability act. Washington, DC:US Government Printing Office. http://www.access.gpo.gov/uscode/uscmain.html.

United States Code (USC). 1976. Title 42--the public health and welfare: 82 (6901-9922k) solid waste disposal. Washington, DC:US Government Printing Office. http://www.access.gpo.gov/uscode/uscmain.html.

United States Department of Health and Human Services (DHHS). 2004. 11th Report on carcinogens. Prepared for the National Institute of Environmental Health Sciences. Durham, NC:Constella Group, Incorporated.

United States Environmental Protection Agency (USEPA). 2006a. EPA region 3 risk-based concentration table: technical background information. Washington, DC:USEPA. http://www.epa.gov/reg3hwmd/risk/human/info/tech.htm.

United States Environmental Protection Agency (USEPA). 2006b. Integrated risk information system (IRIS): IRIS internet users guide. Washington, DC:USEPA. http://www.epa.gov/iris.

United States Environmental Protection Agency (USEPA). 2006c. Pesticides: topical & chemical fact sheets: creosote and its use as a wood preservative. Washington, DC:USEPA. http://www.epa.gov/pesticides/factsheets/chemicals/creosote_main.htm.

United States Environmental Protection Agency (USEPA). 2006d. Pesticides: topical & chemical fact sheets: pentachlorophenol and its use as a wood preservative. Washington, DC:USEPA. http://www.epa.gov/pesticides/factsheets/chemicals/pentachlorophenol_main.htm.

United States Environmental Protection Agency (USEPA). 2006e. Superfund: new report projects number, cost and nature of contaminated site cleanups in the U.S. over next 30 years. Washington, DC:USEPA. http://www.epa.gov/superfund/news/30years.htm.

United States Environmental Protection Agency (USEPA). 2005a. Finding answers: comprehensive environmental response, compensation, and liability act (superfund). Washington, DC:USEPA. http://www.epa.gov/region5/defs/html/cercla.htm.

United States Environmental Protection Agency (USEPA). 2005b. Region 8 - Libby ground water. Washington, DC:USEPA. http://www.epa.gov/region8/superfund/sites/mt/libby_.html.

United States Environmental Protection Agency (USEPA). 2005c. Superfund: CERCLA overview. Washington, DC:USEPA. http://www.epa.gov/superfund/action/law/cercla.htm.

United States Environmental Protection Agency (USEPA). 2005d. Superfund: key dates in superfund. Washington, DC:USEPA. http://www.epa.gov/superfund/action/law/keydates.htm.

United States Environmental Protection Agency (USEPA). 2005e. Superfund: SARA overview. Washington, DC:USEPA. http://www.epa.gov/superfund/action/law/sara.htm.

United States Environmental Protection Agency (USEPA). 2000a. Integrated risk information system (IRIS) toxicological review: vinyl chloride. Washington, DC:USEPA. http://www.epa.gov/iris.

United States Environmental Protection Agency (USEPA). 2000b. Second five-year review report for Libby ground water site, Libby, Lincoln County, Montana. Washington, DC:USEPA. http://www.epa.gov/superfund/action/law/sara.htm.

United States Environmental Protection Agency (USEPA). 1997a. Method 3650B, acid-base partition cleanup revision 2. In SW-846, test methods for evaluating solid waste, physical/chemical methods. Washington, DC:USEPA National Technical Information Service, CD-ROM Version 2.0.

United States Environmental Protection Agency (USEPA). 1997b. Method 8270B, semivolatile organic compounds by gas chromatography/mass spectrometry (GC/MS) revision 3. In SW-846 test methods for evaluating solid waste, physical/chemcial methods. Washington, DC:USEPA National Technical Information Service, CD-ROM Version 2.0.

United States Environmental Protection Agency (USEPA). 1997c. Method 1613, Tetra- through octa-chlorinated dioxins and furans by isotope dilution HRGC/HRMS. In SW-846 test methods for evaluating solid waste, physical/chemcial methods. Washington, DC:USEPA National Technical Information Service, CD-ROM Version 2.0.

United States Environmental Protection Agency (USEPA). 1995. Integrated risk information system (IRIS) toxicological review: dichloromethane. Washington, DC:USEPA. http://www.epa.gov/iris.

United States Environmental Protection Agency (USEPA). 1994a. Integrated risk information system (IRIS) toxicological review: benz(a)anthracene. Washington, DC:USEPA. http://www.epa.gov/iris.

United States Environmental Protection Agency (USEPA). 1994b. Integrated risk information system (IRIS) toxicological review: benzo(a)pyrene (BaP). Washington, DC:USEPA. http://www.epa.gov/iris.

United States Environmental Protection Agency (USEPA). 1994c. Integrated risk information system (IRIS) toxicological review: benzo(b)fluoranthene. Washington, DC:USEPA. http://www.epa.gov/iris.

United States Environmental Protection Agency (USEPA). 1994d. Integrated risk information system (IRIS) toxicological review: benzo(k)fluoranthene. Washington, DC:USEPA. http://www.epa.gov/iris.

United States Environmental Protection Agency (USEPA). 1994e. Integrated risk information system (IRIS) toxicological review: chrysene. Washington, DC:USEPA. http://www.epa.gov/iris.

United States Environmental Protection Agency (USEPA). 1994f. Integrated risk information system (IRIS) toxicological review: dibenz(a,h)anthracene. Washington, DC:USEPA. http://www.epa.gov/iris.

United States Environmental Protection Agency (USEPA). 1994g. Integrated risk information system (IRIS) toxicological review: indeno(1,2,3-cd)pyrene. Washington, DC:USEPA. http://www.epa.gov/iris.

United States Environmental Protection Agency (USEPA). 1993. Integrated risk information system (IRIS) toxicological review: pentachlorophenol. Washington, DC:USEPA. http://www.epa.gov/iris.

United States Environmental Protection Agency (USEPA). 1992. Integrated risk information system (IRIS): EPA's approach for assessing the risks associated with chronic exposure to carcinogens. Washington, DC:USEPA. http://www.epa.gov/iris.

United States Environmental Protection Agency (USEPA). 1991. Drinking water criteria document for PAH. Prepared by the office of health and environmental assessment, environmental criteria and assessment office, Cincinnati, OH for the Office of Water Regulations and Standards. Washington, DC:USEPA.

United States Environmental Protection Agency (USEPA). 1989. Risk assessment guidance for superfund (RAGS) volume I human health evaluation manual (part A). Washington, DC:USEPA. http://www.epa.gov/oswer/riskassessment/ragsa/index.htm.

United States Environmental Protection Agency (USEPA). 1986. Guidelines for the health risk assessment of chemical mixtures. Washington, DC:USEPA. http://www.epa.gov/ncea/raf/pdfs/chem_mix/chemmix?1986.pdf.

Van Duuren BL, Sivak A, Segal A. 1966. The tumor producing agents of tobacco leaf and tobacco smoke condensate. J Natl Cancer Inst 37:519-26.

Vesselinovitch SD, Kyriazis AP, Mihailovich N, Rao KV. 1975a. Conditions modifying development of tumors in mice at various sites by benzo(a)pyrene. Cancer Res 35(11):2948-53.

Vesselinovitch SD, Kyriazis AP, Mihailovich N, Rao KV. 1975b. Factors influencing augmentation and/or acceleration of lymphoreticular tumors in mice by benzo(a)pyrene treatment. Cancer Res 35(8):1963-9.

Viluksela M, Bager Y, Tuomisto JT, Scheu G, Unkila M, Pohjanvirta R, Flodstrom S, Kosma VM, Maki-Paakkanen J, Vartiainen T and others. 2000. Liver tumor-promoting activity of 2,3,7,8-tetrachlorodibenzo-*p*-dioxin (TCDD) in TCDD-sensitive and TCDD-resistant rat strains. Cancer Res 60(24):6911-20.

Visciano P, Perugini M, Amorena M, Ianieri A. 2006. Polycyclic aromatic hydrocarbons in fresh and cold-smoked Atlantic salmon fillets. J Food Prot 69(5):1134-8.

Von Tungeln LS, Xia Q, Herreno-Saenz D, Bucci TJ, Heflich RH, Fu PP. 1999. Tumorigenicity of nitropolycyclic aromatic hydrocarbons in the neonatal B6C3F1 mouse bioassay and characterization of ras mutations in liver tumors from treated mice. Cancer Lett 146(1):1-7.

Vyskocil A, Viau C, Camus M. 2004. Risk assessment of lung cancer related to environmental PAH pollution sources. Hum Exp Toxicol 23:115-27.

Walker NJ, Tritscher AM, Sills RC, Lucier GW, Portier CJ. 2000. Hepatocarcinogenesis in female Sprague-Dawley rats following discontinuous treatment with 2,3,7,8-tetrachlorodibenzo-*p*-dioxin. Toxicol Sci 54(2):330-7.

Wang B, Chambers L. 1997. Procedures for the extraction of tissues and purification of extracts for analysis of polychlorinated dibenzo-*p*-dioxins (PCDD) and polychlorinated dibenzofurans (PCDF). Texas A&M University:standard operating procedures for Geochemical and Environmental Research Group (GERG).

Watanabe T, Ohe T, Hirayama T. 2005. Occurrence and origin of mutagenicity in soil and water environment. Environ Sci 12(6):325-46.

Weisburger JH, William GM. 1988. Interactions of chemical carcinogens. Internl Conf Environ Mutag 3:288-94.

Williams GM, Iatropoulos MJ, Weisburger JH. 1996. Chemical carcinogen mechanisms of action and implications for testing methodology. Exp Toxicol Pathol 48(2-3):101-11.

Wislocki PG, Bagan ES, Lu AYH. 1986. Tumorigenicity of nitrated derivatives of pyrene, benz(a)anthracene, chrysene and benzo(a)pyrene in the newborn mouse assay. Carcinogenesis 7(8):1317-22.

Wogan GN, Hecht SS, Felton JS, Conney AH, Loeb LA. 2004. Environmental and chemical carcinogenesis. Semin Cancer Biol 14:473-86.

Wong O, Harris F. 2005. Retrospective cohort mortality study and nested case-control study of workers exposed to creosote at 11 wood-treating plants in the United States. J Occup Environ Med 47:683-97.

Wyde ME, Cambre T, Lebetkin M, Eldridge SR, Walker NJ. 2002. Promotion of altered hepatic foci by 2,3,7,8-tetrachlorodibenzo-*p*-dioxin and 17beta-estradiol in male Sprague-Dawley rats. Toxicol Sci 68(2):295-303.

Wynder EL, Hoffmann D. 1959. The carcinogenicity of benzofluoranthene. Cancer 12:1194-9.

Yach D, Wipfli H. 2006. A century of smoke. Ann Trop Med Parasitol 100(5):465-79.

Zacharewski T, Safe L, Safe S. 1989. Comparative analysis of polychlorinated dibenzo-*p*-dioxin and dibenzofuran congeners in Great Lakes fish extracts by gas chromatography and *in vitro* enzyme induction activities. Environ Sci Technol 23:730-5.

VITA

Name:	Tracie Denise Phillips
Address:	School of Rural Public Health, Bldg A Room 101, 1266 Texas A&M University, College Station, TX, 77843-1266
Education:	Ph.D., Toxicology, Texas A&M University, 2006 B.S., Bioenvironmental Sciences, Texas A&M University, 2001